Topics in Current Chemistry 328

Sophie Jackson *Editor*

Molecular Chaperones

Springer

328
Topics in Current Chemistry

For further volumes:
http://www.springer.com/series/128

Aims and Scope

The series Topics in Current Chemistry presents critical reviews of the present and future trends in modern chemical research. The scope of coverage includes all areas of chemical science including the interfaces with related disciplines such as biology, medicine and materials science.

The goal of each thematic volume is to give the non-specialist reader, whether at the university or in industry, a comprehensive overview of an area where new insights are emerging that are of interest to larger scientific audience.

Thus each review within the volume critically surveys one aspect of that topic and places it within the context of the volume as a whole. The most significant developments of the last 5 to 10 years should be presented. A description of the laboratory procedures involved is often useful to the reader. The coverage should not be exhaustive in data, but should rather be conceptual, concentrating on the methodological thinking that will allow the non-specialist reader to understand the information presented.

Discussion of possible future research directions in the area is welcome.

Review articles for the individual volumes are invited by the volume editors.

Readership: research chemists at universities or in industry, graduate students.

Sophie Jackson
Editor

Molecular Chaperones

With contributions by

A. Ahmad · T. Aumüller · A.J. Baldwin · J.L.P. Benesch · E.B. Bertelsen · R.A. Dabbs · H. Ecroyd · G. Fischer · R.B. Freedman · J.E. Gestwicki · G.R. Hilton · S.E. Jackson · H. Lioe · M.P. Mayer · A. Rousaki · C. Schiene-Fischer · F. Stengel · A.K. Wallis · M.R. Wilson · A.R. Wyatt · J.J. Yerbury · E.R.P. Zuiderweg

Springer

Editor
Sophie Jackson
Department of Chemistry
University of Cambridge
Cambridge
United Kingdom

ISSN 0340-1022 ISSN 1436-5049 (electronic)
ISBN 978-3-642-34551-7 ISBN 978-3-642-34552-4 (eBook)
DOI 10.1007/978-3-642-34552-4
Springer Heidelberg New York Dordrecht London

Library of Congress Control Number: 2012952678

Printed on acid-free paper

Springer is part of Springer Science+Business Media (www.springer.com)

Preface

Molecular chaperones were first identified more than 30 years ago and have been the subject of considerable research ever since. Their importance in a wide range of different cellular processes has been recognised and in the past decade great strides have been made in understanding them from a structural and mechanistic perspective. This issue of *Topics in Current Chemistry* reviews work in the field over the past decade.

Numerous definitions for the term molecular chaperone exist – one long-standing definition is that they are a functional class of unrelated families of protein that assist the folding or assembly of other polypeptide-containing structures in vivo, but are not components of these assembled structures when they are performing their normal biological functions. Although many think of molecular chaperones in terms of how they affect protein folding, this class of proteins has a much wider role in the cell, and chaperones are involved in assembly and disassembly of macromolecular complexes, play essential roles in targeting and translocation of proteins to specific cellular locations and compartments, are central to many cellular degradation pathways, also regulate cell signalling and through heat shock factor 1 regulate the cellular stress response. Collectively, molecular chaperones in conjunction with other systems govern proteostasis in vivo.

So many families of molecular chaperones are now known it is not possible to discuss in detail the latest research for all of these. Instead, this issue is focussed on six key families for which there have been major advances in knowledge over the last 10 years.

The first two chapters focus on molecular chaperones which can perhaps be described as true protein folding catalysts, as they accelerate the rate of otherwise slow, rate-limiting steps in folding, that is, disulphide bond formation/rearrangement and peptidyl prolyl isomerisation. PDI, protein disulphide isomerase, is one of the most abundant proteins in the endoplasmic reticulum and plays a critical role in the oxidative folding of many ER and extracellular proteins. Chapter 1 describes recent advances in our understanding of the structure and function of PDI, as well as the Dsb family of chaperones which carry out similar functions in prokaryotes. The diversity of potential pathways and intermediates in the oxidative folding of proteins is illustrated using BPTI and detailed mechanistic studies on how PDI facilitates the folding of such systems are provided. The challenges in investigating a complex system in which the chaperone has multiple domains with differing

structures and functions but where high-resolution structural information can only be obtained on individual domains are nicely exemplified. Recent work establishing how the individual domains interact both structurally and functionally with each other to provide a holistic view of PDI's mechanism of action is described.

Chapter 2 describes all three families of known peptidyl prolyl isomerases (PPIases) including the FKBPs, cyclophilins and parvulins. These chaperones catalyse conformational interconversions of peptide bonds which can be critical to the correct folding of many proteins. The structural and chemical features of PPIases and the catalytic cycle are described, and a discussion of chaperoning *versus* catalysis is also included.

One common feature of molecular chaperones is that many are multi-domain and/or oligomeric proteins. The intra-domain and inter-molecular dynamics of these systems can play a very important role in their function, and this is particularly true for the small heat shock proteins (sHsps). Chapter 3 describes the dynamic architecture of this class of chaperones and how their oligomeric state affects their chaperoning activity. Another common feature of many chaperones is that different classes cooperate together in chaperoning networks, some acting, as the small heat shock proteins do, as "holdases" in conjunction with other classes of chaperones that act as "foldases". This is well illustrated in this chapter, the authors coining the phrase "paramedics of the cell" to describe the sHsps which effectively keep proteins alive until the medics (in this case other classes of chaperones) can treat them.

The Hsp70 family of molecular chaperones, which in bacteria comprises DnaK, DnaJ and a nucleotide exchange factor such as GrpE, has a central role in many cellular processes. Hsp70 is a classic chaperone with ATPase activity which is linked with conformational rearrangements in its multi-domain structure. Chapter 4 describes in detail the structure of the Hsp70 system and how ATP binding and hydrolysis linked with conformational changes create a functional cycle which binds and releases unfolded polypeptide chains in a controlled manner. This chapter highlights the importance of allostery in molecular chaperone machines and it goes on to demonstrate how allosteric effectors may act as drugs targeting cellular chaperones. This chapter introduces the idea that chaperones are closely associated with many disease states including neurodegenerative disorders and cancer, and this theme is continued in Chapter 5 on Hsp90s, which not only describes the importance of Hsp90 inhibitors as cancer therapeutics, but also recent work which has begun to establish that chaperones, in particular Hsp90, may also be important in the development of therapeutic agents against viral infection, protozoan parasites and other human pathogens as well as a large number of neurodegenerative disorders. Chapter 5 also describes the biological activity of this important chaperone and the many structural and functional studies that have generated considerable insight into the mechanism of its action. As with the chapter on the Hsp70 system, this section illustrates how ATP binding and hydrolysis, and the binding of cochaperones, are linked with conformational changes in Hsp90 which results in activation of client (substrate) proteins.

The first five chapters are focussed on major classes of intracellular chaperones whilst the final chapter, Chapter 6, describes recent work in the increasingly important field of extracellular molecular chaperones. The function of a number of extracellular chaperones such as clusterin, α2 microglobulin, haptoglobulin, apoE, serum amyloid P component, caseins and fibrinogens are all described, in addition to the link between these molecular chaperones and various disease states, in particular neurodegenerative diseases.

Together, it is hoped that this issue of *Topics in Current Chemistry* provides a useful resource for anyone coming into the field of molecular chaperones as well as those of us who have been working in this area for many years. I would like to take this opportunity to thank all the authors for their contributions and the staff at Springer for their patience.

Cambridge, UK Sophie E. Jackson

Contents

Top Curr Chem (2013) 328: 1–34
DOI: 10.1007/128_2011_171

Published online: 1 June 2011

Assisting Oxidative Protein Folding: How Do Protein Disulphide-Isomerases Couple Conformational and Chemical Processes in Protein Folding?

A. Katrine Wallis and Robert B. Freedman

Abstract Oxidative folding is the simultaneous process of forming disulphide bonds and native structure in proteins. Pathways of oxidative folding are highly diverse and in eukaryotes are catalysed by protein disulphide isomerases (PDIs). PDI consists of four thioredoxin-like domains, two of which contain active sites responsible for disulphide interchange reactions. The four domains are arranged in a horseshoe shape with the two active sites facing each other at the opening of the horseshoe. An extended hydrophobic surface at the bottom of the horseshoe is responsible for non-covalent, hydrophobic interactions with the folding protein. This binding site is capable of distinguishing between fully-folded and partially- or un-folded proteins. PDI is not only a catalyst of the formation of disulphide bonds, but also catalyses folding steps which involve significant conformational change in the folding protein. This review brings together the latest catalytic and structural data aimed at understanding how this is achieved.

Keywords Endoplasmic reticulum · Enzyme mechanism · Mobility · Oxidative folding · Protein conformation

Contents

A.K. Wallis (✉) and R.B. Freedman (✉)
School of Life Sciences, University of Warwick, CV4 7AL Coventry, UK
e-mail: A.K.Wallis@warwick.ac.uk; R.B.Freedman@warwick.ac.uk

1 Introduction and Scope

Conventional chaperones facilitate conformational processes; they assist polypeptides along pathways to folded rather than misfolded products, and these products differ from each other – and from unfolded precursors and intermediate states – in terms of non-covalent, conformational parameters. Covalent chemistry is often involved, in the form of hydrolysis of ATP, and a key issue is how the cycle of ATP binding, hydrolysis and product release is coupled through structural cycles in the chaperone to support folding of the protein substrate [1–3]. However, the linkage of covalent chemical change (ATP hydrolysis) to the conformational process of protein folding is clearly indirect. Oxidative protein folding is different; here, an unfolded protein with free thiol groups on cysteine residues is oxidised to a product, with a specific stable conformation and a specific set of disulphide bonds linking those residues. In this case, covalent and conformational processes are intimately coupled; the native conformation is stabilised by the 'native' set of disulphide linkages, and conversely, those linkages are more stable than disulphides between cysteine residues in an unfolded protein, being stabilised by the native conformation. Native conformation and the 'native' disulphides associated with it are classical thermodynamic 'linked functions' (Fig. 1a).

These issues are critical in thinking about how oxidative protein folding is facilitated in the cell. Disulphide bonds are characteristic of proteins found at the cell surface or exported from the cell into extracellular spaces. Oxidative folding in eukaryotes takes place within the lumen of the ER (endoplasmic reticulum, the first compartment in the cell's 'protein export' pathway). The environment of the ER lumen is crowded and complex. Folding proteins are present in an environment rich in a range of molecular chaperones, folding catalysts and enzymes catalysing

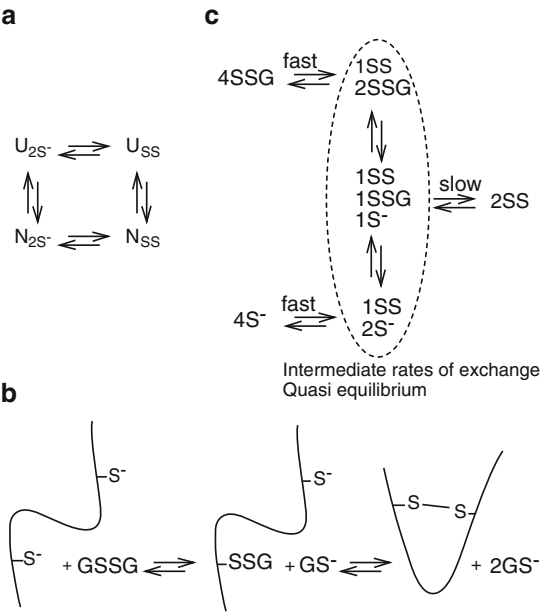

Fig. 1 Formation of disulphide bonds. (**a**) Folding, i.e. changes in conformation and formation of disulphide bonds are thermodynamically linked functions. (**b**) Formation of disulphide bond using oxidised glutathione (GSSG) as oxidant. (**c**) The folding pathway of RNase T1 from the fully-reduced and glutathione mixed-disulphide form

co- and post-translational modifications [4]. The ER lumen also contains machinery for quality control; proteins enter this compartment co-translationally, while being synthesised by ribosomes at the cytoplasmic face of the ER membrane, but only exit to distal compartments of the cell's export pathway if they are correctly folded and assembled [5, 6]. Members of the protein disulphide-isomerase (PDI) family play an essential role in oxidative folding [7, 8] and an in vitro oxidative folding system – comprising a reduced protein substrate, PDI and a suitable source of oxidising equivalents – reproduces the key features of oxidative folding in the cell in terms of rate, pathway and products (see [9] and below).

Hence, although one might question whether a 'reductionist' approach to the mechanism of oxidative protein folding is appropriate, this review will analyse the processes occurring in such an in vitro system, focussing on the catalytic and structural properties of PDI, and aiming to address the question posed in the title. Oxidative protein folding in prokaryotes takes place in the bacterial periplasm and involves members of the distinct Dsb family [10, 11]; there are instructive parallels with PDIs, but the cellular contexts and factors involved are sufficiently different to require separate treatment. So discussion of Dsb proteins will be limited and used to highlight similarities and contrasts with PDI. We will not discuss the relatively newly-discovered system of protein disulphide formation in the mitochondrial matrix, which involves very different machinery that is coupled to the mitochondrial electron transfer system [12].

As background, Sect. 2 will review what is known about the process of oxidative protein folding in vitro in the absence of enzymatic catalysis.

2 Oxidative Folding of Proteins In Vitro Demonstrates a Diversity of Pathways

The pathway of oxidative folding of proteins has been a highly controversial field, but the controversies have receded as a larger number of cases has been studied – under a wider range of conditions and with improved analytical techniques – revealing that there is no general pathway followed by all proteins under all conditions, but an interesting diversity of pathways [9, 11, 13–16]. For such studies of oxidative folding in vitro, the protein in question is fully reduced in denaturing conditions and then transferred into conditions where refolding is favoured by dilution of the denaturant in presence of a thiol/disulphide mixture at concentrations, overall redox potential and pH which facilitate rapid thiol:disulphide exchange reactions (Fig. 1b). Conditions vary, but mixes of oxidised and reduced glutathione (GSSG + GSH) or oxidised and reduced DTT (DTT_{SS} + $DTT_{(SH)2}$) are frequently used, at pH 7–8 and at temperatures from 10 to 37°C. In cases where reduced and intermediate species are highly insoluble, low concentrations of urea or guanidinium chloride may also be present to allow refolding to compete effectively with aggregation.

For detailed analysis of the oxidative folding pathway, the favoured approach is now to withdraw samples at various refolding times, quench rapidly by acidification to pH 2–3 (to inhibit all thiol:disulphide exchange processes which depend on the free thiolate $–S^-$ species), and resolve species by HPLC. Quantitative analysis of peak heights over time allows interpretation of the pathway in terms of the succession of intermediates and the kinetics of their interconversion, while preparative HPLC can be used to isolate such intermediates and define them by determining the number and position of disulphide bonds (primarily by mass spectrometry).

Two features of oxidative folding must be distinguished – the chemical formation of disulphide bonds (disulphide regeneration) and the formation of native tertiary structure (conformational folding). The methods above allow establishment of a protein's disulphide regeneration pathway and the diversity of such pathways is striking; as analysed by Chang [17] the diversity is '. . . mainly manifested in (a) the extent of heterogeneity of folding intermediates, (b) the presence or absence of predominant intermediates containing *native* disulfide bonds and (c) the level of accumulation of fully oxidised *scrambled* isomers as folding intermediates'. However this does not define at what stage(s) in the disulphide regeneration pathway conformational folding occurs; when are crucial features of the native conformation established including compactness, defined secondary structure, overall backbone topology and native tertiary structure?

Isolated intermediates can be studied to define their conformations, stabilities and functional activities (see [18–21] for early examples). In favourable cases significant structural information can be determined by multi-dimensional NMR (e.g. [22]). Where such intermediates are insufficiently stable or not available in sufficient yield for high resolution structural studies, mutants of the native protein can be generated; hence an intermediate lacking a specific disulphide bond can be modelled by expressing a double mutant protein with corresponding cysteine to

alanine or cysteine to serine mutations [23–25]. Characterisation of the conformations of intermediates in the disulphide regeneration pathway by these methods provides the key information for defining the overall pathway of oxidative folding.

2.1 *RNase Oxidative Folding Involves Isomerisation of Non-Native to Native Disulphides, Associated with Structure Formation*

The classic example of ribonuclease A, long studied by Scheraga and colleagues, is a good starting point [14, 15]. Under most conditions its oxidative folding pathway can be regarded as comprising three phases – pre-equilibration, structure formation and completion (Fig. 2a). In the first phase there are rapid formation, breakage and isomerisation of disulphide bonds to generate a mix of species containing one, two,

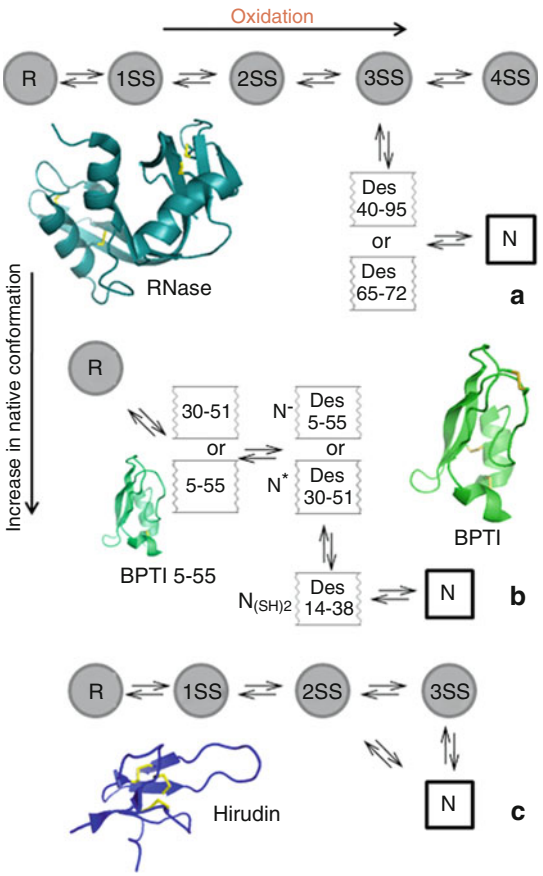

Fig. 2 Folding pathway of small disulphide-bonded proteins. Steps requiring oxidation but little formation of native fold are shown *left* to *right*. Steps involving formation of native fold but no net oxidation or reduction are shown *up* to *down*. The folding pathways shown are (**a**) RNase, (**b**) BPTI and (**c**) Hirudin. The structures shown were generated using pymol (http://www.pymol.org). PDB accession numbers: 5RSA, 2ZJX, 6PTI and 1HRT

three and four disulphide bonds. The 1SS ensemble (species containing a single disulphide) is highly heterogeneous, but not entirely random, being biased towards species containing local disulphides between near-neighbours, or 'native' disulphides [26], but there is no stable tertiary structure and all these species interconvert rapidly, representing a single 1SS kinetic ensemble. Similar ensembles of 2SS, 3SS and 4SS species form and interconvert rapidly, forming a quasi-equilibrium mixture determined by the imposed redox and other conditions; these species all contain non-native disulphide bonds, lack stable tertiary structure and all their thiol and disulphide groups are freely reactive (including in the fully-oxidised 4SS species which are termed 'scrambled').

The second phase, which is rate-determining in most conditions, is the emergence from the 3SS ensemble of defined species that contain three native disulphides and have stable native-like structure, which 'protects' these disulphides and prevents their re-equilibration with the 3SS pool. Species lacking one native disulphide are termed des-species, so des[40–95]RNase A is a species containing three of the four native disulphides but lacking the Cys40–Cys95 disulphide bond. The oxidative folding pathway of RNase under standard conditions is dominated by the slow appearance of des[40–95]RNase and des[65–72]RNase from the quasi-equilibrium mixture, by disulphide isomerisations within the 3SS ensemble. These two des-intermediates have near native conformations in which the disulphides are mainly buried (or stabilised by elements of native structure) while the free thiols are exposed [21, 25]. So, the absence of the final disulphide bond in des[40–95]RNase has minimal impact on the backbone fold, but this species is more dynamic; notably, rates of proton exchange from buried backbone amide groups are increased by 10^2- to 10^6-fold.

In the final phase of oxidative folding of RNase, the two predominant des-species convert to the fully-oxidised native protein in a simple oxidative step with little structural change. Hence, in this pathway, the key step in which native conformation is established involves the parallel formation of native disulphides from non-native disulphides by isomerisations within the pool of 3SS isomers.

2.2 *BPTI Folding Involves a Limited Set of Disulphide Intermediates in which Structure Forms at an Early Stage*

The well-studied case of bovine pancreatic trypsin inhibitor (BPTI), which contains three native disulphides, provides an interesting contrast [13, 27–29]. In this case, the 1SS ensemble is highly non-random, being dominated by a species containing only the 'native' 30–51 link, plus a small fraction of the 1SS species containing only the 'native' 5–55 link (Fig. 2b). In contrast to the unstructured and permissive situation with 1SS forms of RNase A, these species contain significant amounts of native-like structure [18, 24] which constrains the formation of a second SS bond, so that oxidation of either of these species predominantly generates the 14–38 'native' disulphide link. The products are therefore des[5–55]BPTI, (containing

the native 30–51 and 14–38 bonds) and des[30–51]BPTI (containing the native 5–55 and 14–38 bonds). These species have considerable native-like conformation and are sometimes referred to as N′ and N* respectively. Indeed the C30A/C51A mutant of BPTI, an analogue of des[30–51]-BPTI (i.e. N*), has been crystallised and its structure determined to high resolution [23]; the rms difference between its structure and that of wild-type BPTI is as small as that between BPTI structures determined from different crystal forms.

Unlike in the des species of the RNAse A pathway, the remaining free thiol groups in these des-BPTI folding intermediates are buried and unreactive, so that significant unfolding would be required to allow them to react and form the final disulphide. As a result, these des-species are long-lived and cannot directly generate the native fully-oxidised protein; the rate-determining step in the pathway is the isomerisation of these species to generate des[14–38]BPTI, sometimes termed ($N_{(SH)2}$), which resembles the structured des species on the RNase pathway in having fully native-like conformation with buried native disulphides (30–51 and 5–55) and the free thiols of Cys14 and Cys38 exposed at its surface. It should be noted that this direct conversion of one des-species of BPTI to another is an isomerisation, not a reduction to a 1SS state followed by a reoxidation; its mechanism must involve attack by a free thiol of the protein on the 14–38 disulphide bond, breaking this bond and forming a transient intermediate containing a non-native disulphide. Thus although the main intermediates on the BPTI pathway contain only 'native' disulphide bonds, the formation of non-native disulphides and their isomerisation to native disulphides is critical in this pathway, as it is in that of RNase A.

As a radical alternative, the oxidative folding of BPTI has been studied using H_2O_2 as oxidant. This small uncharged reagent can penetrate to buried sites in proteins, and, as a result, this reagent rapidly oxidises the long-lived des-intermediates in the BPTI refolding pathway. Since H_2O_2 is generated by thiol oxidases in the ER, its oxidative activity may be physiologically significant [30].

2.3 Diversity of Pathways and Intermediates

In both RNase A and BPTI, the formation of native conformation is associated with the generation of specific folded des-species, i.e. folding precedes the formation of the final disulphide bond. However, this is not a universal feature. In the case of the leech blood clotting inhibitor, hirudin, which contains three disulphides, the first phase of folding is similar to that of RNase A, the establishment of a quasi-equilibrium mix of unstructured 1SS, 2SS and 3SS species (Fig. 2c), but the next (and final) step is the simultaneous formation of the native conformation and native set of disulphide bonds by oxidation or isomerisation of unstructured species in the 2SS and 3SS ensembles respectively [31].

The diversity of pathways is further emphasised by the cases of α-lactalbumin and lysozyme. α-Lactalbumin is a 4SS Ca^{2+} binding protein whose oxidative folding has been studied both in absence and presence of Ca^{2+} [17]. In absence of Ca^{2+}, the

folding pathway resembles that of hirudin with a highly heterogeneous population of intermediates, including fully oxidised 'scrambled' species; here, native conformation only forms in association with the regeneration of the fourth and final native disulphide bond. However, in presence of Ca^{2+}, one of the 2SS intermediates is stabilised in a native-like conformation by binding a Ca^{2+} ion, and this stable partly-structured intermediate constrains the remainder of the folding pathway, so that under these conditions the pathway resembles that of BPTI, exhibiting a limited number of intermediates containing mostly native disulphide bonds.

Oxidative folding of lysozyme is complicated by the presence of alternative folding pathways, and the insolubility of intermediates, so that effective refolding only occurs in 2 M urea [22] or 0.5 M guanidinium chloride [32]. However, the pathways have been established, and – in the slow refolding pathway – the species des[76–94]lysozyme has been identified as a key structured intermediate in which the free thiol of Cys94 is buried; its conversion to the final native product is slow since it requires a local unfolding to expose this buried residue [22].

These and other examples of oxidative refolding pathways are discussed extensively elsewhere [11, 16]. The clear message is that pathways are diverse and involve both disulphide formation and isomerisation steps. The crucial conformational folding steps are linked to formation of a key 'native' disulphide and many pathways involve partly-folded intermediates which require some degree of unfolding in order for the overall oxidative folding process to proceed to completion.

Disulphide regeneration has been discussed above simply in terms of free thiol (protein–SH) groups, and disulphides (–SS–), but where the reoxidation conditions include a 'redox buffer' comprising a monothiol and its disulphide (e.g. reduced and oxidised glutathione, GS^- + GSSG), the system will also contain mixed disulphides between the protein and reagent (protein–SSG). The net formation of a protein disulphide in such conditions passes via mixed disulphide intermediates (Fig. 1b) and the crucial step to form a protein disulphide is intramolecular.

$$\text{Protein}^{\text{S}^-}_{\text{SSG}} \rightarrow \text{Protein SS} + \text{GS}^-$$

Glutathione is present at high levels within the ER lumen (5–10 mM), so this issue is relevant to the situation in vivo. This feature is generally ignored, but the role of such intermediates was explored in the oxidative refolding of ribonuclease T_1, a protein containing two native disulphides [33]. This system showed rapid formation of species containing one disulphide and two free thiols (1SS,$2S^-$) and then appearance of mono- and di-glutathionylated derivatives, (1SS,$1S^-$,1SSG) and (1SS,2SSG), which formed a quasi-equilibrium mixture that slowly converted to the native (2SS) material. Interestingly, the same quasi-equilibrium mix of 1SS species was formed if refolding was initiated from fully unfolded and glutathionylated (4SSG) starting material (Fig. 1c). Parallel studies by intrinsic fluorescence indicated some formation of structure at an early stage, but native-like fluorescence and enzyme activity only appeared concomitant with the formation of the final 2SS species [33, 34]. This work, and studies exploring the role of glutathione

concentrations in the folding of BPTI [28, 35], emphasise that defining ensembles of disulphide regeneration intermediates simply in terms of the number of intramolecular protein SS groups present understates their complexity.

3 Catalysis of Oxidative Folding In Vitro by PDI

An enzyme capable of catalysing oxidative protein folding was first detected in the early 1960s [36, 37]. Early work showed that its key action on refolding of RNase was in catalysing disulphide isomerisation rather than net oxidation [38] and hence the enzyme was subsequently named as PDI. Indirect evidence for the cellular function of PDI in assisting oxidative folding of newly synthesised proteins came from its cellular and sub-cellular location and its expression pattern over time [39]; later cross-linking and reconstitution studies, plus genetic studies in *Saccharomyces cerevisiae*, confirmed its essential role in the formation of native disulphide bonds [40]. This section focuses on the action of PDI as a catalyst of defined oxidative folding pathways of proteins; the structure of PDI and the molecular detail of its interactions are discussed in a later section.

3.1 Pathway and Kinetics of PDI-Catalysed Oxidative Folding

The first study of PDI's action on a defined oxidative folding pathway [41] indicated that it was a true catalyst of oxidative protein folding of BPTI; the intermediates in the pathway were not significantly altered but the enzyme increased the rates of every step involving both protein conformational change and disulphide oxidoreduction or isomerisation. Hence PDI catalyses steps in which disulphide interchange and conformational change are coupled. Subsequent work on BPTI and a wide range of other substrates has confirmed and elaborated this conclusion.

Working in conditions intended to mimic those within the ER (pH 7.4, GSH 2 mM, GSSG 0.5 mM), Creighton et al. [42] demonstrated very significant catalysis by PDI of oxidative refolding of BPTI. Initial oxidation of fully reduced BPTI was significantly accelerated, indicating that PDI catalyses disulphide formation in unstructured protein substrates; this was confirmed by studies on a simple 28-residue unstructured peptide containing cysteine residues at positions 2 and 27 [43]. In this model system, all the steps involved in oxidation of the peptide by GSSG were catalysed by PDI, including the key intramolecular step in which the two cysteine residues at opposite ends of the peptide come together to form a disulphide ($P^{S-}_{SSG} \rightarrow P(SS) + GS^-$). However, catalysis was even more marked at later stages of the BPTI oxidative folding pathway; the major 2SS intermediates des[5–55] (N′) and des[30–51](N*) appeared and disappeared more rapidly in presence of PDI (Fig. 3) and 80% of starting material was converted to native

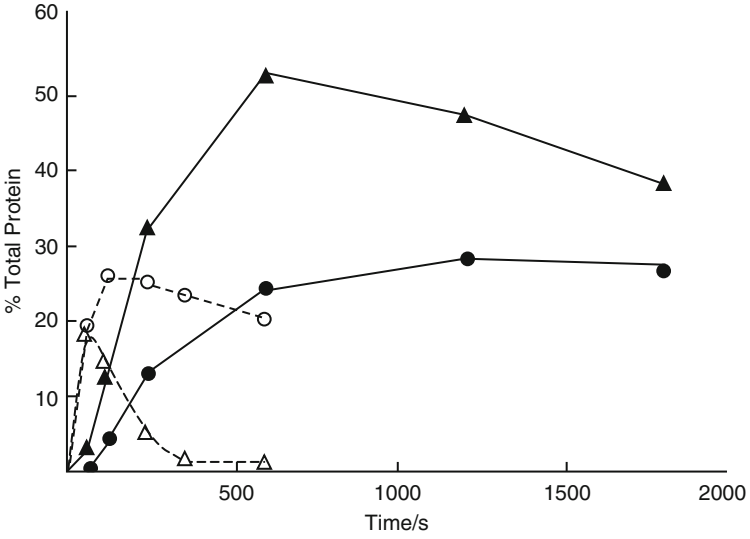

Fig. 3 Catalysis of BPTI folding by PDI. Accumulation of intermediates, N′ (des[5–55]) (*triangles*) and N* (des[30–51]) (*circles*), during folding of reduced BPTI using 0.5 mM GSSG and 2 mM GSH at pH 7.4 in the presence and absence of 1.6 μM PDI (*open and filled symbols* respectively). Adapted from [42], Fig. 9

BPTI within 10 min (with a half-time of ~2 min) whereas, in absence of PDI, only ~10% regeneration of native BPTI occurred over 30 min [42]. Weissman and Kim [44] elaborated this result by isolating the dominant 2SS intermediates and studying their conversion to native BPTI, in absence and presence of PDI (Fig. 4). For both major intermediates, this requires rate-determining SS isomerisation in highly structured 2SS species [des[5–55] → des[14–38] (N′ → $N_{(SH)2}$) and des[30–51] → des[14–38] (N* → $N_{(SH)2}$) respectively] and the accelerations by PDI are >1,000-fold in each case. Under these conditions, the final step of the oxidative folding pathway [des[14–38] → N ($N_{(SH)2}$ → N)], which involves net oxidation to form the 14–38 disulphide, but little conformational change, is quite rapid and was only slightly accelerated by PDI.

Comparable studies have now been carried out to analyse the effects of PDI on oxidative refolding of RNase A at 25 and 37°C [45]. The results indicate that PDI catalyses all steps involving disulphide oxidation, reduction or rearrangement and that addition of PDI results in net catalysis of the entire oxidative refolding process without altering the major parallel pathways involving the formation of two native-like 3SS intermediates des[65–72] and des[40–95]RNase. Hence, under these conditions, PDI does not create any additional pathways or eliminate either of the two major parallel pathways. Further insight has followed from studies on oxidative refolding of RNase at lower temperature. The uncatalysed oxidative refolding pathway of RNase at 15°C resembles that at higher temperatures, but two additional structured 3SS species – des[58–110] and des[26–84] – are

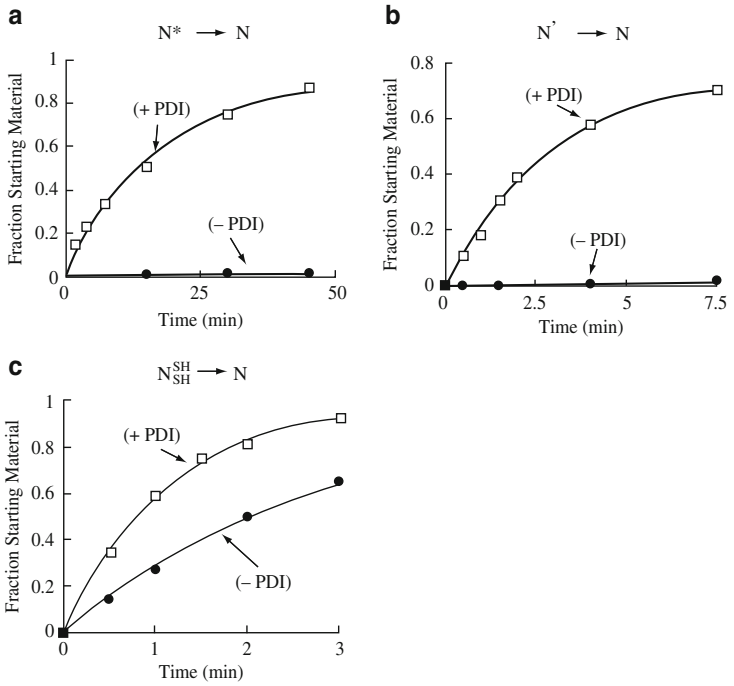

Fig. 4 Effect of PDI on conversion of BPTI des species to native protein. The three des species N′ (des[5–55]), N* (des[30–51]) and $N_{(SH)2}$ (des[14–38]) were isolated and allowed to fold in the presence and absence of PDI (7 μM) at pH 7.2, 0.5 mM GSSG and 2 mM GSH. Figure 2 from [44]

generated and accumulate. As at the higher temperature, the rate-determining step in the pathway is the conversion of the unstructured 3SS ensemble to specific structured des-species but, at this lower temperature, all four possible des–species are formed and two of them are kinetically-trapped and do not convert readily to the native fully-oxidised protein. In presence of PDI at 15°C, these trapped species are rapidly converted back to a mixture of unstructured 3SS intermediates which then progress to the native state via the normal predominant des-species [46]. PDI catalysis of these re-shuffling steps is therefore comparable to its effects on N* and N′ in the BPTI oxidative refolding pathway.

A further example is provided by lysozyme where PDI has been shown to increase dramatically both yield and rate of oxidative refolding [47] (Fig. 5). Despite the significant catalysis of the overall process, the pathway of oxidative folding is not significantly affected by PDI because PDI effectively catalyses conversion of the major des[76–94] intermediate to native lysozyme. As noted above, this species is highly native-like in structure, with the thiol group of Cys94 buried and inaccessible, so that formation of the final 76–94 bond can only occur in association with significant unfolding. Hence, in this pathway, PDI assists the key step by catalysing disulphide formation that is associated with transient unfolding

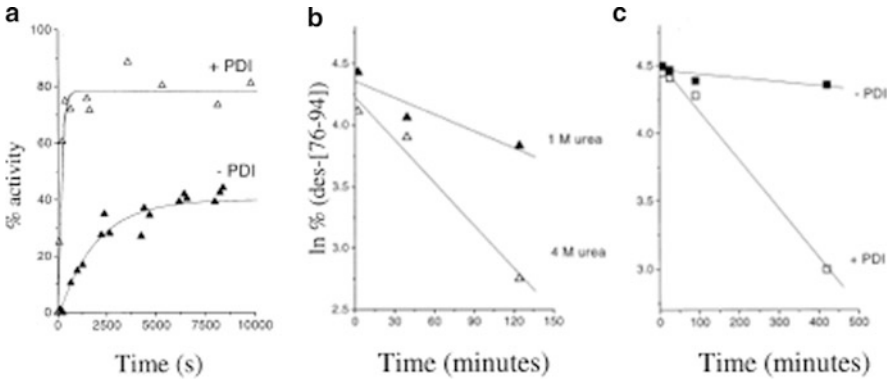

Fig. 5 Effect of PDI on folding of lysozyme. (**a**) Refolding of 6 μM lysozyme in 1 M urea with and without 2 μM PDI (pH 7.4) determined by recovery of activity. (**b**) Rearrangement of 55 μM des[76–94] at pH 8.5 in the presence of 1 and 4 M urea and absence of GSH/GSSG. (**c**) Effect of PDI on oxidation of des[76–94] (55 μM) at pH 7.4 in the presence of 1 M urea, 2.0 mM GSH and 0.4 mM GSSG adapted from [47]

of the structured protein substrate; this interpretation is confirmed dramatically by the observation that in absence of PDI this conversion occurs at a higher rate in 4 M urea than in 1 M urea!

3.2 Oxidative Refolding Catalysed by Bacterial Dsb Proteins

In bacteria, as in eukaryotes, disulphide bonds are infrequent in cytoplasmic proteins but they are found in secreted bacterial proteins and in proteins located in the periplasm. Genetic analysis of the pathway of formation of these disulphides identified several genes whose products are a structurally diverse group of proteins named DsbA, DsbB, etc. according to the gene encoding them. DsbA, DsbB and DsbC have been well-characterised in structural and functional terms [10, 11].

DsbA contains a disulphide group at its active site and is a strong disulphide oxidant (Table 1); it readily oxidises model peptides and a wide range of reduced proteins. DsbA was originally assumed to be functionally equivalent to PDI, but is actually rather different; it is a very effective oxidant of reduced BPTI but very ineffective in generating native BPTI because it does not catalyse the isomerisations of the various des-species on the BPTI oxidative folding pathway nor isomerisations in other oxidative folding pathways [53, 54]. This clear difference between DsbA and PDI is also apparent in their actions on the simple 28-residue peptide substrate mentioned above; PDI was 10- to 20-fold more effective than DsbA in catalysing the intramolecular step leading to the formation of the disulphide bond between cysteine residues at either end of the peptide [55].

When recombinant mammalian proteins are expressed in bacteria and targeted for export to the periplasm, their oxidative folding is generally not efficient [56, 57].

Table 1 Redox potential of selected redox pairs

	Redox potential (mV)	References
O_2/H_2O	820	
DsbA, wt (CPHC)	−122	[48]
DsbA, mutant (CGHC)	−143	[48]
PDI, wt (CGHC)	−175	[49]
Unfolded protein	App −220	For references see [50]
Trx, mutant (CGHC)	−235	[51, 52]
GSH/GSSG	−240	
Trx, wt (CGPC)	−270	[51]

Trx thioredoxin

Most authentic bacterial disulphide-bonded proteins contain only one or few disulphides and lack the complex disulphide bonding patterns found in eukaryotic proteins. This, together with DsbA's lack of isomerase activity, has prompted the suggestion that DsbA can catalyse formation of the native set of disulphide bonds only in proteins where the disulphides link consecutive cysteine residues; in such cases, formation of the native bonds would occur directly in co-translational folding. Examples both supporting and contradicting this proposal have been cited [58, 59]. However, even for authentic bacterial protein substrates, oxidation by DsbA is frequently insufficient to generate the native set of disulphides; periplasmic isomerase activity is required and is provided by the DsbC and DsbG proteins. DsbC has catalytic activity in the overall oxidative refolding of BPTI and in the crucial isomerisations of the kinetically-trapped des-intermediates, but does not catalyse the oxidation of fully-reduced BPTI in these conditions [60]. DsbC also stimulates formation of native oxidised RNase A in a DsbA- and DsbB-dependent reconstituted system [54]. Hence the bacterial system differs from that in eukaryotes in its separation of oxidoreductase and isomerase functions between different proteins [10, 11], whereas these functions are found together in eukaryotic PDIs.

3.3 Peptide Binding and Chaperone Activity of PDI: Partial Reactions of Oxidative Folding?

In the light of the evidence that PDI can catalyse disulphide isomerisations which involve transient unfolding of highly-structured kinetically-trapped intermediates, one would assume that PDI can interact with and stabilise the transition states of such reactions, possibly by binding to regions of unfolded peptide. This capability was explored by using short unstructured peptides as models of unfolded regions in proteins [61–63]. Several peptides (lacking cysteine residues) bound to purified PDI and this binding, monitored by cross-linking of radio-labelled peptides, was saturable, required native PDI and was inhibited by unlabelled peptides or by 'scrambled' RNase but not by native RNase, implying that the peptide binding under study was

a specific interaction at the site at which PDI binds non-covalently to its protein substrates. Conversely, binding of scrambled RNase was observed directly and was inhibited by the presence of peptides. In ER-derived vesicles from mammalian pancreas, this binding of peptides was specific for PDI and for a closely-related, pancreas-specific homologue of PDI termed PDIp; no other ER chaperones had comparable affinities [62]. Further work on this system established that peptide binding by PDIp is highly specific for peptides containing tyrosine or tryptophan residues while that by PDI shows less clear-cut sequence specificity [64].

The ability of PDI to bind unfolded peptides and polypeptides is also demonstrated by its activity towards non-disulphide-containing proteins in conventional chaperone assays. Wang's group showed that PDI suppresses aggregation and increases yield of active enzyme when rhodanese or glyceraldehyde-3-phosphate dehydrogenase are refolded by rapid dilution of denaturant; PDI also suppresses aggregation of rhodanese during thermal aggregation [65, 66]. These are not secretory proteins and hence this is clearly not a physiological activity, but a model for exploring properties of PDI. The activities are not 'enzymic' in that PDI did not enhance rates of folding and did not increase yields of refolding when present in 'catalytic', sub-stoichiometric quantities. Rather, with these protein substrates and many others, PDI resembles conventional molecular chaperones in that it enhances yield of folding and suppresses misfolding, but only when present in substantial molecular excess. The action therefore appears to be one of binding unfolded or misfolded substrates, reducing their free concentrations and hence preventing their aggregation or irreversible misfolding.

This action, even in absence of an enzymic role, may be significant in vivo. PDI interacts with the C-terminal region of monomeric procollagen chains during the assembly of trimeric procollagen in cells; the interaction does not depend on the presence of cysteine residues in this region, implying that PDI is acting as a chaperone in this context [67, 68]. The chaperone activity of PDI is probably also expressed in the remarkable fact that PDI acts as a permanent structural subunit of two ER-located enzymes, prolyl-4-hydroxylase (P4H) and triglyceride transfer protein (MTP) [69, 70]. Prolyl-4-hydroxylase is an $\alpha_2\beta_2$ tetramer in which the β chains are PDI molecules and the α chains are members of a wider Fe^{2+}- and α-keto-glutarate-dependent hydroxylase family. The sites required for substrate (collagen) binding and for hydroxylation activity are within the α subunits, but these subunits are insoluble when expressed in isolation. To generate active enzyme requires co-expression of both subunits (or major fragments of both subunits) and it has been difficult to achieve this in convenient recombinant systems. The microsomal triglyceride transfer protein is an αβ heterodimer of which the β subunit is PDI while the α subunit is a 97kDa polypeptide related to the egg-yolk lipid-binding protein, lipovitellin. So both these enzymes contain PDI plus another polypeptide with the major functional sites associated with the non-PDI component; nevertheless, PDI is not a passive component, being essential for the assembly of functional activity [71]. These observations suggest that, in these enzymes, PDI acts as a chaperone which then remains stably associated with its substrate.

3.4 *Oxidative Refolding In Vitro in Presence of PDI as a Model for Oxidative Folding in the Cell*

In presence of PDI under optimal conditions, oxidative refolding of BPTI, RNase A and others (e.g. hirudin [17]) occurs with a half-time of 30–150 s which is consistent with the rate at which some nascent proteins achieve the native fully-oxidised state in vivo. These simple model systems do not fully reflect the complexity of the situation in vivo of course, but this similarity in rate suggests that catalysis by PDI is the key factor ensuring rapid oxidative folding in vivo.

An attempt to examine oxidative folding in a defined but more complex system, was made in a comparative study of BPTI oxidative folding in presence of mammalian PDI or of the complete set of soluble protein contained in the ER lumen of cultured mouse cells [72]. The activity of the ER luminal content was exactly what would have been predicted from its content of PDI, implying that no other luminal proteins contributed significantly to oxidative folding activity.

A further issue in reconstituting oxidative folding is the source of oxidising equivalents. In most of the studies above, net oxidative capacity was provided by a 'redox buffer' comprising both oxidised and reduced forms of glutathione (GSSG + GSH), the major thiol and disulphide components of the ER lumen; conventionally these redox components are present at 0.5–5 mM and with GSH in a 2- to 5-fold excess, similar to the conditions found in the ER environment [73–75]. However, oxidising equivalents within the ER are ultimately derived from molecular oxygen via Ero1, a flavin-dependent oxidase located in the ER membrane (Ero1p in yeast, Ero1α and Ero1β in higher eukaryotes) [76, 77]. In the absence of glutathione components, oxidative refolding of reduced RNase with stoichiometric consumption of O_2 was reconstituted by in vitro systems comprising PDI + Ero1, initially using yeast enzymes [78, 79] and subsequently human enzymes [80]. In these systems, as in the cell, PDI is absolutely required for oxidative folding, the flow of oxidising equivalents is from Ero1 to PDI to protein substrate, there is no direct interaction between Ero1 and substrate and the role of Ero1 is to recycle reduced PDI. Half-times for recovery of native RNase were in the range 5–10 min, but these studies did not optimise kinetics or study the pathway of oxidative folding. However, these reconstituted systems showed a lag in recovery of RNase activity, as observed for the simpler in vitro systems, presumably corresponding to the 'pre-equilibration' and 'structure-formation' phases of the RNase oxidative folding pathway described above. Hence, despite the different origin of the oxidising equivalents, the features of PDI-catalysed oxidative folding in these O_2- and Ero1-dependent systems are very similar to those in conventional in vitro refolding systems.

A more realistic system for monitoring oxidative folding in the cell is provided by translating mRNAs in presence of ER-derived vesicles in a reducing environment, and then switching to oxidative conditions; the translation products translocate into the interior of the vesicles co-translationally and then undergo oxidative folding post-translationally [42, 81, 82]. In the case of BPTI, translation of mRNA

encoding the natural precursor, prepro-BPTI in such conditions, led to cleavage of the pre-sequence and accumulation of reduced proBPTI in the vesicles; on addition of excess GSSG, this was converted efficiently to native oxidised product with a $t_{1/2}$ of 1–2 min [42]. The kinetics and pathway observed in this system are very similar to that observed for oxidation of reduced pro-BPTI in presence only of PDI and a GSSG + GSH redox buffer.

A similar situation can be set up by treating whole living cells with agents which rapidly reduce or oxidise the ER luminal content. When secretory proteins are biosynthesised and labelled in cells in the presence of DTT, the products are retained in the ER in the reduced state and their oxidative folding is blocked; the block can be removed and oxidative folding initiated in a cellular environment through removal of the DTT by washing or by addition of excess oxidant [83]. Although the model proteins that have dominated in vitro folding work have not been studied in these cellular systems, work with a wide range of other proteins has led to similar overall conclusions. Thus minimum half-times for oxidative folding in this cellular situation are of the order of 2–5 min and proteins undergo defined oxidative folding pathways [77, 83, 84]. Crucially, these pathways involve species with non-native disulphide bonds as significant intermediates, and similar intermediates are also observed in newly synthesised proteins in unperturbed whole cell systems where folding is coupled to translation [5, 84, 85].

Hence none of these more complex systems suggests there are crucial differences between the process in the cell and that in the simpler PDI-catalysed model systems considered above (Sect. 3.1) in terms of the mechanism and pathway of oxidative folding experienced by the substrate protein.

4 Molecular Analysis of Human PDI and Homologues

Early chemical modification and inhibition studies implied that the active site(s) of PDI involved reactive thiol or dithiol group(s) capable of forming covalent disulphide bonds with substrate proteins (Fig. 6), but structural and mechanistic analysis was transformed by the cloning and sequencing of (rat) PDI [86]. This revealed an approximately repetitive pattern in the PDI amino-acid sequence (a–b–b′–a′) with each repeating unit corresponding to roughly 100 residues. Subsequent work has confirmed that each of these regions corresponds to a structural domain.

4.1 Structure of the Thioredoxin-Like Domains

High resolution structures have been solved of all four domains of human PDI individually and of the human **bb′** domains as a pair (PDB accession numbers: 1MEK, 2BJX, 3BJ5, 1X5C and 2K18). These show that PDI contains two domains, **a** and **a′** that closely resemble thioredoxin, with redox-active CGHC active sites, as

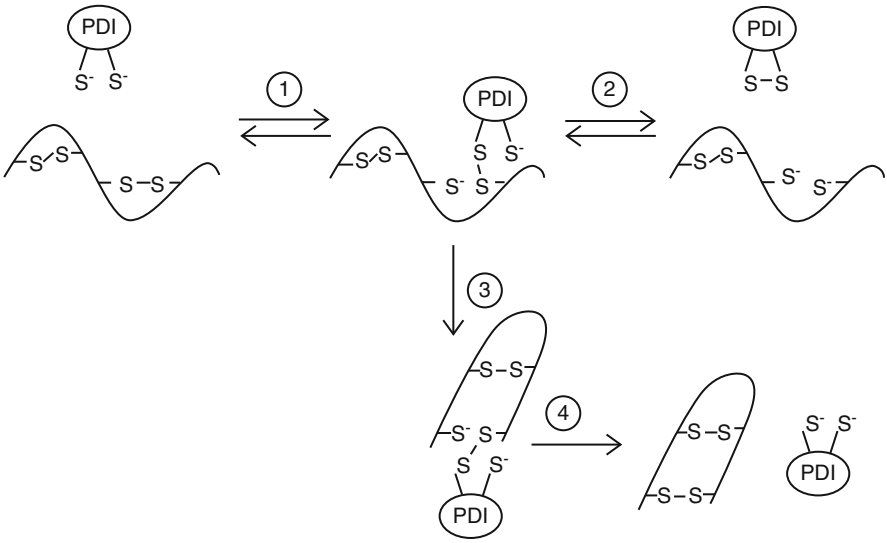

Fig. 6 Disulphide reactions catalysed by PDI. For simplicity only one active site of PDI is shown. (*1*) The N-terminal cysteine of the reduced active site performs a nucleophile attack on a disulphide bond resulting in a mixed disulphide. (*2*) The C-terminal cysteine then reacts with the mixed disulphide resulting in an oxidised active site and reduced substrate. If the same reactions run from right to left starting with an oxidised active site then the substrate is oxidised. (*3*) Once a mixed disulphide is formed the free cysteines created can participate in isomerisation reactions. (*4*) A free cysteine attacks the mixed disulphide resulting in PDI being released with a reduced active site. The disulphides in the substrate have undergone isomerisation. The figure is not drawn to scale; in the case of small disulphide bonded proteins such as discussed in Sect. 2, PDI is much bigger than substrate and the protein would fit within the 'U' of PDI

well as two domains, **b** and **b′** that have the same overall conformation (the thioredoxin fold) but lack redox active sites. The overall domain organisation of PDI is **a**–**b**–**b′**–**x**–**a′**–**c**, where **x** is a 19 residue linker between domains and **c** is a very negatively charged extension. Up to 20 other members of the PDI family have been identified in humans and other vertebrates and 5 more remote relatives of human PDI have been identified in yeast. All family members contain various combinations of **a**-type and **b**-type thioredoxin-like domains (plus other domains in some cases).

The core thioredoxin fold is a mixed α/β fold, where the secondary structure elements are organised βαβαββα [87]. This basic fold has been adapted in a number of ways in different proteins, so that occasionally an α helix is missing or extra secondary structural elements are present. In thioredoxin itself and the PDI domains, there is an extra β strand and α helix prior to the core thioredoxin fold, hence the arrangement of elements is: $\beta_1\alpha_1\beta_2\alpha_2\beta_3\alpha_3\beta_4\beta_5\alpha_4$ (Fig. 7). The β strands form a central β sheet, where β_4 is antiparallel to the other strands. The helices α_1 and α_3 pack onto one side of the β sheet and α_2 is placed on the other side forming an αβα sandwich. Although the fold is conserved, the sequence homology

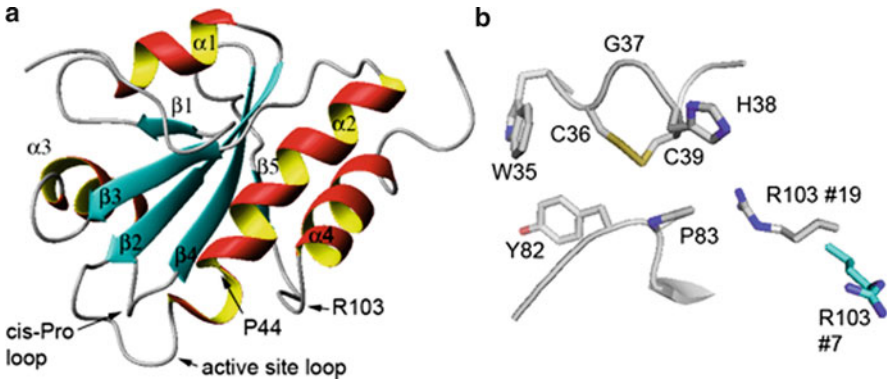

Fig. 7 Structure of domain **a** and its active site. (**a**) The thioredoxin fold. The secondary structure of PDI **a** is shown (pdb 1MEK). (**b**) The active site of PDI **a**. The active site WCGHC sequence is shown as well as the *cis*-Pro loop (Tyr82, Pro83). Arg103 which modifies the pK_a of the C-terminal cysteine residue by moving close to and away from the active site is shown in two conformations (1MEK structure #7 and #19 out of 40 deposited NMR structures) to illustrate how mobile it is. The structures shown were generated using pymol (http://www.pymol.org)

between thioredoxin domains is low and type **b** domains are not easily predicted based on sequence alignment.

The active site (CXXC) is located in the loop immediately prior to and extending into the N-terminal part of α_2. In the **a** and **a′** domains, this α helix contains a conserved proline residue resulting in a kink (Fig. 7a). Another conserved proline is present in the loop immediately before β_4. This proline is in the *cis* configuration (*cis*-Pro) and although distant in the primary sequence it is adjacent to the active site in the structure (Fig. 7). Mutation of the *cis*-Pro in DsbA to an alanine residue, which adopts a *trans* configuration, results in a significant destabilisation of the protein and loss of catalytic activity [88]. The equivalent P → A mutation in yeast PDI abolishes catalytic activity [89]. The presence of the *cis*-Pro has also been suggested to reduce the risk of the active site cysteine residues ligating metal ions [90].

None of these features are conserved in the type **b** domains, which despite retaining the thioredoxin fold show little sequence homology with the type **a** domains and each other. The structure of the **b** domain shows that all of these features are missing, including the *cis*-Pro before β_4 [91]. In the **b′** domain, the *cis*-Pro is retained (although the reason for this is not clear) but all of the other above-mentioned features of the catalytic domains are missing. The **b′** domain shows an extended hydrophobic surface which constitutes the main substrate binding site for PDI (for more detail see Sect. 4.3).

4.2 The Thioredoxin-Like Active Site

The active site sequences CGHC of PDI (Fig. 7b) are very similar to those of thioredoxin (CGPC) and DsbA (CPHC) [92] and a range of other proteins involved

in thiol chemistry. Recognition of the relationship between all these proteins provides valuable comparators and allows insight into the whole family from studies on one protein. The ability of the various proteins containing this active site motif to catalyse oxidation, reduction or isomerisation depends on kinetic factors and thermodynamic parameters, particularly the standard redox potential of the dithiol/disulphide pair formed by the neighbouring cysteines. Hence the environment surrounding these cysteines is of great importance, particularly the electrostatic environment which influences thiol/thiolate ($-SH/S^-$) equilibria.

In a protein where the pK_a of the N-terminal cysteine residue of the pair is very low, such as DsbA (pK_a 3.3–3.5 [48, 93, 94]) the dithiolate state is favoured, generating a highly oxidising disulphide group. In contrast, the pK_a of the N-terminal cysteine residue in thioredoxin is 6.3–7.1 [95, 96], favouring the disulphide form and generating a highly reducing dithiol site. A major determinant of the dithiol/disulphide redox potential in these proteins is the two amino acids between the cysteines which influence the redox potential by electrostatic interactions that modify the pK_a of the N-terminal cysteine and by steric effects that directly modify the stability of the disulphide bond. Mutation of these residues does indeed dramatically change the redox potential. Changing the active site of thioredoxin to resemble that of PDI (CGPC → CGHC) increases the redox potential of thioredoxin by 35 mV (Table 1) and enhances by 100-fold the ability of thioredoxin to fold reduced or scrambled RNAse [51, 52]. This mutant thioredoxin is also able to complement yeast strains deficient in *PDI1*a (whereas complementation with wild-type thioredoxin does not rescue this strain), indicating that a reactive thiol group capable of catalysing isomerisation is essential for correct disulphide bond formation in vivo [97]. Recent determinations of the active site redox potentials in PDI show that in wild-type full-length human PDI the potentials of the redox sites in the **a** and **a**′ domains are very similar (−163 and −169 mV respectively) and that each can be converted to a much more reducing potential (−229 and −226 mV respectively) by the mutation CGHC → CGPC that modifies the sites to resemble thioredoxin [98].

Conversely, mutating the active site of DsbA to resemble that of PDI (CPHC → CGHC) lowers the reduction potential of the active site and increases the pK_a of the N-terminal cysteine [48]. This study also surprisingly showed that the nature of the dipeptide between the active site cysteines dramatically influences the overall thermodynamic stability of the thioredoxin domain despite the residues being surface exposed and the mutants causing no major structural changes. In general most of the changes to the redox potential in DsbA active site mutants can be explained by changes in the pK_a of the N-terminal cysteine, i.e. the higher the pK_a the lower the redox potential [48, 94]. However this is not the case when comparing wild type and mutants of thioredoxin [99] nor when comparing DsbA and thioredoxin with PDI; changing the active site to that resembling PDI shifts the redox potential in the right direction but not all the way. Hence it is clear that other factors are also important. Recently it was discovered that the residue preceding the conserved *cis*-Pro also appears to be of great importance for catalytic activity. Mutations in DsbA and thioredoxin have shown that the nature of this residue

influences the redox potential of the active site cysteines dramatically and the effect is additive to changes in the CXXC motif (see above) [100]. This residue is also very important for the interaction of thioredoxin and DsbA with both up- and downstream partner proteins [100]. In PDI there has been no study of this residue but it is generally an aromatic residue (phenylalanine or tyrosine) which forms part of the hydrophobic patch surrounding the active sites in domains **a** and **a′** (Fig. 7b). The conserved tryptophan immediately before the active site is also part of this hydrophobic patch and believed to be involved in the interaction of substrate with the active site. The tryptophan is clearly important for the ability of yeast PDI to refold RNase. Mutation of this tryptophan to glutamate or lysine simultaneously in **a** and **a′** leads to loss of >50% of the activity [89] in agreement with earlier mutation studies of the equivalent residue in thioredoxin which showed that other aromatic residues were tolerated but not alanine [101].

As described above, the role of the N-terminal cysteine residues is relatively easy to rationalise. This is in contrast to the role of the C-terminal cysteines. An active site where the C-terminal cysteine is mutated (→CxxS or CxxA) can function perfectly well as an isomerase [102] and this is indeed the active site found in Erp44, a member of the mammalian PDI superfamily believed to be involved in retaining partially folded proteins in the ER during stress [103]. However, without a C-terminal cysteine, it is possible for the substrate protein to be trapped in unproductive mixed disulphides, whereas a C-terminal cysteine could react with the mixed disulphide, generating an oxidised active site and releasing the substrate (the so-called escape route). Too low a pK_a for this C-terminal cysteine will cause this reaction to be too rapid, abbreviating the lifetime of mixed disulphides and not allowing the time necessary for isomerisation, resulting in reduction becoming the favoured reaction. To overcome these apparently conflicting demands, PDI possesses the ability to manipulate the pK_a of the C-terminal cysteines during catalysis [104]. This is achieved via motion of a highly-conserved surface-exposed arginine residue (R103 in PDI domain **a**) which is present in the loop between β_5 and α_4. A close inspection of the NMR structure of the PDI domain **a** showed that the distance from the guanidino group to the active site is highly variable (5.9–20.3 Å) [105] (Fig. 7b). When in close proximity to the active site, the arginine is thought to influence the pK_a values of the active site C-terminal cysteine residue, making it far more reactive. Hence PDI mutated in this residue is impaired in its ability to catalyse disulphide bond formation and reduction, but is more efficient in isomerisation, which does not require the C-terminal cysteine residue [104].

4.3 Activities of Isolated Domains

Much of our understanding of the activity of PDI comes from a reductionist approach where the functions of individual domains and shortened constructs have been determined. The **a** and **a′** domains, containing the active sites, have very similar reactivity, although the **a′** domain is considerably less stable particularly in its

oxidised state. These isolated domains can oxidise a reduced peptide or reduced BPTI [106] but unlike PDI they show low ability to introduce a disulphide bond into a partially folded protein and their catalysis of disulphide isomerisation is very impaired when compared to full-length PDI [106, 107]. Similar results have been obtained using RNAse instead of BPTI as a substrate [108]. Likewise isolated domain **a** is impaired in the insulin reduction assay [109].

The isolated **b** and **b′** domains have no catalytic activity. However the **b′** domain has been shown to bind radioactively labelled hydrophobic peptides in a cross-linking assay [63]. These peptides mimic the binding of unfolded proteins and indeed the **b′** domain is essential for PDI's ability to bind substrates (see Sect. 3.3 above). However, binding of larger peptides or entire proteins requires the presence of neighbouring domains too and hence **b′** forms the core of an extended binding site involving several domains [110]. Recently, the core binding site in **b′** has been identified by observing chemical shift changes in NMR titration experiments [111, 112]. The majority of the residues involved in this binding site are in the core β sheet that forms the bottom of the binding site, as well as in α_1 and α_3 which border the site (Fig. 8).

Although the main binding site is situated in the **b′** domain, it appears that the **a′** domain is essential and sufficient to suppress the formation of α-synuclein fibres in in vitro assays [113]. The fibre formation does not involve any thiol chemistry and hence must be a result of interaction of the misfolded protein with PDI a process that would usually require interaction with the **b′** domain. The involvement of **a′** in substrate binding was also suggested by a recent NMR study that looked at the binding of the peptide mastoparan to PDI from the fungus *Humicola insolens*, which showed that binding involved a continuous hydrophobic patch over the **b′** and **a′** domains [114].

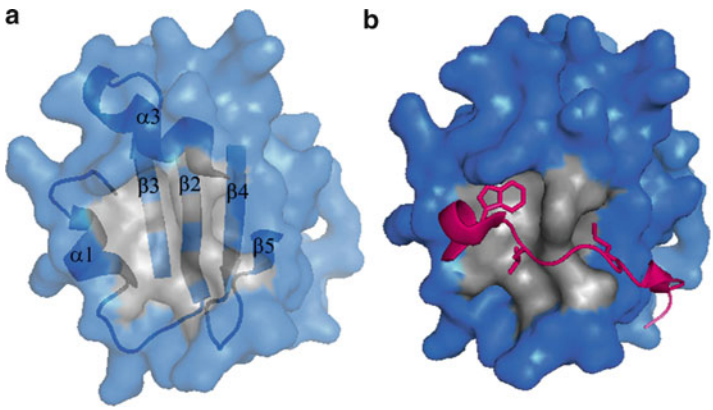

Fig. 8 The substrate binding site of PDI **b′** (pdb reference 3BJ5). (**a**) The structure has a hydrophobic binding site on one face of the domain. Residues contributing to this site (*grey*) are placed in the central β sheet as well as helix 1 and 3, shown in *cartoon representation* (**b**). The x linker (*pink*) binds to the hydrophobic binding site on b′ (*grey*). The side chains of M339, L343 and W347 are shown as these residues form the main contacts

It has long been known that PDI can be found as a dimer under some conditions; dimerisation appears to be mediated via the **b′** domain [115]. Self-association appears to be weak but may be a physiological relevant feature of the protein due to its very high abundance in the ER [116].

4.4 Overall Molecular Structure and Synergistic Action of Catalytic and Binding Domains

No high-resolution structure of full-length vertebrate PDI exists but in the past few years there has been an increase in structural insight into PDI due to the determination of high resolution structures of some members of the mammalian PDI family and fungal PDIs [yeast pdi (pdb accession 2B5E and 3BOA) ERp44 (pdb: 2R2J) and ERp57 (pdb: 3F8U)]. The high-resolution structure of yeast PDI (Pdi1p) was an important development, providing insight into the overall organisation of PDI [89]. The domain arrangement of yeast PDI and of the human homologue ERp57, where the structure was determined in complex with a partner protein, give a compact structure with four well-defined domains organised roughly as a U or horseshoe, with the tips – which are formed by the **a** and **a′** domains – close in space (Fig. 9a) [117]. SAXS data on human PDI imply a similar overall arrangement of domains [118]. As inferred from sequence analysis, and earlier experimental work on mammalian PDI and fragments, the linkers between domains **a** and **b** and between **b** and **b′** are very short, whereas that between **b′** and **a′** – the **x**-linker – is an

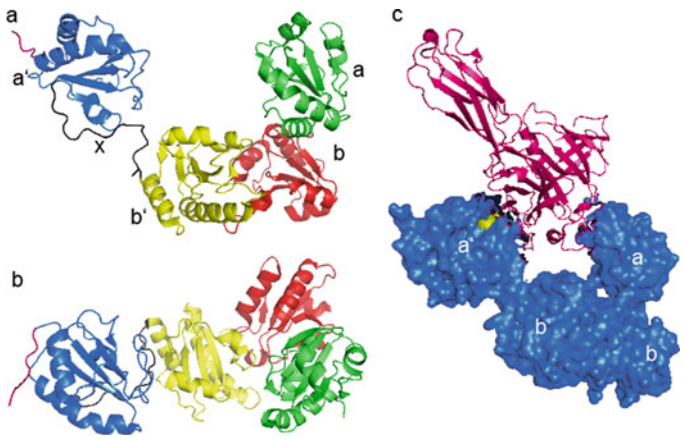

Fig. 9 The overall structure of Erp57. (**a**) The U-shape formed by the domains, where domain **a** is *green*, **b** *red*, **b′** *yellow* and **a′** *blue*. The **x** linker is shown in *black* and **c** in *pink*. (**b**) Turned 90 °C round the *x* axis and shows the **b** domain is not in the same plane as the other three domains. (**c**) Interaction between erp57 (*blue*) and tapasin (*pink*). Tapasin is bound via a mixed disulphide to the active site in domain **a** and interacts extensively with **a** and **a′**. However, there are no contacts to domain **b′**

extended region of defined structure distinct from the thioredoxin-like domains that it connects [119–123]. The domains are not entirely co-planar and domain **b** is displaced, allowing the other three to generate a continuous inner surface (Fig. 9b).

This domain architecture provides a structural basis for understanding the overall function of PDI in that the key defined functional sites line the inner surface of the horseshoe, providing opportunities for multi-point attachment of substrates. The active site dithiol sequences in **a** and **a′** are relatively close in space (~26 Å), facing each other across the open end of the horseshoe, while the inner surface is essentially an extended hydrophobic region mainly contributed by residues of the **b′** domain, but also by parts of the **a** and **a′** domains. Crucially, this hydrophobic surface on **b′**, observed first in the crystal structure of full-length yeast PDI, corresponds to the region which has been shown to constitute the core ligand binding site by direct NMR titration studies on human **b′x** and **bb′x** fragments (see Sect. 4.3). A more recent NMR study on a **b′xa′** fragment of PDI from a different fungal species, confirms this definition of the binding site [124].

These structural insights support the conclusion that the activity of PDI depends on synergy between domains with distinct functional roles [107, 125]. Whereas, individual domains have thioredoxin-like thiol:disulphide oxidoreductase activity (**a** and **a′**), or ability to bind short unfolded peptides (**b′**), they lack full isomerase function towards protein substrates (see Sect. 4.3). Using multi-domain constructs containing only one functional oxidoreductase domain, Darby et al. [107] showed that the **abb′** and **b′xa′c** fragments were the smallest fragments with significant activity in catalysing disulphide formation and reduction in the 28-residue model peptide described previously (Sect. 3.1). These fragments were comparable in activity to full-length PDI with one active-site inactivated by mutation; hence a combination involving the **b′** domain and either redox-active domain is sufficient in this reaction. However, when the fragments were assayed for their ability to catalyse the $N' \rightarrow N_{(SH)2}$ and $N^* \rightarrow N_{(SH)2}$ isomerisations in the BPTI refolding pathway, which involve extensive unfolding and refolding, only the larger **bb′xa′c** fragment had significant activity. Direct and competitive binding studies with a range of peptides and proteins produced comparable results, showing that the **b′** domain is the core of the non-covalent ligand binding site, but that adjacent domains contribute significantly to the binding of larger ligands [63].

Hence the physiological role of PDI in oxidative folding of protein substrates involves extensive PDI/substrate interactions, potentially involving all domains, although the dithiol redox-active sites in the **a** and **a′** domains contribute the core covalent interactions, and the **b′** domains the core non-covalent interactions [125]. This picture has now been extended into other functional interactions of PDI. In vivo assembly studies on prolyl-4-hydroxylase (see Sect. 3.3) have shown that sites in three domains (**a**, **b′**, **a′**) all contribute significantly to the interaction that allows mammalian PDI (β subunits) to assemble with α subunits to form intact, functional prolyl-4-hydroxylase [126, 127].

Similarly, domains and fragments of PDI have been tested for their ability to interact with Ero proteins (see Sect. 3.4) and reconstitute the pathway of O_2-dependent reoxidation and refolding of reduced RNase; the data from reconstitution of yeast

and human systems suggest some differences, but show that the **b′xa′** region is essential for the functional interaction by which Ero proteins transfer oxidising equivalents to PDI [79, 80]. The basis for electron transfer between Ero1α and PDI has been defined more precisely in recent work; studies on active-site mutants of full-length PDI showed that Ero1α can directly oxidise the **a′** domain redox site, but not that of the **a** domain [98], and work on PDI/ERp57 chimaeras showed that Ero1α selects PDI for oxidation because it has specific affinity for the hydrophobic binding site on the PDI b′ domain [128].

The structural basis for genuine PDI/substrate and PDI/partner interactions has not been clarified at high resolution, but clues come from the interactions that occur in crystals of yeast PDI and ERp57. Two X-ray structures of yeast PDI have been determined from crystals grown at different temperatures, but both involve extensive intermolecular interactions with one PDI molecule fitting into the space between the **a**, **b′** and **a′** domains of an adjacent molecule. Similarly, full-length ERp57 has not been crystallised alone, but as a complex with a partner protein, tapasin (Fig. 9), which interacts most extensively with the **a** and **a′** domains, contacting homologous sites on these domains close to the redox-active sites. The fact that these interactions are observed in crystals suggests that the contact sites are important for function and also implies that, in PDI and homologues, occupancy of these sites is essential to suppress motion and define a fixed structure.

The distance between ERp57 redox active sites in the ERp57/tapasin complex is greater than that in yeast PDI (34 cf. 26 Å) but, given that these structures represent ERp57/partner and yeast PDI/pseudo-substrate complexes, it is not clear whether these distances are imposed by the bound partner or represent preferential distances for isolated yeast PDI or ERp57 in solution. What is clear is that interaction between **b** and **b′** domains is relatively fixed [129]. The surface area buried between the **b** and **b′** domains is considerably greater than that between **a** and **b**, or **b′** and **a′** domains, and comparison of structures (e.g. yeast PDI crystallised in alternative conditions, full-length ERp57/tapasin and isolated ERp57 **bb′** fragment) shows little change in relative disposition of the **b** and **b′** domains (rmsd < 1.7 Å, change in relative angle $< 20°$) implying that the **bb′** region provides a solid base or trunk whereas **a** and **a′** may be more mobile ‘arms’.

5 Current Questions

5.1 Substrate Interactions

Despite significant recent progress, we still lack essential structural, thermodynamic and kinetic information on the interaction between PDI and its substrates. The most detailed structural information comes from ligand titration studies monitored by NMR, which reveal that the binding site in human PDI is a hydrophobic cavity on the **b′** domain formed by the surface of the core β–sheet and flanking helices α1 and α3 [111, 112]. This corresponds to the site occupied by the **x**-linker in the crystal

structure of human PDI **b′x** which shows three hydrophobic residues of the linker (M339, L343 and W347) extending their side chains into this hydrophobic cavity on **b′** [130]. This coincidence of sites suggests that ligand binding is associated with displacement of the **x**-linker, which therefore acts as a cap over the site (Fig. 7b). In the absence of ligand there appears to be interconversion between 'capped' and 'uncapped' (or 'closed' and 'open') states; the balance between the states can be perturbed by a wide variety of mutations and reported on by the fluorescence of W347 [130, 131] and NMR relaxation dispersion experiments confirm the dynamic interconversion between the states (M.J. Howard and R.A. Williamson, personal communication). The displacement of **x** by ligand can be monitored in HSQC spectra of **b′x** where the resonance arising from the tryptophan residue in the linker (W347) can be readily resolved and shown to shift from a 'closed' to 'open' position as a function of increasing ligand concentration [112]. Most of the hydrophobic residues that form the central section of the peptide ligand mastoparan (ALAALA) are involved in the interaction with the ligand binding site [111]. These results provide solid information on where ligands bind on PDI, but give no direct information on the conformation adopted by ligands bound at this site or on specific interactions between residues in ligands and the binding site.

PDI shows very broad specificity for ligand binding and has been shown to bind to a wide range of peptides with no identifiable sequence or composition defining good PDI ligands [64]. Conversely, there is no known ligand that is completely specific for PDI and does not bind to other proteins; bacitracin has been claimed as such a specific ligand, and cell biologists have used inhibition by bacitracin as diagnostic of PDI-mediated processes, but this has been shown to be invalid [109]. Affinities for ligand binding to PDI derived from NMR shift titrations with peptides and fully unfolded small proteins give values in the range 1–100 μM [111]. Native RNAse has a K_d of >2 mM by this method, so clearly the binding site is able to discriminate folded and unfolded proteins. This discrimination has been confirmed by SPR studies on the binding of unfolded (reduced/alkylated), misfolded (C38S/C55S double-mutant) and native, wild-type BPTI to full-length human PDI and its **bb′x** fragment. At 25° the K_d for misfolded and unfolded BPTI is 1–10 μM whereas for native, wild-type BPTI it is 1–10 mM, and over a range of temperatures, the affinity was consistently greatest for unfolded and lowest for native BPTI (Unpublished data).

Some comparative studies on PDI homologues have provided interesting insight into differences between them in ligand-binding properties. Sequence alignments indicate that PDIp, PDILT and ERp27 have hydrophobic ligand binding sites on their **b′** domains, entirely comparable to that in PDI. The ligand-binding properties of the pancreas-specific PDI (PDIp) have been directly compared with those of PDI itself and they reveal a clear specificity of PDIp for peptide ligands containing aromatic amino acids, especially tyrosine, and for the corresponding hydroxyl–aryl group in non-peptide ligands [64, 132]. By contrast, ERp57 and ERp72 do not have a hydrophobic patch at the position corresponding to the ligand binding site in PDI; instead they have a charged, polar surface [129]. ERp57 does not bind unfolded proteins directly but does so indirectly by binding specifically to lectin chaperones (calnexin or calreticulin) which recruit unfolded glycoproteins as folding

substrates; similarly, its function in loading peptides onto the MHC complex involves indirect interactions via other partner proteins [117].

These structural and affinity data on ligand binding leave significant questions unanswered. Assuming that physiological substrates bind to PDI over an extended area (i.e. at multiple 'sites') are there multiple, roughly-equivalent binding modes available to any one peptide or unfolded protein, or is there a single preferred binding mode? What are the rates of association and dissociation? In the course of PDI-catalysed oxidative folding, does the substrate dissociate and re-associate with PDI several times or remain bound throughout? Does the mode of binding change as the substrate undergoes conversion through the stages of 'disulphide-regeneration' and 'conformational folding' defined in Sect. 2? Given that the major interaction sites for protein ligands and for the cellular oxidant Ero1α both involve the **b′xa′** region of PDI, and that they compete for binding [128], are there differences in the precise regions involved? New types of experiment will be required to address such questions.

5.2 Enzyme and Substrate Dynamics

There are several clear lines of evidence indicating that PDI is a dynamic molecule, especially in terms of flexibility between adjacent domains leading to alternative conformations (see below). While this work emphasises the dynamic nature of PDI, it does not yet give a completely consistent picture, does not yield quantitative data on the modes, rates and amplitudes of PDI's internal motions and (crucially) does not demonstrate clearly how these motions might be coupled to function.

Yeast PDI structure has been solved independently from crystals grown at 4 and 25°C [89, 116]. The two structures differ most obviously in a rotation of the **a** domain through 123° relative to domain **b** whereas the interdomain angles **b**–**b′** and **b′**–**a′** change by less than 20°. The rotation is focused on the short interdomain loop beginning at Ser139, and it is the Ramachandran angles of Ser139 that undergo the largest change, notably a change in ψ from −11° to +138°. Experiments restricting the mobility of the **a** domain with respect to the rest of the molecule indicate that this mobility of the **a** domain is crucial for the function of the enzyme. The suggestion that the **a** domain works as a flexible arm mobile with respect to the **bb′** base seems plausible but further work is required to define this. In particular there appears to be a difference in this respect between yeast and human PDI where the mobility of the **a′** domain is more significant. The evidence from fluorescence and NMR showing that the **x** region can occupy two alternative positions in the **bb′x** and **b′x** constructs of human PDI in solution, either capping the ligand binding site or displaced from it [112, 130], implies considerable mobility of the **a′** domain relative to **b′**. This conclusion is supported by studies of the full length protein with several proteases, showing that the **a′** domain is much more prone to release than the **a** domain, and fluorescence data confirming the existence of alternative conformations of the **x**-linker [131]. Hence in contrast to the picture in yeast PDI, the major interdomain plasticity of human PDI appears to be relative movement of

a′ and **b′** domains mediated by the **x**-linker. Yeast PDI is < 30% identical in sequence to human PDI and notably the short interdomain linker between domains **a** and **b** and the **x**-linker between **b′** and **a′** are not well-conserved. Furthermore a number of functional differences have been noted. It is not yet clear whether this apparent difference in dynamic properties will be resolved by further work or represents a genuine difference between the molecules. A further comparison can be made with another human PDI homologue, ERp72, which has similar overall domain architecture to PDI, differing only in the presence of an additional **a**-type domain at the N-terminus (giving $\mathbf{a^0abb'xa'c}$); in this case the major sites of interdomain mobility appear to be between **b′** and **a′** (as in human PDI), and between $\mathbf{a^0}$ and **a** [129, 133].

An interesting approach to the relationship between substrate binding, redox state and PDI dynamics was developed from studies on PDI action on cholera toxin [134]. The toxin comprises two polypeptides linked by a disulphide, which is taken up at the cell surface, retrotranslocated to the lumen of the ER and undergoes reduction there to release the cytotoxic A subunit. Tsai et al. demonstrated that PDI catalysed this reduction, generating unfolded toxin A chains, and provided evidence that only reduced PDI was capable of binding the toxin. They inferred that PDI was a 'redox-dependent chaperone' with unfolding activity, but this result was challenged by evidence that the conditions used for generating oxidised PDI involved addition of high concentrations of GSSG (glutathione disulphide) which competed with toxin for the peptide/protein binding site on PDI [135]. Furthermore, these authors showed that the oxidised and reduced forms of PDI did not differ in affinity for procollagen C-propeptide or for the α subunit of prolyl-4-hydroxylase. They concluded that 'our experiments do not rule out the possibility that a conformational change in PDI regulates binding, but only that this conformational change is not necessarily a consequence of a change in the redox state of PDI'.

This question has now been studied using more refined structural tools in work on PDI from the fungus *H. insolens* [114, 136]. Unfortunately there are little functional data on this PDI and it is not closely related in sequence to human PDI or even to yeast PDI from *S. cerevisiae*. Nevertheless, it has a similar overall domain organisation and structural studies using high-field NMR and SAXS methods have generated intriguing data. The **b′xa′** fragment of *H. insolens* PDI shows structural and functional differences in properties depending on the oxidation state of the **a′** domain; upon oxidation, this fragment showed changes in overall dimensions as determined by SAXS, had higher affinity for the non-specific ligand ANS and showed redox-dependent perturbations in the environments, dynamics and H/D exchange properties of residues within the **b′** domain. This fragment contains the binding-site for peptide ligands and mapping this site in detail revealed that it included part of the surface of the **a′** domain as well as a significant hydrophobic patch on the **b′** domain, corresponding to the site identified in human PDI. The results could be interpreted as indicating a conformational change on oxidation of the **a′** active-site leading to greater separation between the **a′** and **b′** domains and greater exposure of the ligand-binding site. Conversion to the reduced form of PDI fragment (e.g. following oxidation of bound substrate by transfer of oxidising

equivalents from the **a**′ domain active site) would then lead to domain movement, relative concealment of the binding-site, reduced affinity for ligand and hence ligand release. The model is attractive but not yet fully proven and corresponding findings have not been made for human PDI. Furthermore, the redox-dependent change in affinity for ligands is opposite to that proposed by Tsai et al. [135].

The indirect evidence for conformational changes in PDI associated with its functional cycle suggests that the best strategy for defining this cycle in more detail would be to trap complexes involving PDI + substrate (preferably using mutants of PDI and/or substrate that cannot complete a full cycle of oxidative folding). Such complexes might be less mobile and more conformationally homogeneous than the materials studied so far, allowing crystallisation and high-resolution structure determination. This seems likely to be a productive strategy, but success is not guaranteed. One negative indicator is the fact that the well characterised complexes of PDI, prolyl 4-hydroxylase and microsomal triglyceride transfer protein (referred to in Sect. 3.3) have not yielded to structural analysis. Both these complexes are potential drug targets and considerable effort has been expended on attempts to characterise them in detail. It might be thought that these stable complexes of PDI with a partner protein would be useful models for static PDI/substrate complexes. However the fact that neither has yielded a high resolution crystal structure suggests that these complexes are themselves dynamic and/or heterogeneous; this may reflect the fact that each of these complexes functionally interacts with and modifies a further protein partner, procollagen or apolipoprotein B, respectively.

5.3 What Next?

Work on the molecular basis of PDI's action has gathered pace over the past 5 years but much still remains to be clarified. How do unfolded and highly-folded substrates interact with PDI? How does PDI act upon them? To what extent does PDI undergo conformational change during its catalytic cycle, and how is conformational change in PDI coupled to changes in its substrate, to facilitate a coupling of 'disulphide regeneration' and 'conformational folding'?. These questions highlight the fact that we lack a detailed structural and dynamic description of complexes between full-length PDI and physiological protein substrates and of the intermediate states along the pathway of PDI-catalysed oxidative folding. To answer such questions we will need to prepare and trap species representing different steps along this pathway and describe their dynamics and the range of structural states that they explore.

References

1. Lin Z, Rye HS (2006) GroEL-mediated protein folding: making the impossible, possible. Crit Rev Biochem Mol Biol 41:211–239
2. Papo N, Kipnis Y, Haran G et al (2008) Concerted release of substrate domains from GroEL by ATP is demonstrated with FRET. J Mol Biol 380:717–725

3. Altschuler GM, Willison KR (2008) Development of free-energy-based models for chaperonin containing TCP-1 mediated folding of actin. J R Soc Interface 5:1391–1408
4. Chakravarthi S, Jessop CE, Bulleid NJ (2009) Oxidative folding in the endoplasmic reticulum. In: Buchner J, Moroder L (eds) Oxidative folding of peptides and proteins. RSC Publishing, Cambridge
5. van Anken E, Braakman I (2005) Versatility of the endoplasmic reticulum protein folding factory. Crit Rev Biochem Mol Biol 40:191–228
6. Hebert DN, Molinari M (2007) In and out of the ER: protein folding, quality control, degradation, and related human diseases. Physiol Rev 87:1377–1408
7. Ellgaard L, Ruddock LW (2005) The human protein disulphide isomerase family: substrate interactions and functional properties. EMBO Rep 6:28–32
8. Appenzeller-Herzog C, Ellgaard L (2008) The human PDI family: versatility packed into a single fold. Biochim Biophys Acta 1783:535–548
9. Freedman RB (1995) The formation of protein disulphide bonds. Curr Opin Struct Biol 5:85–91
10. Gleiter S, Bardwell JC (2008) Disulfide bond isomerization in prokaryotes. Biochim Biophys Acta 1783:530–534
11. Mamathambika BS, Bardwell JC (2008) Disulfide-linked protein folding pathways. Annu Rev Cell Dev Biol 24:211–235
12. Riemer J, Bulleid N, Herrmann JM (2009) Disulfide formation in the ER and mitochondria: two solutions to a common process. Science 324:1284–1287
13. Creighton T (1995) Disulphide-coupled protein folding pathways. Philos Trans R Soc Lond B Biol Sci 348:5–10
14. Narayan M, Welker E, Wedemeyer WJ et al (2000) Oxidative folding of proteins. Acc Chem Res 33:805–812
15. Wedemeyer WJ, Welker E, Narayan M et al (2000) Disulfide bonds and protein folding. Biochemistry 39:4207–4216
16. Arolas JL, Aviles FX, Chang JY et al (2006) Folding of small disulfide-rich proteins: clarifying the puzzle. Trends Biochem Sci 31:292–301
17. Chang JY (2004) Evidence for the underlying cause of diversity of the disulfide folding pathway. Biochemistry 43:4522–4529
18. Darby NJ, van Mierlo CP, Creighton TE (1991) The 5–55 single-disulphide intermediate in folding of bovine pancreatic trypsin inhibitor. FEBS Lett 279:61–64
19. van Mierlo CP, Darby NJ, Creighton TE (1992) The partially folded conformation of the Cys-30 Cys-51 intermediate in the disulfide folding pathway of bovine pancreatic trypsin inhibitor. Proc Natl Acad Sci USA 89:6775–6779
20. Ewbank JJ, Creighton TE (1993) Structural characterization of the disulfide folding intermediates of bovine alpha-lactalbumin. Biochemistry 32:3694–3707
21. Talluri S, Rothwarf DM, Scheraga HA (1994) Structural characterization of a three-disulfide intermediate of ribonuclease A involved in both the folding and unfolding pathways. Biochemistry 33:10437–10449
22. van den Berg B, Chung EW, Robinson CV et al (1999) Characterisation of the dominant oxidative folding intermediate of hen lysozyme. J Mol Biol 290:781–796
23. Eigenbrot C, Randal M, Kossiakoff AA (1990) Structural effects induced by removal of a disulfide-bridge: the X-ray structure of the C30A/C51A mutant of basic pancreatic trypsin inhibitor at 1.6 A. Protein Eng 3:591–598
24. van Mierlo CP, Darby NJ, Keeler J et al (1993) Partially folded conformation of the (30–51) intermediate in the disulphide folding pathway of bovine pancreatic trypsin inhibitor. 1 H and 15 N resonance assignments and determination of backbone dynamics from 15 N relaxation measurements. J Mol Biol 229:1125–1146
25. Laity JH, Lester CC, Shimotakahara S et al (1997) Structural characterization of an analog of the major rate-determining disulfide folding intermediate of bovine pancreatic ribonuclease A. Biochemistry 36:12683–12699

26. Vinci F, Ruoppolo M, Pucci P et al (2000) Early intermediates in the PDI-assisted folding of ribonuclease A. Protein Sci 9:525–535
27. Weissman JS, Kim PS (1991) Reexamination of the folding of BPTI: predominance of native intermediates. Science 253:1386–1393
28. Weissman JS, Kim PS (1995) A kinetic explanation for the rearrangement pathway of BPTI folding. Nat Struct Biol 2:1123–1130
29. Goldenberg DP (1992) Native and non-native intermediates in the BPTI folding pathway. Trends Biochem Sci 17:257–261
30. Karala AR, Lappi AK, Saaranen MJ et al (2009) Efficient peroxide-mediated oxidative refolding of a protein at physiological pH and implications for oxidative folding in the endoplasmic reticulum. Antioxid Redox Signal 11:963–970
31. Chang JY (1994) Controlling the speed of hirudin folding. Biochem J 300(Pt 3):643–650
32. Roux P, Ruoppolo M, Chaffotte AF et al (1999) Comparison of the kinetics of S–S bond, secondary structure, and active site formation during refolding of reduced denatured hen egg white lysozyme. Protein Sci 8:2751–2760
33. Ruoppolo M, Freedman RB, Pucci P et al (1996) Glutathione-dependent pathways of refolding of RNase T1 by oxidation and disulfide isomerization: catalysis by protein disulfide isomerase. Biochemistry 35:13636–13646
34. Ruoppolo M, Freedman RB (1995) Refolding by disulfide isomerization: the mixed disulfide between ribonuclease T1 and glutathione as a model refolding substrate. Biochemistry 34:9380–9388
35. Kibria FM, Lees WJ (2008) Balancing conformational and oxidative kinetic traps during the folding of bovine pancreatic trypsin inhibitor (BPTI) with glutathione and glutathione disulfide. J Am Chem Soc 130:796–797
36. Goldberger RF, Epstein CJ, Anfinsen CB (1963) Acceleration of reactivation of reduced bovine pancreatic ribonuclease by a microsomal system from rat liver. J Biol Chem 238:628–635
37. Venetianer P, Straub FB (1963) The enzymic reactivation of reduced ribonuclease. Biochim Biophys Acta 67:166–168
38. Givol D, Goldberger RF, Anfinsen CB (1964) Oxidation and disulfide interchange in the reactivation of reduced ribonuclease. J Biol Chem 239:PC3114–PC3116
39. Freedman RB (1984) Native disulphide bond formation in protein biosynthesis: evidence for the role of protein disulphide isomerase. Trends Biochem Sci 9:438–441
40. Freedman RB, Hirst TR, Tuite MF (1994) Protein disulphide isomerase: building bridges in protein folding. Trends Biochem Sci 19:331–336
41. Creighton TE, Hillson DA, Freedman RB (1980) Catalysis by protein-disulphide isomerase of the unfolding and refolding of proteins with disulphide bonds. J Mol Biol 142:43–62
42. Creighton TE, Bagley CJ, Cooper L et al (1993) On the biosynthesis of bovine pancreatic trypsin inhibitor (BPTI). Structure, processing, folding and disulphide bond formation of the precursor in vitro and in microsomes. J Mol Biol 232:1176–1196
43. Darby NJ, Freedman RB, Creighton TE (1994) Dissecting the mechanism of protein disulfide isomerase: catalysis of disulfide bond formation in a model peptide. Biochemistry 33:7937–7947
44. Weissman JS, Kim PS (1993) Efficient catalysis of disulphide bond rearrangements by protein disulphide isomerase. Nature 365:185–188
45. Shin HC, Scheraga HA (2000) Catalysis of the oxidative folding of bovine pancreatic ribonuclease A by protein disulfide isomerase. J Mol Biol 300:995–1003
46. Shin HC, Song MC, Scheraga HA (2002) Effect of protein disulfide isomerase on the rate-determining steps of the folding of bovine pancreatic ribonuclease A. FEBS Lett 521:77–80
47. van den Berg B, Chung EW, Robinson CV et al (1999) The oxidative refolding of hen lysozyme and its catalysis by protein disulfide isomerase. EMBO J 18:4794–4803
48. Huber-Wunderlich M, Glockshuber R (1998) A single dipeptide sequence modulates the redox properties of a whole enzyme family. Fold Des 3:161–171

49. Lundstrom J, Holmgren A (1993) Determination of the reduction-oxidation potential of the thioredoxin-like domains of protein disulfide-isomerase from the equilibrium with glutathione and thioredoxin. Biochemistry 32:6649–6655
50. Hatahet F, Ruddock LW (2009) Protein disulfide isomerase: a critical evaluation of its function in disulfide bond formation. Antioxid Redox Signal 11:2807–2850
51. Krause G, Lundstrom J, Barea JL et al (1991) Mimicking the active site of protein disulfide-isomerase by substitution of proline 34 in *Escherichia coli* thioredoxin. J Biol Chem 266:9494–9500
52. Lundstrom J, Krause G, Holmgren A (1992) A Pro to His mutation in active site of thioredoxin increases its disulfide-isomerase activity 10-fold. New refolding systems for reduced or randomly oxidized ribonuclease. J Biol Chem 267:9047–9052
53. Zapun A, Creighton TE (1994) Effects of DsbA on the disulfide folding of bovine pancreatic trypsin inhibitor and alpha-lactalbumin. Biochemistry 33:5202–5211
54. Bader MW, Xie T, Yu CA et al (2000) Disulfide bonds are generated by quinone reduction. J Biol Chem 275:26082–26088
55. Darby NJ, Creighton TE (1995) Catalytic mechanism of DsbA and its comparison with that of protein disulfide isomerase. Biochemistry 34:3576–3587
56. Qiu J, Swartz JR, Georgiou G (1998) Expression of active human tissue-type plasminogen activator in Escherichia coli. Appl Environ Microbiol 64:4891–4896
57. Gebendorfer KM, Winter J (1999) The periplasm of *E. coli* – oxidative folding of recombinant proteins. In: Buchner J, Moroder L (eds) Oxidative folding of peptides and proteins. RSC Publishing, Cambridge
58. Berkmen M, Boyd D, Beckwith J (2005) The nonconsecutive disulfide bond of *Escherichia coli* phytase (AppA) renders it dependent on the protein-disulfide isomerase, DsbC. J Biol Chem 280:11387–11394
59. Messens J, Collet JF, Van Belle K et al (2007) The oxidase DsbA folds a protein with a nonconsecutive disulfide. J Biol Chem 282:31302–31307
60. Zapun A, Missiakas D, Raina S et al (1995) Structural and functional characterization of DsbC, a protein involved in disulfide bond formation in *Escherichia coli*. Biochemistry 34:5075–5089
61. Klappa P, Hawkins HC, Freedman RB (1997) Interactions between protein disulphide isomerase and peptides. Eur J Biochem 248:37–42
62. Klappa P, Stromer T, Zimmermann R et al (1998) A pancreas-specific glycosylated protein disulphide-isomerase binds to misfolded proteins and peptides with an interaction inhibited by oestrogens. Eur J Biochem 254:63–69
63. Klappa P, Ruddock LW, Darby NJ et al (1998) The b′ domain provides the principal peptide-binding site of protein disulfide isomerase but all domains contribute to binding of misfolded proteins. EMBO J 17:927–935
64. Ruddock LW, Freedman RB, Klappa P (2000) Specificity in substrate binding by protein folding catalysts: tyrosine and tryptophan residues are the recognition motifs for the binding of peptides to the pancreas-specific protein disulfide isomerase PDIp. Protein Sci 9:758–764
65. Cai H, Wang CC, Tsou CL (1994) Chaperone-like activity of protein disulfide isomerase in the refolding of a protein with no disulfide bonds. J Biol Chem 269:24550–24552
66. Song JL, Wang CC (1995) Chaperone-like activity of protein disulfide-isomerase in the refolding of rhodanese. Eur J Biochem 231:312–316
67. Wilson R, Lees JF, Bulleid NJ (1998) Protein disulfide isomerase acts as a molecular chaperone during the assembly of procollagen. J Biol Chem 273:9637–9643
68. McLaughlin SH, Bulleid NJ (1998) Thiol-independent interaction of protein disulphide isomerase with type X collagen during intra-cellular folding and assembly. Biochem J 331 (Pt 3):793–800
69. Kivirikko KI, Pihlajaniemi T (1998) Collagen hydroxylases and the protein disulfide isomerase subunit of prolyl 4-hydroxylases. Adv Enzymol Relat Areas Mol Biol 72:325–398
70. Hussain MM, Shi J, Dreizen P (2003) Microsomal triglyceride transfer protein and its role in apoB-lipoprotein assembly. J Lipid Res 44:22–32

71. Kersteen EA, Higgin JJ, Raines RT (2004) Production of human prolyl 4-hydroxylase in Escherichia coli. Protein Expr Purif 38:279–291
72. Zapun A, Creighton TE, Rowling PJ et al (1992) Folding in vitro of bovine pancreatic trypsin inhibitor in the presence of proteins of the endoplasmic reticulum. Proteins 14:10–15
73. Hwang C, Sinskey AJ, Lodish HF (1992) Oxidized redox state of glutathione in the endoplasmic reticulum. Science 257:1496–1502
74. Bass R, Ruddock LW, Klappa P et al (2004) A major fraction of endoplasmic reticulum-located glutathione is present as mixed disulfides with protein. J Biol Chem 279:5257–5262
75. Dixon BM, Heath SH, Kim R et al (2008) Assessment of endoplasmic reticulum glutathione redox status is confounded by extensive ex vivo oxidation. Antioxid Redox Signal 10: 963–972
76. Sevier CS, Kaiser CA (2008) Ero1 and redox homeostasis in the endoplasmic reticulum. Biochim Biophys Acta 1783:549–556
77. Mezghrani A, Fassio A, Benham A et al (2001) Manipulation of oxidative protein folding and PDI redox state in mammalian cells. EMBO J 20:6288–6296
78. Tu BP, Ho-Schleyer SC, Travers KJ et al (2000) Biochemical basis of oxidative protein folding in the endoplasmic reticulum. Science 290:1571–1574
79. Kulp MS, Frickel EM, Ellgaard L et al (2006) Domain architecture of protein-disulfide isomerase facilitates its dual role as an oxidase and an isomerase in Ero1p-mediated disulfide formation. J Biol Chem 281:876–884
80. Wang L, Li SJ, Sidhu A et al (2009) Reconstitution of human Ero1-Lalpha/protein-disulfide isomerase oxidative folding pathway in vitro. Position-dependent differences in role between the a and a′ domains of protein-disulfide isomerase. J Biol Chem 284:199–206
81. Bulleid NJ, Freedman RB (1988) Defective co-translational formation of disulphide bonds in protein disulphide-isomerase-deficient microsomes. Nature 335:649–651
82. Marquardt T, Hebert DN, Helenius A (1993) Post-translational folding of influenza hemagglutinin in isolated endoplasmic reticulum-derived microsomes. J Biol Chem 268: 19618–19625
83. Braakman I, Helenius J, Helenius A (1992) Manipulating disulfide bond formation and protein folding in the endoplasmic reticulum. EMBO J 11:1717–1722
84. Jansens A, van Duijn E, Braakman I (2002) Coordinated nonvectorial folding in a newly synthesized multidomain protein. Science 298:2401–2403
85. Land A, Zonneveld D, Braakman I (2003) Folding of HIV-1 envelope glycoprotein involves extensive isomerization of disulfide bonds and conformation-dependent leader peptide cleavage. FASEB J 17:1058–1067
86. Edman JC, Ellis L, Blacher RW et al (1985) Sequence of protein disulphide isomerase and implications of its relationship to thioredoxin. Nature 317:267–270
87. Gruber CW, Cemazar M, Heras B et al (2006) Protein disulfide isomerase: the structure of oxidative folding. Trends Biochem Sci 31:455–464
88. Charbonnier JB, Belin P, Moutiez M et al (1999) On the role of the cis-proline residue in the active site of DsbA. Protein Sci 8:96–105
89. Tian G, Xiang S, Noiva R et al (2006) The crystal structure of yeast protein disulfide isomerase suggests cooperativity between its active sites. Cell 124:61–73
90. Su D, Berndt C, Fomenko DE et al (2007) A conserved cis-proline precludes metal binding by the active site thiolates in members of the thioredoxin family of proteins. Biochemistry 46:6903–6910
91. Kemmink J, Dijkstra K, Mariani M et al (1999) The structure in solution of the b domain of protein disulfide isomerase. J Biomol NMR 13:357–368
92. Bardwell JC, McGovern K, Beckwith J (1991) Identification of a protein required for disulfide bond formation in vivo. Cell 67:581–589
93. Nelson JW, Creighton TE (1994) Reactivity and ionization of the active site cysteine residues of DsbA, a protein required for disulfide bond formation in vivo. Biochemistry 33:5974–5983

94. Grauschopf U, Winther JR, Korber P et al (1995) Why is DsbA such an oxidizing disulfide catalyst? Cell 83:947–955
95. Dyson HJ, Jeng MF, Tennant LL et al (1997) Effects of buried charged groups on cysteine thiol ionization and reactivity in *Escherichia coli* thioredoxin: structural and functional characterization of mutants of Asp 26 and Lys 57. Biochemistry 36:2622–2636
96. Forman-Kay JD, Clore GM, Gronenborn AM (1992) Relationship between electrostatics and redox function in human thioredoxin: characterization of pH titration shifts using two-dimensional homo- and heteronuclear NMR. Biochemistry 31:3442–3452
97. Chivers PT, Laboissiere MC, Raines RT (1996) The CXXC motif: imperatives for the formation of native disulfide bonds in the cell. EMBO J 15:2659–2667
98. Chambers JE, Tavender TJ, Oka OB et al (2010) The reduction potential of the active site disulfides of human protein disulfide isomerase limits oxidation of the enzyme by Ero1alpha. J Biol Chem 285:29200–29207
99. Chivers PT, Prehoda KE, Raines RT (1997) The CXXC motif: a rheostat in the active site. Biochemistry 36:4061–4066
100. Ren G, Stephan D, Xu Z et al (2009) Properties of the thioredoxin fold superfamily are modulated by a single amino acid residue. J Biol Chem 284:10150–10159
101. Krause G, Holmgren A (1991) Substitution of the conserved tryptophan 31 in *Escherichia coli* thioredoxin by site-directed mutagenesis and structure-function analysis. J Biol Chem 266:4056–4066
102. Kersteen EA, Barrows SR, Raines RT (2005) Catalysis of protein disulfide bond isomerization in a homogeneous substrate. Biochemistry 44:12168–12178
103. Wang L, Vavassori S, Li S et al (2008) Crystal structure of human ERp44 shows a dynamic functional modulation by its carboxy-terminal tail. EMBO Rep 9:642–647
104. Karala AR, Lappi AK, Ruddock LW (2010) Modulation of an active-site cysteine pKa allows PDI to act as a catalyst of both disulfide bond formation and isomerization. J Mol Biol 396:883–892
105. Lappi AK, Lensink MF, Alanen HI et al (2004) A conserved arginine plays a role in the catalytic cycle of the protein disulphide isomerases. J Mol Biol 335:283–295
106. Darby NJ, Creighton TE (1995) Functional properties of the individual thioredoxin-like domains of protein disulfide isomerase. Biochemistry 34:11725–11735
107. Darby NJ, Penka E, Vincentelli R (1998) The multi-domain structure of protein disulfide isomerase is essential for high catalytic efficiency. J Mol Biol 276:239–247
108. Ruoppolo M, Orru S, Talamo F et al (2003) Mutations in domain a′ of protein disulfide isomerase affect the folding pathway of bovine pancreatic ribonuclease A. Protein Sci 12:939–952
109. Karala AR, Ruddock LW (2010) Bacitracin is not a specific inhibitor of protein disulfide isomerase. FEBS J 277:2454–2462
110. Freedman RB, Klappa P, Ruddock LW (2002) Model peptide substrates and ligands in analysis of action of mammalian protein disulfide-isomerase. Methods Enzymol 348:342–354
111. Denisov AY, Maattanen P, Dabrowski C et al (2009) Solution structure of the bb' domains of human protein disulfide isomerase. FEBS J 276:1440–1449
112. Byrne LJ, Sidhu A, Wallis AK et al (2009) Mapping of the ligand binding site on the b' domain of human PDI; interaction with peptide ligands and the x-linker region. Biochem J 423:209–217
113. Cheng H, Wang L, Wang CC (2009) Domain a′ of protein disulfide isomerase plays key role in inhibiting alpha-synuclein fibril formation. Cell Stress Chaperones 15:415–421. doi:10.1007/s12192-009-0157-2
114. Serve O, Kamiya Y, Maeno A et al (2010) Redox-dependent domain rearrangement of protein disulfide isomerase coupled with exposure of its substrate-binding hydrophobic surface. J Mol Biol 396:361–374
115. Wallis AK, Sidhu A, Byrne LJ et al (2009) The ligand-binding b′ domain of human protein disulphide-isomerase mediates homodimerization. Protein Sci 18:2569–2577

116. Tian G, Kober FX, Lewandrowski U et al (2008) The catalytic activity of protein-disulfide isomerase requires a conformationally flexible molecule. J Biol Chem 283:33630–33640
117. Dong G, Wearsch PA, Peaper DR et al (2009) Insights into MHC class I peptide loading from the structure of the tapasin-ERp57 thiol oxidoreductase heterodimer. Immunity 30:21–32
118. Li SJ, Hong XG, Shi YY et al (2006) Annular arrangement and collaborative actions of four domains of protein-disulfide isomerase: a small angle X-ray scattering study in solution. J Biol Chem 281:6581–6588
119. Kemmink J, Darby NJ, Dijkstra K et al (1997) The folding catalyst protein disulfide isomerase is constructed of active and inactive thioredoxin modules. Curr Biol 7:239–245
120. Freedman RB, Gane PJ, Hawkins HC et al (1998) Experimental and theoretical analyses of the domain architecture of mammalian protein disulphide-isomerase. Biol Chem 379: 321–328
121. Ferrari DM, Soling HD (1999) The protein disulphide-isomerase family: unravelling a string of folds. Biochem J 339(Pt 1):1–10
122. Alanen HI, Salo KE, Pekkala M et al (2003) Defining the domain boundaries of the human protein disulfide isomerases. Antioxid Redox Signal 5:367–374
123. Pirneskoski A, Klappa P, Lobell M et al (2004) Molecular characterization of the principal substrate binding site of the ubiquitous folding catalyst protein disulfide isomerase. J Biol Chem 279:10374–10381
124. Serve O, Kamiya Y, Maeno A et al (2009) Redox-dependent domain rearrangement of protein disulfide isomerase coupled with exposure of its substrate-binding hydrophobic surface. J Mol Biol 396:361–374
125. Freedman RB, Klappa P, Ruddock LW (2002) Protein disulfide isomerases exploit synergy between catalytic and specific binding domains. EMBO Rep 3:136–140
126. Pirneskoski A, Ruddock LW, Klappa P et al (2001) Domains b′ and a′ of protein disulfide isomerase fulfill the minimum requirement for function as a subunit of prolyl 4-hydroxylase. The N-terminal domains a and b enhances this function and can be substituted in part by those of ERp57. J Biol Chem 276:11287–11293
127. Koivunen P, Salo KE, Myllyharju J et al (2005) Three binding sites in protein-disulfide isomerase cooperate in collagen prolyl 4-hydroxylase tetramer assembly. J Biol Chem 280:5227–5235
128. Inaba K, Masui S, Iida H et al (2010) Crystal structures of human Ero1alpha reveal the mechanisms of regulated and targeted oxidation of PDI. EMBO J 29:3330–3343
129. Kozlov G, Maattanen P, Thomas DY et al (2010) A structural overview of the PDI family of proteins. FEBS J 19:3924–3936
130. Nguyen VD, Wallis K, Howard MJ et al (2008) Alternative conformations of the x region of human protein disulphide-isomerase modulate exposure of the substrate binding b′ domain. J Mol Biol 383:1144–1155
131. Wang C, Chen S, Wang X et al (2010) Plasticity of human protein disulphide isomerase: evidence for mobility around the x-linker region and its functional significance. J Biol Chem 35:26788–26797
132. Klappa P, Freedman RB, Langenbuch M et al (2001) The pancreas-specific protein disulphide-isomerase PDIp interacts with a hydroxyaryl group in ligands. Biochem J 354: 553–559
133. Kozlov G, Maattanen P, Schrag JD et al (2009) Structure of the noncatalytic domains and global fold of the protein disulfide isomerase ERp72. Structure 17:651–659
134. Tsai B, Rodighiero C, Lencer WI et al (2001) Protein disulfide isomerase acts as a redox-dependent chaperone to unfold cholera toxin. Cell 104:937–948
135. Lumb RA, Bulleid NJ (2002) Is protein disulfide isomerase a redox-dependent molecular chaperone? EMBO J 21:6763–6770
136. Nakasako M, Maeno A, Kurimoto E et al (2010) Redox-dependent domain rearrangement of protein disulfide isomerase from a thermophilic fungus. Biochemistry 49:6953–6962

Top Curr Chem (2013) 328: 35–68
DOI: 10.1007/128_2011_151

Published online: 20 May 2011

Peptide Bond *cis*/*trans* Isomerases: A Biocatalysis Perspective of Conformational Dynamics in Proteins

Cordelia Schiene-Fischer, Tobias Aumüller, and Gunter Fischer

Abstract Peptide bond *cis*/*trans* isomerases (PCTIases) catalyze an intrinsically slow rotational motion taking part in the conformational dynamics of a protein backbone in all of its folding states. In this way, PCTIases assist other proteins to shape their functionally active structure. They have been associated with viral, bacterial, and parasitic infection, signal transduction, cell differentiation, altered metabolic activity, apoptosis, and many other physiological and pathophysiological processes. The need to understand, characterize, and control biochemical steps which contribute to the folding of proteins is a problem being addressed in many laboratories today. This review discusses the biochemical basis that the peptidyl prolyl *cis*/*trans* isomerase (PPIase) family of PCTIases uses for the control of bioactivity. Special emphasis is given to recent developments in the field of biocatalytic features of PPIases, the mechanism of catalysis, and enzyme inhibition.

Keywords Cyclophilin · Cyclosporine · FK506 · FKBP · Folding helper · Immunophilin · Pin1 · Proline · Protein backbone · Protein dynamics · Protein folding · Rapamycin · Signal transduction

Contents

C. Schiene-Fischer (✉), T. Aumüller, and G. Fischer
Max Planck Research Unit for Enzymology of Protein Folding, Weinbergweg 22, 06120 Halle/Saale, Germany
e-mail: fischer@enzyme-halle.mpg.de

Abbreviations

APIase	Secondary amide peptide bond *cis*/*trans* isomerase
CsA	Cyclosporine A
CypA	Cyclophilin A; cyclophilin18
NMR	Nuclear magnetic resonance
PCTI	Peptide bond *cis*/*trans* isomerization
PCTIase	Peptide bond *cis*/*trans* isomerase
PPIase	Peptidyl prolyl *cis*/*trans* isomerase
SFA	Sanglifehrin A

1 Introduction

Important conformational features of the protein backbone are related to the peptide bond. The highly mobile electrons of its nitrogen and oxygen atoms cause planarity, a high barrier to rotation and high polarity [1] which results in peptide bond *cis*/*trans* isomerization (PCTI). The picture of proteins provided by X-ray crystal structures is suggestive of the conformational homogeneity of peptide bonds in native proteins, adopting either *trans* or *cis* conformation. Isomer propensities in unfolded chains and native proteins have been the subject of theoretical considerations, empirical studies and statistical analyses of structural databases of proteins [2–9]. The majority of data has provided collective evidence of the marked peptide bond *cis*/*trans* isomerization (PCTI) based conformational heterogeneity of certain peptide bonds in a polypeptide chain under all biologically relevant conditions. Members of peptide bond *cis*/*trans* isomerases (PCTIases) are characterized by catalyzing the interconversion of the two energetically preferred conformers of the planar peptide bond, the *cis* ($\omega \approx 0°$) and the *trans* conformer ($\omega \approx 180°$) in oligopeptides and in all protein folding states. They are able to enhance the rate of the intrinsically slow rotational motions caused by PCTI, thus affecting the conformational dynamics of the protein in a site-directed manner.

In this review we will discuss the essential characteristics of catalyzed conformational interconversions, the enzymes, and their inhibitors mainly from a

chemical perspective. Because examples for PCTIase catalysis relevant to physiological processes have significantly increased in the last few years, their discussion would go beyond the scope of this review. Several reviews have addressed the biological role of PCTIases in a comprehensive manner [10–18].

1.1 *Overview of Peptide Bond* cis/trans *Isomerization and Peptide Bond* cis/trans *Isomerases*

The peptide bond preceding proline, the prolyl bond, is especially disposed by its stereochemical nature to maintain *cis*/*trans* ratios around unity in short peptides, unfolded polypeptide chains, or unstructured regions of native proteins. Conformational heterogeneity is less pronounced, but still visible, for secondary amide peptide bonds (also termed non-proline peptide bonds), because a typical *cis*/*trans* ratio is about 10^{-3} in an unfolded chain [19].

Generally, elementary conformational transitions in protein folding and protein re-structuring take place spontaneously and the energy barriers to bond rotation regarding angles ϕ, ψ, and χ are mostly rather low ranging around $\Delta G^{\neq} \leq 6$ kT. Barriers of this magnitude form an upper speed limit for folding [20]. All of these features make the experimentally easily accessible refolding of small proteins a fast reaction on the timescale of biological events. Thus, the discovery of PCTIases had to await the identification of a sufficiently slow conformational interconversion worth being catalyzed in the de novo folding and the re-structuring of proteins. This event was shown to be the PCTI of the prolyl bond [21]. Dependent on the sequential context, barriers to rotation of the prolyl bond range from 16 to 22 kcal/mol. In essence, PCTI leads to slow periodic changes in the positions of neighboring chain segments, because the propagation direction and Cα–C′α atom distances for the polypeptide backbone are different in each isomer [7]. Notably, unfolded chains and folding intermediates do not represent the sole and perhaps not even the main physiological states of a protein which undergo spontaneous PCTI. Native state prolyl bond isomers in dynamic equilibrium with each other have been identified and characterized for many proteins, mostly using NMR spectroscopy [22, 23].

However, the wide range of *cis*/*trans* isomer ratios and interconversion rates, which depend on the sequential and spatial context of the prolyl bond, allows for some isomers to escape NMR-based detection. Despite being a minor isomer (0.017%), a significant functional effect of the *trans* Ser-Pro55 conformer could be detected in the side chain reactivity of native RNase T1 [24]. In rare cases, secondary amide peptide bonds were also shown to be involved in native state heterogeneity [25, 26].

Chemically, the prolyl bond relates to a tertiary amide group where the NH hydrogen of a secondary amide peptide bond is replaced by intramolecular substitution with the side chain alkyl group. The other 19 gene coded amino acids form secondary amide peptide bonds, rendering the prolyl bond the only imidic bond, which is especially important for the structural and functional features of proteins.

Later it became obvious in investigations of simple peptide models as well as in the refolding of denatured proteins that relatively high rotational barriers exist not only for prolyl bonds but also for secondary amide peptide bonds [19, 27]. Consequently, two major types of PCTIases have been identified. Peptidyl prolyl *cis/trans* isomerases (PPIases) necessarily require a proline residue in the P1′ position of a substrate chain (nomenclature according to Schechter and Berger [28]) exhibiting almost no activity against non-prolyl peptide bonds [29]. Secondary amide peptide bond *cis/trans* isomerases (APIases) catalyze the PCTI of non-proline peptide bonds. Proline occurring at the P1′ subsite of a potential substrate chain is detrimental to APIase catalysis. Subsite specificity of APIases has already been noted but detailed examinations are lacking. The categorization of PPIase families based on their amino acid sequence dissimilarities is underlined by comparing effects of signature inhibitors (see Sect. 4). Currently, the families comprise three members: cyclophilins, FK506 binding proteins (abbreviated: FKBP), and parvulins. Three-dimensional structures of PPIases have similarities, despite rather divergent amino acid sequences [30, 31]. The existence of a fourth family with the single member PTPA (protein phosphatase 2A phosphatase activator) has not yet been confirmed by independent investigations [32]. The PPIase families have distinct substrate specificities and prove to be sensitive to different types of inhibitors. The identification of cyclophilins and FKBP responsible for the immunosuppressive properties of cyclosporine A (CsA) and FK506 by gain-of-function often leads to these families being called immunophilins (see Sect. 4.1) [33–35].

Prototypical PPIases are monomerically active enzymes ranging in size from 92 to 163 amino acids. PPIases are widely distributed throughout all living organisms, being present even in the very small genome of *Mycoplasma genitalum* [36]. Consequently, by means of amino acid sequence homology, a cyclophilin was identified as a virally encoded protein although it proved to be inactive when assayed for activity with a standard PPIase substrate [37].

1.2 History of Peptide Bond cis/trans *Isomerases*

The first peptidyl prolyl *cis/trans* isomerase (PPIase, EC 5.2.1.8.) was discovered, isolated, and characterized from pig kidney in 1984 [38], which was later found to be identical to the CsA binding protein cyclophilin A (CypA) [39, 40]. Notably, the oligopeptide-based activity assay used for the discovery could be complemented by enzyme-catalyzed protein folding reactions [41–43]. Surprisingly, as was already true for CypA, an immunosuppressive drug molecule played a key role for the identification of a further family of this enzyme class, the FK506 binding proteins (FKBP), because the human PPIase FKBP12 was identified as the major cellular binding partner for the peptide macrolide FK506 [44, 45]. In the mid-1990s, a 92 residue member of the parvulins was identified in *Escherichia coli*, forming the prototype of the third family of PPIases [46]. Soon after having described these prototypic enzymes, the first human isoenzymes were characterized for all families

of PPIases [47–49]. Considering its significance in signaling processes in mammals, the discovery of the pSer(pThr)-Pro specific parvulin Pin1 was of particular importance [49, 50].

The ribosome machinery is thought to release some proteins in their native state, thus leading to the expectation that peptide bond *cis*/*trans* isomerases maybe in its close vicinity. Consequently, the 48-kDa FKBP-like protein trigger factor was identified in 1995 as the peripheral PPIase of the large subunit of the *E. coli* ribosome which was shown to associate with nascent polypeptide chains [51–54].

In 2002, 2D-^{1}H NMR exchange spectra, dipeptide-based UV/Vis stopped flow investigations, and measurements of the refolding kinetics of RNase T1 variants led to the identification of the secondary amide peptide bond *cis*/*trans* isomerase (APIase) activity for *E. coli* DnaK, a member of the Hsp70 family of chaperones [55]. Based on the structural changes of geldanamycin that occur during HSP90 binding, it was inferred that this protein could also join the APIase family of PCTIases [56]. However, thermodynamic and kinetic studies on the binding of geldanamycin derivatives to wild-type and mutant Hsp90 did not provide evidence of this hypothesis [57].

1.3 Domain Composition of the Enzyme Families

As stated above, the sequence similarities of the respective catalytic domains served as a feature to sort PPIases into the different families. They are defined by distinct signature pattern (PROSITE, ID: PDOC00154, ID: PDOC00426, ID: PDOC00840). However, the larger isoenzymes of each PPIase family are of a modular nature, consisting of several PPIase and/or protein domains with different functionalities, whereas single-domain PPIases consist only of the catalytic domain. Additionally, some single- and multi-domain PPIases harbor a targeting sequence that determines the subcellular localization of the mature protein. Several supplementary domains of human PPIases mediate protein–protein interactions. Interestingly, additional domains are recruited differently among human PPIase families (Figs. 1–3). Some FKBPs but none of the cyclophilins and parvulins contain multiple catalytic domains. A major component of the multi-domain FKBPs is a TPR domain which usually comprises three TPR motifs, which is known to mediate interactions with Hsp90 or the calcium-binding EF hand domains (Fig. 2). Cyclophilin supplementary domains include the RNA recognition motif rrm, WD40 protein–protein interaction domains, zinc finger domains, and the Ran-binding domain RanBD1. Only Cyp40 and RanBP2 contain TPR motifs frequently found in FKBP. Amongst the human PPIases, only Cyp58 (Cyp-60, PPIL2) was shown to have an additional enzyme domain, the U-box that exhibits ubiquitin protein ligase activity (Fig. 1). The human parvulin Par14 has a DNA-binding domain, whereas the phosphospecific parvulin Pin1 contains a group IV WW domain with specificity to pSer(pThr) peptide sequences (Fig. 3). Interestingly, a Trim5-CypA fusion protein formed by the insertion of a CypA pseudogene within the Trim5 gene accounts for post-entry restriction of HIV-1 in owl monkeys [12, 59].

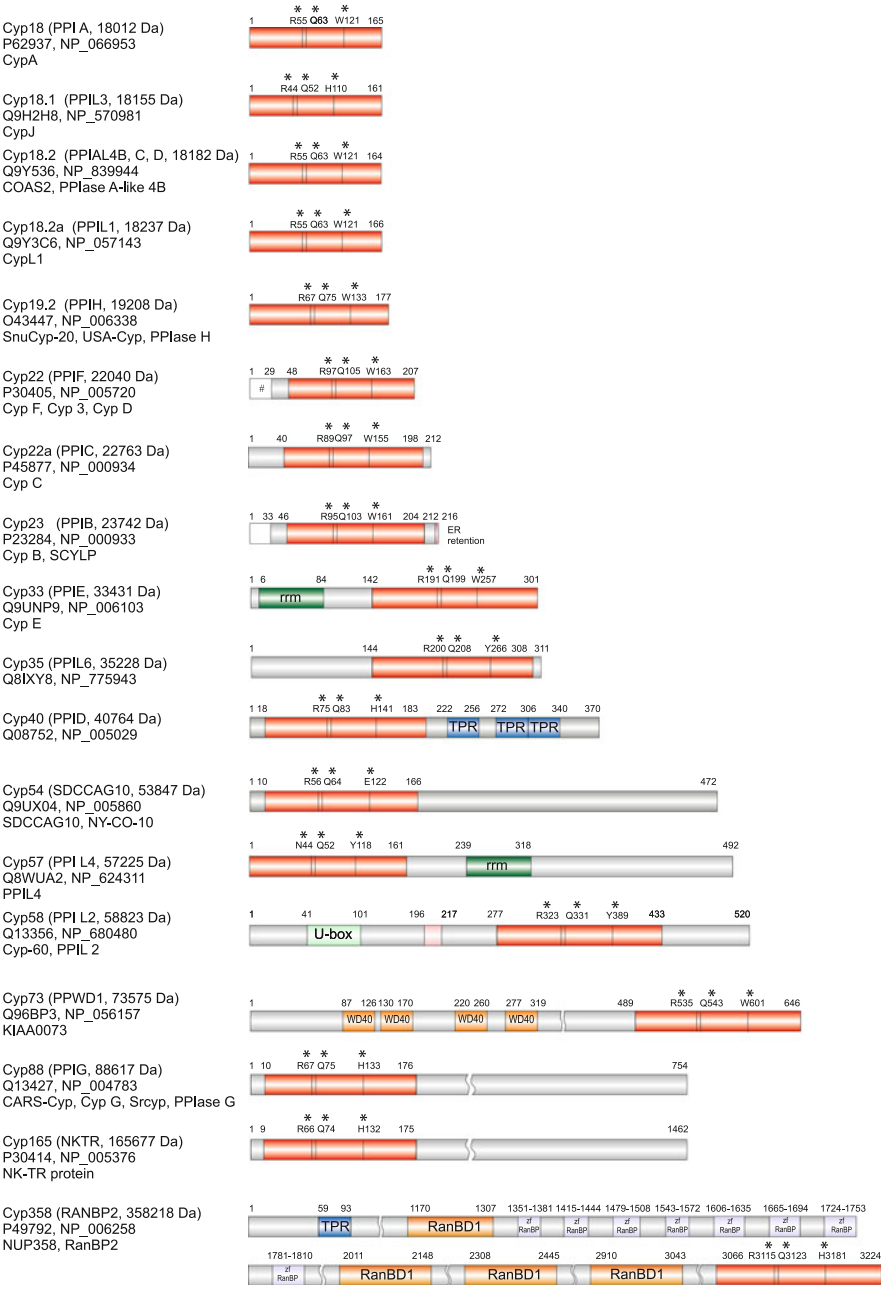

Fig. 1 Human cyclophilins. Protein nomenclature is according to Fischer (1994) [90]. The gene name and the size of the unprocessed protein are shown in *brackets*. In the *second row*, the accession numbers of UniProtKB/Swiss-Prot database and NCBI Reference Sequence are given. In the *third row*, alternative protein names are given. The amino acid residues that border the

This type of cyclophilin was considered to be a promising anti-HIV-1 gene therapy candidate [60].

Phylogenetic conservation of domain composition can be followed by comparing the PPIases of different organisms. The cyclophilins and FKBPs of *Arabidopsis thaliana* and *Caenorhabditis elegans* have supplementary domains similar to those in humans. Both organisms express single-domain PPIases as well as multi-domain PPIases. FKBP were found to contain TPR motifs and EF hand domains (only *C. elegans*), cyclophilins are found to be supplemented with rrm, U-box domains, or WD-40 domains. Higher plants contain a Pin1-type parvulin lacking the WW domain of *h*Pin1, whereas the Pin1 of *C. elegans* is similar to its human congener. Both organisms contain a single Par14 homolog. Importantly, an *At*FKBP is reminiscent of the ribosome-bound *Ec*Trigger factor containing N- and C-terminal ribosome-binding domains. This gives rise to the assumption that trigger factors can only be found in bacteria and in chloroplasts. In addition, a chloroplast-localized parvulin is unique in that it contains an additional rhodanese domain [61].

The numbers of PPIases and their domain organization vary greatly in phylogenetically distant organisms. The *Saccharomyces cerevisieae* PPIases have rather different supplementary domains compared to human PPIases. Of the eight cyclophilins, two have distinct supplementary domains, the TPR domains. Two of the total four FKBP have additional nucleolin-related domains. The yeast Pin1 ESS1 has an additional WW domain, like human Pin1.

In *E. coli*, the two cyclophilins do not contain additional domains. Several *Ec*FKBP are supplemented by dimerization domains, a metal binding domain, or the ribosome-binding domains of trigger factor. The prototypic parvulin (Par10) is coexpressed with the *Ec*SurA protein resulting from duplication of the parvulin domain.

As an exception, a novel group of dual-family PPIases exists in protozoan parasites that contain both a C-terminal cyclophilin and an N-terminal FKBP domain [62]. The APIase domain of DnaK is adjacent to the N-terminal ATPase domain.

2 Enzyme Activity Assays

A fruitful approach in the development of PCTIase assays has been to utilize methods used for the kinetic investigations of PCTI. PCTI coupled to a fast irreversible process with high PCTI specificity in a case in which k_{obs}(isomerization) << k_{obs} (coupled reaction) forms the most versatile approach. The slow kinetic phases which are then finally monitored in the time courses of the coupled reaction represent

Fig. 1 (Continued) protein domains or modules are designated according to UniProtKB/Swiss-Prot, Pfam or ClustalW alignment. The cyclophilin domain is depicted in *red*. Signal sequences are shown as *colorless boxes*. *Rrm* RNA recognition motif, *TPR* tetratricopeptide repeat, *U-box* U-box domain, *WD40* WD40 repeat, *RanBD1* Ran binding protein 1 domain, *zf RanBP* Zn-finger Ran-binding. *Asterisk* indicates amino acid residues in positions corresponding to the functionally important amino acid residues of CypA (catalysis: Arg55, Gln63; CsA binding: Trp121). *Hash* indicates "potential"

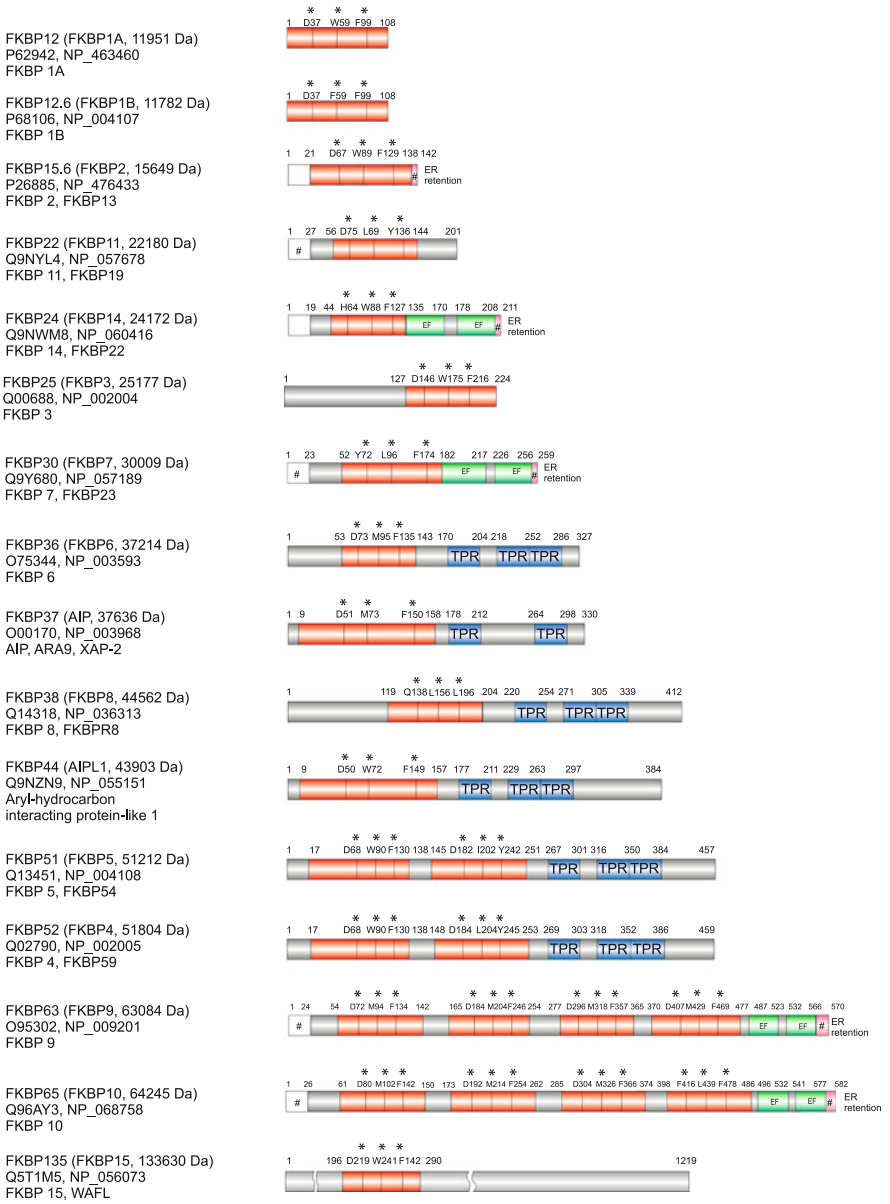

Fig. 2 Human FKBP. Protein nomenclature is according to Fischer (1994) [90]. The gene name and the size of the unprocessed protein are shown in *brackets*. In the *second row*, the accession numbers of UniProtKB/Swiss-Prot database and NCBI Reference Sequence are given. In the *third row*, alternative protein names are given. The amino acid residues that border the protein domains or modules are designated according to UniProtKB/Swiss-Prot, Pfam or ClustalW alignment. The FKBP domain is depicted in *red*. Signal sequences are shown as *colorless boxes*. *TPR* tetratricopeptide repeat, *EF* EF hand. *Asterisk* indicates amino acid residues in positions corresponding to amino acid residues of FKBP12 important for catalysis (Asp37, Trp59, Phe99). *Hash* indicates "potential"

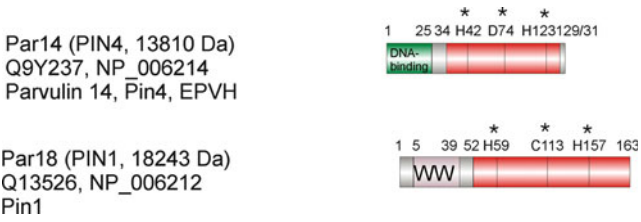

Fig. 3 Human parvulins. Protein nomenclature is according to Fischer (1994) [90]. The gene name and the size of the unprocessed protein are shown in *brackets*. In the *second row*, the accession numbers of UniProtKB/Swiss-Prot database and NCBI Reference Sequence are given. In the *third row*, alternative protein names are given. The amino acid residues that border the protein domains or modules are designated according to UniProtKB/Swiss-Prot, Pfam or ClustalW alignment. The parvulin domain is depicted in *red*. *WW* WW domain, DNA binding of Par14 is according to Sekerina et al. [30]. *Asterisk* indicates amino acid residues important for catalysis

the rate of the conformational interconversion. Regardless of whether the measured PCTI is spontaneous or PCTIase catalyzed, this condition holds in either case. Usually, protein folding [21, 63, 64], proteolytic reactions [65, 66], protein phosphorylation [24, 67], protein dephosphorylation [68], membrane transport and pore regulation [69–71], as well as antibody recognition [72] represent coupled reactions adaptable to PCTI assays. Because of the unimolecular nature of PCTI, resulting kinetics are first-order and thus rate constants are straightforward to obtain. Rate constants can be calculated for either *cis* to *trans* or *trans* to *cis* isomerization, depending on which isomer is reactive in the coupled reaction. In standard protease-coupled PPIase assays the high K_M values of the oligopeptide substrates allow for calculation of specificity constants by $k_{cat}/K_M = (k_{obs} - k_0)/E_0$, where k_{obs} is the experimental first-order rate constant of the catalyzed prolyl isomerization, k_0 represents its spontaneous rate, and E_0 is the PPIase concentration [38].

Solvent jumps into aqueous buffer from substrate peptide-containing non-aqueous media such as LiCl/trifluoroethanol [73] or micelles [74] exploit solvent-altered PCTI ratios that are transiently retained in water. Rapid pH changes can also be employed for the PCTIase assays [55]. Fluorescence quenched substrates provide for a favorable signal-to-noise ratio for this type of assay [75]. Thereby, time courses of PCTI yield composite rate constants are characterized by $k_{ob} = k_{cis\ to\ trans} + k_{trans\ to\ cis}$. These assays avoid artifacts resulting from PCTIase degradation that could potentially be able to disturb protease-coupled assays.

Dynamic ^{1}H-NMR methods provide a powerful tool for assaying PCTIase activity against both oligopeptide and protein substrates [22, 76]. They do not require a prior perturbation of the PCTI equilibrium by chemical means. In ^{1}H NMR experiments, the *cis* and *trans* signals of a substrate experience line broadening and coalescence in the presence of a PCTIase [77, 78]. In two-dimensional NOESY experiments, exchange cross peak intensities at different mixing times give access to the rate constants of catalyzed PCTI [76, 79, 80].

In addition, ^{15}N-NMR experiments measuring the increase in the transverse relaxation rates R_2 showed that the rates of conformational dynamics of the enzyme strongly correlate with the microscopic rates of substrate turnover [81, 82].

Notably, NMR-based PCTIase assays require enzyme concentrations up to 10^5-fold higher when compared with coupled and solvent-assisted assays. Autocatalysis, which has already been found in the refolding of denatured PPIases [83, 84], is a possible complication at high PCTIase concentrations.

3 Biocatalytic Features

We know that the chemical reactivity of peptide bond isomers free in solution is rather similar and the energy barrier to their interconversion is relatively low on the time scale of most non-elementary chemical reactions in aqueous solution. Thus, the question arises as to whether there are molecular reasons for a key role of PCTIase catalysis in the cell. However, in the presence of a protein as a reactant or a catalyst, extended binding regions allow a much greater proportion of the reactants to interact in the ground state or transition state, thus causing isomer-specific bioreactions.

Owing to the reversible nature of the uncoupled PCTI, the basic catalytic pathway can be described by the following minimal reaction scheme:

$$E + S_{cis} \rightleftharpoons ES_{cis} \rightleftharpoons ES_{trans} \rightleftharpoons E + S_{trans}.$$

The impact of PPIase or APIase catalysis on a substrate chain is based on the following molecular processes:

1. Abolition of the transient discrimination of unreactive *cis*/*trans* isomers in coupled reactions. This happens for isomer-specific reactions where a reactant is an isomerase substrate undergoing PCTI in solution. Net effects are seen, for example, in changed reaction pathways [85] or abrogation of multiphasic reaction kinetics [86].
2. Accelerated decay of metastable folding states of proteins.
3. Permanent enhancement of the polypeptide backbone dynamics in the presence of a PCTIase (chain lubrication). This might uncover progression through the catalytic cycle of a coupled enzyme reaction and could also be effective in regulation of membrane channels or control of other bioactivity.
4. Generation of mechanical forces necessary to cause structural distortions. Catalysis causes increased frequency of a directed protein backbone movement.

In addition, PPIases have been found to exhibit other properties which may only be indirectly related to catalysis:

1. They occasionally act as holding chaperones for unfolded polypeptide chains (see Sect. 3.3).
2. They show proline-directed affinity for protein ligands.
3. They can alter *cis*/*trans* ratios of bound relative to free substrates.
4. They can be utilized as presenter proteins (or matchmakers) of a few microbial metabolites to uncover gain-of-function (see Sect. 4.1).

When $[E]_0 << [S]_0$, then it has been shown that PPIases do not change the *cis*/*trans* ratio of the free substrate. However, the isomer ratios of Michaelis complexes can differ from those of the unbound molecules. Sometimes either the *trans* or the *cis* isomer binds better to the enzyme. This behavior must play a role in determining the total amount of an isomer in solution when the substrate and PPIase are present in stoichiometric amounts or when there is an excess of the PPIase. Unfortunately, knowledge about the nature and the concentrations of intracellular PPIase substrates is insufficient. However, high intracellular concentrations in the range of 5–10 μM have been found for cyclophilins and FKBPs [87–89], indicating that changes of the *cis*/*trans* ratio of a substrate have to be considered in vivo.

The biological consequences of either spontaneous or enzyme-catalyzed native state PCTIs of substrate proteins can be imagined, for example, alternative conformations defined by regulatory protein loops [58].

Consequently, it has been proposed that PCTI is unique in that it resembles a molecular switch [90] or timer [91, 92] in the cell showing the following characteristics [90]:

1. There are two switch positions, *cis* and *trans*, which may correspond to either an "on" or "off" functional state. Other switch positions are unstable.
2. The energy needed to operate the switch spontaneously is high on the energy scale relevant for cell signaling and protein folding.
3. The switch involves the chemo-mechanical coupling in the whole molecule that undergoes isomerization. Lever effects might lead to an amplification of atomic displacements on remote sites [7]. The reversibility of the isomerization causes an oscillatory mechanical movement, which may be the movement of a particular segment of the protein backbone or may generate increased backbone dynamics of the whole protein.

Decreased switching resistance of PCTI in a substrate chain in the presence of a PCTIase is a general feature of this "on"/"off" switch. In addition, the degree to which barriers are lowered depends on general features of enzymatic catalysis such as isoenzyme pattern, substrate specificity, enzyme concentration, and expressional regulation, as well as enzyme inhibition and activation. In this way, the catalyzed conformational interconversion may be expected to provide subtle regulation of protein properties.

The *Pseudomonas syringae* AvrRpt2 protease activation exemplifies true "on"/"off" switching by cyclophilin catalysis because the difference in protease activity between the "off" state and the cyclophilin-mediated "on" state is more than 10^5-fold [93, 94].

3.1 Basic Catalytic Parameters

Most prototypic PPIases are perfectly evolved [95] and display high catalytic power as defined by k_{cat}/K_M values which are in the diffusion controlled range of 10^7 s^{-1} M^{-1} [75, 96] and are highly conserved throughout evolution. The high cellular

enzyme concentrations for prototypic PPIases (see Sect. 3) might considerably exceed those of a potential substrate. In some cases, such as in human FKBP, prototypic PPIases do not represent the most abundant enzymes underlining the need for a complete expression profile of all PPIases. For example, human FKBP51 is abundantly expressed in numerous tissues and in many cases is in molar excess over FKBP12 [88]. Furthermore, PPIases such as CypA and Pin1 are subject to considerable up-regulation under stress conditions and in many other pathophysiological situations including cancer and inflammation [97–101].

Taken together, high catalytic efficiency and high enzyme concentration could make prolyl isomerizations of potential protein substrates very fast in the cell. Under these conditions, the limiting rates might approach the magnitude of turnover numbers k_{cat} which were found to range up to 10^4 s^{-1} as measured for oligopeptide substrates in vitro [102, 103]. Thus, the magnitude of the acceleration factor in relation to the spontaneous prolyl isomerization could exceed 10^6-fold, shifting exchange rates and thus the lifetimes of the isomeric states into the micro- to millisecond range. PPIases appear to exhibit significantly lower k_{cat} values for unfolded protein substrates, which is probably due to changes in the rate limiting chemical step from catalysis to conformational rearrangements of the enzyme. The latter process is thought to accompany the dissociation of the PPIase/product complex [104, 105]. Several studies showed that biologically relevant native state PCTI can be efficiently catalyzed by PPIases [22, 76, 106].

The presence of a pSer(pThr)-Pro moiety defines a major but not the exclusive structural feature of Pin1 substrates. Although cyclophilins and Pin1 utilize different substrate motifs for favored active site recognition, functional replacement in the cell remains possible [107, 108]. How can a protein become a Pin1 substrate? A solvent-exposed disordered chain segment containing the pSer(pThr)-Pro moiety may constitute a basis for Pin1 recognition. One of the most important long-range structural effects caused by Ser(Thr)-Pro phosphorylation is loss of structure and increased backbone flexibility around the phosphate residue, resulting in the local unfolding of the polypeptide chain [109]. Thus, potential Pin1 substrates might emerge from many protein phosphorylations catalyzed by proline-directed protein kinases.

Mapping specificity determinants of PPIase and APIase catalysis is still at an early stage. At best, some data sets have been described in terms of physiologically irrelevant oligopeptide substrate parameters, which might not entirely match the situation of native or native-like protein substrates. The picture that has emerged from prototypic PPIases is one characterized by the essential role of the proline residue in P1′ position for substrate specificity [29, 55]. Reversing the stereocenter at P1′ and P1 positions led to decreased activity of prototypic PPIases for all families [110] but did not prevent substrate binding. Generally, strong proline-directed binding, though experimentally more easily accessible when compared to catalysis [111], does not indicate high catalytic interconversion rates of the bound polypeptide chain.

The activity assay of cyclophilins on various oligopeptide substrates revealed that this enzyme family is probably rather promiscuous with respect to modifications by gene coded amino acids at the P1 position [47, 75]. This position is more

relevant for FKBP and parvulin catalysis [46, 75, 112]. Systematic investigations regarding other positions are still lacking. The binding segment of HIV-1 capsid$^{1\text{-}151}$ fragment in its CypA complex extends over at least nine residues in support of the combined subsite concept for PPIase catalysis in which the positioning of a substrate in the active cleft must activate a still unknown number of remote subsites in the transition state of the reaction [113]. The number of critical subsites was shown to vary between the PPIase families [114]. The task of identifying specificities for protein substrates has recently been approached using FKBP-catalyzed refolding of a small library for Xaa160-Pro161 of the N2 domains of the gene-3-protein of phage fd [104]. The bimolecular specificity constants for FKBP12 catalysis strongly resemble those of a Xaa-Pro tetrapeptide library but at reduced catalytic efficacy. Interestingly, grafting of the IF1 chaperone domain of *Ec*SlyD into FKBP12 increased the k_{cat}/K_M values toward N2 domains relative to FKBP12 by about 10^3-fold, exceeding the value found for oligopeptide substrates. Concomitantly, FKBP-like substrate specificity was lost for the chimeric enzyme. This finding suggests a rate limiting step of catalysis that is independent of the nature of the substrate.

Prototypic PPIases consisting of a single catalytic domain do not need cofactors or ATP for catalytic activity in standard assays. APIases of the Hsp70 type are catalytically active against oligopeptide substrates but must make use of a cofactor assisted, ATP-consuming mechanism in order to eject the unfolded polypeptide chain from the catalytic site [55]. Larger PPIases exist which consist of one or more PPIase domains complemented by other functional protein segments or domains (see Sect. 1.3). In several cases, enzymatic activity has not been found for recombinantly produced catalytic domains or full length proteins of the larger PPIases, although the choice of the assay substrate could be critical. In a few cases a cofactor-regulated activity was detected such as was found for FKBP38. Binding of Ca^{2+}/calmodulin to the inactive, non-FK506 binding apo-FKBP38 plays a major role in shaping the active site such that it can subsequently be inhibited by FK506 [115]. Activity control by Ni^{2+} ions has been found for the FKBP-like *Ec*SlyD [116]. In this case, the Ni^{2+} interacting C-terminal alpha-helix of the protein is packed against the catalytic site of the PPIase domain eliciting structural alterations of the catalytic pocket [117].

Interestingly, the enzymatic activity of several cyclophilins and FKBP can be reversibly regulated by formation of internal disulfide bonds [118–120]. PPIase activity of the isolated *At*FKBP13 was suppressed several fold in the thiol form of the protein [121]. On the other hand, the modification of Cys41 and Cys69 of *Ec*Par10 by Michael addition of juglone results initially in a very rapid reaction which does not directly influence the PPIase activity, followed by a slow active site restructuring which abrogated PPIase catalysis [122].

Whether post-translational modifications of PPIases play an important role in altering their fundamental biochemical properties such as substrate specificity has not yet been investigated thoroughly but such modifications can be predicted to occur in the cell. For example, glutathionylation under basal conditions strongly influences the secondary structure composition of CypA, and it plays a key role in

redox regulation of immunity [123–125]. Moreover, unlike the singly modified FKBP12, CypA was found to be acetylated at multiple lysine residues in a human leukemia cell line [126]. Acetylation of Lys125 decreased k_{cat}/K_m of the CypA-catalyzed isomerization of a tetrapeptide substrate by 26-fold. Inhibition by CsA is reduced to a similar extent [127].

Pseudomonas aeruginosa ExoS enzyme can make use of CypA as a substrate for ADP-ribosylation at Arg55 and Arg69 sites. Examination of the effect of this modification on PPIase activity gave a moderate (19%) decrease in k_{cat}/K_M for Xaa-Pro containing peptides. However, once ribosylated, CypA is no longer able to serve as a matchmaker protein for calcineurin inhibition by CsA [128].

Although the phosphorylation of PPIases, including FKBP12 and CypA, has been detected frequently, many questions remain about the influence of this post-translational modification on their biochemical functions [18, 129–133].

Most PPIases are ubiquitously available proteins in the cell and thus particularly well suited for multifunctional uses, a trait that has been termed moonlighting [134]. However, great care must be taken with non-PCTIase related activities so as to ensure they do not result from protein contaminations. For example, the calcium/magnesium-dependent nuclease activity reported for cyclophilins [135, 136] originated from an impurity present in the preparations of the cyclophilins [137, 138].

The cyproase proteolytic function of an *E. coli* cyclophilin variant is also not well understood yet [139]. A silent catalytic triad of a serine protease has been identified by 3D database modeling in CypA (and is present in many other cyclophilins too) [140]. Although the three residues are correctly aligned, protease activity has not yet been reported for cyclophilins or their variants.

Several cysteine SH-groups of PPIases appear to be highly reducing. The chloroplast-located cyclophilin *At*CYP20-3 (also known as "ROC4") is linked to photosynthetic electron transport and redox regulation to the folding of SAT1, thereby enabling the cysteine-based thiol biosynthesis pathway to adjust to light and stress conditions [141]. By means of a CsA-independent pathway, peroxiredoxin II (Prx II) was reduced by CypA without help from any other reductant. These results strongly suggest that CypA might function as an immediate electron donor in supporting the reactive-oxygen degrading properties of Prx proteins [142]. Consequently, recombinant CypA administered to cortical neuronal cultures protected neurons from oxidative stress [143]. A PPIase independent large-scale conformational change was observed for an HIV-1 capsid protein variant upon CypA binding. This change appears to be mediated by Cys198 of the capsid and markedly affected disassembly of the viral core [144].

3.2 Catalytic Mechanism

Despite several mechanistic hypotheses and a considerable body of data demonstrating significant PCTI rate acceleration by PPIases, and thus a highly evolved

catalytic machinery, a detailed description of the catalytic mechanism is still lacking [96, 145]. It is a matter of fact that the effects of side chain mutations on catalytic efficiency of a PPIase cannot be predicted on the basis of the current atomistic models, and catalytic antibodies raised against transition-state analogs did not show an enzyme-like rate enhancement [146].

Current knowledge is insufficient to conclude that PCTIases all have a common catalytic mechanism. By comparison, catalytic parameters allow us to propose that cyclophilins and parvulins are grouped together mechanistically whereas the catalytic machinery of FKBPs is less evolved. Surprisingly, mutational studies on FKBP12 suggested that the presence of a hydrophobic cavity can satisfy all requirements for catalysis [147, 148]. On the other hand, neither non-aqueous solvents [149] nor micelles could approximate the power of FKBP catalysis [74]. It is possible that mechanistic considerations on the basis of mutational analysis of recombinantly expressed PPIase variants is misleading due to problems with contaminations of mutant protein preparations in *E. coli*. For example, after selective removal of *E. coli* PPIases the apparent residual activity of recombinant *h*CypA Arg55Ala decreases from 0.1% [150] to <0.02% of wtCyPA activity (Fanghanel and Fischer, unpublished) in a tetrapeptide assay. Furthermore, the sticky nature of PPIases makes them a common minor impurity in many protein samples from recombinant or authentic sources.

An important lessons from ^{15}N-NMR relaxation experiments is that conformational dynamics of CypA residues Arg55, Lys82, Leu98, Ser99, Ala101, Asn102, Ala103, and Gly109 strongly correlate with the microscopic rates of turnover for a tetrapeptide substrate [81]. CypA active site variants suffer from greatly reduced k_{cat}/K_M values when compared to wtCypA because turnover numbers k_{cat} decrease dramatically [151]. By contrast, ground state affinities were shown to differ by only threefold to sixfold.

Several lines of evidence from high resolution crystal structures and NMR indicate that interconverting conformational substates exist in CypA and FKBP12 that were found to be relevant for chemical steps of catalysis [151, 152]. Eyring-plots of k_{cat}/K_M values suggested two functional states of free CypA but a single one for FKBP12 [153].

It is unlikely that there is a single factor responsible for the catalytic rate enhancement achieved by PCTIases. Our hypothesis, which is based on large inverse solvent deuterium isotope effects and proton inventory studies (Fanghänel and Fischer, unpublished), favors a concerted mechanism in which the lone electron pair of the peptide bond is fixed on nitrogen by an H-bond donor of the protein. Simultaneously, the transition state of the reaction is electrostatically stabilized by an enzyme bound, general base-polarized water molecule that might act as spectator stabilizing the positively charged carbon of the perpendicularly oriented carbonyl group. Solvent assistance by a Gln63-bound water molecule has been proposed on the basis of X-ray structures of substrate-like dipeptide inhibitors complexed with CypA [154]. Interestingly, the CypA Gln63Thr variant exhibits a nearly inactivating (>>3,000-fold) reduction in catalytic efficiency in a tetrapeptide-4-nitroanilide assay [155]. This model is further supported by structural investigations of CypA complexes formed with backbone modified substrate analogs

such as Ala-Gly-*trans*-ψ[CS-N]-Pro-Phe-NH-4-nitroanilide (PDB ID: 1VBT) or Ala-DAla-Pro-Phe-4-nitroanilide (PDB ID: 1VBS) in comparison with the unmodified substrate. They all show an overall similarity of active site side chain arrangements in the respective structures while the modified peptides lack a water molecule in the critical location at Gln63. Consequently, the prolyl isomerization in these peptides could not be catalyzed by CypA [110, 156].

3.2.1 Rotational Direction of Isomerized Peptide Bonds

By ab initio Hartree–Fock and density functional methods it was found that *cis*/*trans* isomerization proceeds asymmetrically through only the clockwise rotation about the peptide bond in the gas phase and the solution [157]. In a protein backbone, lever–arm amplification of the isomerization-mediated structural changes is supposed to occur. Chemo-mechanical coupling involving PCTI and anchoring points has been discussed as playing a role for the active movement of motor proteins such as myosin and kinesin because minute chain translations can be magnified to larger ones by lever arm effects [158].

It is especially interesting to address the directionality of the *cis* to *trans* isomerization accompanying the interconversion of the PPIase/*cis*-peptide complex to the PPIase/*trans*-peptide complex. According to reversible reaction features both binary species are Michaelis complexes. Assuming that the central Xaa-Pro dipeptide segment complexed in a PPIase domain active site will remain fixed, either the C-terminal or the N-terminal part of the substrate chain will undergo rotation as the peptide bond flips between the *cis* and the *trans* conformations. The vectorial character of the isomerization mediated effects implies that there is increased backbone dynamics but only in the propagation direction of the effects. ^{1}H-NMR chemical shift differences of a CypA-bound tetrapeptide 4-nitroanilide substrate suggested C-terminal rotation of the substrate chain [77]. Similarly, R2 relaxation time-based evaluation of substrate chain dynamics indicates that the carboxy terminal tail of a tetrapeptide 4-nitroanilide substrate rotates [81]. In contrast, using an accelerated MD method in explicit water the reaction trajectories of CypA-bound acetyl-His-Ala-Gly-Pro-Ile-Ala-*N*-methylamide indicate a different rotational direction because the C-terminal part including the proline ring never rotated during the MD simulation [145]. The latter finding is in line with crystal structure data of Pin1 complexed with pThr-Pro containing substrates and inhibitors. In these complexes, the C-terminal end of the bound peptide was shown to reside in a restrictive environment, effectively limiting the range of conformations accessible to a bound substrate whereas the structural data for the N-terminal part of the substrate indicate a mobile structural element [31]. In theoretical studies of the complex between human CypA and the 146 residue N-terminal domain of HIV-1 capsid protein the targeted proline residue remains fixed during catalyzed PCTI whereas the prolyl bond carbonyl rotates 180° [159]. This finding is complemented

by crystal structures of CypA in complex with HIV-1 capsid protein variants because substrate and product chains are accommodated within the enzyme active site by rearrangement of their N-terminal residues [160].

Asymmetric transmission of structural changes along a polypeptide chain has already been detected for spontaneous prolyl isomerizations in the uncomplexed state of potential PPIase substrates. In 12 native protein pairs exhibiting both prolyl isomers in different crystalline states, the structural changes seen on backbone Cα atom distances are unidirectional relative to the isomerizing bond whereby the magnitude of the isomer-specific effect exceeds 3.0 Å even at atomic positions remote to proline. Both directions, N-terminal and C-terminal to the isomerizing bond, were found to be involved, dependent on the nature of the protein [7]. This is in accordance with the idea that the substrate sequence determines the part of the substrate chain which is motion-coupled to the PCTI.

3.3 Chaperoning vs Catalysis

In vitro studies of refolding yields of denatured proteins in the presence of PCTIases have led them to be named chaperones. Indeed, preventing other proteins from aggregating into non-functional structures appears to be a major characteristic of this enzyme group [161–165]. An important question is: what is the relationship between PCTI catalysis and chaperoning in the cell? There have been significant advances toward answering this question and explaining the increase in refolding yields of denatured proteins by isomerase catalysis. It was shown that PCTIase-catalyzed decay of aggregation-prone folding intermediates could ultimately lead to increased folding yields [85].

Another aspect deserving mention is that the ability to sequester (to hold chains) a polypeptide substrate is an inherent feature of the catalytic machinery of PCTIases. It also contributes, for example, to the catalytic mechanism of proteases, protein kinases, and phosphatases. In all these cases, catalytic power is linked in a compulsory manner to substrate binding to an extended array of S-subsites of the enzymes. Relatively simple experiments permit us to assess whether or not a protein can be classified as a holding chaperone, based on its ability to bind to and transiently hold a client protein [161–163, 165]. In contrast to PCTIases, proteases, protein kinases, and protein phosphatases can be correctly categorized in vivo by conventional methods because they catalyze quasi-irreversible reactions. Here, chemically well-distinguishable product and reactant states exist. As anticipated, proteases reveal their chaperone function when protease inactive variants were shown to prevent the aggregation of denatured substrate proteins as has been exemplified for trypsin [166] and aspartic proteases [167]. However, there is absolutely no doubt that proteases have evolved to catalyze peptide bond hydrolysis in the cell and that chain sequestration is used to assist their catalytic machinery.

The question now arises as to whether or to what extent this single molecular function impacts on the action of PCTIases in the cell. Several molecular features of peptide bond *cis*/*trans* isomerase catalysis present some analytical drawbacks to the accurate analysis of experimental data and these need to be considered in exploring cellular functions: (1) the small chemical differences between *cis* and *trans* isomers, (2) the volatile equilibrium of PCTI, and (3) functional rescue by enzyme isoforms. However, we want to stress, by way of conclusion, that peptide bond *cis*/*trans* isomerases have also evolved to bind to and sequester polypeptides as an auxiliary factor but prerequisite for catalysis. The clues to understanding PPIase and APIase catalysis in the cell are provided by enzymatically inactive variants as well as by pharmacological inhibition using potent inhibitors of high selectivity (see Sect. 4). These studies provide a means of dissecting and assessing the functional characteristics of PCTIases in biological experiments provided enzyme variants can be applied that combine strongly reduced catalytic activity with the ability to sequester a client polypeptide chain [16]. For chromatin modulation in yeast, the chaperone domain of *Sp*FKBP39 suffices to induce effects on DNA supercoiling and nuclease digestion in vitro. However, rDNA silencing is sensitive to activity-reduced active site-mutants of *Sp*FKBP39 in vivo [168]. In particular, experiments on Pin1 provide experimental evidence for the exclusive role of PPIase activity in signaling processes [11, 15, 79]. In addition, it does not make sense chaperoning native proteins to prevent their aggregation in the phosphorylated state.

Due to their high catalytic power, great caution must be exercised when interpreting the lack of changed phenotypes subsequent to knock down or pharmacological inhibition of PPIases. For example, extremely low cellular levels of Ess1, an essential parvulin-like PPIase of yeast, were found to be required and sufficient for optimal and for minimal cell growth of yeast. In this case, about 1.5–20 Ess1 molecules per cell suffice for minimal growth, but the cells die in its absence [242].

4 Enzyme Inhibitors

Since the functional importance of PCTIases for a large variety of biological processes has been revealed, there is an increasing interest in the development of inhibitors as mechanistic tools and potential drugs for various diseases. Selective inhibition among the three families of PPIases can be easily achieved. However, development of specific inhibitors of the human isoenzymes within the respective subfamilies has only been of limited success owing to the conservation of active sites within the subfamilies. In many cases, PPIase inhibitors are found to be surrogates of the prolyl bond in its twisted transition state of isomerization. Thereby, the pharmacophore interacts with catalytically important residues in the enzyme's substrate binding pocket forming reversible adducts. Having now identified the many biochemical functions potentially performed by PPIases (see Sect. 3),

low molecular weight inhibitors can take a major step forward in dissecting the role of PPIases in the cell. However, this review will not be able to convey a comprehensive picture of their potential biological effects. Until now, there have been only a few attempts to develop inhibitors targeted to APIases.

An extensive review of PPIase inhibitor development before 2006 is provided by Wang and Etzkorn [169].

4.1 Inhibitors Characterized by Gain-of-Function

Nature has provided for secondary metabolites such as FK506, rapamycin, sanglifehrin, and CsA, all of which inhibit their target PPIase in the low nanomolar range [39, 44, 170]. However, calcineurin has been shown to be the immunologically relevant receptor for the CypA/CsA and the FKBP12/FK506 complexes in the cell [33, 34]. Once bound, both drugs inhibit the serine/threonine-specific protein phosphatase activity of calcineurin through gain-of-function. In other words, physiological effects observed after the administration of these drugs are due to the compulsory combination of both PPIase inhibition and gain-of-function. Moreover, the PPIase/calcineurin concentration ratio $>>1$ in the cell argues that there is a predominance of gain-of-function at low concentrations of the systemically administered drug. In a few tissue-based assays, cyclophilin concentrations were found to be limiting [171].

Chemically, both CsA and FK506 are of dual-domain composition, with one distinct part of the molecule responsible for PPIase binding and the other part, the "effector domain," mediating the interaction of the PPIase/drug complex with calcineurin [35]. However, the composite surface formed by the PPIase/drug complexes does not play an essential role for calcineurin inhibition. CsA derivatives substituted in residue 3 have been shown to inhibit calcineurin without prior formation of a complex with CypA, as exemplified for [R-α-*N*,*N*-dimethylaminoethylthio-Sar]^3–CsA (Fig. 4) [172]. Unlike CsA, this cyclosporine derivative is unable to inhibit calcineurin after forming the binary complex with CypA. These results indicate that subtle conformational changes in CsA are induced either by CypA binding or substitution in 3-position and these are responsible for calcineurin inhibition and thus immunosuppression [173]. To remove calcineurin inhibition while retaining the high cyclophilin PPIase inhibitory potency of the cyclosporine warhead, modifications at side chains of positions 4 and 6 of CsA can be utilized [174, 175]. Such derivatives have been termed nonimmunosuppressive cyclosporins and have played a pivotal role in dissecting cyclophilin functions (see Sect. 4.2.1).

CsA binds to the active site of CypA with its cyclophilin binding domain (residues 1–3 and 9–11). Its "effector domain" consists of residues 4–8 [176]. CsA inhibits the PPIase activity of a wide variety of cyclophilin isoenzymes;

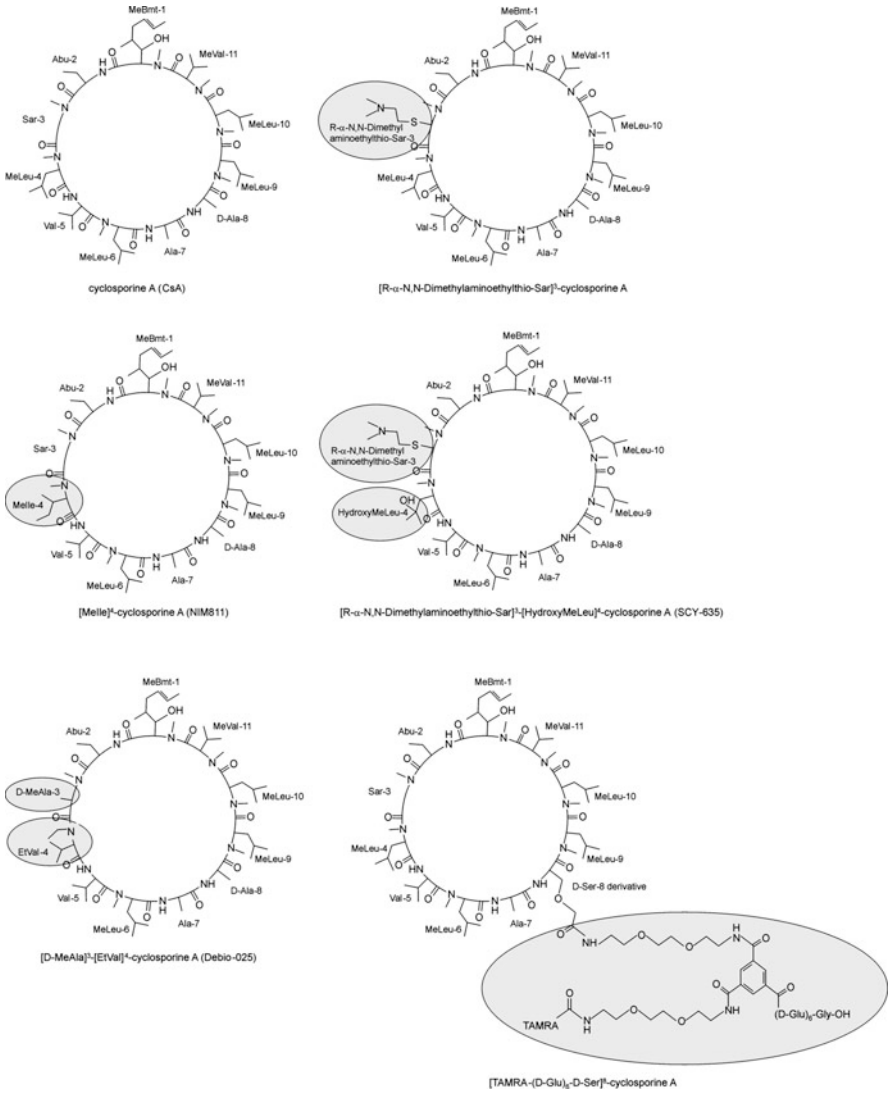

Fig. 4 Schematic representation of the chemical structures of cyclosporine A (CsA) and CsA derivatives

their susceptibility is determined by the presence of Trp121 (CypA numbering) in the catalytic domain of the protein (Fig. 1) [177].

The macrolide lactone FK506 (tacrolimus) contains a hemiketal-masked triketoamide moiety incorporated in a 23-membered ring [178]. FKBP12/FK506 complex formation results in strong inhibition of both the PPIase activity of FKBP12 ($IC_{50} = 0.88$ nM) and the protein phosphatase activity of calcineurin

(IC_{50} = 47 nM) in vitro [33, 179]. In the FKBP12/FK506 complex, the pipecolinyl ring of FK506 is considered to mimic the proline residue of a substrate and its twisted α-dicarbonyl moiety resembles the transition state of *cis*/*trans* isomerization [180]. The strong immunosuppressant FK520 (ascomycin) is a C21 ethyl analog of FK506 with somewhat changed pharmacological properties [181]. Generally, elimination or modifications of the "effector domain" of FK506 or ascomycin, respectively, resulted in the abolition of gain-of-function, whereas the PPIase inhibitory potency remained at a relatively high level. The effector domain includes backbone atoms and substituents at C18 to C23 in the macrocycle and C26 to C34 in the cyclohexyl ring [35, 182]. Thus, C18 hydroxylation of ascomycin completely abolished both immunosuppression and calcineurin inhibition, retaining the high affinity of the parent compound for FKBP12 ($K_D \approx 4$ nM) [183]. The macroring derivative 506BD, which lacks the effector domain backbone, still exhibits the feature of being a strong FKBP12 inhibitor. However, it is nonimmunosuppressive and is able to reverse suppression of Il-2 transcription by FK506 (see Sect. 4.3.1) [184].

Rapamycin (sirolimus), a related macrolide-type tight binding FKBP12 inhibitor (K_I = 0.2 nM), causes immunosuppression by means of a cellular signaling mechanism independent of calcineurin but controlled by gain-of-function [185]. Structurally, the FKBP binding domain of rapamycin is highly similar to FK506, whereas the effector domains of rapamycin and FK506 differ significantly. The FKBP12/rapamycin complex is inert against calcineurin but it binds to and inhibits the mammalian target of rapamycin (mTORC1 or raptor) [186–188]. It is thought that ternary complex formation leads to different signaling responses in different cell types [189]. mTOR is centrally involved in cancer metabolism, growth, and proliferation [190]. CI779 (temsirolimus), a 42-ester derivative of rapamycin with 2,2-bis(hydroxymethyl) propionic acid, RAD001 (everolimus, 42-*O*-(2-hydroxyethyl) rapamycin), and ridaforolimus (42-*O*-dimethylphosphinate rapamycin), are collectively named rapalogs. These immunosuppressive rapamycin derivatives are being applied in the clinics for medical purposes [191].

In the ternary complex formed by FKBP12, rapamycin, and the FRB domain of mTOR, the most extensive contacts with the FRB domain involve the triene part of rapamycin [192]. Thus, the triene-modified rapamycin analog WAY-124,466, can inhibit PPIase, but does not show rapamycin-specific immunosuppressive properties [193]. Cleavage of the cyclohexyl ring of rapamycin leads to loss of immunosuppressive activity at only slightly reduced affinity to FKBP12, indicating that the C37–C39 segment of the cyclohexyl ring also belongs to the effector domain (see Sect. 4.3.1) [194].

Notably, as has emerged for other PPIase inhibitors that utilize gain-of-function, cellular effects of rapamycin are of a composite nature. Beside affecting mTOR signaling, administration of rapalogs can involve profound effects caused by inhibition of the PPIase activity of the 16 human FKBP isoforms. Thus, it is highly probable that adverse or even therapeutic effects observed for rapamycin or rapalogs could result from FKBP inhibition.

4.2 Cyclophilin Inhibitors

4.2.1 Cyclosporine Derivatives

Based on CsA, various derivatives have been developed for inhibition of cyclophilins without targeting calcineurin (Fig. 4). The nonimmunosuppressive cyclosporine molecule NIM811 is modified as compared to CsA at the fourth amino acid from *N*-methyl-leucine to *N*-methyl-isoleucine so as to retain its ability to bind tightly to the active site of cyclophilins but to prevent mediating calcineurin inhibition [195]. NIM811 inhibits the PPIase activity of CypA with a K_I value of 2.1 nM [196]. Debio-025 and SCY-635 are modified at the fourth amino acid from *N*-methyl-leucine to *N*-ethyl-valine or *N*-methyl-hydroxyleucine, respectively. Both compounds have an additional modification at the third amino acid from sarcosine to *N*-methyl-*D*-alanine or dimethylaminoethylthio-sarcosine, respectively [10]. Debio-025 and SCY-635 are potent inhibitors of CypA PPIase activity with K_I values of 0.34 nM and 1.8 nM, respectively [196, 197], and are being tested in clinical phase studies for treatment of hepatitis C virus infections [10].

A disadvantage of the use of a global cyclophilin inhibitor in biological systems is the high susceptibility to inhibition of several cyclophilin isoforms. Treatment with more specific inhibitors would (1) probably elicit less side effects than a global cyclophilin inhibitor and (2) not get dispersed into a cellular sink when sequestered by off-target cyclophilins. Consequently, attempts were made to address the inhibitor to a subfraction of cyclophilins defined by their distribution throughout the organism. Thus, extracellular cyclophilins are specifically targeted by cell-impermeable CsA derivatives. A potent cell-impermeable cyclophilin inhibitor has been synthesized that contains a 6-mer D-glutamic acid moiety and 5(6)-carboxytetramethylrhodamine as a fluorescence probe attached to side chain-modified [D-Ser]^8-CsA [198].

Similarly, selective targeting of CypD, a mitochondrial cyclophilin, was approached by conjugating CsA to the lipophilic triphenylphosphonium cation, enabling its accumulation in mitochondria due to the inner membrane potential [199].

4.2.2 Other Inhibitors

Sanglifehrins are macrolides found to bind to cyclophilins. They display immunosuppressive activity in the murine mixed lymphocyte reaction but lack gain-of-function [170]. Sanglifehrin A (SFA) has a complex molecular structure consisting of a 22-membered macrocycle with a nine carbon tether terminated by a highly substituted spirobicyclic moiety in position 23 [200]. It inhibits the PPIase activity of CypA with an IC_{50} value of 12.8 nM [201]. By X-ray crystallography it was shown that, similar to CsA, the 22-membered macrocycle of SFA is deeply embedded in the active site of CypA [200]. Unlike CsA, which blocks IL-2 production, SFA blocks IL-2 induced proliferation and cytokine production of T cells [202]. Molecular details by which SFA accomplish its immunosuppressive activity are not yet fully explored.

A large number of compounds have recently been developed as inhibitors of cyclophilins either based on rational design or screening of chemical libraries. The high throughput virtual screening program LIDAEUS fed with the two million compounds of the ZINC database as input filtered six compounds with an experimentally determined IC_{50} value against CypA in the micromolar range [203]. Another approach gave quinoxaline derivatives with an IC_{50} value of 0.4 μM for CypA [204].

Several designed inhibitors are based on the idea of peptidomimetic inhibitors using conformationally locked prolyl amide substrate analogs. For example, ground state analogs such as alkene isosteres of prolyl amide bonds or bicyclic lactams were found to have affinities to CypA in the micromolar range [205, 206]. The attempt to design mimics of the twisted amide transition state of cyclophilin substrates led to the synthesis of phosphoamide mimics of the tetrapeptide Ala-Gly-Pro-Phe, which inhibited the PPIase activity of CypA in the low micromolar range [207]. Also, bimolecular oxorhenium metalloconstructs were shown to bind CypA with a slightly better affinity than the corresponding nonmetalated peptides [208]. Aryl-1-indanylketones exhibit a twisted amide structure with an sp^3 hybridized indanyl carbon atom, which might resemble the putative transition state of catalysis. The highest affinity compounds of this class inhibited CypA with K_I values in the high nanomolar range. As a new feature, this compound class was able to discriminate between the two most abundant human cyclophilins, CypA and CypB. It was shown that aryl-1-indanylketones could abolish CypA-mediated chemotaxis of mouse $CD4^+$ T cells but were inert when CypB was the chemoattractant. Notably, cross-inhibition with Pin1 takes place with similar potency [209, 210].

4.3 FKBP Inhibitors

4.3.1 FK506 and Rapamycin Analogs

L-685,818, the C18-hydroxy, C21-ethyl derivative of FK506, and FK1706, the C21-propanone derivative of FK506 are non-immunosuppressive compounds that have affinities toward FKBP12 comparable to FK506 [211, 212]. The nonimmunosuppressive rapamycin derivative ILS-920 was prepared from rapamycin via a [4 + 2] cycloaddition reaction with nitrosobenzene at the C1, C3 diene and by further catalytic hydrogenation. An over 200-fold preference for binding to FKBP52 relative to FKBP12 was reported with a K_D value of 0.48 nM for the ILS-920/FKBP52 complex [213].

The design of several FKBP inhibitors was based on the common structural elements of FK506 and rapamycin which represent the binding domains of these drugs. As mentioned above, the analogs of the FKBP binding domain of FK506, cyclic 506BD, and the acyclic 506BD showed remarkable FKBP12 inhibition with K_I values of 5 and 20 nM, respectively but do not show immunosuppressive activity [184]. In several approaches, dicarbonyl, thiocarbonyl, α-hydroxy carbonyl, sulfonamide, and acyl hydrazide derivatives of pipecolyl-containing compounds,

polycyclic aza-amides and prolyl-containing compounds were characterized as causing micromolar and submicromolar FKBP12 inhibition [214–218]. Bulky hydrophobic alkyl groups as substituents for the pyranose ring region of FK506 as well as alkyl or alkyl aryl esters instead of the lead cyclohexylethyl moiety appeared to be favorable for high affinity [219]. Broadly tested for beneficial effects in neuroregeneration, nonimmunosuppressive open-chain FK506 derivatives such as GPI 1046 (K_I = 306 nM) [220] and V-10,367 (K_I = 0.5 nM) [214] have been developed [221]. Unfortunately, reported inhibition constants are of high variance; the reason why is discussed elsewhere [222].

4.3.2 Other Inhibitors

Beside FK506 and rapamycin, there are other natural polyketides containing an α-ketoacyl pipecolic residue. Members of this structural class are meridamycin and the antascomicins, which bind tightly to FKBP12, competing thereby with FK506, but are not immunosuppressive [223, 224]. The newly isolated nocardiopsin polyketides were also found to bind to FKBP12 [225]. Pregnane derivatives have been found by molecular docking studies to be active site directed FKBP12 ligands [226]. This property has been experimentally confirmed with K_D values in the low micromolar range.

Interestingly, cycloheximide, a well-known inhibitor of eukaryotic protein synthesis, inhibits the PPIase activity of FKBP12 with an IC_{50} value of 3.6 μM [227]. Its derivative *N*-(*N*′,*N*′-dimethylcarboxamidomethyl) cycloheximide forms a relatively specific inhibitor of the apoptosis-related FKBP38 with a K_I value of 85 nM [220].

4.4 Pin1 Inhibitors

Reversible inhibition of parvulins other than Pin1 by small molecules has not yet been established.

Since inhibition of the pSer(pThr)-Pro specific parvulin Pin1 might lead to a new opportunity in cancer therapy, much effort has been invested in the search for efficient inhibitors of this enzyme. The development of parvulin inhibitors started with the irreversible small molecule inhibitor juglone. However, although juglone differentiates the parvulin family of PPIases from cyclophilins and FKBP, its use has been hampered by lack of specificity [122].

The design of reversible inhibitors was initially based on phosphopeptide mimics, which led to inhibitors with low nanomolar inhibition of Pin1. Thus, the substrate-analog inhibitor Ac-Phe-*D*Thr(PO_3H_2)-Pip-Nal-Gln-NH_2 specifically targeted to the PPIase active site with a K_I of 18 nM [228]. Both enzyme kinetics and structural data support the conclusion that the Thr(PO_3H_2)-Pip moiety exhibits a transition state analog conformation [229]. By using composite peptides consisting of a substrate-analog inhibitory motif and a WW domain targeted segment, it was shown that

bivalent binding of ligands toward Pin1 enhanced affinity compared to monovalent binding [230]. Other phosphorylated peptidomimetic Pin1 inhibitors are the (E)- and (Z)-alkenes Ac-Phe-Phe-pSerΨ[CH=C]Pro-Arg-NH_2 with IC_{50} values for Pin1 inhibition in the micromolar range [231]. Phosphorylated perhydropyrrolizine derivatives and pepticinnamin analogs are moderately potent non-peptidomimetic inhibitors of Pin1 with K_I values in the micromolar range [232, 233]. Improved affinities could be reached by structure-based de novo design of phosphorylated compounds using an aminophenylpropanol core [234]. As found for CypA, aryl-1-indanylketones can inhibit Pin1 with K_I values in the range of 400 nM [209]. This finding might indicate similarities in the transition state configuration of the catalytic pathways of both enzymes. The structure-guided evolution of an indole 2-carboxylic acid fragment resulted in the identification of a series of α-benzimidazolyl-substituted amino acids which inhibited Pin1 activity with IC_{50}s < 100 nM [235].

Impressively, screening of more than one million compounds with a Pin1 fluorescence polarization binding assay and a Pin1 PPIase activity assay did not yield any inhibitory compounds that could be confirmed by secondary assays such as ITC or NMR-based ligand binding analysis [234]. On the other hand, dipentamethylene thiuram monosulfide found by a screening approach gave a K_D value of 60 nM when bound to the active site of Pin1 [236].

4.5 DnaK Inhibitors

DnaK from *E. coli* serves as a well-studied model system of Hsp70 chaperones. Compounds targeting the ATP-binding pocket of Hsp70s are not in the scope of this review. A limited number of approaches have identified DnaK inhibitors targeted to its peptide binding domain.

Anti-bacterial fatty acylated benzamido inhibitors of the APIase activity of DnaK were shown to bind to the peptide binding site of DnaK, thereby inhibiting the DnaK-assisted refolding of luciferase [237]. Screening for inhibitors of the DnaK-mediated refolding of firefly luciferase from a dihydropyrimidine library resulted in the identification of micromolar inhibitors of the DnaK refolding activity [238].

5 Conclusion and Perspectives

Clear evidence for the role of PCTI for bioactivity in vitro has been shown by the "on"/"off" peptide bond-based photoswitch implanted in the backbone of RNase S [239]. Elegant studies on the infection of *E. coli* cells by the filamentous phage fd showed that the "on" switch state of infection is realized by the *cis*-to-*trans* isomerization of the Gln212-Pro213 peptide bond of the gene-3-protein whereas re-isomerization to *trans* actuates the "off" position for phage infectivity [91]. Switching the cell-signaling adaptor protein Crk represents another impressive

example for the PCTI-based regulation of signal transduction [240]. Of course, a rate-limiting PCTI switch might be kinetically suspended when the respective peptide bond undergoes enzymatic catalysis by a PCTIase.

However, looking to the future, enzymatically enhanced chain dynamics of substrate proteins deserves closer attention. How the dynamics of a molecule contribute to its function has long been a matter of debate and controversy [241, 243].

To render proteins functional by means of catalytically controlled chain dynamics on the basis of site-specific enzymes is a fascinating new aspect of PCTIase research.

Probing physiological pathways in response to isoenzyme-specific inhibitors of PCTIases will become increasingly important. Characterizing and understanding of these pathways may be an effective strategy for determining previously undescribed PCTIase targets and thus for future drug development.

References

1. Dugave C (ed) (2006) *cis/trans* Isomerization in biochemistry. Wiley-VCH Verlag, Weinheim
2. Stewart DE, Sarkar A, Wampler JE (1990) J Mol Biol 214:253
3. Jabs A, Weiss MS, Hilgenfeld R (1999) J Mol Biol 286:291
4. Wathen B, Jia ZC (2008) J Proteome Res 7:145
5. Exarchos KP, Exarchos TP, Papaloukas C, Troganis AN, Fotiadis DI (2009) BMC Bioinform 10:1471
6. Lorenzen S, Peters B, Goede A, Preissner R, Frommel C (2005) Proteins 58:589
7. Reimer U, Fischer G (2002) Biophys Chem 96:203
8. Kang YK, Jhon JS, Park HS (2006) J Phys Chem B 110:17645
9. Jakob RP, Schmid FX (2009) J Mol Biol 387:1017
10. Gallay PA (2009) Clin Liver Dis 13:403
11. Lu KP, Zhou XZ (2007) Nat Rev Mol Cell Biol 8:904
12. Luban J (2007) J Virol 81:1054
13. Barik S (2006) Cell Mol Life Sci 63:2889
14. Kang CB, Ye H, Dhe-Paganon S, Yoon HS (2008) Neurosignals 16:318
15. Esnault S, Shen ZJ, Malter JS (2008) Crit Rev Immunol 28:45
16. Fischer G, Aumüller T (2004) Rev Physiol Biochem Pharmacol 148:105
17. Bell A, Monaghan P, Page AP (2006) Int J Parasitol 36:261
18. Takahashi K, Uchida C, Shin RW, Shimazaki K, Uchida T (2008) Cell Mol Life Sci 65:359
19. Pappenberger G, Aygun H, Engels JW, Reimer U, Fischer G, Kiefhaber T (2001) Nat Struct Biol 8:452
20. Bieri O, Hellrung B, Schutkowski M, Drewello M, Kiefhaber T (1999) Proc Natl Acad Sci USA 96:9597
21. Brandts JF, Halvorson HR, Brennan M (1975) Biochemistry 14:4953
22. Andreotti AH (2003) Biochemistry 42:9515
23. Ng KKS, Park-Snyder S, Weis WI (1998) Biochemistry 37:17965
24. Weiwad M, Werner A, Rücknagel P, Schierhorn A, Küllertz G, Fischer G (2004) J Mol Biol 339:635
25. Guan RJ, Xiang Y, He XL, Wang CG, Wang M, Zhang Y, Sundberg EJ, Wang DC (2004) J Mol Biol 341:1189

26. Garcia-Pino A, Buts L, Wyns L, Loris R (2006) J Mol Biol 361:153
27. Scherer G, Kramer ML, Schutkowski M, Reimer U, Fischer G (1998) J Am Chem Soc 120:5568
28. Schechter I, Berger A (1967) Biochem Biophys Res Commun 27:157
29. Scholz C, Scherer G, Mayr LM, Schindler T, Fischer G, Schmid FX (1998) Biol Chem 379:361
30. Sekerina E, Rahfeld JU, Muller J, Fanghänel J, Rascher C, Fischer G, Bayer P (2000) J Mol Biol 301:1003
31. Zhang Y, Daum S, Wildemann D, Zhou XZ, Verdecia MA, Bowman ME, Lücke C, Hunter T, Lu KP, Fischer G, Noel JP (2007) ACS Chem Biol 2:320
32. Jordens J, Janssens V, Longin S, Stevens I, Martens E, Bultynck G, Engelborghs Y, Lescrinier E, Waelkens E, Goris J, Van Hoof C (2006) J Biol Chem 281:6349
33. Liu J, Farmer JD Jr, Lane WS, Friedman J, Weissman I, Schreiber SL (1991) Cell 66:807
34. Friedman J, Weissman I (1991) Cell 66:799
35. Schreiber SL (1991) Science 251:283
36. Bang H, Pecht A, Raddatz G, Scior T, Solbach W, Brune K, Pahl A (2000) Eur J Biochem 267:3270
37. Thai V, Renesto P, Fowler CA, Browni DJ, Davis T, Gu WJ, Pollock DD, Kern D, Raoult D, Eisenmesser EZ (2008) J Mol Biol 378:71
38. Fischer G, Bang H, Mech C (1984) Biomed Biochim Acta 43:1101
39. Fischer G, Wittmann-Liebold B, Lang K, Kiefhaber T, Schmid FX (1989) Nature 337:476
40. Takahashi N, Hayano T, Suzuki M (1989) Nature 337:473
41. Bachinger HP (1987) J Biol Chem 262:17144
42. Lang K, Schmid FX, Fischer G (1987) Nature 329:268
43. Fischer G, Bang H (1985) Biochim Biophys Acta 828:39
44. Harding MW, Galat A, Uehling DE, Schreiber SL (1989) Nature 341:758
45. Siekierka JJ, Hung SH, Poe M, Lin CS, Sigal NH (1989) Nature 341:755
46. Rahfeld JU, Schierhorn A, Mann K, Fischer G (1994) FEBS Lett 343:65
47. Bergsma DJ, Eder C, Gross M, Kersten H, Sylvester D, Appelbaum E, Cusimano D, Livi GP, McLaughlin MM, Kasyan K, Porter TG, Silverman C, Dunnington D, Hand A, Pritchett WP, Bossard MJ, Brandt M, Levy MA (1991) J Biol Chem 266:23204
48. Jin YJ, Albers MW, Lane WS, Bierer BE, Schreiber SL, Burakoff SJ (1991) Proc Natl Acad Sci USA 88:6677
49. Lu KP, Hanes SD, Hunter T (1996) Nature 380:544
50. Ranganathan R, Lu KP, Hunter T, Noel JP (1997) Cell 89:875
51. Stoller G, Rücknagel KP, Nierhaus KH, Schmid FX, Fischer G, Rahfeld JU (1995) EMBO J 14:4939
52. Hesterkamp T, Hauser S, Lutcke H, Bukau B (1996) Proc Natl Acad Sci USA 93:4437
53. Blaha G, Wilson DN, Stoller G, Fischer G, Willumeit R, Nierhaus KH (2003) J Mol Biol 326:887
54. Kramer G, Rauch T, Rist W, Vorderwulbecke S, Patzelt H, Schulze-Specking A, Ban N, Deuerling E, Bukau B (2002) Nature 419:171
55. Schiene-Fischer C, Habazettl J, Schmid FX, Fischer G (2002) Nat Struct Biol 9:419
56. Lee YS, Marcu MG, Neckers L (2004) Chem Biol 11:991
57. Onuoha SC, Mukund SR, Coulstock ET, Sengerova B, Shaw J, McLaughlin SH, Jackson SE (2007) J Mol Biol 372:287
58. Gell DA, Feng L, Zhou SP, Jeffrey PD, Bendak K, Gow A, Weiss MJ, Shi YG, Mackay JP (2009) J Biol Chem 284:29462
59. Sayah DM, Sokolskaja E, Berthoux L, Luban J (2004) Nature 430:569
60. Neagu MR, Ziegler P, Pertel T, Strambio-De-Castillia C, Grutter C, Martinetti G, Mazzucchelli L, Grutter M, Manz MG, Luban J (2009) J Clin Invest 119:3035
61. He ZY, Li LG, Luan S (2004) Plant Physiol 134:1248
62. Adams B, Musiyenko A, Kumar R, Barik S (2005) J Biol Chem 280:24308

63. Schiene C, Fischer G (2000) Curr Opin Struct Biol 10:40
64. Schmid FX (2005) In: Buchner J, Kiefhaber T (eds) Protein folding handbook. Wiley-VCH, Weinheim, p 916
65. Fischer G, Bang H, Berger E, Schellenberger A (1984) Biochim Biophys Acta 791:87
66. Brandts JF, Lin LN (1986) Meth Enzymol 131:107
67. Weiwad M, Küllertz G, Schutkowski M, Fischer G (2000) FEBS Lett 478:39
68. Zhou XZ, Kops O, Werner A, Lu PJ, Shen MH, Stoller G, Küllertz G, Stark M, Fischer G, Lu KP (2000) Mol Cell 6:873
69. Brandsch M, Thunecke F, Küllertz G, Schutkowski M, Fischer G, Neubert K (1998) J Biol Chem 273:3861
70. Bailey PD, Boyd CAR, Collier ID, Kellett GL, Meredith D, Morgan KM, Pettecrew R, Price RA (2005) Org Biomol Chem 3:4038
71. Lummis SCR, Beene DL, Lee LW, Lester HA, Broadhurst RW, Dougherty DA (2005) Nature 438:248
72. Wittelsberger A, Keller M, Scarpellino L, Patiny L, Acha-Orbea H, Mutter M (2000) Angew Chem Int Ed 39:1111
73. Garciaecheverria C, Kofron JL, Kuzmic P, Kishore V, Rich DH (1991) J Am Chem Soc 114:2758
74. Kramer ML, Fischer G (1997) Biopolymers 42:49
75. Zoldak G, Aumüller T, Lücke C, Hritz J, Ostenbrink C, Fischer G, Schmid FX (2009) Biochemistry 48:10423
76. Bosco DA, Eisenmesser EZ, Pochapsky S, Sundquist WI, Kern D (2002) Proc Natl Acad Sci USA 99:5247
77. Kern D, Scherer G, Fischer G, Drakenberg T (1995) Biochemistry 34:13594
78. Videen JS, Stamnes MA, Hsu VL, Goodman M (1994) Biopolymers 34:171
79. Lippens G, Landrieu I, Smet C (2007) FEBS J 274:5211
80. Hubner D, Drakenberg T, Forsen S, Fischer G (1991) FEBS Lett 284:79
81. Eisenmesser EZ, Bosco DA, Akke M, Kern D (2002) Science 295:1520
82. Kern D, Eisenmesser EZ, Wolf-Watz M (2005) Nucl Magn Reson Biol Macromol 394:507
83. Scholz C, Zarnt T, Kern G, Lang K, Burtscher H, Fischer G, Schmid FX (1996) J Biol Chem 273:12703
84. Veeraraghavan S, Holzman TF, Nall BT (1996) Biochemistry 35:10601
85. Schiene-Fischer C, Habazettl J, Tradler T, Fischer G (2002) Biol Chem 383:1865
86. Thies MJW, Mayer J, Augustine JG, Frederick CA, Lilie H, Buchner J (1999) J Mol Biol 293:67
87. Agarwal RP, Threatte GA, McPherson R (1987) Clin Chem 33:481
88. Baughman G, Wiederrecht GJ, Chang F, Martin MM, Bourgeois S (1997) Biochem Biophys Res Commun 232:437
89. Ryffel B, Foxwell BM, Gee A, Greiner B, Woerly G, Mihatsch MJ (1988) Transplantation 46:90S
90. Fischer G (1994) Angew Chem Int Ed 33:1415
91. Eckert B, Martin A, Balbach J, Schmid FX (2005) Nat Struct Mol Biol 12:619
92. Lu KP, Finn G, Lee TH, Nicholson LK (2007) Nat Chem Biol 3:619
93. Coaker G, Falick A, Staskawicz B (2005) Science 308:548
94. Aumüller T, Jahreis G, Fischer G, Schiene-Fischer C (2010) Biochemistry 49:1042
95. Burbaum JJ, Raines RT, Albery WJ, Knowles J (1989) Biochemistry 28:9293
96. Fanghänel J, Fischer G (2004) Front Biosci 9:3453
97. Billich A, Winkler G, Aschauer H, Rot A, Peichl P (1997) J Exp Med 185:975
98. Andreeva L, Heads R, Green CJ (1999) Int J Exp Pathol 80:305
99. Yeh ES, Means AR (2007) Nat Rev 7:381
100. Choi KJ, Piao YJ, Lim MJ, Kim JH, Ha J, Choe W, Kim SS (2007) Cancer Res 67:3654
101. Obchoei S, Wongkhan S, Wongkham C, Li M, Yao QZ, Chen CY (2009) Med Sci Monit 15:221

102. Park ST, Aldape RA, Futer O, DeCenzo MT, Livingston DJ (1992) J Biol Chem 267:3316
103. Kofron JL, Kuzmic P, Kishore V, Colon-Bonilla E, Rich DH (1991) Biochemistry 30:6127
104. Jakob RP, Zoldak G, Aumüller T, Schmid FX (2009) Proc Natl Acad Sci USA 106:20282
105. Scholz C, Stoller G, Zarnt T, Fischer G, Schmid FX (1997) EMBO J 16:54
106. Pappenberger G, Bachmann A, Muller R, Aygun H, Engels JW, Kiefhaber T (2003) J Mol Biol 326:235
107. Wu XY, Wilcox CB, Devasahayam G, Hackett RL, Arevalo-Rodriguez M, Cardenas ME, Heitman J, Hanes SD (2000) EMBO J 19:3727
108. Fujimori F, Gunji W, Kikuchi J, Mogi T, Ohashi Y, Makino T, Oyama A, Okuhara K, Uchida T, Murakami Y (2001) Biochem Biophys Res Commun 289:181
109. Kipping M, Zarnt T, Kiessig S, Reimer U, Fischer G, Bayer P (2001) Biochemistry 40:7957
110. Schiene C, Reimer U, Schutkowski M, Fischer G (1998) FEBS Lett 432:202
111. Piotukh K, Gu W, Kofler M, Labudde D, Helms V, Freund C (2005) J Biol Chem 280:23668
112. Harrison RK, Stein RL (1990) Biochemistry 29:3813
113. Gamble TR, Vajdos FF, Yoo SH, Worthylake DK, Houseweart M, Sundquist WI, Hill CP (1996) Cell 87:1285
114. Golbik R, Yu C, Weyher-Stingl E, Huber R, Moroder L, Budisa N, Schiene-Fischer C (2005) Biochemistry 44:16026
115. Edlich F, Weiwad M, Erdmann F, Fanghänel J, Jarczowski F, Rahfeld JU, Fischer G (2005) EMBO J 24:2688
116. Hottenrott S, Schumann T, Plückthun A, Fischer G, Rahfeld JU (1997) J Biol Chem 272:15697
117. Martino L, He YZ, Hands-Taylor KLD, Valentine ER, Kelly G, Giancola C, Conte MR (2009) FEBS J 276:4529
118. Motohashi K, Koyama F, Nakanishi Y, Ueoka-Nakanishi H, Hisabori T (2003) J Biol Chem 278:31848
119. Gopalan G, He Z, Balmer Y, Romano P, Gupta R, Heroux A, Buchanan BB, Swaminathan K, Luan S (2004) Proc Natl Acad Sci USA 101:13945
120. Gourlay LJ, Angelucci F, Baiocco P, Boumis G, Brunori M, Bellelli A, Miele AE (2007) J Biol Chem 282:24851
121. Shapiguzov A, Edvardsson A, Vener AV (2006) FEBS Lett 580:3671
122. Hennig L, Christner C, Kipping M, Schelbert B, Rücknagel KP, Grabley S, Küllertz G (1998) Fischer G 37:5953
123. Vandekerckhove J, Gianazza E, Ghezzi P (2002) Proc Natl Acad Sci USA 99:3505
124. Fratelli M, Demol H, Puype M, Casagrande S, Villa P, Eberini I, Vandekerckhove J, Gianazza E, Ghezzi P (2003) Proteomics 3:1154
125. Ghezzi P, Casagrande S, Massignan T, Basso M, Bellacchio E, Mollica L, Biasini E, Tonelli R, Eberini I, Gianazza E, Dai WW, Fratelli M, Salmona M, Sherry B, Bonetto V (2006) Proteomics 6:817
126. Choudhary C, Kumar C, Gnad F, Nielsen ML, Rehman M, Walther TC, Olsen JV, Mann M (2009) Science 325:834
127. Lammers M, Neumann H, Chin JW, James LC (2010) Nat Chem Biol 6:331
128. DiNovo AA, Schey KL, Vachon WS, McGuffie EM, Olson JC, Vincent TS (2006) Biochemistry 45:4664
129. Steplewski A, Ebel W, Planey SL, Alnemri ES, Robertson NM, Litwack G (2000) Gene 246:169
130. Min SH, Cho JS, Oh JH, Shim SB, Hwang DY, Lee SH, Jee SW, Lim HJ, Kim MY, Sheen YY, Kim YK (2005) Neurochem Res 30:955
131. Eckerdt F, Yuan JP, Saxena K, Martin B, Kappel S, Lindenau C, Kramer A, Naumann S, Daum S, Fischer G, Dikic I, Kaufmann M, Strebhardt K (2005) J Biol Chem 280:36575
132. Shen ZJ, Esnault S, Malter JS (2005) Nat Immunol 6:1280
133. Lu PJ, Zhou XZ, Liou YC, Noel JP, Lu KP (2002) J Biol Chem 277:2381

134. Jeffery CJ (1999) Trends Biochem Sci 24:8
135. Montague JW, Hughes FM, Cidlowski JA (1997) J Biol Chem 272:6677
136. Nicieza RG, Huergo J, Connolly BA, Sanchez J (1999) J Biol Chem 274:20366
137. Schmidt B, Tradler T, Rahfeld JU, Ludwig B, Jain B, Mann K, Rücknagel KP, Janowski B, Schierhorn A, Küllertz G, Hacker J, Fischer G (1996) Mol Microbiol 21:1147
138. Manteca A, Sanchez J (2004) J Bacteriol 186:6325
139. Quemeneur E, Moutiez M, Charbonnier JB, Menez A (1998) Nature 391:301
140. Wallace AC, Laskowski RA, Thornton JM (1996) Protein Sci 5:1001
141. Dominguez-Solis JR, He ZY, Lima A, Ting JL, Buchanan BB, Luan S (2008) Proc Natl Acad Sci USA 106:16386
142. Lee SP, Hwang YS, Kim YJ, Kwon KS, Kim HJ, Kim K, Chae HZ (2001) J Biol Chem 276:29826
143. Boulos S, Meloni BP, Arthur PG, Majda B, Bojarski C, Knuckey NW (2007) Neurobiol Dis 25:54
144. Homme MB, Carter C, Scarlata S (2005) Biophys J 88:2078
145. Hamelberg D, McCammon A (2009) J Am Chem Soc 131:147
146. Ma LF, Hsieh-Wilson LC, Schultz PG (1998) Proc Natl Acad Sci USA 95:7251
147. Ikura T, Ito N (2007) Protein Sci 16:2618
148. Ikura T, Kinoshita K, Ito N (2008) Protein Eng Des Sel 21:83
149. Eberhardt ES, Loh SN, Hinck AP, Raines RT (1992) J Am Chem Soc 114:5437
150. Zydowsky LD, Etzkorn FA, Chang HY, Ferguson SB, Stolz LA, Ho SI, Walsh CT (1992) Protein Sci 1:1092
151. Fraser JS, Clarkson MW, Degnan SC, Erion R, Kern D, Alber T (2009) Nature 462:669
152. Brath U, Akke M (2009) J Mol Biol 387:233
153. Harrison RK, Stein RL (1992) J Am Chem Soc 114:3464
154. Ke HM, Mayrose D, Cao W (1993) Proc Natl Acad Sci USA 90:3324
155. Baum N, Schiene-Fischer C, Frost M, Schumann M, Sabapathy K, Ohlenschlager O, Grosse F, Schlott B (2009) Oncogene 28:3915
156. Schutkowski M, Wöllner S, Fischer G (1994) Biochemistry 34:13016
157. Kang YK (2006) J Phys Chem B 110:21338
158. Tchaicheeyan O (2004) FASEB J 18:783
159. Agarwal PK (2004) Proteins 56:449
160. Howard BR, Vajdos FF, Li S, Sundquist WI, Hill CP (2003) Nat Struct Biol 10:475
161. Pirkl F, Buchner J (2001) J Mol Biol 308:795
162. Bose S, Weikl T, Bugl H, Buchner J (1996) Science 274:1715
163. Chakraborty A, Das I, Datta R, Sen B, Bhattacharyya D, Mandal C, Datta AK (2002) J Biol Chem 277:47451
164. Mok D, Allan RK, Carrello A, Wangoo K, Walkinshaw MD, Ratajczak T (2006) FEBS Lett 580:2761
165. Moparthi SB, Fristedt R, Mishra R, Almstedt K, Karlsson M, Hammarström P, Carlsson U (2010) Biochemistry 49:1137
166. Fischer G, Wawra S (2006) Mol Microbiol 61:1388
167. Hulko M, Lupas AN, Martin J (2007) Protein Sci 16:644
168. Kuzuhara T, Horikoshi M (2004) Nat Struct Mol Biol 11:275
169. Wang XDJ, Etzkorn FA (2006) Biopolymers 84:125
170. Sanglier JJ, Quesniaux V, Fehr T, Hofmann H, Mahnke M, Memmert K, Schuler W, Zenke G, Gschwind L, Maurer C, Schilling W (1999) J Antibiot 52:466
171. Kung L, Batiuk TD, Palomo-Pinon S, Noujaim J, Helms LM, Halloran PF (2001) Am J Transplant 1:325
172. Baumgrass R, Zhang YX, Erdmann F, Thiel A, Weiwad M, Radbruch A, Fischer G (2004) J Biol Chem 279:2470
173. Zhang YX, Baumgrass R, Schutkowski M, Fischer G (2004) Chembiochem 5:1006

174. Sigal NH, Dumont F, Durette P, Siekierka JJ, Peterson L, Rich DH, Dunlap BE, Staruch MJ, Melino MR, Koprak SL (1991) J Exp Med 173:619
175. Fliri H, Baumann G, Enz A, Kallen J, Luyten M, Mikol V, Movva R, Quesniaux V, Schreier M, Walkinshaw M, Wenger R, Zenke G, Zurini M (1993) Ann NY Acad Sci 696:47
176. Theriault Y, Logan TM, Meadows R, Yu L, Olejniczak ET, Holzman TF, Simmer RL, Fesik SW (1993) Nature 361:88
177. Bossard MJ, Koser PL, Brandt M, Bergsma DJ, Levy MA (1991) Biochem Biophys Res Commun 176:1142
178. Tanaka H, Kuroda A, Marusawa H, Hatanaka H, Kino T, Goto T, Hashimoto M, Taga T (1987) J Am Chem Soc 109:5031
179. Weiwad M, Edlich F, Kilka S, Erdmann F, Jarczowski F, Dorn M, Moutty MC, Fischer G (2006) Biochemistry 45:15776
180. Rosen MK, Standaert RF, Galat A, Nakatsuka M, Schreiber SL (1990) Science 248:863
181. Goulet MT, Rupprecht KM, Sinclair PJ, Wyvratt MJ, Parsons WH (1994) Perspect Drug Discovery Des 2:145
182. Itoh S, Decenzo MT, Livingston DJ, Pearlman DA, Navia MA (1995) Bioorg Med Chem Lett 5:1983
183. Kawai M, Lane BC, Hsieh GC, Mollison KW, Carter GW, Luly JR (1993) FEBS Lett 316:107
184. Bierer BE, Somers PK, Wandless TJ, Burakoff SJ, Schreiber SL (1990) Science 250:556
185. Bierer BE, Mattila PS, Standaert RF, Herzenberg LA, Burakoff SJ, Crabtree G, Schreiber SL (1990) Proc Natl Acad Sci USA 87:9231
186. Brown EJ, Albers MW, Shin TB, Ichikawa K, Keith CT, Lane WS, Schreiber SL (1994) Nature 369:756
187. Sabatini DM, Erdjumentbromage H, Lui M, Tempst P, Snyder SH (1994) Cell 78:35
188. Chiu MI, Katz H, Berlin V (1994) Proc Natl Acad Sci USA 91:12574
189. Meric-Bernstam F, Gonzalez-Angulo AM (2009) J Clin Oncol 27:2278
190. Le Tourneau C, Faivre S, Serova M, Raymond E (2008) Br J Cancer 99:1197
191. Fasolo A, Sessa C (2008) Expert Opin Investig Drugs 17:1717
192. Choi JW, Chen J, Schreiber SL, Clardy J (1996) Science 273:239
193. Ocain TD, Longhi D, Steffan RJ, Caccese RG, Sehgal SN (1993) Biochem Biophys Res Commun 192:1340
194. Sedrani R, Jones LH, Jutzi-Eme AM, Schuler W, Cottens S (1999) Bioorg Med Chem Lett 9:459
195. Rosenwirth B, Billich A, Datema R, Donatsch P, Hammerschmid F, Harrison R, Hiestand P, Jaksche H, Mayer P, Peichl P, Quesniaux V, Schatz F, Schuurman HJ, Traber R, Wenger R, Wolff B, Zenke G, Zurini M (1994) Antimicrob Agents Chemother 38:1763
196. Ptak RG, Gallay PA, Jochmans D, Halestrap AP, Ruegg UT, Pallansch LA, Bobardt MD, de Bethune MP, Neyts J, De Clercq E, Dumont JM, Scalfaro P, Besseghir K, Wenger RM, Rosenwirth B (2008) Antimicrob Agents Chemother 52:1302
197. Hopkins S, Scorneaux B, Huang Z, Murray MG, Wring S, Smitley C, Harris R, Erdmann F, Fischer G, Ribeill Y (2010) Antimicrob Agents Chemother 54:660
198. Malesević M, Kühling J, Erdmann F, Balsley MA, Bukrinsky MI, Constant SL, Fischer G (2010) Angew Chem Int Ed 49:213
199. Malouitre S, Dube H, Selwood D, Crompton M (2010) Biochem J 425:137
200. Sedrani R, Kallen J, Cabrejas LMM, Papageorgiou CD, Senia F, Rohrbach S, Wagner D, Thai B, Eme AMJ, France J, Oberer L, Rihs G, Zenke G, Wagner J (2003) J Am Chem Soc 125:3849
201. Zenke G, Strittmatter U, Fuchs S, Quesniaux VFJ, Brinkmann V, Schuler W, Zurini M, Enz A, Billich A, Sanglier JJ, Fehr T (2001) J Immunol 166:7165
202. Zhang LH, Liu JO (2001) J Immunol 166:5611
203. Taylor P, Blackburn E, Sheng YG, Harding S, Hsin KY, Kan D, Shave S, Walkinshaw M (2008) Br J Pharmacol 153:S55

204. Li J, Chen J, Zhang L, Wang F, Gui CS, Qin Y, Xu Q, Liu H, Nan FJ, Shen JK, Bai DL, Chen KX, Shen X, Jiang HL (2006) Bioorg Med Chem 14:5527
205. Hart SA, Etzkorn FA (1999) J Org Chem 64:2998
206. Wang HC, Kim K, Bakhtiar R, Germanas JP (2001) J Med Chem 44:2593
207. Demange L, Moutiez M, Dugave C (2002) J Med Chem 45:3928
208. Clavaud C, Heckenroth M, Stricane C, Menez A, Dugave C (2006) Bioconjug Chem 17:807
209. Daum S, Erdmann F, Fischer G, de Lacroix BF, Hessamian-Alinejad A, Houben S, Frank W, Braun M (2006) Angew Chem Int Ed 45:7454
210. Daum S, Schumann M, Mathea S, Aumüller T, Balsley MA, Constant SL, de Lacroix BF, Kruska F, Braun M, Schiene-Fischer C (2009) Biochemistry 48:6268
211. Dumont FJ, Staruch MJ, Koprak SL, Siekierka JJ, Lin CS, Harrison R, Sewell T, Kindt VM, Beattie TR, Wyvratt M (1992) J Exp Med 176:751
212. Price RD, Yamaji T, Yamamoto H, Higashi Y, Hanaoka K, Yamazaki S, Ishiye M, Aramori I, Matsuoka N, Mutoh S, Yanagihara T, Gold BG (2005) Eur J Pharmacol 509:11
213. Ruan B, Pong K, Jow F, Bowlby M, Crozier RA, Liu D, Liang S, Chen Y, Mercado ML, Feng X, Bennett F, von Schack D, McDonald L, Zaleska MM, Wood A, Reinhart PH, Magolda RL, Skotnicki J, Pangalos MN, Koehn FE, Carter GT, Abou-Gharbia M, Graziani EI (2008) Proc Natl Acad Sci USA 105:33
214. Armistead DM, Badia MC, Deininger DD, Duffy JP, Saunders JO, Tung RD, Thomson JA, Decenzo MT, Futer O, Livingston DJ, Murcko MA, Yamashita MM, Navia MA (1995) Acta Crystallogr D 51:522
215. Holt DA, Konialianbeck AL, Oh HJ, Yen HK, Rozamus LW, Krog AJ, Erhard KF, Ortiz E, Levy MA, Brandt M, Bossard MJ, Luengo JI (1994) Bioorg Med Chem Lett 4:315
216. Choi C, Li JH, Vaal M, Thomas C, Limburg D, Wu YQ, Chen Y, Soni R, Scott C, Ross DT, Guo H, Howorth P, Valentine H, Liang S, Spicer D, Fuller M, Steiner J, Hamilton GS (2002) Biol Med Chem Lett 12:1421
217. Wei L, Wu Y, Wilkinson DE, Chen Y, Soni R, Scott C, Ross DT, Guo H, Howorth P, Valentine H, Liang S, Spicer D, Fuller M, Steiner J, Hamilton GS (2002) Biol Med Chem Lett 12:1429
218. Hudack RA Jr, Barta NS, Guo C, Deal J, Dong L, Fay LK, Caprathe B, Chatterjee A, Vanderpool D, Bigge C, Showalter R, Bender S, Augelli-Szafran CE, Lunney E, Hou X (2006) J Med Chem 49:1202
219. Holt DA, Luengo JI, Yamashita DS, Oh HJ, Konialian AL, Yen HK, Rozamus LW, Brandt M, Bossard MJ, Levy MA, Eggleston DS, Liang J, Schultz LW, Stout TJ, Clardy J (1993) J Am Chem Soc 115:9925
220. Edlich F, Weiwad M, Wildemann D, Jarczowski F, Kilka S, Moutty MC, Jahreis G, Lücke C, Schmidt W, Striggow F, Fischer G (2006) J Biol Chem 281:14961
221. Gold BG (2000) Expert Opin Inv Drug 9:2331
222. Fanghänel J, Fischer G (2003) Biophys Chem 100:351
223. Zink DL, Dahl A, Nielsen J, Wu E, Huang L, Kastner C, Dumont FJ (1995) Tetrahedron Lett 36:997
224. Fehr T, Sanglier JJ, Schuler W, Gschwind L, Ponelle M, Schilling W, Wioland C (1996) J Antibiot 49:230
225. Raju R, Piggott AM, Conte M, Tnimov Z, Alexandrov K, Capon RJ (2010) Chemistry 16:3194
226. Burkhard P, Hommel U, Sanner M, Walkinshaw MD (1999) J Mol Biol 287:853
227. Christner C, Wyrwa R, Marsch S, Küllertz G, Thiericke R, Grabley S, Schumann D, Fischer G (1999) J Med Chem 42:3615
228. Wildemann D, Erdmann F, Alvarez BH, Stoller G, Zhou XZ, Fanghänel J, Schutkowski M, Lu KP, Fischer G (2006) J Med Chem 49:2147
229. Daum S, Fanghänel J, Wildemann D, Schiene-Fischer C (2006) Biochemistry 45:12125
230. Daum S, Lücke C, Wildemann D, Schiene-Fischer C (2007) J Mol Biol 374:147
231. Wang XJ, Xu B, Mullins AB, Neiler FK, Etzkorn FA (2004) J Am Chem Soc 126:15533

232. Siegrist R, Zürcher M, Baumgartner C, Seiler P, Diederich F, Daum S, Fischer G, Klein C, Dangl M, Schwaiger M (2007) Helv Chim Acta 90:217
233. Bayer E, Thutewohl M, Christner C, Tradler T, Osterkamp F, Waldmann H, Bayer P (2005) Chem Commun (Camb) 28:516
234. Guo CX, Hou XJ, Dong LM, Dagostino E, Greasley S, Ferre R, Marakovits J, Johnson MC, Matthews D, Mroczkowski B, Van Arsdale T, Popoff I, Piraino J, Margosiak S, Thomson J, Los G, Murray BW (2009) Bioorg Med Chem Lett 19:5613
235. Potter AJ, Ray S, Gueritz L, Nunns CL, Bryant CJ, Scrace SF, Matassova N, Baker L, Dokurno P, Robinson DA, Surgenor AE, Davis B, Murray JB, Richardson CM, Moore JD (2010) Bioorg Med Chem Lett 20:586
236. Tatara Y, Lin YC, Bamba Y, Mori T, Uchida T (2009) Biochem Biophys Res Commun 384:394
237. Liebscher M, Jahreis G, Lücke C, Grabley S, Raina S, Schiene-Fischer C (2007) J Biol Chem 282:4437
238. Wisen S, Gestwicki JE (2008) Anal Biochem 374:371
239. Wildemann D, Schiene-Fischer C, Aumüller T, Bachmann A, Kiefhaber T, Lücke C, Fischer G (2007) J Am Chem Soc 129:4910
240. Sarkar P, Reichman C, Saleh T, Birge RB, Kalodimos CG (2007) Mol Cell 25:413
241. Daniel RM, Dunn RV, Finney JL, Smith JC (2003) Annu Rev Biophys Biomol Struct 32:69
242. Gemmill TR, Wu XY, Hanes SD (2005) J Biol Chem 280:15510
243. Kamerlin SCL, Warshel A (2010) Proteins 78:1339

Top Curr Chem (2013) 328: 69–98
DOI: 10.1007/128_2012_324

Published online: 11 May 2012

Small Heat-Shock Proteins: Paramedics of the Cell

Gillian R. Hilton, Hadi Lioe, Florian Stengel, Andrew J. Baldwin, and Justin L.P. Benesch

Abstract The small heat-shock proteins (sHSPs) comprise a family of molecular chaperones which are widespread but poorly understood. Despite considerable effort, comparatively few high-resolution structures have been determined for the sHSPs, a likely consequence of their tendency to populate ensembles of interconverting conformational and oligomeric states at equilibrium. This dynamic structure appears to underpin the sHSPs' ability to bind and sequester target proteins rapidly, and renders them the first line of defence against protein aggregation during disease and cellular stress. Here we describe recent studies on the sHSPs, with a particular focus on those which have provided insight into the structure and dynamics of these proteins. The combined literature reveals a picture of a remarkable family of molecular chaperones whose thermodynamic and kinetic properties are exquisitely balanced to allow functional regulation by subtle changes in cellular conditions.

Keywords α-Crystallin, Molecular chaperone, Polydispersity, Protein dynamics, Small heat-shock protein (sHSP)

Contents

G.R. Hilton, H. Lioe, F. Stengel and J.L.P. Benesch (✉)
Physical & Theoretical Chemistry Laboratory, Department of Chemistry, University of Oxford, South Parks Road, Oxford OX1 3QZ, UK
e-mail: justin.benesch@chem.ox.ac.uk

A.J. Baldwin
Departments of Molecular Genetics, Biochemistry, and Chemistry, University of Toronto, Toronto, ON, Canada

Abbreviations

Af	*Archaeoglobus fulgidus*
At	*Arabidopsis thaliana*
Bt	*Bos taurus* (cow)
Dr	*Danio rerio* (zebrafish)
E. coli	*Escherichia coli*
EM	Electron microscopy
EPR	Electron paramagnetic resonance spectroscopy
Hs	*Homo sapiens* (human)
IM	Ion mobility
Mj	*Methanocaldococcus jannaschii*
MS	Mass spectrometry
Mt	*Mycobacterium tuberculosis*
nES	Nanoelectrospray
NMR	Nuclear magnetic resonance spectroscopy
Ps	*Pisum sativum* (pea)
Rn	*Rattus norvegicus* (brown rat)
Sc	*Saccharomyces cerevisiae* (bakers' yeast)
sHSP	Small heat shock protein
Ta	*Triticum aestivum* (wheat)
Tsp	*Taenia saginata* (beef tapeworm)
Xa	*Xanthomonas axoponidis*

Gillian R. Hilton, Hadi Lioe and Florian Stengel contributed equally to this work.

1 Introduction

The small heat-shock proteins (sHSPs) are a family of almost ubiquitous stress proteins [1]. Most organisms encode multiple sHSP genes, an observation particularly clear in the case of higher organisms [2], with Californian Poplar having as many as 36 [3]. In humans the sHSPs number 10 [4] and are implicated in a range of cellular processes including modulation of cytoskeletal dynamics, stabilisation of membranes and apoptosis [5]. These diverse cellular roles appear to be linked by the ability of the majority of the sHSPs to interact with non-native states of proteins [6, 7]. This property is fundamental to their general behaviour as "molecular chaperones" [8], acting to prevent improper polypeptide associations and aggregation [9].

Molecular chaperones play a vital role in protein homeostasis [10], the mechanism through which the cell maintains proper function by balancing the influence of a multitude of biochemical pathways [11]. It has recently become apparent that the native state of proteins is in general less thermodynamically favoured than the amyloid aggregates they can form [12], revealing an underlying metastability of the proteome [13]. Consequently, the breakdown of "proteostasis" can lead to a variety of diseases [14], many of which are characterised by the aggregation and deposition of misfolded proteins [15]. sHSPs represent a central node in the proteostasis "network" [11], and in the main are dramatically up-regulated under conditions of cellular stress to being among the most abundant of all proteins [16, 17]. Furthermore, they are often found associated with protein aggregates obtained post mortem from victims of protein-misfolding disorders [18]. The sHSPs' chaperone function is therefore crucial to the cell's tolerance to stress, and their malfunction is implicated in a range of human pathologies [19–21]. Together these observations suggest that the sHSPs are on the front line of defence against the deleterious consequences of protein unfolding.

Despite their obvious importance, the sHSPs remain relatively poorly characterised on the molecular level. This is largely due to their tendency to populate a range of dynamic oligomeric states at equilibrium, rendering them refractory to many structural biology approaches [22]. As a consequence, high-resolution information exists only for very few members of the family [9]. Recent years have, however, seen considerable developments in the techniques available to structural biologists, and the means to combine data from multiple sources into "hybrid" approaches [23, 24]. Concomitantly there have been significant recent advances in our understanding of the sHSPs. Here we describe the current knowledge of the structure and dynamics of these remarkable molecular chaperones and their interaction with target proteins.

2 The Dynamic Architecture of sHSPs

Proteins are inherently highly dynamic entities [25–27], and an appreciation of how their different structural forms interconvert is necessary to understand how they carry out their cellular roles [24]. These fluctuations can span picoseconds to days,

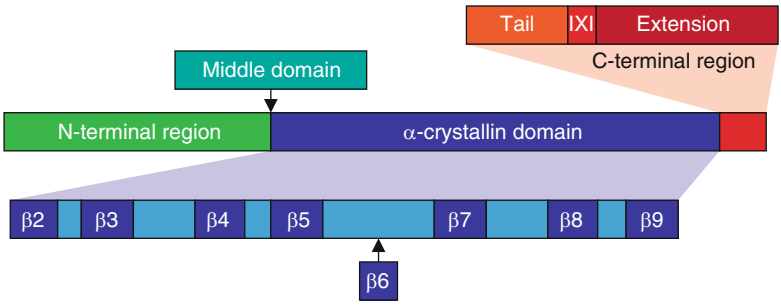

Fig. 1 Domain architecture of the sHSPs. The defining element and most highly conserved region of the sHSP sequence is the α-crystallin domain, which is flanked by the variable N- and C-terminal regions. The α-crystallin domain is composed of seven or eight β-strands, for metazoans or non-metazoans, respectively [37]. In the latter, the sequence between β5 and β7 contains an additional, and distinct, β6 strand. In the metazoans this loop region is shortened, and instead the β7 strand is elongated, into a "β6 + 7" strand. This leads to two alternative modes of dimerisation for the sHSPs (see Fig. 2). The C-terminal region is split into two parts, referred to here as the "tail" and "extension", separated by an IXI motif. The N-terminal region by contrast has no obvious sub-divisions. In HSP26, however, limited proteolysis has revealed a "middle domain" which is inserted between the N-terminal region and α-crystallin domain [35]

have diverse amplitudes and span all levels of protein organisation [28]. Furthermore, the emerging consensus is that sparsely populated "excited" states are frequently responsible for the molecular recognition events underpinning biological function [29–33]. The sHSPs represent a particularly intriguing illustration of this dynamical paradigm: although they share common features, these chaperones undergo intrinsic motions and conformational rearrangements on a wide range of both spatial and temporal scales.

2.1 sHSP Primary Structure

The sHSP family is characterised by the presence of an "α-crystallin" domain [34], derived from the eponymous mammalian sHSP. This central domain is flanked by N- and C-terminal regions (Fig. 1). As perhaps to be expected for a family as large as the sHSPs, exceptions to this basic subdivision exist, including the presence of a "middle domain" [35] or multiple α-crystallin domains [36]. A comprehensive bioinformatics analysis of more than 8,700 sHSP sequences has revealed sHSPs to be composed of on average 161 amino acids [2], corresponding to approximately 17.9 kDa. With an average length of 94 residues, the α-crystallin domain typically composes the bulk of the sequence (approximately 58%). The N-terminus has an average length of 56 residues (35%), whereas at 10 residues (6%) the C-terminus is much shorter.

As the defining element of the sHSP family, the α-crystallin domain is the most conserved region of the sHSP sequence. Interestingly, genomic data has revealed there to be an under-representation of aromatic residues, and an over-representation

of charged amino acids in this domain [2]. Additionally there are notable positions of particularly high conservation, for example the "disease arginine" (at position 120 in αB-crystallin) [37], mutation at which results in a variety of pathologies [38].

The C-terminal region is generally considered to be of two segments, termed here as the "tail" and "extension" [39], which are separated by a highly conserved IXI motif (Fig. 1). The extension appears to be present primarily in higher eukaryotes [39]. In some members of the sHSP family, e.g. human HSP20 [40] and *Taenia saginata* TSP36 [36], the entire C-terminal region is absent. The N-terminal region is however essentially omnipresent and, in the main, considerably longer. It displays almost no sequence conservation, and is responsible for the majority of the sequence variation between sHSPs in the same organism [2]. Additionally, sites available for post-translational modification appear to be found largely in this part of the protein [41]. It is quite possible that this variability of the N-terminus may have a role to play in ensuring that a cell's cohort of sHSPs can recognise a wide range of target proteins.

2.2 The Protomeric α-Crystallin Domain Dimer

High-resolution structures have been very hard to come by for the sHSPs, and the vast majority stem from isolated α-crystallin domains, truncated of the terminal regions. All of these structures, however, reveal a common basic fold of the α-crystallin domain, namely an immunoglobulin-like β-sandwich comprising up to nine β-strands (Fig. 2). The different structures align very well, and are replicated in the two structures solved for full-length, oligomeric sHSPs [42, 43]. However a significant difference can be seen between the structures from animals relative to other organisms (Fig. 2). In the structures determined for plant [43], archaeal [42, 44], and bacterial [45] sHSPs dimerisation occurs via reciprocal donation of the β6 strand, located in a loop, into the β-sandwich of a neighbouring monomer. By contrast, in the mammalian sHSPs the β6 strand has fused with β7 [46–48] into an elongated "β6 + 7" strand which had previously been suggested by spectroscopic experiments, and predicted to enable dimerisation [49–51].

Interestingly, SAXS data has indicated that this dimeric interface observed in truncated forms of the mammalian sHSPs has significant flexibility [52]. Further insight comes from X-ray crystallography which has found three distinct alternative registers formed by the paired β6 + 7 strands, causing a translation in the dimer interface, two residues at a time, spanning approximately 15 Å [46, 48, 53] (Fig. 2). These polymorphic states are termed, in order of decreasing overlap between anti-parallel β6 + 7 strands, AP_I, AP_{II} and AP_{III} [48]. Solid-state nuclear magnetic resonance spectroscopy (NMR) revealed that dimerisation of αB-crystallin mediated by β6 + 7 pertains also to full-length protein, but to date only one register, AP_{II}, has been observed [54]. While relating hydrogen/deuterium exchange rates determined for full-length αB-crystallin [55] to the structure of the truncated dimer certainly reveals the interfaces to be dynamic, it remains to be elucidated to what

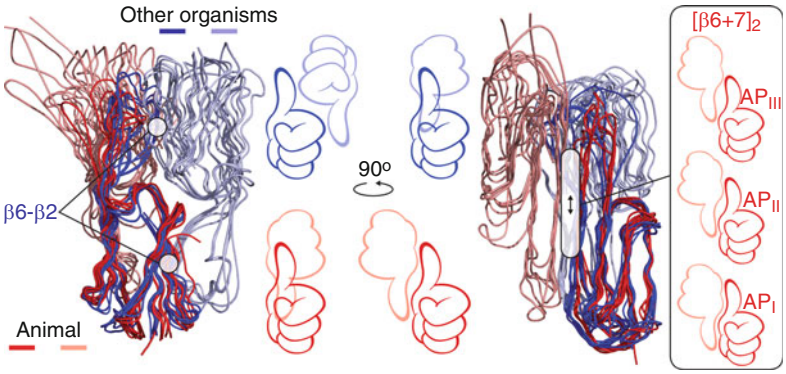

Fig. 2 Distinct dimeric α-crystallin cores. The overall fold of the α-crystallin domain is an immunoglobulin-like β-sandwich with a protruding loop, reminiscent of a "thumbs-up" hand gesture. The structures are highly conserved amongst sHSPs, and accordingly monomers from animals (*red*) and other organisms (*blue*) align very well. The corresponding dimeric partners (*light red* and *light blue*, respectively), however, are found in distinctly different locations, rotated ≈ 180° relative to each other. This is as a result of the non-metazoan proteins dimerising through reciprocal interaction between β6 and β2 strands; whereas the metazoan proteins dimerise through their extended β6 + 7 strands. The latter dimerisation form has been observed in three distinct registers, termed AP_I, AP_{II} and AP_{III}

extent multiple AP interfaces are populated in the oligomers at equilibrium in solution, and whether they interconvert. However, irrespective of these registry shifts, it is clear that, despite very similar basic monomer structures, two distinctly different modes of dimerisation have evolved across the kingdoms of life.

2.3 Heterogeneous N-Termini; Dynamic C-Termini

In contrast to the recent wealth of structural insight into the α-crystallin domain, equivalent information about the termini remains relatively limited. In the crystal structure of *Methanocaldococcus jannaschii* HSP16.5 none of the N-termini are resolved [42]; however EM data revealed additional density within the central cavity of the oligomer [56]. In HSP14.0 from *Sulfolobus tokodaii* two crystal forms were obtained, with the N-termini resolved in one but not the other [44]. Similarly, in the crystal structure of the *Triticum aestivum* HSP16.9 oligomer, half of the N-termini are unresolved; the remainder are structured and found in the centre of the oligomer [57]. Atomic models generated for the N-termini of HSP16.5 [58] and αB-crystallin [59, 60] using sparse spectroscopic restraints, and the N-termini resolved in the crystal structures of HSP16.9 [43], TSP36 [61] and HSP14.0 [44], reveal a propensity to form helical secondary structure.

In apparent contradiction with these results, in hydrogen/deuterium exchange studies of two plant sHSPs, HSP16.9 and *Pisum sativum* HSP18.1, rapid

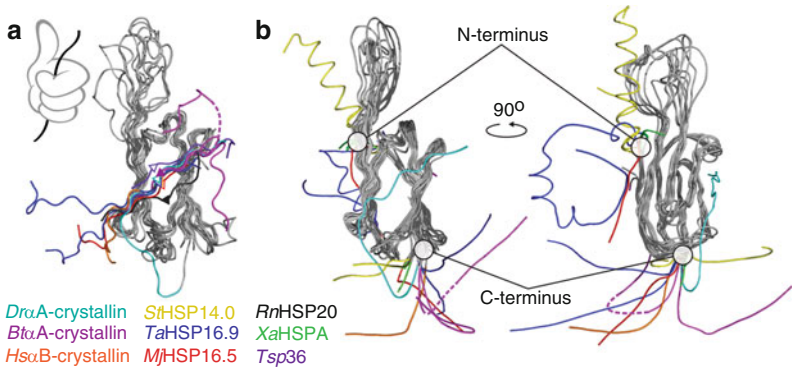

Fig. 3 Variability in the termini. C-termini make inter-dimer contacts, binding over the groove between β4 and β8 strands; by analogy with Fig. 2, the α-crystallin core "hand" grasps the C-terminal "string" from an adjacent monomer (**a**). This interaction has been observed in all crystal structures in which the C-terminal IXI motif is resolved. In other cases (*Tsp*36, *Rn*HSP20) the groove is instead occupied by residues from the N-terminus. Notably both directions of binding have been observed (direction indicated by *triangles* placed in the location of the X in the IXI, *solid arrows* bind *top-right* to *bottom left*). Note that this interaction can even be intra-molecular, as observed in the structure of *Dr*αA-crystallin (*cyan*). The angle which the C-terminus makes from the α-crystallin domain is very variable (**b**). Illustrated are all C-termini resolved in sHSP crystal structures, and it is notable that this variability in angle is found even for the same protein, either in the same oligomer (*Ta*HSP16.9) or in different crystal forms (*St*HSP14.0, *Bt*αA-crystallin). N-terminal residues are observed in fewer structures, but also reveal heterogeneity. This ability of the terminal regions to adopt different orientations is likely crucial for the sHSPs' ability to populate multiple oligomeric states

exchange of the N-terminal backbone amides was observed [62, 63]. Even those positions involved in inter-dimer contacts approached complete exchange with 100 s, and only a single exchanging population was observed [63]. This reveals that all 12 of the N-termini in these dodecameric proteins are essentially equivalent, but does not rule out that at any given moment a sub-population thereof may be structured and form relatively transient interactions. Taking these results in combination with the evidence from the crystal structures suggests that the N-termini populate multiple slowly inter-converting conformations in the centre of the oligomer, perhaps helping to maintain the integrity of the assemblies [64]. Such intrinsic heterogeneity could conceivably be important in recognising and binding variable target proteins by presenting diverse geometries for interaction [65].

In the structures of HSP16.9 and HSP16.5 the C-terminal tails were revealed to span between dimers, such that the IXI motif binds into a groove between strands β4 and β8 (Fig. 3a). Similar "cross-linking" interactions mediated by the C-termini were observed both in X-ray structures of α-crystallin constructs lacking the C-terminal extension [48] and solid-state NMR data on the full-length protein [54], both obtained at temperatures below freezing. Interestingly, however, for the α-crystallins at physiological temperature in solution it appears that the IXI motif is actually predominantly detached from the oligomer [66–68]. This apparent

contradiction can be rationalised by the strong temperature dependence of fluctuations of the tail [66], and points to a careful thermodynamic regulation of the IXI binding [69]. Unlike the tail, NMR studies have revealed that the C-terminal extension, for those sHSPs in which it is present, is intrinsically disordered and tumbles freely in solution [70, 71]. This region of sequence is primarily hydrophilic and is thought to facilitate the detachment of the remainder of the C-terminus [72]. Considering that α-crystallins with truncated extensions are associated with cataract [73], a picture emerges in which the dynamics of the C-terminus are crucial to chaperone function, potentially through regulating access to the β4/β8 groove in a form of "auto-inhibitory" regulation [43, 54].

2.4 Oligomeric Assembly Is Mediated by Flexible Terminal Interactions

While the sHSPs are prefixed by "small" due to their low monomeric molecular mass, relative to the other heat-shock proteins (HSPs), this is something of a misnomer. The sHSPs are typically oligomeric, with the majority studied so far comprising 12 or more subunits and having masses in excess of 200 kDa [9], making them among the largest of the HSPs. Though only two high-resolution structures (for HSP16.5 and HSP16.9) exist for such oligomers, in both cases they are stabilised by inter-dimer connections formed by the terminal regions of the protein as well as specific interactions between the α-crystallin core building blocks [42, 57].

In these structures the C-termini decorate the surface of the oligomer, holding it together by bridging between the α-crystallin domains of adjacent dimers [42, 57] (Fig. 3a). It is notable that the angle made between the domain and the tail is variable, even within the same oligomer [57] (Fig. 3b). Such flexibility in the tail is mediated by a "hinge-loop" just C-terminal to the core domain [48, 74] and, it is tempting to speculate, explains how the sHSPs can be found in a range of oligomeric forms [75]. Furthermore, it is notable that for the α-crystallins the area of sequence around the IXI is palindromic [46, 48], which may allow an additional degree of variability in assembly. The versatility of the C-terminus is reminiscent of that in the coat protein VP1 whose conformational flexibility mediates its variable assembly in simian virus 40 [76].

In the case of TSP36, which lacks a C-terminus, the β4/8 groove in the α-crystallin domain is instead occupied by N-terminal residues [61]. The presence of IXI motifs in both the C-terminus and extreme N-terminus of a number of sHSPs, such as the α-crystallins, raises the possibility that there may be some extent of inter-changeability between the two termini. Alternatively, the structure of HSP16.9 demonstrated the ability of the N-termini to extend across the central cavity of the oligomer, intertwined in a pairwise manner [57]. Considering HSP16.9 is a monodisperse dodecamer, this may amount to a specific interaction acting to lock the protein into a single oligomeric stoichiometry, reminiscent of the role played by the protein P30 in the bacteriophage PRD1 [77].

Conceivably, as the N-termini in the main appear heterogeneous, it is possible that they interact with each other relatively non-specifically, driven together by hydrophobic interactions [64]. Constructs of the α-crystallins, truncated of the N-terminus but retaining the C-terminus, were only able to form oligomers to very low abundance relative to sub-oligomeric species [48]. However, in the case of HSP16.5, the protein was still observed as an oligomer after removal of the N-terminus [78], but was completely disassembled after further removal of the C-terminus [79]. It appears therefore that the N-termini are not necessarily required for oligomerisation, but contribute to the thermodynamic stability of the resultant assemblies. While the importance of the N-terminus therefore appears to vary between sHSPs, it clearly has a role to play in defining oligomerisation, the details of which warrant further investigation.

2.5 sHSPs Assemble into Multiple Polyhedral Topologies

Members of the sHSP family populate a continuum of oligomeric states, from monodisperse to extremely polydisperse [56]. Notably, plant sHSPs typically exist as single oligomers, generally dodecamers [80]. Conversely, many mammalian sHSPs co-populate a wide range of oligomeric states at equilibrium; for example the α-crystallins adopt all possible stoichiometries between approximately 10 and 50 subunits [81, 82]. Between these two extremes, sHSPs have been characterised that populate an intermediate number of oligomeric states, with certain amongst them preferred, such as for example *Saccharomyces cerevisiae* HSP26 [83] and Acr2 from *Mycobacterium tuberculosis* [84]. This tendency towards polydispersity has proven to be a major hindrance in the structural characterisation of sHSPs [22].

Nonetheless, the X-ray structures determined for sHSPs at conditions in which a single oligomeric state was populated provide considerable insight. HSP16.5 crystallised as a 24mer, in which the subunits are assembled into an octahedron, with a protomeric dimer comprising each edge (Fig. 4a) [42]. Remarkably, insertion of additional residues in the N-terminus resulted in an expanded symmetric oligomer, with 24 dimers assembled into a cuboctahedron [75] (Fig. 4a). The dodecamer of HSP16.9, by contrast, assembles into a "double-ring" topology, i.e. two triangular rings stacked on top of each other (Fig. 4a) [43]. Docking of a dimer into the electron microscopy (EM) reconstruction of Acr1 from *M. tuberculosis* reveals an alternative arrangement for dodecameric sHSPs, namely a tetrahedron (Fig. 4a) [84]. This striking oligomerisation into polyhedral geometries reveals the important observation that all the α-crystallin core dimers within the oligomers are essentially equivalent structural environments, connected via terminal interactions (Fig. 4b). It is plausible that this characteristic results in there being no great energetic difference for a dimer residing in a specific oligomeric stoichiometry, and therefore enables multiple oligomeric states to be populated at equilibrium [66]. As polyhedral arrangements result in dimers being arranged symmetrically while also

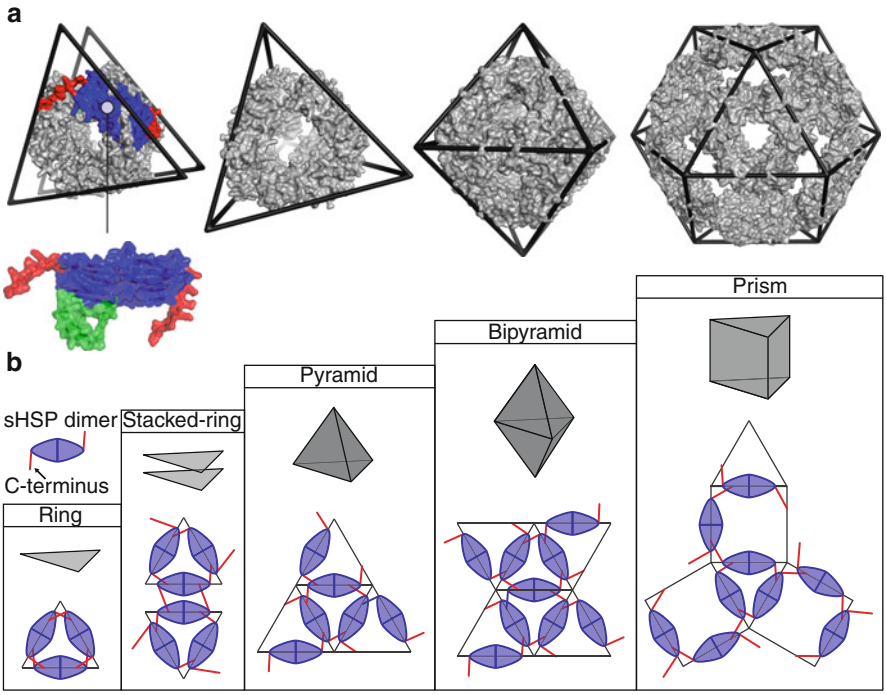

Fig. 4 Polyhedral architecture of the sHSPs. The structures, from *left to right*, of HSP16.9 (12mer), Acr1 (12mer), HSP16.5 (24mer), and a modified HSP16.5 (48mer) display striking polyhedral geometries (**a**). They assemble as a double ring, tetrahedron, octahedron and cuboctahedron, respectively (*in sequence*, *left to right*). In each case the α-crystallin domain dimers (*blue*) are collinear with the edges of the polyhedron, as illustrated for HSP16.9. The dimers are held together by extended C-termini (*red*, cf. Fig. 3), and the N-termini (*green*) are sequestered on the inside of the oligomers. This assembly of core dimers into polyhedra via C-termini can be illustrated schematically using nets of several classes of polyhedra (**b**). Nets are shown based on a triangular base-unit, but could easily be drawn for larger polygons in these classes (e.g. a square pyramid). Similar nets can be drawn for any given polyhedron such that all the C-termini are "satisfied", binding dimers together at the vertices

satisfying similar terminal interactions, it has been proposed that polydisperse sHSPs share these scaffolds [85].

2.6 *Hybrid Approaches to Determine the Structure of Polydisperse sHSPs*

The inherent polydispersity and plasticity of sHSPs are a significant impediment to their structural characterisation. These characteristics are likely however to be important to their cellular function, for example in preventing the unwanted crystallisation of the α-crystallins despite their high concentration in the eye lens [86], but

accordingly render the determination of X-ray structures of these proteins extremely challenging [22]. This has in recent years led to the application of both novel and integrated structural biology approaches to the sHSPs. The size limit of traditional solution NMR approaches has been circumvented to provide insights into the α-crystallins, either by examining truncated forms [50] or regions of marked flexibility [70, 71]. Moreover, the large oligomeric species have even be examined directly by means of solid-state NMR [54, 59], or via selective labelling of amino acids in methyl transverse relaxation optimised spectroscopy (TROSY) solution NMR [66] and electron paramagnetic resonance (EPR) approaches [51, 87, 88].

These varied strategies all provide structural information, ensemble-averaged onto the monomer level. In order to translate these insights onto the quaternary structure, studies have combined NMR data with that obtained from EM [59, 85], small-angle X-ray scattering (SAXS) [54, 59] or ion-mobility spectrometry (IM) [85], all of which report on the oligomeric form. Particular challenges are posed in the cases of polydisperse sHSPs and techniques are required which can separate, and address individually, the constituent oligomeric states. Single-particle analysis of EM data provides the opportunity to generate three-dimensional reconstructions of particles after their sorting according to size [89, 90]; currently however, the highest resolution of separation for macromolecular assemblies is afforded by MS approaches [91]. In the case of αB-crystallin, the archetypal polydisperse sHSP, early EM analysis revealed a broad range of oligomeric sizes and masses, with apparently variable symmetries [92, 93]. MS enabled the identification and relative quantification of the underlying individual oligomeric states, revealing a broad distribution of stoichiometries centred around ∼28 subunits [81, 82] (Fig. 5a).

Recently, an EM reconstruction for αB-crystallin was obtained by assuming that the principal oligomer states shared common symmetry elements [94]. This was combined with solid-state NMR [59] and cross-linking MS [60] data to generate model oligomers constructed from hexameric sub-complexes [59, 60]. An orthogonal approach, using IM–MS to discriminate between candidates based on a variable polyhedral architecture, and cross-validation with EM data, revealed alternative structures for this protein [85] (Fig. 5a). While these studies have reported plausible models for αB-crystallin, they differ in terms of symmetry and size distribution. While definitive structures therefore remain elusive, it is clear that the emergence of novel and hybrid approaches have provide new impetus to the structural study of this notorious target for structural biology.

2.7 sHSP Oligomers Can Transition Between Compact and Expanded Forms

Aside from the variability in quaternary structure afforded by polydispersity, it appears that sHSPs oligomers themselves can exist in multiple conformations (Fig. 5b). A cryoEM study of HSP26 revealed two distinct populations of 24mers, differing by approximately 5% in diameter [90, 95]. Additionally, subunit

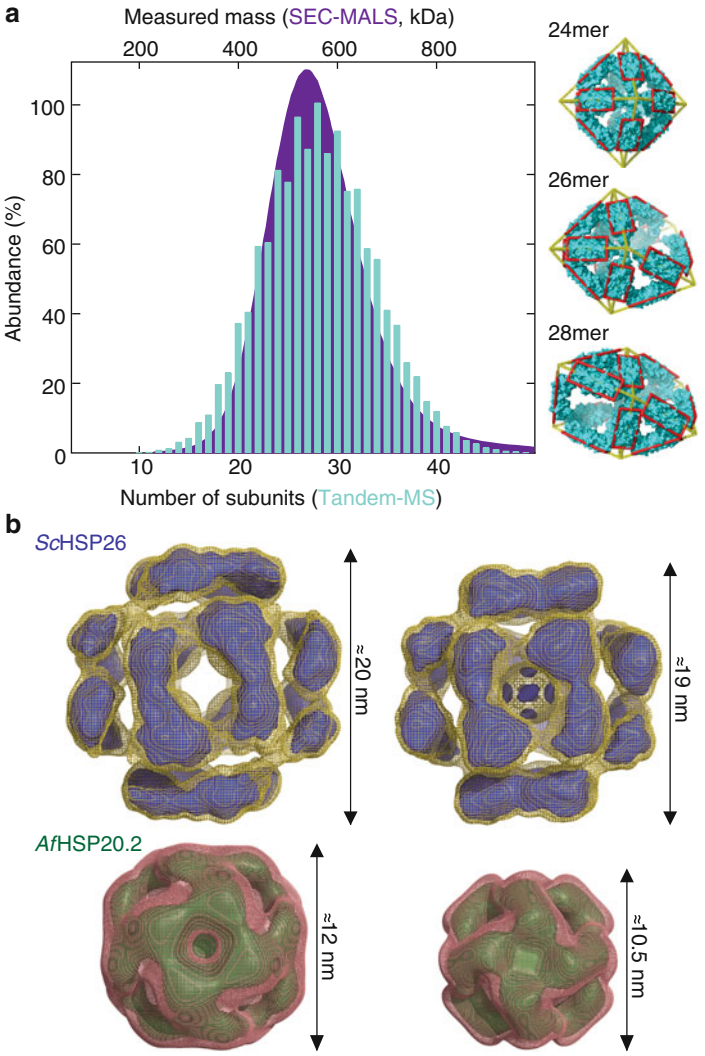

Fig. 5 Macro- and micro-heterogeneity of the sHSPs. Many sHSPs are polydisperse, populating a range of oligomeric states at equilibrium (**a**). The most famous example of this macro-heterogeneity is αB-crystallin, which forms oligomers spanning 200–1,000 kDa, as determined using size-exclusion chromatography coupled to multi-angle light scattering (SEC-MALS) (*purple*) [91]. Mass spectrometry measurements have revealed the underlying distribution of oligomers (*cyan*) to be centred on 28 subunits, with those stoichiometries composed of an even number of subunits to be preferred [82]. Ion-mobility mass spectrometry measurements allowed the filtering of structural models, based on polyhedral scaffolds (Fig. 4), to reveal the likely architecture of the 24mer, 26mer and 28mer forms [85]. These structures are based on an octahedron, augmented triangular prism and gyrobifastigium, respectively (*right*). Aside from populating multiple stoichiometries, different conformations of individual sHSP oligomeric states have been observed (**b**). Electron microscopy investigations of both *Sc*HSP26 and *Af*HSP20.2 suggested the possibility of sHSPs populating "expanded" and "compact" forms, differing in overall size but not topology. This micro-heterogeneity adds an additional level to the quaternary complexity of the sHSPs

exchange of HSP26 could only be quantitatively understood by invoking at least two separate dissociation rate constants, consistent with two types of oligomers [83]. Differences were noted between negative-stain EM reconstructions of *Arabidopsis thaliana* HSP21, in the presence or absence of cross-linker, hinting at the possibility of multiple conformations differing in terms of compactness [96]. A similar observation was also made in a negative-stain EM study of the octahedral HSP16.5 and *Archaeoglobus fulgidus* HSP20.2 24mers. For both proteins the relative proportions of the two forms varied as a function of temperature, demonstrating that the two states can interconvert [97]. Previous studies of HSP16.5 had reported some heterogeneity of the protein [56, 98, 99]. As such it appears that sHSPs not only display "macro-heterogeneity", that is populating multiple oligomeric stoichiometries, but that these individual stoichiometries can adopt multiple quaternary structures in a form of "micro-heterogeneity". Moreover, for HSP20.2 the larger form was predominant at temperatures both above and below the physiological temperature of the organism, suggesting a functional role for these quaternary conformational fluctuations.

The underlying structural origin of these expansions and contractions of the oligomers is unclear. There is evidence that they might stem from packing differences enforced by rearrangement of the inter-dimer contacts formed by the terminal regions [95]. For HSP26, they may be caused by its unique middle domain, which undergoes a conformational switch upon heat shock [100]. Alternatively, the α-crystallin domain dimeric building-block itself might fluctuate in length, for example due to changes in register at the interface [48, 53], which would propagate to have consequences on the overall size of the oligomer. Alternative registers have so far only been observed for mammalian sHSPs, which have an extremely labile dimer interface formed by the β6 + 7 strand [50, 82]. However, considering that the interface of dimers formed via the β6 loop are also easily broken [101], it is not inconceivable that a similar mechanism might also occur in sHSPs from lower organisms.

2.8 sHSPs Co-Assemble into a Recycling Oligomeric Ensemble

In addition to the complexity afforded by both macro- and micro-heterogeneity, it has long been known that members of the sHSP family co-assemble into hetero-oligomers *in vivo* [102]. Isolated sub-populations of oligomers re-equilibrate to the parent distribution [103] in a process mediated by the movement of individual subunits [104]. The combinations of sHSPs which are compatible for co-assembly are dependent on their evolutionary relationships [80]; however the subunit exchange of the individual oligomers appears to be a general property of these proteins [105–108]. As such, the sHSPs should not be considered as static homomeric proteins, but rather as a continually "recycling" ensemble of hetero-oligomers.

Subunit exchange occurs via the dissociation of the oligomer, with a rate strongly dependent on solution conditions [82, 105]. This reveals that the sHSPs are in a rapid equilibrium with a small population of sub-oligomeric forms. The

identity of the exchanging unit depends on the sHSP in question, with monomers [82], dimers [108] and mixtures thereof [101] all having been observed directly in high-resolution mass spectrometry experiments. This equilibrium between oligomers and smaller species is shifted towards dissociation at elevated temperatures, with appreciable concentrations of the latter observed under heat-shock conditions for some sHSPs [80, 83, 109], but not for others [80, 82]. Concomitant to this dissociation, high-order oligomers have also been observed, such that sHSPs which are monodisperse under ambient temperatures effectively become polydisperse at elevated temperature [110, 111]. These processes of assembly, dissociation and exchange are also affected by modifications to the sHSPs thought to regulate or compromise sHSP activity such as post-translational modification [72, 112, 113] or mutation [114–116]. Given these characteristics, it is tempting to speculate that such quaternary dynamics are important for chaperone function, presumably by exposing target-protein binding regions either on the sub-oligomeric species, or *en route* to dissociation [9, 57].

3 The Molecular Chaperone Function of sHSPs

As might be expected from their evolutionary diversity, sHSPs have been reported to be involved in a range of cellular processes. The role which is common to most members of the family is the ability to act as molecular chaperones [117, 118]. This function of the sHSPs was first demonstrated when it was found that α-crystallin could prevent the accumulation of aggregation-prone eye-lens proteins [119]. This *in vitro* observation was later confirmed *in vivo* when αA-crystallin knockout mice developed inclusion bodies rendering the eye lens opaque [120]. Furthermore, disruption of the αB-crystallin and the adjacent HSPB2 sHSP genes resulted in degeneration of some skeletal muscles [121]. Since the pioneering work on α-crystallin, many other sHSPs have been demonstrated to have molecular chaperone activity, and it is quite likely that the ability to interact with non-native states even underpins the mechanism of their other activities in the cell [6].

3.1 High-Capacity Holdase Function of sHSPs Sequesters Destabilised Targets from Aggregation

It has been established for some time that the molecular chaperone role of sHSPs is to bind target proteins whose native structure is destabilised by a range of stresses [119, 122–125]. Under such conditions, these proteins can have a tendency to form amorphous or amyloid aggregate morphologies [18]. Rather than refolding the targets, as is the case for the ATP-dependent "foldase" chaperones such as HSP60, HSP70 and HSP90 [126], the sHSPs instead act in an ATP-independent manner to trap them as they unfold [119, 122–125]. The resultant complexes formed between

the sHSP and target proteins can range in mass up to several MDa [111, 127, 128]. The binding capacities of the sHSPs vary between different members of the family, but can be very high, with the chaperones capable of protecting stoichiometric quantities of target [128, 129]. The capacity appears to be somewhat dependent on the identity of the target protein [127, 129], perhaps purely reflecting the mass of the target [7, 130]. As such, the sHSPs can be viewed as high-capacity "sponges" for non-native proteins, preventing the deleterious consequences of their aggregation [131].

The majority of assays for studying sHSP activity rely on assessing the ability of the chaperone to suppress the aggregation of model proteins, due to the difficulties in purifying inherently unstable targets [132]. It is not uncommon that the apparent efficiency of protection is dependent on the choice of model protein [133]. As such these *in vitro* assays might not be expected to capture all aspects of *in vivo* function [134]. Nevertheless, the capacity of sHSPs to interact with a range of destabilised model proteins renders it likely that they have multiple targets in the cell [9, 57]. Determining the characteristics of actual cellular substrates has however been hampered by the absence of easily assayed phenotypes associated with sHSP deletions in yeast or *Escherichia coli* [135, 136]. However, a study using *Synechocystis* sp. PCC 6803, in which only a single sHSP is encoded and the deletion of which results in lack of thermo-tolerance [137], identified interactions with numerous proteins [132]. These interactors displayed no commonality in sequence or structure, and spanned functions ranging from transcription, translation, to cell signalling, and secondary metabolism [132]. A similarly heterogeneous set of targets was also observed in yeast, corroborating the apparent broad specificity of sHSPs [138]. The general chaperone function of the sHSPs therefore appears to be to act as "holdases", sequestering target proteins and thereby impeding the deleterious consequences of their aggregation [131].

3.2 sHSP Activity Is Influenced by Environmental Conditions

Multiple different stresses have been reported to stimulate the activity of sHSPs. Primary to these is heat shock, with sHSPs generally thought to be more effective chaperones at elevated temperature. For example, HSP26 has been demonstrated to undergo significant structural and dynamical changes around 40°C, consistent with a thermal activation of the protein [83, 100, 109]. While HSP26 is unusual in containing a middle domain, HSP18.1 undergoes a similar dynamic transition in oligomerisation from an inactive "storage form" into a functional chaperone with temperature [111]. In fact chaperone functions at temperatures far in excess of those normally termed "heat shock" have been reported [139]. On the other hand, some sHSPs have been shown to retain chaperone activity below heat shock temperatures [140], demonstrating that thermal activation is not a universal requirement for sHSP function.

Solution pH is also known to affect the molecular properties of the sHSPs. Studies of αB-crystallin have revealed dramatic changes in the thermodynamics and kinetics of the inter-subunit interfaces [50, 54, 66, 82]. This is reflected in pH-dependent changes in chaperone function *in vitro* [141–143], and a role for αB-crystallin in responding to cellular acidification [144–146]. sHSPs have also been demonstrated to provide protection against toxicity from metal ions *in vivo* [147]. The α-crystallins have been shown to bind metal ions directly [48], potentially silencing any tendency to oxidise [148, 149], and resulting in modulation of their chaperone function [150, 151]. This behaviour is interesting in light of the role of the redoxins, which switch from their enzymatic function to become molecular chaperones upon oxidative stress [152, 153].

While it has been generally accepted that the function of sHSPs is as ATP-independent molecular chaperones, there have been reports suggesting that the sHSPs can bind nucleotides [154, 155]. This finding is supported by the observation of sulphate ions accumulated at the dimer interface in recent crystal structures [48, 156]. Mapping changes in residue-specific protease susceptibility of αB-crystallin upon the addition of nucleotide [157] on the structure of the core domain suggest that the location of the sulphate may represent ATP-binding sites [53]. This is in line with the notion that nucleotide binding (rather than hydrolysis) might regulate activity [154], a mode of action that contrasts with the canonical chaperones, in which the turnover of ATP drives their action [158].

Members of the sHSPs can become post-translationally modified upon stress, with phosphorylation in particular implicated in affecting their function [159–161]. Accordingly, profound effects of phosphorylation on the chaperone activity have been observed *in vitro* [112, 162–164]. However, the identity of the target protein and solution conditions both strongly influence whether the post-translational modification leads to an increase or decrease in chaperone efficacy [133]. As such, while the evidence clearly points to phosphorylation regulating the function of sHSPs, a simple description of the mechanism appears unlikely [165]. Overall, from the differences in activity observed for the sHSPs as a result of multiple and varied stimuli, a picture emerges of a family of molecular chaperones which are exquisitely and directly controlled by the insult responsible for a particular stress condition.

3.3 sHSPs Co-Operate with the Cellular Machinery to Allow Reactivation or Degradation of Targets

While the sHSPs are active under stress conditions and act to bind non-native target proteins, they do not themselves appear to enable their refolding. Instead the target protein is subsequently retrieved from the sHSP:target complex and refolded upon interaction with ATP-dependent chaperones [166–169]. This renaturation pathway involves the HSP70/HSP40 system (DnaK/J in prokaryotes), a nucleotide exchange factor, and HSP100 working in concert with the sHSPs to liberate and refold unfolded substrate proteins [170].

While it has been demonstrated that the sHSPs facilitate the disaggregation of insoluble protein deposits [135, 170–174], the mechanism by which this is achieved is presently unclear. Recent studies suggest that different sHSPs may play varying roles in the resolubilisation process [175]. It is likely that they act to compete kinetically for the inter-molecular interactions that would otherwise ultimately lead to the formation of stable aggregates, instead holding proteins in a conformation more amenable to subsequent refolding [170].

While the link between the sHSPs and ATP-dependent foldases is clear, recent evidence also points to their interaction with the protein degradation machinery [176]. A number of studies have linked sHSPs with the proteasome/ubiquitin pathway [177–180], and the *E. coli* sHSPs IbpA and IbpB have been shown to be substrates of the Lon protease [181]. Though this field warrants considerably more attention, the involvement of sHSPs in both the refolding and degradation pathways reveals them as crucial switching points in determining the fate of unfolded proteins [182].

3.4 sHSPs Possess Multiple Sites that Become Exposed to Bind Targets

Considerable effort has been expended in an attempt to elucidate the region of the sHSPs which interact directly with the target proteins. Different studies have implicated the N-terminal region [65, 134, 183, 184], the C-terminus [185, 186] and the α-crystallin core [149, 187, 188]. Indeed, isolated α-crystallin domains from some sHSPs have been shown to have a certain amount of molecular chaperone activity [48, 52]. Taking these results together implies that there is no single binding site within the oligomer, but rather that these are dependent on the sHSP or target protein in question [6] (Fig. 6).

A commonality observed in the majority of putative interacting regions which have been elucidated is that they are hydrophobic in nature [6]. This is unsurprising, considering that it is the exposure of complementary hydrophobic surfaces on target proteins which renders them aggregation prone. It has been shown that the number of accessible hydrophobic sites on the sHSP increase upon heat shock [80, 167, 189], prompting the question whether this is a consequence of structural rearrangements of the sHSP oligomer.

A popular hypothesis, based on cumulative evidence from studies of several different members of the family which demonstrated oligomeric dissociation at heat-shock temperatures, is that a sub-oligomeric species form of the sHSP initially binds the target [109, 137, 190]. This mechanism does not appear to be universal, however, as a number of examples have emerged showing that dissociation, or its corollary, the rate of subunit exchange, is not necessarily correlated with chaperone activity [72, 80, 82, 191, 192]. In this regard it is informative to consider the case of HSP26. An early study of this protein demonstrated it to undergo dissociation into sub-oligomeric species at heat shock temperatures, suggesting this event to predicate chaperone activity [109]. However, subsequent studies revealed that chaperone

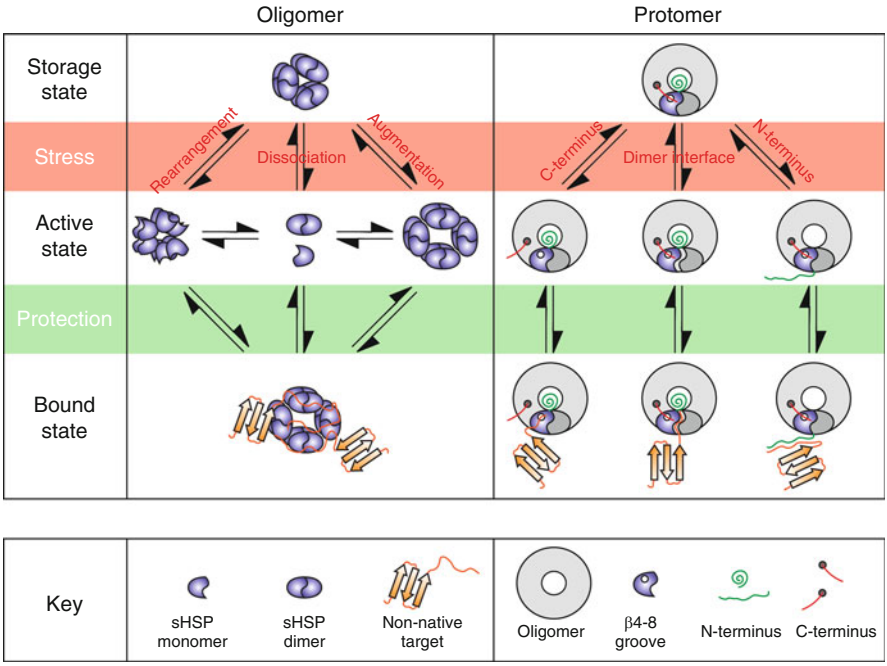

Fig. 6 Molecular basis for activation of binding of target by the sHSPs. A range of structural and dynamical changes in the sHSPs have been observed which have been ascribed to switching the chaperone into an "active" state. These are separated here according to effects on the oligomer (*left*) or protomer (*right*) level. The former include dissociation of the oligomer; a conformational rearrangement of a domain within the oligomers; or a change in oligomeric distribution. At present no universal pathway has emerged, and activation is likely to be sHSP dependent. Ultimately, and common to all sHSPs studied, large and heterogeneous sHSP:target complexes are formed. On the protomer level evidence for the exposure of the β4–β8 groove by detachment of the C-terminus, exposure of the dimer interface and unfurling the N-terminus has been proposed. The diversity in mechanism is likely to reflect the evolutionary diversity of both the sHSPs and their targets

activity was unaffected if the oligomer was cross-linked such that it could not dissociate [191]. Instead, a thermally regulated conformational change in the middle domain [100], which in the unrestrained protein is concomitant to changes in oligomerisation [83], has been implicated as underlying activation of this sHSP. This example illustrates that even if a protein undergoes dissociation into sub-oligomeric species at heat-shock temperatures, this does not necessarily imply that the sub-oligomeric species is the active target-binding form.

An alternative model is motivated by a recent cross-linking study between HSP18.1 and malate dehydrogenase which suggested that the N-terminal region was primarily responsible for binding [65]. However, examination of the structure of its homologue HSP16.9 reveals at least some of the N-termini to be sequestered within the centre of the oligomer [43], a location structurally incompatible with the high binding capacity of the chaperone. It is possible therefore that the N-terminal

arm unfurls from the central cavity of the protein to become exposed at heat-shock temperatures in an intrinsically disordered state which can present diverse geometries of interaction sites for binding [65]. One can even envisage a situation whereby the N-terminus acts to modulate the surface of the oligomer, similar to the way in which the specificity of protein phosphatase 1 is governed by the binding of its unstructured regulator proteins such as spinophilin [193]. Such a release of the N-termini would necessitate the loss of the directional inter-dimer constraints they form in the crystal structure of HSP16.9. Circumstantial evidence for this mechanism therefore comes from that fact that at heat-shock temperatures the oligomeric form of this protein is no longer confined to a dodecamer [110].

This change in protein partitioning, with most of the protein being re-allocated from a monodisperse oligomer at ambient temperatures into a polydisperse ensemble, arises purely from thermal motions that transfer subunits between oligomers of varying relative stability. This is particularly pronounced for HSP18.1 [111] where, interestingly, the resultant distribution of higher oligomers that was observed in this study was very similar to that populated by the α-crystallins at ambient temperatures [82, 162], conditions under which they remain chaperone-active. This raises the possibility that a polydisperse ensemble of oligomers may not only be a direct consequence of sHSP activation, but may even itself be of direct functional benefit.

In combination these studies suggest that there are not only multiple binding sites on the oligomer but also different mechanisms for their exposure to target proteins (Fig. 6). A common thread appears to be that the native oligomer represents a chaperone-inactive "storage form", which undergoes a transition to a chaperone-active form. Such a change may exist purely to prevent unwanted, retarding associations with non-native states during non-stress conditions. Alternatively it may signal a switch between different cellular functions, analogous to redoxins which have been observed to become chaperone active upon a stress-induced change in the oligomeric state [152, 153]. Overall, however, it is clear that there are considerable mechanistic variations in the chaperone function of different sHSPs, emphasising the broad specificity of these chaperones in protecting the proteome.

3.5 sHSP:Target Complexes are Plastic and Polydisperse

The complexes formed when sHSPs are incubated with target proteins are very large and extremely heterogeneous [127, 128]. This is in stark contrast to the defined stoichiometries of interaction observed for foldase chaperones and their targets [158]. Such heterogeneity severely hampers structural interrogations, but can be overcome using the high resolution of separation afforded by MS approaches [91]. Employing a tandem-MS strategy [81], the different complexes formed between HSP18.1 and luciferase were identified and quantified [111]. Despite these experiments being performed with an excess of chaperone, remarkably over 300 stoichiometries of interaction were observed, variable in both the number of

sHSP and target subunits [111]. In light of the observation that sHSP:target complexes scale with the amount of target protein [127], a glimpse of the bewildering polydispersity of these complexes is obtained.

The complexes are not static entities; indeed they can continue to incorporate ever-increasing amounts of substrate [111, 127, 128]. Moreover, the sHSP subunits continue to exchange with free sHSP oligomers and other complexes [127]. By contrast, target proteins appear unable to transfer from one complex to another [127]. Hydrogen/deuterium exchange experiments revealed no difference in backbone amide protection between the sHSP free in solution or in complex [62], and α-lactalbumin associated with α-crystallin is still visible in proton NMR spectra, implying that it must spend a significant proportion of its time tumbling independently in solution [194]. These data therefore reveal that the interaction between sHSP and target protein is, at least in some cases, only transient, presumably to facilitate subsequent transfer to the refolding machinery.

In addition to these inherent dynamics and variability, it also appears that sHSP: target complexes can adopt different morphologies [128, 130]. Interestingly it appears that this is target-protein dependent: the same sHSPs formed different morphologies with different targets [128, 130] but complexes of different sHSPs and the same target appear similar [128]. This can be rationalised by the observation that the sHSPs bind target proteins early during the unfolding process, when their structure is largely preserved [62, 130]. In summary, the complexes formed between sHSPs and targets are extremely polydisperse and dynamic, which renders their structural characterisation very challenging, but is likely integral to their cellular function.

4 Paramedics Within the Proteostasis Network

Molecular chaperones are crucial for the maintenance of cellular protein homeostasis [10]. sHSPs are an important part of this network, being dramatically upregulated and activated during cellular stress, and sequestering destabilised targets from aggregation. In this way, sHSPs can be regarded as the paramedics of the cell [83], rapidly stabilising the targets prior to their attention by the refolding or degradation machinery. Aside from this important role in overcoming the kinetics of aggregation, the sHSPs also act to increase the proteostasis capacity of the cell. By temporarily storing the aggregation-prone proteins, awaiting refolding or degradation, they act as a vital buffer between protein unfolding and its potentially deleterious consequences.

While the sHSPs form a crucial part of the proteostasis network [11], they themselves can be thought of as a highly dynamic sub-network. As discussed above, many studies have shown that sHSPs can adopt a range of plastic oligomeric states, containing chains from multiple different sHSPs. As many organisms express multiple sHSPs in the same cellular compartment, this will lead to their

coassembly upon synthesis. If all particular subunit arrangements are allowed the number possible of oligomers N_{Oli} is given by

$$N_{\mathrm{Oli}} = \sum_{i}^{n} \frac{[N_{\mathrm{sHSP}} + P_i - 1]!}{P_i![N_{\mathrm{sHSP}} - 1]!}$$

where N_{sHSP} is the number of sHSPs capable of coassembly and i the number of sHSP subunits in a particular oligomeric stoichiometry P.

As an example, for monodisperse hetero-dodecamers ($P_i = 12$), if there are six compatible sHSPs ($N_{\mathrm{sHSP}} = 6$), as is the case for class I sHSPs in the Arabidopsis cytosol [3], the number of potential oligomers is 6,188. In the analogous calculation for class I cytosolic sHSPs in Californian poplar ($N_{\mathrm{sHSP}} = 18$) [3], almost 52,000,000 combinations are possible. While what proportion of these potential hetero-oligomers are formed *in vivo* will be influenced by factors such as tissue specificity and relative expression rates and levels, the number of possibilities is nonetheless remarkable. Combined with the observation that the oligomers rapidly exchange subunits, this suggests that sHSPs should not be regarded as individual oligomers but rather an extensive and interconverting ensemble.

The very large numbers of compatible sHSPs in plants are not replicated in mammals but instead it appears that a different mechanism to achieve the same effect might be at play. In the case of α-crystallin in the eye lens, where both isoforms A and B are expressed and populate oligomeric states between 10 and 50mers [66], 1,271 combinations are possible. Additionally, αB-crystallin is found outside the lens, and is one of seven sHSPs abundant in muscle, leading to potentially over 264,000,000 different complexes. Although, specificities of interaction between sHSP pairs [195] will act to reduce this number in the cell, the polydispersity of many members of the family can act as a means to magnify the diversity of hetero-oligomers.

Indeed, in the case of plant sHSPs it has been shown that a mono- to polydisperse transition occurs under heat-shock conditions, and therefore both the large number of sHSPs and polydispersity can combine to create astonishingly large possible numbers [111]. It remains to be proven to what extent this diversity exists *in vivo*, and how it acts to regulate molecular chaperone function. It is however enlightening to consider the parallels with the immune system in higher eukaryotes, whereby a relatively small number of genes (~300) can give rise to over 10^8 different antibodies [196], allowing the recognition of the diverse structures of antigens. It is tempting to speculate that evolution of such an extensive sHSP ensemble, within the context of the wider chaperone network [197], allows organisms to protect themselves against the diversity of unfolding client proteins and thereby maintain proteostasis.

Acknowledgments We are very grateful for the stimulating interactions we have had with all of our collaborators in the study of sHSPs, and thank all of the Benesch group for helpful discussion. We thank the Wellcome Trust (GRH, FS), the European Molecular Biology Organization (HL, AJB), European Union 7th Framework Program "PROSPECTS" (FS), Canadian Institutes of Health Research (AJB), and the Royal Society (JLPB).

References

1. Narberhaus F (2002) Alpha-crystallin-type heat shock proteins: socializing minichaperones in the context of a multichaperone network. Microbiol Mol Biol Rev 66(1):64–93 (table of contents)
2. Kriehuber T et al (2010) Independent evolution of the core domain and its flanking sequences in small heat shock proteins. FASEB J 24(10):3633–3642
3. Waters ER, Aevermann BD, Sanders-Reed Z (2008) Comparative analysis of the small heat shock proteins in three angiosperm genomes identifies new subfamilies and reveals diverse evolutionary patterns. Cell Stress Chaperones 13(2):127–142
4. Kappe G et al (2003) The human genome encodes 10 alpha-crystallin-related small heat shock proteins: HspB1-10. Cell Stress Chaperones 8(1):53–61
5. Nakamoto H, Vigh L (2007) The small heat shock proteins and their clients. Cell Mol Life Sci 64(3):294–306
6. Haslbeck M et al (2005) Some like it hot: the structure and function of small heat-shock proteins. Nat Struct Mol Biol 12(10):842–846
7. Basha E, O'Neill H, Vierling E (2012) Small heat shock proteins and alpha-crystallins: dynamic proteins with flexible functions. Trends Biochem Sci 37(3):106–117
8. Ellis RJ, van der Vies SM (1991) Molecular chaperones. Annu Rev Biochem 60:321–347
9. McHaourab HS, Godar JA, Stewart PL (2009) Structure and mechanism of protein stability sensors: chaperone activity of small heat shock proteins. Biochemistry 48(18):3828–3837
10. Hartl FU, Bracher A, Hayer-Hartl M (2011) Molecular chaperones in protein folding and proteostasis. Nature 475(7356):324–332
11. Balch WE et al (2008) Adapting proteostasis for disease intervention. Science 319 (5865):916–919
12. Baldwin AJ et al (2011) Metastability of native proteins and the phenomenon of amyloid formation. J Am Chem Soc 144(36):14160–14163
13. Olzscha H et al (2011) Amyloid-like aggregates sequester numerous metastable proteins with essential cellular functions. Cell 144(1):67–78
14. Powers ET et al (2009) Biological and chemical approaches to diseases of proteostasis deficiency. Annu Rev Biochem 78:959–991
15. Chiti F, Dobson CM (2006) Protein misfolding, functional amyloid, and human disease. Annu Rev Biochem 75:333–366
16. Beck M et al (2009) Visual proteomics of the human pathogen Leptospira interrogans. Nat Methods 6(11):817–823
17. Malmstrom J et al (2009) Proteome-wide cellular protein concentrations of the human pathogen Leptospira interrogans. Nature 460(7256):762–765
18. Ecroyd H, Carver JA (2009) Crystallin proteins and amyloid fibrils. Cell Mol Life Sci 66 (1):62–81
19. Arrigo AP et al (2007) Hsp27 (HspB1) and alphaB-crystallin (HspB5) as therapeutic targets. FEBS Lett 581(19):3665–3674
20. Sun Y, MacRae TH (2005) The small heat shock proteins and their role in human disease. FEBS J 272(11):2613–2627
21. Carra S et al (2011) Alteration of protein folding and degradation in motor neuron diseases: implications and protective functions of small heat shock proteins. Prog Neurobiol (in press). doi:10.1016/j.bbr.2011.03.031
22. Horwitz J (2009) Alpha crystallin: the quest for a homogeneous quaternary structure. Exp Eye Res 88(2):190–194
23. Cowieson NP, Kobe B, Martin JL (2008) United we stand: combining structural methods. Curr Opin Struct Biol 18(5):617–622
24. Robinson CV, Sali A, Baumeister W (2007) The molecular sociology of the cell. Nature 450 (7172):973–982

25. Frauenfelder H, Sligar SG, Wolynes PG (1991) The energy landscapes and motions of proteins. Science 254(5038):1598–1603
26. Karplus M, McCammon JA (1983) Dynamics of proteins: elements and function. Annu Rev Biochem 52:263–300
27. Wüthrich K, Wagner G (1978) Internal motion in globular proteins. Trends Biol Sci 3(4):227–230
28. Russel D et al (2009) The structural dynamics of macromolecular processes. Curr Opin Cell Biol 21(1):97–108
29. Boehr DD, Nussinov R, Wright PE (2009) The role of dynamic conformational ensembles in biomolecular recognition. Nat Chem Biol 5(11):789–796
30. Henzler-Wildman K, Kern D (2007) Dynamic personalities of proteins. Nature 450 (7172):964–972
31. Karplus M, Kuriyan J (2005) Molecular dynamics and protein function. Proc Natl Acad Sci USA 102(19):6679–6685
32. Smock RG, Gierasch LM (2009) Sending signals dynamically. Science 324(5924):198–203
33. Baldwin AJ, Kay LE (2009) NMR spectroscopy brings invisible protein states into focus. Nat Chem Biol 5(11):808–814
34. Kappe G, Boelens WC, de Jong WW (2010) Why proteins without an alpha-crystallin domain should not be included in the human small heat shock protein family HSPB. Cell Stress Chaperones 15(4):457–461
35. Haslbeck M et al (2004) A domain in the N-terminal part of Hsp26 is essential for chaperone function and oligomerization. J Mol Biol 343(2):445–455
36. Kappe G et al (2004) Tsp36, a tapeworm small heat-shock protein with a duplicated alpha-crystallin domain, forms dimers and tetramers with good chaperone-like activity. Proteins 57(1):109–117
37. Poulain P, Gelly JC, Flatters D (2010) Detection and architecture of small heat shock protein monomers. PLoS One 5(4):e9990
38. Benndorf R, Welsh MJ (2004) Shocking degeneration. Nat Genet 36(6):547–548
39. Carver JA (1999) Probing the structure and interactions of crystallin proteins by NMR spectroscopy. Prog Retin Eye Res 18(4):431–462
40. Chernik IS et al (2007) Small heat shock protein Hsp20 (HspB6) as a partner of 14-3-3gamma. Mol Cell Biochem 295(1–2):9–17
41. MacCoss MJ et al (2002) Shotgun identification of protein modifications from protein complexes and lens tissue. Proc Natl Acad Sci USA 99(12):7900–7905
42. Kim KK, Kim R, Kim SH (1998) Crystal structure of a small heat-shock protein. Nature 394 (6693):595–599
43. van Montfort RL et al (2001) Crystal structure and assembly of a eukaryotic small heat shock protein. Nat Struct Biol 8(12):1025–1030
44. Takeda K et al (2011) Dimer structure and conformational variability in the N-terminal region of an archaeal small heat shock protein, StHsp14.0. J Struct Biol 174(1):92–99
45. Hilario E et al (2011) Crystal structures of Xanthomonas small heat shock protein provide a structural basis for an active molecular chaperone oligomer. J Mol Biol 408(1):74–86
46. Bagnéris C et al (2009) Crystal structures of alpha-crystallin domain dimers of alphaB-crystallin and Hsp20. J Mol Biol 392(5):1242–1252
47. Baranova EV et al (2011) Three-dimensional structure of alpha-crystallin domain dimers of human small heat shock proteins HSPB1 and HSPB6. J Mol Biol 411(1):110–122
48. Laganowsky A et al (2010) Crystal structures of truncated alphaA and alphaB crystallins reveal structural mechanisms of polydispersity important for eye lens function. Protein Sci 19 (5):1031–1043
49. Berengian AR, Parfenova M, McHaourab HS (1999) Site-directed spin labeling study of subunit interactions in the alpha-crystallin domain of small heat-shock protein – comparison of the oligomer symmetry in alpha A-crystallin, HSP 27, and HSP 16.3. J Biol Chem 274(10):6305–6314

50. Jehle S et al (2009) [alpha]B-crystallin: a hybrid solid-state/solution-state NMR investigation reveals structural aspects of the heterogeneous oligomer. J Mol Biol 385(5):1481–1497
51. Koteiche HA, McHaourab HS (1999) Folding pattern of the alpha-crystallin domain in alpha A-crystallin determined by site-directed spin labeling. J Mol Biol 294(2):561–577
52. Feil IK et al (2001) A novel quaternary structure of the dimeric alpha-crystallin domain with chaperone-like activity. J Biol Chem 276(15):12024–12029
53. Clark AR et al (2011) Crystal structure of R120G disease mutant of human alphaB-crystallin domain dimer shows closure of a groove. J Mol Biol 408(1):118–134
54. Jehle S et al (2010) Solid-state NMR and SAXS studies provide a structural basis for the activation of alphaB-crystallin oligomers. Nat Struct Mol Biol 17(9):1037–1042
55. Hasan A et al (2004) Thermal stability of human alpha-crystallins sensed by amide hydrogen exchange. Protein Sci 13(2):332–341
56. Haley DA et al (2000) Small heat-shock protein structures reveal a continuum from symmetric to variable assemblies. J Mol Biol 298(2):261–272
57. van Montfort R, Slingsby C, Vierling E (2001) Structure and function of the small heat shock protein/alpha-crystallin family of molecular chaperones. Adv Protein Chem 59:105–156
58. Koteiche HA et al (2005) Atomic models by cryo-EM and site-directed spin labeling: application to the N-terminal region of Hsp16.5. Structure 13(8):1165–1171
59. Jehle S et al (2011) N-terminal domain of alphaB-crystallin provides a conformational switch for multimerization and structural heterogeneity. Proc Natl Acad Sci USA 108(16):6409–6414
60. Braun N et al (2011) Multiple molecular architectures of the eye lens chaperone alphaB-crystallin elucidated by a triple hybrid approach. Proc Natl Acad Sci USA 108 (51):20491–20496
61. Stamler R et al (2005) Wrapping the alpha-crystallin domain fold in a chaperone assembly. J Mol Biol 353(1):68–79
62. Cheng GL et al (2008) Insights into small heat shock protein and substrate structure during chaperone action derived from hydrogen/deuterium exchange and mass spectrometry. J Biol Chem 283(39):26634–26642
63. Wintrode PL et al (2003) Solution structure and dynamics of a heat shock protein assembly probed by hydrogen exchange and mass spectrometry. Biochemistry 42(36):10667–10673
64. Kim R et al (2003) On the mechanism of chaperone activity of the small heat-shock protein of Methanococcus jannaschii. Proc Natl Acad Sci USA 100(14):8151–8155
65. Jaya N, Garcia V, Vierling E (2009) Substrate binding site flexibility of the small heat shock protein molecular chaperones. Proc Natl Acad Sci USA 106(37):15604–15609
66. Baldwin AJ et al (2011) Quaternary dynamics of aB-crystallin as a direct consequence of localised tertiary fluctuations in the C-terminus. J Mol Biol 413(2):310–320
67. Treweek TM et al (2010) A quantitative NMR spectroscopic examination of the flexibility of the C-terminal extensions of the molecular chaperones, [alpha]A- and [alpha]B-crystallin. Exp Eye Res 91(5):691–699
68. Ghahghaei A et al (2009) Structure/function studies of dogfish alpha-crystallin, comparison with bovine alpha-crystallin. Mol Vis 15:2411–2420
69. Hilton GR et al (2012) A labile C-terminal interaction mediates the quaternary dynamics of αB crystallin. Phil Trans R Soc B (under consideration)
70. Carver JA et al (1992) Identification by H-1-NMR spectroscopy of flexible C-terminal extensions in bovine lens alpha-crystallin. FEBS Lett 311(2):143–149
71. Carver JA, Lindner RA (1998) NMR spectroscopy of alpha-crystallin. Insights into the structure, interactions and chaperone action of small heat-shock proteins. Int J Biol Macromol 22(3–4):197–209
72. Aquilina JA et al (2005) Subunit exchange of polydisperse proteins: mass spectrometry reveals consequences of alphaA-crystallin truncation. J Biol Chem 280(15):14485–14491
73. Takemoto LJ (1997) Changes in the C-terminal region of alpha-A crystallin during human cataractogenesis. Int J Biochem Cell Biol 29(2):311–315

74. Laganowsky A, Eisenberg D (2010) Non-3D domain swapped crystal structure of truncated zebrafish alphaA crystallin. Protein Sci 19(10):1978–1984
75. Shi J et al (2006) Cryoelectron microscopy and EPR analysis of engineered symmetric and polydisperse Hsp16.5 assemblies reveals determinants of polydispersity and substrate binding. J Biol Chem 281(52):40420–40428
76. Liddington RC et al (1991) Structure of simian virus 40 at 3.8-A resolution. Nature 354 (6351):278–284
77. Abrescia NG et al (2004) Insights into assembly from structural analysis of bacteriophage PRD1. Nature 432(7013):68–74
78. Koteiche HA, McHaourab HS (2002) The determinants of the oligomeric structure in Hsp16.5 are encoded in the alpha-crystallin domain. FEBS Lett 519(1–3):16–22
79. Bertz M et al (2010) Structural and mechanical hierarchies in the alpha-crystallin domain dimer of the hyperthermophilic small heat shock protein Hsp16.5. J Mol Biol 400 (5):1046–1056
80. Basha E et al (2010) Mechanistic differences between two conserved classes of small heat shock proteins found in the plant cytosol. J Biol Chem 285(15):11489–11497
81. Aquilina JA et al (2003) Polydispersity of a mammalian chaperone: mass spectrometry reveals the population of oligomers in alphaB-crystallin. Proc Natl Acad Sci USA 100 (19):10611–10616
82. Baldwin AJ et al (2011) αB-crystallin polydispersity is a consequence of unbiased quaternary dynamics. J Mol Biol 413(2):297–309
83. Benesch JLP et al (2010) The quaternary organization and dynamics of the molecular chaperone HSP26 are thermally regulated. Chem Biol 17(9):1008–1017
84. Kennaway CK et al (2005) Dodecameric structure of the small heat shock protein Acr1 from Mycobacterium tuberculosis. J Biol Chem 280(39):33419–33425
85. Baldwin AJ et al (2011) The polydispersity of αB-crystallin is rationalised by an interconverting polyhedral architecture. Structure 19(12):1855–1863
86. Tardieu A (1988) Eye lens proteins and transparency: from light transmission theory to solution X-ray structural analysis. Annu Rev Biophys Biophys Chem 17:47–70
87. Alexander N et al (2008) De novo high-resolution protein structure determination from sparse spin-labeling EPR data. Structure 16(2):181–195
88. McHaourab HS, Berengian AR, Koteiche HA (1997) Site-directed spin-labeling study of the structure and subunit interactions along a conserved sequence in the alpha-crystallin domain of heat-shock protein. 27. Evidence of a conserved subunit interface. Biochemistry 36 (48):14627–14634
89. Scheres SH et al (2007) Disentangling conformational states of macromolecules in 3D-EM through likelihood optimization. Nat Methods 4(1):27–29
90. White HE et al (2004) Recognition and separation of single particles with size variation by statistical analysis of their images. J Mol Biol 336(2):453–460
91. Benesch JLP, Ruotolo BT (2011) Mass spectrometry: an approach come-of-age for structural and dynamical biology. Curr Opin Struct Biol 21(5):641–649
92. Haley DA, Horwitz J, Stewart PL (1998) The small heat-shock protein, alphaB-crystallin, has a variable quaternary structure. J Mol Biol 277(1):27–35
93. Haley DA, Horwitz J, Stewart PL (1999) Image restrained modeling of alpha B-crystallin. Exp Eye Res 68(1):133–136
94. Peschek J et al (2009) The eye lens chaperone alpha-crystallin forms defined globular assemblies. Proc Natl Acad Sci USA 106(32):13272–13277
95. White HE et al (2006) Multiple distinct assemblies reveal conformational flexibility in the small heat shock protein Hsp26. Structure 14(7):1197–1204
96. Lambert W et al (2011) Subunit arrangement in the dodecameric chloroplast small heat shock protein Hsp21. Protein Sci: Publ Protein Soc 20(2):291–301
97. Haslbeck M et al (2008) Structural dynamics of archaeal small heat shock proteins. J Mol Biol 378(2):362–374

98. Cao A et al (2008) Preheating induced homogeneity of the small heat shock protein from Methanococcus jannaschii. Biochim Biophys Acta Proteins Proteomics 1784(3):489–495
99. Kim DR et al (2003) Activation mechanism of HSP16.5 from Methanococcus jannaschii. Biochem Biophys Res Commun 307(4):991–998
100. Franzmann TM et al (2008) Activation of the chaperone Hsp26 is controlled by the rearrangement of its thermosensor domain. Mol Cell 29(2):207–216
101. Sobott F et al (2002) Subunit exchange of multimeric protein complexes. Real-time monitoring of subunit exchange between small heat shock proteins by using electrospray mass spectrometry. J Biol Chem 277(41):38921–38929
102. Siezen RJ, Bindels JG, Hoenders HJ (1978) The quaternary structure of bovine alpha-crystallin. Size and charge microheterogeneity: more than 1000 different hybrids? Eur J Biochem 91(2):387–396
103. Siezen RJ, Owen EA (1983) Physicochemical characterization of high-molecular-weight alpha-crystallin subpopulations from the calf lens nucleus. Biochim Biophys Acta 749 (3):227–237
104. van den Oetelaar PJ et al (1990) A dynamic quaternary structure of bovine alpha-crystallin as indicated from intermolecular exchange of subunits. Biochemistry 29(14):3488–3493
105. Bova MP et al (1997) Subunit exchange of alpha A-crystallin. J Biol Chem 272 (47):29511–29517
106. Bova MP et al (2000) Subunit exchange of small heat shock proteins – analysis of oligomer formation of alpha A-crystallin and Hsp27 by fluorescence resonance energy transfer and site-directed truncations. J Biol Chem 275(2):1035–1042
107. Guan YH et al (2006) Subunit exchange of MjHsp16.5 studied by single-molecule imaging and fluorescence resonance energy transfer. J Am Chem Soc 128(22):7203–7208
108. Painter AJ et al (2008) Real-time monitoring of protein complexes reveals their quaternary organization and dynamics. Chem Biol 15(3):246–253
109. Haslbeck M et al (1999) Hsp26: a temperature-regulated chaperone. EMBO J 18 (23):6744–6751
110. Benesch JLP, Sobott F, Robinson CV (2003) Thermal dissociation of multimeric protein complexes by using nanoelectrospray mass spectrometry. Anal Chem 75(10):2208–2214
111. Stengel F et al (2010) Quaternary dynamics and plasticity underlie small heat shock protein chaperone function. Proc Natl Acad Sci USA 107(5):2007–2012
112. Ito H et al (2001) Phosphorylation-induced change of the oligomerization state of alpha B-crystallin. J Biol Chem 276(7):5346–5352
113. Kato K et al (1994) Dissociation as a result of phosphorylation of an aggregated form of the small stress protein, hsp27. J Biol Chem 269(15):11274–11278
114. Michiel M et al (2009) Abnormal assemblies and subunit exchange of alpha B-crystallin R120 mutants could be associated with destabilization of the dimeric substructure. Biochemistry 48(2):442–453
115. Treweek TM et al (2007) Site-directed mutations in the C-terminal extension of human alphaB-crystallin affect chaperone function and block amyloid fibril formation. PLoS One 2 (10):e1046
116. Hayes VH, Devlin G, Quinlan RA (2008) Truncation of alphaB-crystallin by the myopathy-causing Q151X mutation significantly destabilizes the protein leading to aggregate formation in transfected cells. J Biol Chem 283(16):10500–10512
117. Ke L et al (2011) HSPB1, HSPB6, HSPB7 and HSPB8 protect against RhoA GTPase-induced remodeling in tachypaced atrial myocytes. PLoS One 6(6):e20395
118. Vos MJ et al (2010) HSPB7 is the most potent polyQ aggregation suppressor within the HSPB family of molecular chaperones. Hum Mol Genet 19(23):4677–4693
119. Horwitz J (1992) Alpha-crystallin can function as a molecular chaperone. Proc Natl Acad Sci USA 89(21):10449–10453

120. Brady JP et al (1997) Targeted disruption of the mouse alpha A-crystallin gene induces cataract and cytoplasmic inclusion bodies containing the small heat shock protein alpha B-crystallin. Proc Natl Acad Sci USA 94(3):884–889
121. Brady JP et al (2001) AlphaB-crystallin in lens development and muscle integrity: a gene knockout approach. Invest Ophthalmol Vis Sci 42(12):2924–2934
122. Jakob U et al (1993) Small heat-shock proteins are molecular chaperones. J Biol Chem 268 (3):1517–1520
123. Lee GJ, Pokala N, Vierling E (1995) Structure and in vitro molecular chaperone activity of cytosolic small heat shock proteins from pea. J Biol Chem 270(18):10432–10438
124. Merck KB et al (1993) Structural and functional similarities of bovine alpha-crystallin and mouse small heat-shock protein – a family of chaperones. J Biol Chem 268(2):1046–1052
125. Chang Z et al (1996) Mycobacterium tuberculosis 16-kDa antigen (Hsp16.3) functions as an oligomeric structure in vitro to suppress thermal aggregation. J Biol Chem 271 (12):7218–7223
126. Richter K, Haslbeck M, Buchner J (2010) The heat shock response: life on the verge of death. Mol Cell 40(2):253–266
127. Friedrich KL et al (2004) Interactions between small heat shock protein subunits and substrate in small heat shock protein-substrate complexes. J Biol Chem 279(2):1080–1089
128. Stromer T et al (2003) Analysis of the interaction of small heat shock proteins with unfolding proteins. J Biol Chem 278(20):18015–18021
129. Basha E, Friedrich KL, Vierling E (2006) The N-terminal arm of small heat shock proteins is important for both chaperone activity and substrate specificity. J Biol Chem 281 (52):39943–39952
130. Stengel F et al. Dissecting heterogeneous molecular chaperone complexes using a mass spectrum deconvolution approach. Chem Biol (in press)
131. Eyles SJ, Gierasch LM (2010) Nature's molecular sponges: small heat shock proteins grow into their chaperone roles. Proc Natl Acad Sci USA 107(7):2727–2728
132. Basha E et al (2004) The identity of proteins associated with a small heat shock protein during heat stress in vivo indicates that these chaperones protect a wide range of cellular functions. J Biol Chem 279(9):7566–7575
133. Ecroyd H et al (2007) Mimicking phosphorylation of alphaB-crystallin affects its chaperone activity. Biochem J 401(1):129–141
134. Giese KC et al (2005) Evidence for an essential function of the N terminus of a small heat shock protein in vivo, independent of in vitro chaperone activity. Proc Natl Acad Sci USA 102(52):18896–18901
135. Mogk A et al (2003) Small heat shock proteins, ClpB and the DnaK system form a functional triade in reversing protein aggregation. Mol Microbiol 50(2):585–595
136. Petko L, Lindquist S (1986) Hsp26 is not required for growth at high temperatures, nor for thermotolerance, spore development, or germination. Cell 45(6):885–894
137. Giese KC, Vierling E (2002) Changes in oligomerization are essential for the chaperone activity of a small heat shock protein in vivo and in vitro. J Biol Chem 277(48):46310–46318
138. Haslbeck M et al (2004) Hsp42 is the general small heat shock protein in the cytosol of Saccharomyces cerevisiae. EMBO J 23(3):638–649
139. Ehrnsperger M et al (1999) The dynamics of Hsp25 quaternary structure. Structure and function of different oligomeric species. J Biol Chem 274(21):14867–14874
140. Farahbakhsh ZT et al (1995) Interaction of alpha-crystallin with spin-labeled peptides. Biochemistry 34(2):509–516
141. Bennardini F, Wrzosek A, Chiesi M (1992) Alpha B-crystallin in cardiac tissue. Association with actin and desmin filaments. Circ Res 71(2):288–294
142. Koretz JF, Doss EW, LaButti JN (1998) Environmental factors influencing the chaperone-like activity of alpha-crystallin. Int J Biol Macromol 22(3–4):283–294
143. Poon S et al (2002) Mildly acidic pH activates the extracellular molecular chaperone clusterin. J Biol Chem 277(42):39532–39540

144. Bassnett S, Duncan G (1986) Variation of pH with depth in the rat lens measured by double-barrelled ion-sensitive microelectrodes. In: Duncan G (ed) The lens: transparency and cataract. Proceedings of the EURAGE/BBS symposium, Eurage, Rijswijk, pp. 77–85
145. Mathias RT, Riquelme G, Rae JL (1991) Cell to cell communication and pH in the frog lens. J Gen Physiol 98(6):1085–1103
146. Poole-Wilson PA (1978) Measurement of myocardial intracellular pH in pathological states. J Mol Cell Cardiol 10(6):511–526
147. Matuszewska E et al (2008) Escherichia coli heat-shock proteins IbpA/B are involved in resistance to oxidative stress induced by copper. Microbiology 154(Pt 6):1739–1747
148. Ahmad MF et al (2008) Selective Cu^{2+} binding, redox silencing, and cytoprotective effects of the small heat shock proteins alphaA- and alphaB-crystallin. J Mol Biol 382(3):812–824
149. Narayanan S et al (2006) alphaB-crystallin competes with Alzheimer's disease beta-amyloid peptide for peptide-peptide interactions and induces oxidation of Abeta-Met35. FEBS Lett 580(25):5941–5946
150. Biswas A, Das KP (2008) Zn^{2+} enhances the molecular chaperone function and stability of alpha-crystallin. Biochemistry 47(2):804–816
151. Ganadu ML et al (2004) Effects of divalent metal ions on the alphaB-crystallin chaperone-like activity: spectroscopic evidence for a complex between copper(II) and protein. J Inorg Biochem 98(6):1103–1109
152. Jang HH et al (2004) Two enzymes in one; two yeast peroxiredoxins display oxidative stress-dependent switching from a peroxidase to a molecular chaperone function. Cell 117 (5):625–635
153. Lee JR et al (2009) Heat-shock dependent oligomeric status alters the function of a plant-specific thioredoxin-like protein, AtTDX. Proc Natl Acad Sci USA 106(14):5978–5983
154. Biswas A, Das KP (2004) Role of ATP on the interaction of alpha-crystallin with its substrates and its implications for the molecular chaperone function. J Biol Chem 279 (41):42648–42657
155. Muchowski PJ, Clark JI (1998) ATP-enhanced molecular chaperone functions of the small heat shock protein human alphaB crystallin. Proc Natl Acad Sci USA 95(3):1004–1009
156. Hilario E et al (2006) Crystallization and preliminary X-ray diffraction analysis of XAC1151, a small heat-shock protein from Xanthomonas axonopodis pv. citri belonging to the alpha-crystallin family. Acta Crystallogr Sect F Struct Biol Cryst Commun 62(Pt 5):446–448
157. Muchowski PJ et al (1999) ATP and the core: "alpha-crystallin" domain of the small heat-shock protein alphaB-crystallin. J Biol Chem 274(42):30190–30195
158. Saibil HR (2008) Chaperone machines in action. Curr Opin Struct Biol 18(1):35–42
159. Ito H et al (1997) Phosphorylation of alphaB-crystallin in response to various types of stress. J Biol Chem 272(47):29934–29941
160. Wang K, Gawinowicz MA, Spector A (2000) The effect of stress on the pattern of phosphorylation of alphaA and alphaB crystallin in the rat lens. Exp Eye Res 71(4):385–393
161. Marin R, Landry J, Tanguay RM (1996) Tissue-specific posttranslational modification of the small heat shock protein HSP27 in Drosophila. Exp Cell Res 223(1):1–8
162. Aquilina JA et al (2004) Phosphorylation of alpha B-crystallin alters chaperone function through loss of dimeric substructure. J Biol Chem 279(27):28675–28680
163. Koteiche HA, McHaourab HS (2002) Effect of phosphorylation on the chaperone function of alpha B crystallin. Invest Ophthalmol Vis Sci 43:3567
164. Koteiche HA, McHaourab HS (2003) Mechanism of chaperone function in small heat-shock proteins – phosphorylation-induced activation of two-mode binding in alpha B-crystallin. J Biol Chem 278(12):10361–10367
165. Gaestel M (2002) sHsp-phosphorylation: enzymes, signaling pathways and functional implications. Prog Mol Subcell Biol 28:151–169
166. Ehrnsperger M et al (1997) Binding of non-native protein to Hsp25 during heat shock creates a reservoir of folding intermediates for reactivation. EMBO J 16(2):221–229

167. Lee GJ et al (1997) A small heat shock protein stably binds heat-denatured model substrates and can maintain a substrate in a folding-competent state. EMBO J 16(3):659–671
168. Lee GJ, Vierling E (2000) A small heat shock protein cooperates with heat shock protein 70 systems to reactivate a heat-denatured protein. Plant Physiol 122(1):189–198
169. Veinger L et al (1998) The small heat-shock protein IbpB from Escherichia coli stabilizes stress-denatured proteins for subsequent refolding by a multichaperone network. J Biol Chem 273(18):11032–11037
170. Liberek K, Lewandowska A, Zietkiewicz S (2008) Chaperones in control of protein disaggregation. EMBO J 27(2):328–335
171. Matuszewska M et al (2005) The small heat shock protein IbpA of Escherichia coli cooperates with IbpB in stabilization of thermally aggregated proteins in a disaggregation competent state. J Biol Chem 280(13):12292–12298
172. Mogk A et al (2003) Refolding of substrates bound to small Hsps relies on a disaggregation reaction mediated most efficiently by ClpB/DnaK. J Biol Chem 278(33):31033–31042
173. Haslbeck M et al (2005) Disassembling protein aggregates in the yeast cytosol. The cooperation of Hsp26 with Ssa1 and Hsp104. J Biol Chem 280(25):23861–23868
174. Cashikar AG, Duennwald M, Lindquist SL (2005) A chaperone pathway in protein disaggregation. Hsp26 alters the nature of protein aggregates to facilitate reactivation by Hsp104. J Biol Chem 280(25):23869–23875
175. Ratajczak E, Zietkiewicz S, Liberek K (2009) Distinct activities of Escherichia coli small heat shock proteins IbpA and IbpB promote efficient protein disaggregation. J Mol Biol 386 (1):178–189
176. Vos MJ et al (2011) Small heat shock proteins, protein degradation and protein aggregation diseases. Autophagy 7(1):101–103
177. den Engelsman J et al (2003) The small heat-shock protein alpha B-crystallin promotes FBX4-dependent ubiquitination. J Biol Chem 278(7):4699–4704
178. Parcellier A et al (2003) HSP27 is a ubiquitin-binding protein involved in I-kappaBalpha proteasomal degradation. Mol Cell Biol 23(16):5790–5802
179. Lin DI et al (2006) Phosphorylation-dependent ubiquitination of cyclin D1 by the SCF (FBX4-alphaB crystallin) complex. Mol Cell 24(3):355–366
180. Ahner A et al (2007) Small heat-shock proteins select deltaF508-CFTR for endoplasmic reticulum-associated degradation. Mol Biol Cell 18(3):806–814
181. Bissonnette SA et al (2010) The IbpA and IbpB small heat-shock proteins are substrates of the AAA+ Lon protease. Mol Microbiol 75(6):1539–1549
182. Meyer AS, Baker TA (2011) Proteolysis in the Escherichia coli heat shock response: a player at many levels. Curr Opin Microbiol 14(2):194–199
183. Stromer T et al (2004) Analysis of the regulation of the molecular chaperone Hsp26 by temperature-induced dissociation: the N-terminal domain is important for oligomer assembly and the binding of unfolding proteins. J Biol Chem 279(12):11222–11228
184. Aquilina JA, Watt SJ (2007) The N-terminal domain of alphaB-crystallin is protected from proteolysis by bound substrate. Biochem Biophys Res Commun 353(4):1115–1120
185. Lindner RA et al (2000) Mouse Hsp25, a small heat shock protein – the role of its C-terminal extension in oligomerization and chaperone action. Eur J Biochem 267(7):1923–1932
186. Smulders R et al (1996) Immobilization of the C-terminal extension of bovine alphaA-crystallin reduces chaperone-like activity. J Biol Chem 271(46):29060–29066
187. Bhattacharyya J et al (2006) Mini-alphaB-crystallin: a functional element of alphaB-crystallin with chaperone-like activity. Biochemistry 45(9):3069–3076
188. Sharma KK, Kaur H, Kester K (1997) Functional elements in molecular chaperone alpha-crystallin: identification of binding sites in alpha B-crystallin. Biochem Biophys Res Commun 239(1):217–222
189. Sharma KK et al (1998) Interaction of 1,1′-bi(4-anilino)naphthalene-5,5′-disulfonic acid with alpha-crystallin. J Biol Chem 273(15):8965–8970

190. Shashidharamurthy R et al (2005) Mechanism of chaperone function in small heat shock proteins: dissociation of the HSP27 oligomer is required for recognition and binding of destabilized T4 lysozyme. J Biol Chem 280(7):5281–5289
191. Franzmann TM et al (2005) The activation mechanism of Hsp26 does not require dissociation of the oligomer. J Mol Biol 350(5):1083–1093
192. Augusteyn RC (2004) Dissociation is not required for alpha-crystallin's chaperone function. Exp Eye Res 79(6):781–784
193. Ragusa MJ et al (2010) Spinophilin directs protein phosphatase 1 specificity by blocking substrate binding sites. Nat Struct Mol Biol 17(4):459–464
194. Carver JA et al (2002) The interaction of the molecular chaperone alpha-crystallin with unfolding alpha-lactalbumin: a structural and kinetic spectroscopic study. J Mol Biol 318 (3):815–827
195. Fontaine JM et al (2005) Interactions of HSP22 (HSPB8) with HSP20, alphaB-crystallin, and HSPB3. Biochem Biophys Res Commun 337(3):1006–1011
196. Tonegawa S (1983) Somatic generation of antibody diversity. Nature 302(5909):575–581
197. Gong Y, Kakihara Y, Krogan N, Greenblatt J, Emili A, Zhang Z, Houry WA (2009) An atlas of chaperone-protein interactions in Saccharomyces cerevisiae: implications to protein folding pathways in the cell. Mol Syst Biol 5:275, Epub June 16, 2009

Top Curr Chem (2013) 328: 99–154
DOI: 10.1007/128_2012_323

Published online: 11 May 2012

Allostery in the Hsp70 Chaperone Proteins

Erik R. P. Zuiderweg, Eric B. Bertelsen, Aikaterini Rousaki, Matthias P. Mayer, Jason E. Gestwicki, and Atta Ahmad

Abstract Heat shock 70-kDa (Hsp70) chaperones are essential to in vivo protein folding, protein transport, and protein re-folding. They carry out these activities using repeated cycles of binding and release of client proteins. This process is under allosteric control of nucleotide binding and hydrolysis. X-ray crystallography, NMR spectroscopy, and other biophysical techniques have contributed much to the understanding of the allosteric mechanism linking these activities and the effect of co-chaperones on this mechanism. In this chapter these findings are critically reviewed. Studies on the allosteric mechanisms of Hsp70 have gained enhanced urgency, as recent studies have implicated this chaperone as a potential drug target

E.R.P. Zuiderweg (✉) and E.B. Bertelsen
Department of Biological Chemistry, The University of Michigan, Ann Arbor, MI 48109, USA
e-mail: zuiderwe@umich.edu

A. Rousaki
Program in Biophysics, The University of Michigan, Ann Arbor, MI 48109, USA

Institute of Organic Chemistry and Chemical Biology, Goethe University, Max-von-Laue-Str. 7, 60438 Frankfurt, DE

M.P. Mayer
Zentrum für Molekulare Biologie der Ruprecht-Karls-Universität Heidelberg, Heidelberg, Germany

J.E. Gestwicki
Department of Biological Chemistry, The University of Michigan, Ann Arbor, MI 48109, USA

Lifesciences Institute, The University of Michigan, Ann Arbor, MI 48109, USA

Department of Pathology, The University of Michigan, Ann Arbor, MI 48109, USA

A. Ahmad
Department of Biological Chemistry, The University of Michigan, Ann Arbor, MI 48109, USA

Lifesciences Institute, The University of Michigan, Ann Arbor, MI 48109, USA

in diseases such as Alzheimer's and cancer. Recent approaches to combat these diseases through interference with the Hsp70 allosteric mechanism are discussed.

Keywords Dynamics · DnaJ · DnaK · Interactions · Structure

Contents

1 General Introduction

Heat shock 70-kDa proteins, Hsp70s, were first identified in bacteria as being over-expressed in response to cellular stress such as elevated temperatures, nutrient deprivation, heavy metals, oxidative stress, and viral infections [1]. Hsp70s rescue proteins that have been partially denatured, misfolded, and/or have become aggregated by these conditions. Hsp70s can unfold these clients in a complicated process fueled by ATP hydrolysis under allosteric control [2]. The unfolded clients are then free to refold properly. In addition to their roles in the stress response, Hsp70s are also expressed in normal, unstressed cells, where they act as chaperones, catalyzing the overall folding yield of newly expressed proteins by unfolding off-pathway intermediates [3, 4].

Hsp70s occur in all domains of life: archaea, eubacteria, and eukaryotes. In the eukaryotes, (specialized) Hsp70s are found in the cytosol, nucleus, mitochondria, chloroplasts, and endoplasmic reticulum. Hsp70s have been shown to be the most conserved proteins found in all organisms [5]. In archaea and eubacteria Hsp70 is referred to as DnaK. In yeasts they are called SSA, in mammals including humans they are referred to as HSPA. The latter are enumerated in Table 1. Most species encode for at least three Hsp70s.

In stressed human cells, the 13 Hsp70 isoforms account for 2% of all protein mass [6]. In addition to Hsp70's role in protein re-folding, Hsp70s direct irreversibly denatured proteins to degradation by the ubiquitin-proteasome system [7] or by the lysosomal proteolysis system [8]. Hsp70s are assisted by co-chaperones called J-proteins (Hsp40) [9] and nucleotide exchange factors (NEF) [10]. Apart from

Table 1 Homology for the hydrophobic NBD-SBD linker for the human HSPA (HSPA8 count) as compared to Hsp110 of *S. cervicea* (bottom)

Systematic name	Old name	390	391	392	393	394	395	396	397	398
HspA1A	Hsp70 1A/1B	D	L	L	L	L	D	V	A	P
HspA1L	Hsp70 1-like	D	L	L	L	L	D	V	A	P
Hspa2	Hsp70 2	D	L	L	L	L	D	V	T	P
HSPA5	Grp78, Bip	D	L	V	L	L	D	V	C	P
HSPA6	Hsp70 6	D	L	L	L	L	D	V	A	P
HSPA8	Hsc70	D	L	L	L	L	D	V	T	P
HSPA9	Mt-Hsp70, mortalin	D	V	L	L	L	D	V	T	P
HSP12A	Hsp70 12A	A	V	I	K	V	R	R	S	P
HSPA12b	Hsp70 12B	G	V	V	R	V	R	R	S	P
HSPA13	Hsp70 13	A	L	E	I	P	N	K	H	L
HSPA14	Hsp70 14	D	S	L	M	I	E	C	S	A
		395	396	397	398	399	400	401	402	403
HSP110	SSB-1	E	D	I	H	P	Y	S	V	S

their function in protein (re)folding, the Hsp70 proteins also mediate uncoating of clathrin-coated vesicles [11], trafficking of nuclear hormone receptors [12], and antigen presentation by MHCs [13]. Because of these varied roles, Hsp70 is considered a core mediator of protein homeostasis.

Hsp70s have been implicated in numerous diseases. For example, Hsp70s are upregulated in tumors [14], and they are required for the survival of these cells [15–17]. Enhanced expression of Hsp70 in tumor cells is likely caused by conditions which mimic stress [18, 19]. Hsp70s are thought to play at least three roles in cancer. First, they are thought to attempt to neutralize the conformational changes in mutant proteins [20, 21] which are common in tumorigenic cells. Second, Hsp70s are found to inhibit specifically cell death pathways [19, 22–26]. Third, mitochondrial Hsp70 can directly inactivate p53 tumor suppressor protein [27, 28]. Hsp70s are also involved in several CNS disorders. Diseases such as Alzheimer's, Pick's disease, progressive supranuclear palsy, corticobasal degeneration, and argyrophilic grain disease are characterized by the aberrant accumulation of hyperphosphorylated tau, called tau-tangles [29]. Hsp70s participate in the clearance of tau-tangles through a mechanism that is currently not well understood. Because of these emerging roles of Hsp70s in multiple diseases, there is renewed interest in understanding the mechanisms of this chaperone, with the goal of creating new medicines that best exploit the complex mechanisms of allostery in the Hsp70 system.

2 Hsp70 Overall Architecture and ATP Hydrolysis

Because Hsp70s are extremely well conserved proteins (53% identity, 68% homology between the Hsp70 of *E. coli* and Hsc70 of humans), the conclusions of studies using an Hsp70 from one organism are often considered to approximate the behavior of the others. Thus, we primarily discuss the properties and allosterics

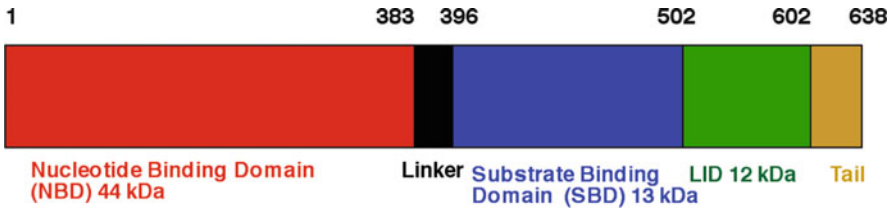

Fig. 1 Hsp70 domain architecture in DnaK *E. coli* count

of the Hsp70s in the context of the *E. coli* ortholog, called DnaK, because it is one of the best studied. Further, in this review we will often use the names DnaK and Hsp70 interchangeably.

DnaK contains three domains (see Fig. 1). The N-terminal 45-kDa Nucleotide Binding Domain (NBD) is formally divided into four subdomains: IA (1–37, 112–184, 363–383), IB (38–111), IIA (185–227, 310–362) and IIB (228–309), all in DnaK *E. coli* numbering. IA-IB and IIA-IIB form the two arms of a V-shaped structure [30, 31]. Nucleotide is bound at the center of the V-shaped cleft and is coordinated by residues derived from all four subdomains. The distribution is skewed: the adenosine and deoxy-ribose moieties are wedged into the interface of subdomains IIA and IIB. The α-phosphate and β-phosphate interact mostly with residues from subdomain IIA, whereas the γ-phosphate and the ATP-coordinated Mg^{2+} ion are mostly in contact with residues of subdomain IA. Only one residue from subdomain IB is involved in interaction with nucleotide. It is Lys70 which is absolutely essential for catalysis (Lys71 Hsc70 for which the definitive mutagenesis experiment was carried out [32]). The lysine ε-amino group is likely involved in the activation of the water molecule that carries out the nucleophilic attack on the gamma phosphate [32]. Mutations of other residues involved in nucleotide or Mg^{2+} binding affect k_{cat} and/or K_M, but no single mutation completely abolishes hydrolysis [33]. Hence there is no single residue acting as the sole general base catalyst. Even the nature of the monovalent ions that help coordinate the γ-phosphate in the active site is important: ATP hydrolysis is five times slower in NaCl than in KCl [34].

The NBD is connected via a linker to the Substrate Binding Domain (SBD). The linker is 10–12 residues in length and is highly conserved, showing a characteristic D/E-V/I/L-L-L-D-V-*-P hydrophobic sequence [35]. The SBD is a β-basket of 13 kDa, which is made up of two antiparallel β-sheets of four strands each [36]. The substrate-binding pocket is located between the two β sheets, is highly hydrophobic, and displays a high affinity for hydrophobic residues such as Leu [37]. A short linker connects the SBD to the 15-kDa alpha-helical LID which shields the substrate-binding pocket [37]. Beyond the LID is a tail region of varying length (approximately 50 residues) and sequence. In *E. coli* DnaK this tail is disordered and dynamic [38]. Recent work indicates that it may act as a disordered tether linked to a weak substrate-binding motif which enhances chaperone function by

transiently interacting with folding clients [39]. In human Hsp70s the very C-terminus of the tail region contains sequences that are important for the interaction with the CHIP [12], a ubiquitin ligase, or for ER targeting [40].

3 The Hsp70 Functional Cycle

Misfolded proteins (substrates) display stretches of exposed hydrophobic amino acids. The most quoted [41], but not universal [42], view is that co-chaperones of the DnaJ class (Hsp40) are the first to recognize and bind to such substrates, and escort them to the Hsp70 protein. In the DnaK–DnaJ–substrate complex, the substrate is transferred to the hydrophobic cleft located on the Hsp70 SBD. The cleft is solvent-accessible in the ATP state of the chaperone. By combined action of DnaJ and bound substrate, the Hsp70 hydrolyzes ATP. This leads to a large-scale conformational change in which the substrate becomes more tightly bound. EM-structural analysis of an Hsp70 bound to a full-length protein client confirms that the binding takes place through the SBD [43]. Nucleotide exchange factors (NEF; GrpE in the case of *E. coli*) help the Hsp70 to acquire ATP, reversing the conformational change, and reducing the affinity of the Hsp70 for the substrate, after which it is released. This cycle constitutes the so-called "holdase" and release function of the Hsp70 (see Fig. 2). This function is utilized to transport un/mis-folded proteins between organelles or to protect the un/mis-folded proteins from aggregation until more favorable folding conditions exist [44].

In addition to the holdase function, the Hsp70's main function is to help in the protein (re)folding process. Hsp70s such as DnaK, in the presence of DnaJ, GrpE, and ATP, can refold heat-denatured luciferase [45], polymerase [46], and resolubilize protein aggregates [47]. In fact, in the eukaryotic cytosol, Hsp70s are the predominant protein (re)folding machine, handling more substrates (20% of the proteome) [48] than the eukaryotic GroEL analog TRiC (7% of the proteome) [49]. Protein refolding must involve an active unfolding step of the substrate [4, 50, 51]. Possible mechanisms are (1) that Brownian motion of the chaperone loosens the bound misfolded protein, in a process called entropic pulling [52], (2) that misfolded proteins are inherently unstable and will transiently expose additional hydrophobic sequences which are trapped by additional DnaJ and/or DnaK, leading to progressive unfolding in a multi-molecular complex, (3) a combination of (1) and (2) [47], and (4) that the closure of the Hsp70 lid upon binding to the client is a molecular wedge to alter the conformation of the bound substrate [43]. Unfolded protein is subsequently released by action of the NEF, after which it can spontaneously refold. Especially in the refolding function (Hsp70 as "foldase" actually, better, "un-foldase") timing and kinetics must be critical to success.

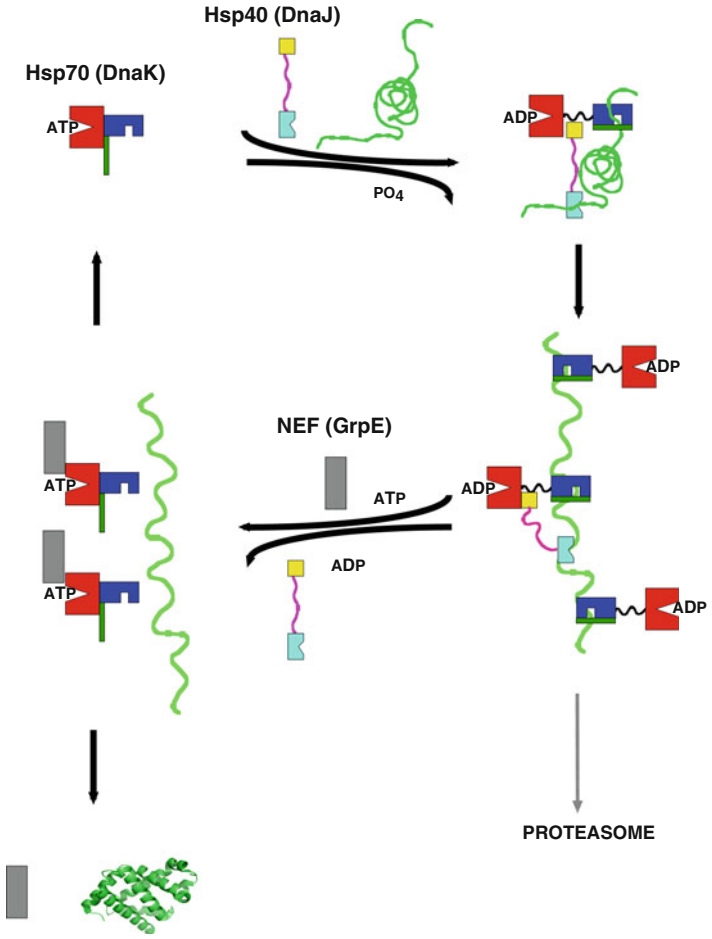

Fig. 2 The Hsp70 functional cycle as an unfoldase. DnaK NBD is in *red*, SBD is in *blue*, LID is in *dark green*. DnaJ J-domain is in *yellow*, DnaJ SBD is in *cyan*, DnaJ GF-region is in *pink*. Substrate (client) is in *green*. NEF is in *gray*. The oligomeric complex with several Hsp70s and Hsp40s is unproven. Successful cycles result in unfolded protein that can spontaneously refold. Unsuccessful cycles result in protein degradation by the proteasome

4 Allostery and Structures of Hsp70

Hsp70s are allosteric proteins in which ATP binding at the NBD causes substrate release at the SBD, and in which substrate binding causes hydrolysis of ATP, and in which hydrolysis of ATP enhances substrate binding. In the ADP state substrate binding is tight, while in the ATP state, the substrate binding affinity is reduced by one to two orders of magnitude [53–55] (depending on substrate and species; see Table 2). As the distance between the nucleotide binding cleft and substrate binding cleft is more than 50 Å, the clefts must communicate indirectly by allostery.

Table 2 Thermodynamics and kinetics of DnaK substrate-binding allostery

σ^{32}(132–144) binding to DnaK [54]				CALLQSRLLLSAPRRAAA binding to DnaK [55]		
	K_D	k_{on}	k_{off}	K_D	k_{on}	k_{off}
ATP	1.8 μM	1.3×10^6 M^{-1} s^{-1}	2.31 s^{-1}	2.2 μM	4.5×10^5 M^{-1} s^{-1}	1.8 s^{-1}
ADP	78 nM	1.17×10^4 M^{-1} s^{-1}	0.001 s^{-1}	63 nM	9.3×10^3 M^{-1} s^{-1}	0.004 s^{-1}
Ratio ATP/ADP	23	109	2,566	35	48	450
ΔΔG or ΔΔG‡	1.9 kCal M^{-1}	2.8 kCal M^{-1}	4.7 kCal M^{-1}	2.1 kCal M^{-1}	2.3 kCal M^{-1}	3.7 kCal M^{-1}

Our discussion here will focus mostly on allosterics as observed in DnaK, the Hsp70 of bacteria *E. coli*. This is because much of the early Hsp70 work was carried out for DnaK and also because the majority of the recent structural information on allostery has been collected on DnaK. We are, as of this writing, not aware of any structural/kinetic/thermodynamic findings that are fundamentally different for the mammalian Hsp70s. The latter differ from DnaK *E. coli* mostly in the utilization of different co-chaperones.

The difference in the affinity for substrate in the case of DnaK-ATP and DnaK-ADP corresponds to a free energy of allostery of only 2 kcal/mol (see Table 2) [53–55]. This is less energy than is contained in a typical H-bond. However, the substrate off-rate is different by three orders of magnitude between the ADP and ATP state, which corresponds to a respectable change of 4–5 kcal/mol in the free-energy of the dissociation activation barrier.

DnaK's allostery can be measured in a number of ways. In vitro assays include stimulation of ATP-hydrolysis upon substrate binding [56], which can be monitored by detecting the release of ortho-phosphate by γ^{32}P radio-isotope assays [57], colorimetric assays [58], or ^{31}P NMR spectroscopy [59]. In addition, substrate binding at the SBD may be monitored by change in the emission maximum of the intrinsic fluorescence of Trp102 of DnaK [60], which is located in the subdomain IB of the NBD [61]. The fluorescence change can hence be used to monitor allosteric communication. Furthermore, the quintessential substrate release upon ATP binding can be monitored by a decrease in the fluorescence anisotropy of fluoroscein-labeled substrate peptides [62]. Nucleotide and substrate binding result in global changes in the DnaK molecule. The linker between NBD and SBD is more easily cleaved in the ADP state than in the ATP state [61]. Also, amide proton exchange in the SBD is different in ADP and ATP states [63]. Finally, extensive chemical shift changes of the NMR lines of the NBD occur when peptide becomes bound to the SBD [64], and, conversely, the NMR spectrum of the SBD changes upon ADP/ATP exchange in the NBD [65].

In vivo assays of Hsp70 functionality include evaluation of capability of cells to survive heat shock [66], and, for DnaK in particular, its ability to stimulate lambda-phage growth in *E. coli* [67]. A stringent test is the refolding of mutated or heat-denatured luciferase, which will only occur in the presence of ATP and co-chaperones of the DnaJ and NEF class [45]. Recently, suspicions that all of these functional/biophysical assays may not perfectly correlate with each other have been put forth [68, 69].

Much about allosteric mechanisms of proteins can usually be learned from the comparison of the structures of different allosteric states of the proteins. The classical example is the comparison of the crystal structures of oxyhemoglobin and deoxyhemoglobin. The conformational differences seen provided strong clues about the allosteric mechanism, which was eventually verified with biochemical and genetic experiments. A similar structural analysis has been a longstanding goal in the Hsp70 field. While structures for isolated NBDs [37, 70–72], SBDs [37, 73, 74], and LID [37, 75] were published almost two decades ago, structural biology techniques have only recently captured a few constructs that contain both NBD and SBD

[38, 64, 76, 77]. For the Hsp70s, at least four allosteric states should be compared: NBD(ATP)-SBD(apo), NBD(ATP)-SBD(sub), NBD(ADP)-SBD(sub), and NBD (ADP)-SBD(apo). In addition, one can add NBD(apo)-SBD(apo) and NBD(apo)-SBD(sub). However, nucleotide-free NBD can exist only transiently during the ADP → ATP exchange and should not be considered to be a physiologically relevant state. Nevertheless, biochemical evidence suggests that its properties are not unlike the ADP-bound state [61]. ATP hydrolysis in the NBD(ATP)-SBD(sub) state is relatively rapid (0.05–0.5 s^{-1}) [56]. Consequently, the lifetime of this state is too short for structural studies. This leaves three other relevant states to be studied. The NBD(ADP)-SBD(sub) state is completely stable in the absence of NEFs and so is the NBD(ADP)-SBD(apo) state. The NBD(ATP)-SBD(apo) state is stable enough for most biophysical experiments (ATP hydrolysis rate is 5×10^{-4} s^{-1}) [56], but not for NMR or X-ray structure determination.

In addition to these fundamental considerations, there are technical problems. The Hsp70s tend to aggregate in both ADP and ATP states, especially when the SBD cleft is unoccupied, and the NBD-SBD linker is very susceptible to proteolytic cleavage. These properties hamper both NMR and X-ray studies. Hsp70s are "large" for NMR, precluding high-resolution structure determinations to be made (except for the isolated SBD [73, 78]). As multi-domain proteins of dynamical nature, Hsp70s also are a challenge for X-ray crystallography, both in crystallization and in the effect of packing on the relative (sub)domain positions in the crystal.

Because of these technical issues, only one of the four allosterically relevant structures is available to date: it is the NBD(ADP)-SBD(sub) state, determined in solution from a *combined* analysis of X-ray structural data of the subdomains, with NMR residual dipolar couplings which delineate the relative domain orientations. The structure was obtained for wt-DnaK in the presence of ADP, phosphate, and the peptide NRLLLTG ($K_D = 5$ μM) [38]. In this structure, the LID domain is docked to the SBD, but the SBD-LID unit moves rather unrestricted with respect to the NBD [38] as can be seen from the NMR intensity data presented in Fig. 3. Using ^{15}N NMR relaxation data, it was established that the dynamics of the SBD is consistent with motion in a cone of 70° opening angle with respect to the NBD, and that the time scale of the motion is shorter than 1 ns. The study substantiated earlier NMR studies that noted that the NBD and SBD behave as independent units in the ADP state [65, 79]. So the NMR data from two groups show that there is no stable communication between NBD and SBD in the ADP state. Hence, one expects that the two domains must interact in the ATP state.

By itself this is an interesting finding: conventional understanding is that allostery involves (at least) two well-defined states, in which the interaction free energy between the allosterically-coupled units differs. Possibly this outlook may be derived from the fact that virtually all structural studies of allosteric systems have been studied by crystallography, a method which can only characterize well-defined states. Possibly, allostery involving dynamic, "non-communicating" states is widespread, but has gone undetected. Alternatively, we observe here a primitive form of allostery. It must be simpler evolutionarily to develop interface

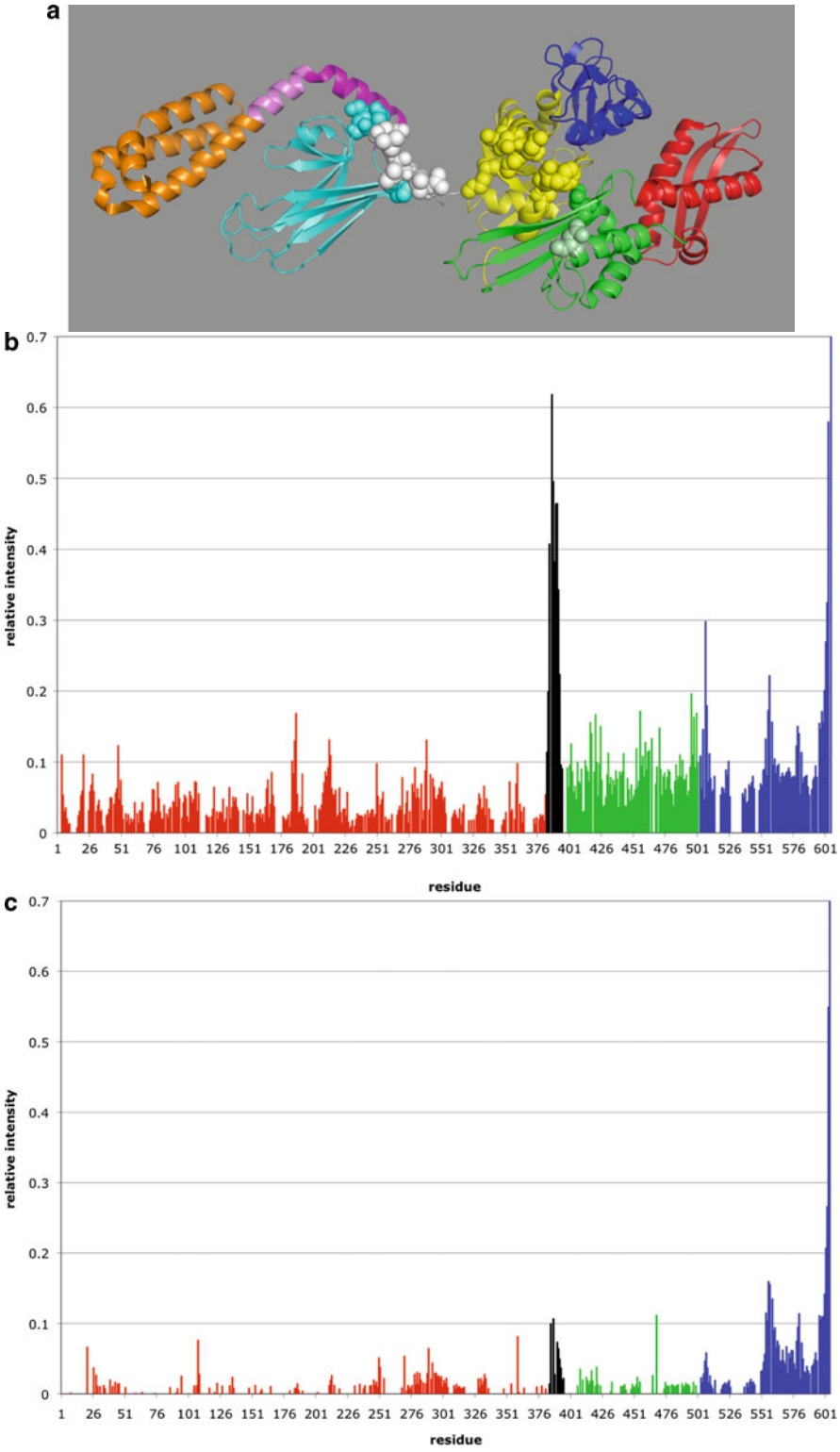
a
b
relative intensity
0.7
0.6
0.5
0.4
0.3
0.2
0.1
0
1 26 51 76 101 126 151 176 201 226 251 276 301 326 351 376 401 426 451 476 501 526 551 576 601
residue
c
relative intensity
0.7
0.6
0.5
0.4
0.3
0.2
0.1
0
1 26 51 76 101 126 151 176 201 226 251 276 301 326 351 376 401 426 451 476 501 526 551 576 601
residue

complementarity in only one instead of two allosteric states. Hsp70s, which are some of the most ancient proteins [5], may have conserved this mechanism.

The following other two-domain structures are available, but neither of these contains wild-type proteins.

First, an NMR solution conformation is available for a truncated construct of the DnaK of *Thermos thermophilus*, in the ADP state, but without bound substrate [64]. This protein, an NBD(ADP)-SBD(apo) state construct, is missing the complete alpha-helical LID domain. It does not show relative domain motions. Its overall domain alignment is within experimental uncertainty, identical to that of wt-DnaK-*E. coli* NBD(ADP)-SBD(sub). Whether the lack of inter-domain motion is caused by the lack of the LID, the lack of substrate, or the fact that the experimental data were recorded at 55 °C, a temperature well below the temperature of optimal activity of *T. thermophilus* (65–80 °C), is currently unknown.

Second, a crystal structure of a two-domain construct of bovine Hsc70 truncated at residue 554 was reported [76]. The C-terminus binds to the substrate-binding cleft. In this construct, NBD and SBD were found to interact. However, the mutations E213A and D214A, which were essential to the crystallization process, are found to be on the interface between NBD and SBD (see Fig. 4). It is likely that these aggressive mutations are the cause of the observed hydrophobic packing between NBD and SBD. We believe that the crystal structure for this Hsc70 triple-mutant [76] is artifactual.

Third, a crystal structure of DnaK(1–509) from *Geobacillus kaustophilus* bound in the ADP state was reported [77]. The construct is missing the alpha-helical LID domain. The crystal contains dimers, in which the SBD of one monomer binds to the NBD-SBD linker of the other monomer. While this is not likely to be a physiologically relevant state, the structure does show that the NBD and SBD are significantly separated from each other, in agreement with NMR solution structure of wt-DnaK in the ADP state [38].

Fourth, a crystal structure of SSE1, an Hsp110 from *S. cerevisiae*, has appeared [80]. Hsp110s are homologous to Hsp70s, and bind ATP stably without hydrolyzing it. Despite the fact that the Hsp110 crystal structure is a dimer mediated by LID–LID interactions, the NBD-SBD interface may be representative of the Hsp70 ATP state.

Fig. 3 (**a**) The relative orientation of the SBD (*left*) and NBD (*right*) for DnaK(1–605) in the ADP – NRLLLTG state in solution [38]. NBD domain IA: *yellow*, IB: *blue*, IIA: *green*, IIB: *red*, linker: *white*, beta domain: *cyan*, LID-helix-A: *magenta*, LID-helix-B: *pink*, Lid: *orange*. Residues rendered in space fill are important for the NBD-SBD allosteric communication as determined by mutagenesis studies from several other workers as discussed in the text. (**b**) Dynamical properties of the ADP-NRLLLTG state of the DnaK backbone as determined from cross-peak intensity of HNCO NMR data [38]. High intensity indicates high mobility, low intensity indicates low mobility. Colors: NBD: *red*, Linker: *black*, SBD: *green*, LID: *blue*. (**c**) Dynamical properties of the ATP-APO state of the DnaK (1–605)(T199A/V436F) backbone as determined from cross-peak intensity of HNCO NMR data. High intensity indicates high mobility, low intensity indicates low mobility. Colors: NBD: *red*, Linker: *black*, SBD: *green*, LID: *blue* (Bertelsen and Zuiderweg, unpublished)

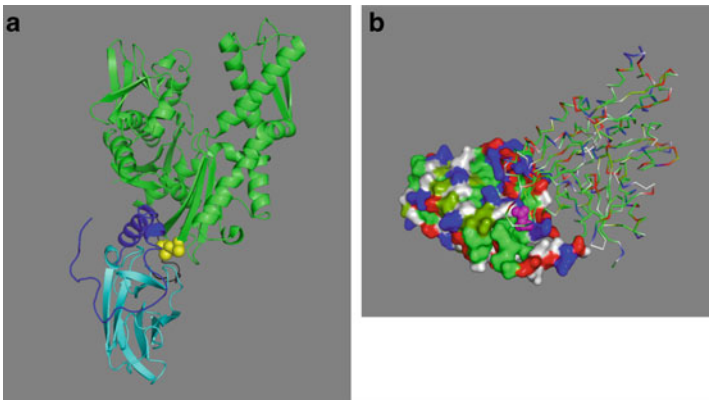

Fig. 4 A crystal structure of human Hsc70 Δ(555–646) E213A/D214A [76]. (**a**) *Left*, overall docking. *Green*: SBD, *cyan*: SBD-beta; *blue* LID; *black* NBD-SBD linker. A213 and A214 are *yellow*. (**b**) *Right*, docking of the NBD (ribbon) on the SBD/LID/Linker (surface). The linker is at the *bottom*. Color coding: *green*: apolar, *red*: negative, *blue*: positive, *white*: polar, *mud-green*: Thr + Tyr. The mutations A213 and A214 on the NBD are in *pink* and interact directly with a hydrophobic SBD surface

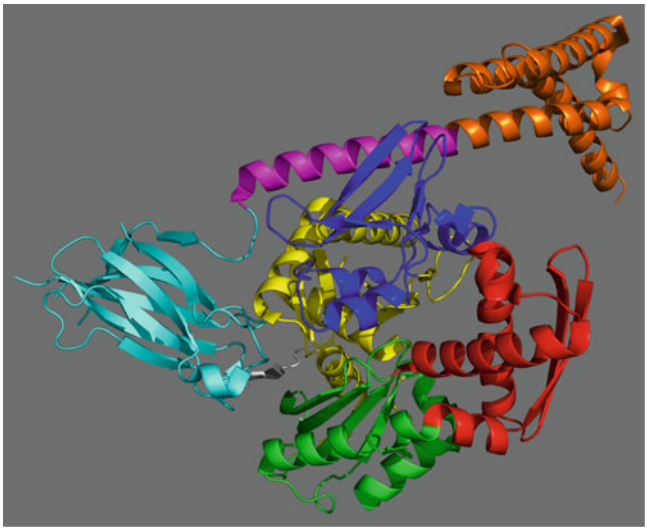

Fig. 5 A crystal structure of Hsp110 of *S. cervisea* [80] Orientation and color coding is as in Fig. 3a. (NBD domain IA: *yellow*, IB: *blue*, IIA: *green*, IIB: *red*, linker: *white*, beta domain: *cyan*, LID-helix-A: *magenta*, LID-helix-B: *pink*, Lid: *orange*)

It is depicted in Fig. 5. The structure shows a docked NBD and SBD, in agreement with the expectation for the ATP state of Hsp70. The linker is engaged as an additional strand of the two-stranded beta sheet in NBD subdomain IIA. This docking would explain the extensive solution NMR chemical shift changes upon ATP/ADP exchange

seen for residues in these strands [64, 65, 81, 82]. The LID in Hsp110 has moved away from the SBD and is docked against subdomain IB. This docking would explain the fact that the fluorescence of Trp102 in subdomain IB of DnaK is affected by the ATP-ADP conformational change, but not in the absence of the LID [61]. Despite all these expected features, there is still doubt as to the validity of Hsp110 as a model for the Hsp70 ATP-apo state. In particular, the lack of homology for the linker (see Table 1) is of great concern. The linker plays a key role in the allosteric function of the Hsp70s (see below). The linker sequence VLLLD, strongly conserved between Hsp70 members, is DIHPY in Hsp110. On the one hand, the differences in linker are quite to be expected as they would explain why Hsp110 is locked in the ATP state; on the other hand, one questions whether the observed docking in Hsp110 can be representative of the presumed docking in the Hsp70s since the differences in physico-chemical properties of the linker residues are so large.

A recent NMR contribution from the Gierasch group [83] is weighing in on this discussion. They observe chemical shift changes in the two-stranded beta sheet in NBD subdomain IIA between DnaK NBD constructs with and without the linker, but only in the ATP state. While no actual structure determination was carried out, these results were interpreted to reflect that, only in the ATP state, the linker may form an additional strand of the two-stranded beta sheet in NBD subdomain IIA. Hence, this study supports the claim that the crystal structure of SSE1 [80] may indeed be a model for the ATP state of the Hsp70 chaperones.

Nevertheless, as of this writing, this leaves us with only one reliable structure for a full-length and authentic Hsp70: it is the solution structure of wt-DnaK in the NBD(ADP)-SBD(sub)state in which no communication between NBD and SBD takes place [38, 65]. Hence all understanding of the allosteric mechanism for Hsp70s has to be derived from either structural studies of the individual domains and their changes upon ligand binding or biochemical/biophysical studies of the full-length proteins without direct structural insights.

Fortunately, many such studies are available, and will be reviewed below.

5 Global Characteristics of the Allosteric Change

The γ-OH of Hsc70 active-site residue T13 (T11 in DnaK *E. coli* numbering) forms a hydrogen bond with an oxygen of the ATP γ-phosphate. This hydrogen bond is one of the few direct links between the nucleotide and NBD subdomain IA (see above). Mutation of T13 to valine did not affect the efficiency of ATP hydrolysis, but completely abrogated the allosteric communication between NBD and SBD [84]. The mutation T13S was allosterically active [84] and structural studies revealed that its γ-OH took the position of the γ-OH of Thr. These findings underscore the importance of this single hydrogen bond for the allosteric mechanism. Possibly it is the key linkage signaling the nucleotide state to subdomain IA, which, in turn, propagates the signal to the SBD (see below). However, the

mechanism is probably more complicated: mutation of Hsc70 residue K71 (K70 in *E. coli* numbering), the only ATP-contact residue derived from subdomain IB (and essential for ATP hydrolysis [32]) also abrogating the ATP-induced conformational change (as determined by SAXS) [32]. Hsc70 point-mutations E175S, D199S, and D206S also bind ATP and also impair the ability of ATP to induce a conformational change [32] (E171, D194, and D201 in *E. coli* numbering). All of these residues are involved in coordinating Na^+ or K^+ ions, which in turn neutralize the ATP γ-phosphate. The mutation E543K on the LID can "rescue" the ATP-induced transition for E175S/E543K, D199S/E543K, and D206S/E543K. E543 (D540 *E. coli*) forms a salt-bridge with R469 (R467 *E. coli*), stabilizing the LID-closed, ADP state. It is likely that the E543K mutation destabilizes the ADP state, facilitating the ATP-induction of the LID-open state. Hence, it is likely that the mutations E175S, D199S, and D206S attenuate, but do not eliminate, allosteric communication. The γ-OH of T204 (T199 *E. coli*) was initially thought to be a candidate for the nucleophile attacking the ATP. However, its mutation to Ala yielded a protein that could still turn over ATP (albeit less efficiently), and in which allostery was intact [85]. The same mutation in *E. coli* (T199A) had the same phenotype [61, 86]. A rather rigorous mutation in the DnaK substrate binding cleft, V436F, retained significant substrate binding capability, and retained allostery [61, 87, 88].

Some representative mutations of surface residues that yield Hsp70 constructs that still can hydrolyze ATP and bind substrate, but which lack allosteric coupling, are Y145A, N147A, and D148A [86]; P143G and R151A [89]; K155D and R167D [35]. Mutagenesis of most residues of the NBD-SBD linker leads to loss of allosteric communication [35, 90]. On the SBD, mutations K414I [62] and P419A [91, 92] eliminate allostery. N415G and D326V attenuate allostery [93]. All mentioned positions are listed in DnaK *E. coli* numbering and are shown in Fig. 3. The NBD surface mutations all occur in subdomain IA facing the SBD in the solution structure except for D326V on subdomain IIB, rendered in a different shade of green in Fig. 3. The SBD mutations occur on the solvent exposed loops that face the NBD in the solution structure of the ADP state. These areas are potentially in contact in the ATP state. Recent work showed that these areas have been subject to co-evolutionary mutagenesis [93], further bolstering the observation that they could be in contact in the ATP allosteric state.

SAXS experiments showed considerable changes in overall molecular shape between the ATP and ADP allosteric states of Hsc70 [94, 95]. The ADP state is extended and monomeric, while the ATP state has a more globular shape. However, the SAXS experiments on the ATP state should be critically viewed, considering that this state has a strong tendency to aggregate at the concentrations needed for SAXS.

Both hydrogen exchange and limited proteolytic digestion studies of DnaK show that ATP binding stabilizes the NBD, while simultaneously destabilizing most of the SBD [61, 63].

Gierasch and coworkers observed that the TROSY NMR spectra of the isolated NBD and isolated SBD superimposed well on the TROSY NMR spectrum for DnaK in the ADP state, but not for DnaK in the ATP state [65, 79]. This data suggested that

NBD and SBD do not interact in the ADP state, but do interact in the ATP state. The former observation was fully confirmed in the solution structure of DnaK in the ADP state (see Fig. 3). In this figure the intensities of the HNCO cross peaks are plotted as well [38]. Larger peaks indicate greater mobility of the associated amino acid residues. Clearly, the SBD and LID domains have equal mobilities, while the NBD domain has a different mobility. NBD-SBD domain docking in the ATP state is confirmed with NMR mobility data on a DnaK construct in the ATP state as shown in Fig. 3c. This figure also shows that part, but not all, of the LID is undocked in the ATP state.

Extensive domain dynamics has also been observed in FRET studies of the yeast Scc1 DnaK homolog [96]. Fluorophores attached to NBD position 341 (318 in DnaK *E. coli* count) and SBD position 448 (425) are closer to each other in the presence of ATP than in the presence of ADP. The distance distribution is much wider for the ADP state than the ATP state, in agreement with the relative mobility of the NBD and SBD in that state. Fluorophores attached to SBD position 448 (425) and LID position 590 (564) are closer to each other in the presence of ADP than in the presence of ATP, showing that the LID undocks in the latter state. Again, the distance distribution is wider for the ADP state than the ATP state, suggesting that the LID can also undock in the ADP state.

As deduced from the following observations, the determinants for the allosteric communication appear to be solely embedded in the NDB and the beta domain of the SBD and the NBD-SBD linker. The LID domain, which certainly has to move away from the beta domain to allow substrate binding and release, does not directly drive the allostery. Mutant DnaK in which the complete LID was deleted (1–507) showed wild-type activity in the ATP-hydrolysis and ligand fluorescence assays (see Fig. 6) [74]. When the severely truncated DnaK(1–507) was expressed in a DnaK-deficient strain, it still supported significant bacteriophage growth [74]. It is unknown, but unlikely, that this construct is also functional in protein refolding, given the pivotal role of the LID in regulating the kinetics of substrate binding and release [97–104].

Other workers have also shown that other "lidless" constructs retain considerable allostery [97, 98, 101–104]. It seems prudent to conclude that the conformational changes of the LID domain are a result rather than a cause of the Hsp70 allostery. However, comparisons of the kinetics of ligand binding and hydrolysis between wild-type and constructs lacking the LID showed that the LID domain affects the kinetics of substrate binding and release in a dramatic fashion [97, 98, 101–104]. Fine control of substrate binding and release kinetics must be essential to the protein refolding machinery – maybe even more so than thermodynamics (see below).

6 The Key Role of the NBD-SBD Linker

The ten-residue linker between NBD and SBD is mostly hydrophobic and strongly conserved between Hsp70s (see Table 1). This linker is more exposed in the ADP than in the ATP state according to proteolysis assays [105] and hydrogen exchange

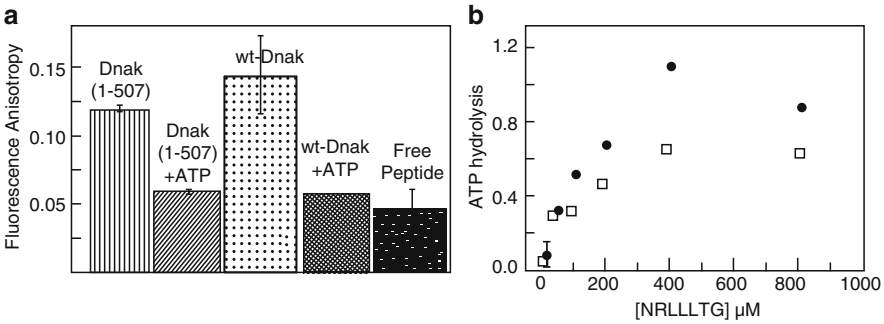

Fig. 6 In vitro studies of DnaK(1–507) allosteric function. (**a**) ATP-induced release of peptide F-APPY in DnaK(1–507) measured by fluorescence anisotropy. The *first bar* represents the anisotropy value for peptide bound to 1.1 mM DnaK(1–507). The *second bar* represents the anisotropy value 5 min after addition of 0.44 mM ATP. The *third and fourth bars* represent the values for wt-DnaK under comparable conditions, and the *last bar* indicates the anisotropy value of free peptide. *Error bars* reflect the standard deviation from a mean of three measurements. (**b**) Peptide stimulation of ATPase activity of DnaK(1–507) (P) and wt-DnaK (m). As DnaK (1–507) is titrated with the peptide NRLLLTG, the ATPase activity is stimulated in a manner similar to that of wt-DnaK. The hydrolysis rate is reported as moles of ATP hydrolyzed per minute per mole of DnaK(1–507) or wt-DnaK. The *error bar* on the first point reflects the standard deviation from a mean of three measurements and is valid for both assays. From [74]

experiments [63]. This is fully confirmed with the NMR dynamics data in Fig. 3: in the ADP state the linker is very mobile, while the linker in the ADP state is docked. Combined with the knowledge that mutations in the linker are detrimental to the allosteric coupling [90, 106], these results imply a significant role for the linker in allosteric signal transduction between the NBD and SBD.

Mayer and co-workers were the first to observe that the ATP-hydrolysis rate by the isolated NBD of DnaK(2–393) was 41-fold faster than that of DnaK(2–385) [35]. The difference between these constructs lies in the presence or absence of the linker sequence ^{386}VKDVLLLD^{393}. As such, the mere presence of the linker in this truncated construct mimicked, partially, the hallmark allosteric stimulatory effect of substrate binding in the context of the wild-type protein. The mutation D393A abolished the enhancement. This demonstrated that the linker itself is necessary and sufficient for allosteric control of the NBD. Together with the observations that mutations of the hydrophobic residues interfere with allostery [90, 106], and with the observation that mutation of D388 did not interfere with allostery [35], the essential part of the linker is demarcated as ^{389}VLLLD^{393}.

The effect of the presence of linker on the ATP hydrolysis rate was independently observed by Gierasch and co-workers, who found that DnaK(1–392) was a 13-fold more efficient enzyme than DnaK(1–388) [65]. These workers used NMR investigations to characterize the differences between the NBD constructs. The domains in the ADP state revealed major chemical shift differences for about 50 residues between DnaK(1–392) and DnaK(1–388). In addition, the four C-terminal residues of DnaK(1–388) were seen to be mobile. Significantly, the C-terminus of

DnaK(1–392) was not mobile, indicating that the linker is docked in this construct. Using selective labeling experiments, it was possible to show that L177 and I373 in the IA-IIA hydrophobic cleft undergo large chemical shift changes between the two constructs. The sidechain of L177 is part of the surface of the IA-IIA hydrophobic cleft. I373 is completely buried but packed against L177. It was suggested that the shifts of these residues indicate that the linker binds in this cleft. Recent work strongly suggests that DnaK residues 215–220, which form the edge strand of the beta sheet in subdomain IIA, interact with the NBD-SBD linker in the ATP state but not in the ADP state [83]. There is some indication that the linker forms an extra strand of the beta sheet. Very likely this interaction is crucial to the propagation of the allosteric signal from the NBD to the SBD [80].

Mayer and coworkers set out to identify the electrostatic partner for linker residue D393 on the NBD surface [35]. Mutagenesis of likely candidate residues R151, K155, and R167 in the IA-IIA cleft showed those to be important for the regulation of allostery in the context of the full molecule. However, charge reversal mutations of these residues in the context of DnaK(2–393) exacerbated the ATP hydrolysis enhancement effect instead of abolishing it. So, it is unlikely that D393 interacts with these positive residues in DnaK(2–393). This leaves one with the suspicion that the interaction of the linker in the context of the isolated NBD could be different to that in the full protein. In this context it is interesting to note that crystal structures of linker-extended Hsc70 NBD constructs did not show electron density for the linker, and their three-dimensional structures were identical to those of constructs without the linker [107].

7 Allosteric Changes in the NBD

The linker interacts differently with the NBD in the ATP state compared to in the ADP state [35, 65, 83] . Hence, one expects differences for the structures of the NBD in these different states. Remarkably, only very small differences were observed between the conformation of the (isolated) NBD by X-ray crystallography in the presence of a variety of nucleotide analogs (see Fig. 7), making it difficult to explain *why* the linker docks in one state but not the other. However, NMR spectra showed distinct differences in chemical shifts between the ADP and ATP states in Hsc70 [81] and in DnaK [82, 108], especially in the groove between NBD subdomains IA and IIA. This strongly suggests that conformational changes also occur in solution for the isolated NBD (Fig. 7).

Since these conformational changes are not observed in the crystal, the energy difference between them is likely to be small, which is in agreement with the overall characteristics of the Hsp70s as described at the outset. The solution-detected differences reveal much of the workings of the Hsp70 allosteric machine. With the modern NMR method of residual dipolar couplings, relative domain orientation can be determined in solution, even though detailed changes and translations cannot [109]. Using these methods it was possible to detect up to 9° rotation between the

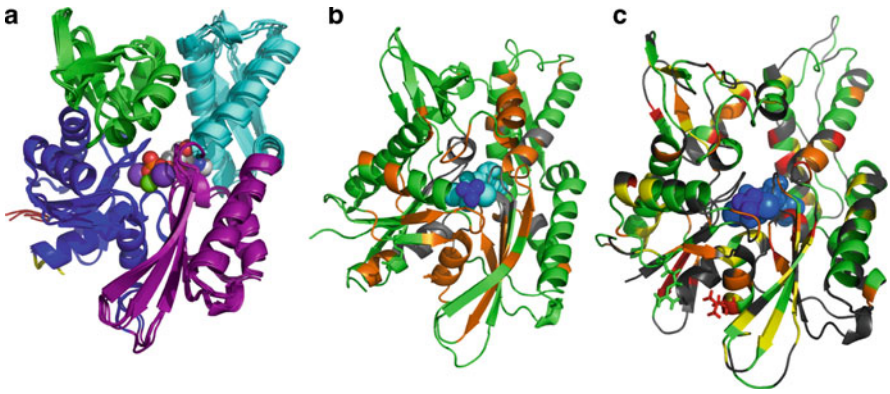

Fig. 7 (**a**) Superposition of five crystal structures for bovine Hsc70 NBD: wt-APO (2QW9.pdb), wt-ADP.PO_4 (3HSC.pdb and 2QWL.pdb), wt-ADP.VO_4 (2QWM.pdb) and K71M-ATP (1KAX.pdb). The N-terminus is in *red*, the C-terminus is in *yellow*. (**b**) ^{15}N-^{1}H chemical shift differences between the ATP and ADP.Pi conformation of Hsc-70-NBD. *Orange*: significant shift, *green*: no shift, *gray*: not known. (**c**) ^{15}N-^{1}H chemical shift differences between the AMPPNP and ADP.Pi conformation of TTh-NBD. *Red*: large shifts; *orange*: medium shifts; *yellow*: small shifts; *green*: no shift; *gray*: not known. ADP is in *light blue*, PO_4^{3-} in *dark blue*

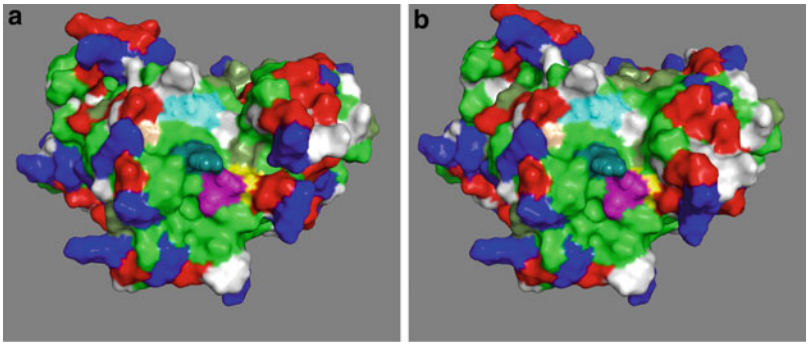

Fig. 8 The SBD's view of the IA/IIA interface of DnaK-TTh. (**a**) *Left*: in the ADP state. (**b**) *Right*: in the AMPPNP state [82]. Color coding: hydrophobics, *green*; positive, *blue*; negative, *red*; polar, *white*. The C-terminus (residue 372) is *magenta*. Residue L174 (L177 in DnaK *E. coli*) in *yellow*, residue R148 (R151 in *E. coli*) in *cyan*, residue A152 (K155 in *E. coli*) sand, residue R164 (R167 in *E. coli*) in teal

different subdomains for the isolated NBD of DnaK *T. thermophilus* (TTh) when comparing the ADP and AMPPNP states [82]. In particular, the hydrophobic cleft between subdomains IA and IIA is different between the AMPPNP state and the ADP state. The structure calculations suggest that the groove is narrow and deep in the ATP state and broad and shallow in the ADP state (see Fig. 8). However, the calculations are based on rotations of entire subdomains without translational information, and the accuracy of the presented structural models is very limited.

Nevertheless, the rotation of subdomain IIA relatively to subdomain IA is real (with 97% significance), which will obviously affect the details of the groove between the subdomains. Figure 8 also shows the locations of the different relevant residues discussed in the previous paragraph.

The NMR data show that the nucleotide-binding cleft is "closed" in the ATP state and is "open" in the ADP state. These studies suggest that the crystal structures of the isolated NBD all correspond to the "closed" ATP state, irrespective of the bound ligand.

Different orientations of the NBD subdomains have also been observed, by crystallography, for NBDs complexed with different nucleotide exchange factors [71, 110–113]. These studies show that subdomain rotations are also possible in the crystal. Similar changes have been seen for actin and hexokinase, which show considerable structural homology with the Hsp70 NBD [31]. The nucleotide binding cleft is more open in the Hsp70-NEF-complexes. The open state of Hsc70 with an NEF in the crystal resembles the ADP state of DnaK *TTh* without an NEF in solution [82]. This would suggest that the NEF captures and stabilizes the more open ADP state.

What local changes could allow these global rotations? The sugar-ribose moiety and alpha-phosphate of ATP is exclusively in contact with subdomains IIA and IIB. Only the beta and gamma phosphates contact subdomain IA (hydrogen bonds with Thr14 NH and Thr13 NH, respectively), and form the only link between lobes II and I (from inspection of the structure of Hsc70-K71M, with bound ATP). Breakage of the gamma-phosphate, as has occurred in the ADP state of the protein, may therefore weaken the link between the lobes, allowing for (dynamic) rearrangement of the relative positions of these lobes. In this way, the state of the deeply buried nucleotide can be signaled to the surface of the NBD by (dynamic) subdomain rotations. The rotations are probably responsible for the change in access to the hydrophobic cleft between IA and IIA as was described above.

Mayer and co-workers have discovered an interesting mutation R151K in DnaK, which abolishes all allosteric communication [63, 89]. R151K is located in subdomain IA and its sidechain is partially exposed to the groove between subdomains IA and IIA. In the Hsc70 crystal structure the guanidinium group of the homologous R151 is within hydrogen bond distance of the carbonyl oxygen of P143. P143, in turn, stabilizes E175, which protrudes into the nucleotide-binding pocket (see Fig. 9). The authors hypothesize that the NBD nucleotide state affects this network reversely, possibly by a proline *cis-trans* isomerization and a more extensive conformational change in segments 139–163 and 165–177, which flank the IA-IIA cleft. This change then leads to a change in the linker docking. Substrate binding hypothetically reverts all of these conformational changes, in particular in Pro143 (*cis-trans* isomerization) and E171, thereby bringing the catalytic K70 with its coordinated water molecule into the ideal position for ATP gamma-phosphate cleavage.

Whether this hypothetical mechanism actually contributes to nucleotide-cleft signaling awaits investigation of the mutant R151K by structural analysis.

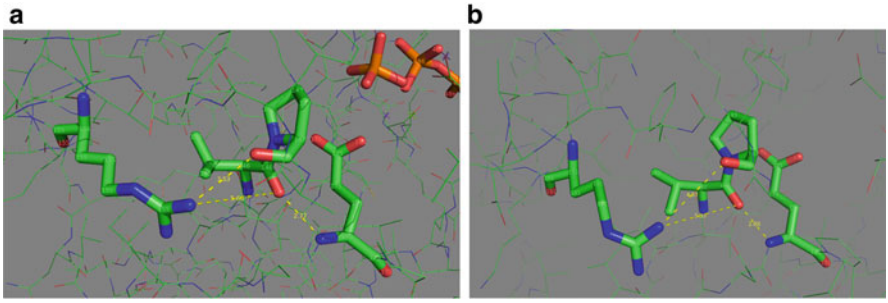

Fig. 9 (**a**) *Left*: the hypothetical "proline switch" in Hsc70 ADP.Pi. (**b**) *Right*: the hypothetical "proline switch" in DnaK-*E. coli* without nucleotide. Following [89]

8 Allosteric Changes in the SBD

The SBD has been extensively investigated (see Fig. 10). Its topology is unique in the PDB [36]. A crystal structure of an SBD-LID construct of DnaK showed that the substrate-binding cleft is lined with hydrophobic residues to which a hydrophobic substrate (NRLLLTG) binds [37]. The cleft shows one particularly deep pocket that accommodates the sidechain of Leu4 of the substrate. The backbone of the substrate is stabilized by H-bonds to the main chain of the SDB. The SBD is a rather "flat" molecule, with the binding cleft spanning the short axis. The cleft just about covers the seven-residue substrate; hence it is believed that an Hsp70 can in principle bind to stretches of seven exposed residues in un- or misfolded proteins.

In the substrate-bound form, the LID is closed. LID helices A and B (the rising and horizontal helices in Fig. 10) are stabilized by a combination of hydrophobic and charge interactions, while the part that covers the cleft has exclusively charge–charge interactions [37, 115]. Recent NMR data [38] confirms that, in solution and with NBD present, the complete LID domain is docked to the beta basket in the ADP state and when substrate is present (also see Fig. 3b). Figure 3c shows that the latter section of the lid un-docks when the ligand is absent with the NBD the ATP state. This result confirms, with direct data, the long-standing belief that the lid must come off the cleft for binding or release of substrate protein.

Interestingly, the NMR dynamics data in Fig. 3c suggest that the release does not engage the entire LID, and confirms an early hypothesis based on slight structural differences at exactly this hinge point between different molecules in the crystallographic unit cell [37]. However, it disagrees with our earlier hypotheses that the entire LID can come off, which was based on observations of displacements of the entire helix with respect to the beta domain for different SBD constructs [73, 78]. Muga and co-workers [115] found that mutations at the N-terminus of the horizontal helix destabilize the ADP but not the ATP state, also suggesting that the entire helix comes off in the ATP state. Other data also suggest that the entire helix B can come off: for DnaK it is well known that W102 fluorescence changes upon binding of ATP [100, 116]. The change is compatible with a reduction in solvent exposure of this residue, which is located in NBD subdomain IB. This change in fluorescence is lost

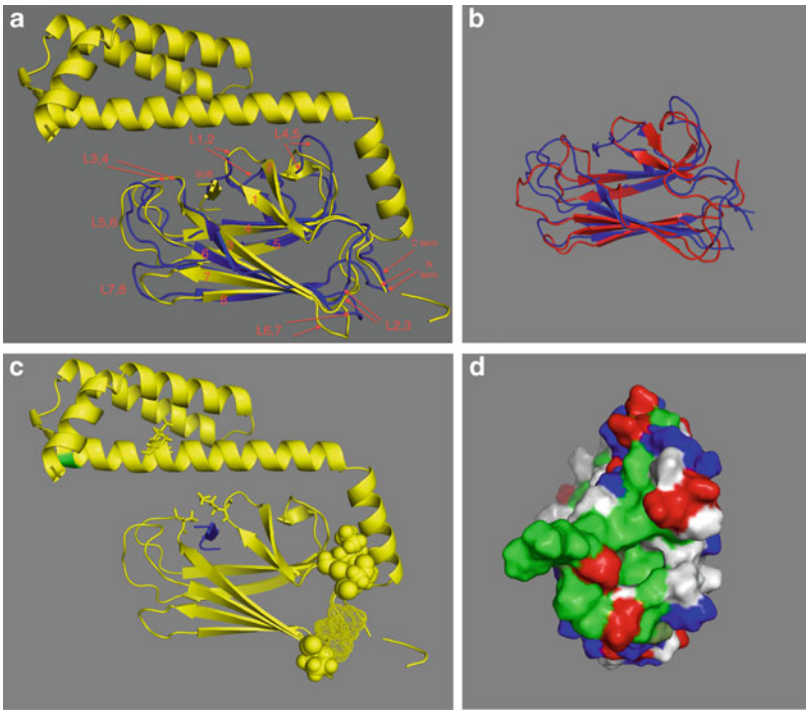

Fig. 10 (**a**) Comparison of *E. coli* DnaK(389–605)-NRLLLTG (*yellow* [37]) with DnaK (393–507)-NRLLLTG (*blue* [114]), with nomenclature following [37]. (**b**) Comparison of DnaK (393–507)-NRLLLTG (*blue* [114]) with DnaK(393–507).apo (*red* [74]) (**c**) DnaK(389–605)-NRLLLTG. The ligand is in *blue*. Residue 552 is in *green*. L542Y, L543E on the LID are in *sticks*. K414, N415 and P419 are in *space fill*, T417 and I418 are in *dots*. (**d**) The N-terminal "face" of DnaK(389–605)-NRLLLTG. Phobics are in *green*, positives in *blue*, negatives in *red*, polars *white*. The structure protruding at 3 o'clock is the residual NBD-SBD linker, with Asp393 (*red*) close to the SBD core

upon removal of the entire LID as in truncation DnaK(1–507) [99, 117]. Nevertheless, allosteric communication, as judged by peptide-release stimulation by ATP and ATP hydrolysis stimulation by peptide, is still fully functional in DnaK(1–507) [74, 117]. This suggested that, in the ATP-apo state, the LID may directly collide with NBD subdomain IB. It is of interest to note that the crystal structure of Hsp110, potentially a model for Hsp70 in the ATP state, shows direct contact between the LID helix and subdomain IA [80]. Muga and co-workers [117] also found that the W102 fluorescence change remains in DnaK(1–537), suggesting that N-terminus of helix B, must come off to allow changing interaction with subdomain IA.

The following results may shed light on this conundrum. Using EPR spinlabels and cysteine cross linking, Mayer et al. [68] show that the LID can hinge at residue 515 (between helix A and B) and also at residue 530 (in helix B, close to the binding cleft, see in Fig. 3c) but that these different modes depend on the nature of the substrate offered: binding/release of entire proteins requires the first mode.

Gierasch and co-workers [79] used NMR to study the DnaK(387–552, L542Y, L543E), a construct containing both beta basket and helices A and B of the LID. The mutations were made to avoid self-binding of the truncated lid [78] (see Fig. 10c). Changes in chemical shifts of DnaK(387–552, L542Y, L543E) upon titration of NRLLLTG were small, and localized around the substrate cleft. The pattern of hydrogen exchange protection with and without bound substrate were largely the same, although the overall stability of the domain was slightly enhanced by the substrate. Analysis of NOEs and hydrogen bonding confirmed that DnaK (387–552, L542Y, L543E) showed very little and certainly no widespread conformational change upon ligand binding. These studies present a question: if no changes occur in the SBD structure upon substrate binding, how does substrate binding get transmitted to the NBD?

The above results are at variance with the results of an earlier NMR investigation, in which DnaK(393–507), containing only the beta basket, was investigated [74]. As stated above, lidless DnaK(1–507) is functional protein in vitro and, at least partially, in vivo. Hence, one expects that the basket alone should display allosteric effects. The properties of substrate-bound and substrate free basket differed greatly. In the presence of substrate, the basket was rigid (confirmed with ^{15}N relaxation measurements; L. Wang and E. Zuiderweg, unpublished), and the solution structure was identical to the corresponding region of the crystal structure of substrate-bound DnaK(389–605) [114] (Fig. 10a). In contrast, unliganded basket is a dynamic molecule which fluctuates between different conformations on the milli/microsecond time scale [74]. All resonances for loops 3, 4, 5, and 6 (see Fig. 10a for nomenclature) were broadened away beyond detection, suggesting a dynamical collapse, or melting, of part of the substrate binding cleft. Less, but still significant, broadening was observed for Q424, V425, F426, and S427, which in the liganded structure form the latter half of beta strand 3. It was concluded that the latter part of this strand is dynamically disordered in the apo state. Broadening was also observed for the amide protons T417 and I418 in loop 2,3 which are quite remote from the cleft, and which "face" the NBD in the structure in Fig. 3. Hence, the NMR data show a conformational/dynamical linkage between events in the substrate binding cleft and loop 2,3.

^{15}N relaxation studies on the basket showed that the rotational correlation time of the domain decreases from 12 to 7 ns upon binding of NRLLLTG (L. Wang and E. Zuiderweg, unpublished). Such a change in rotational correlation time is compatible with a change from dimer to monomer. Dilution experiments suggest that $K_{\text{dimer}} < 1$ μM. Ligand-linked monomerization could explain why the substrate NRLLLTG binds with considerably lower apparent affinity (600 μM) [74] than to wild-type protein (5 μM) [37], even though the structure of the bound complex is similar to the wt structure (Fig. 10). Isotope-edited NOE experiments on mixed ^{15}N-^{14}N labeled protein preparations showed NOEs between the ^{15}N and ^{14}N labeled proteins, confirming the existence of a dimer for the APO state of the basket (S. Stevens and E. Zuiderweg, unpublished). Significantly, the inter-monomer NOEs suggested that dimerization was not mediated by the substrate-binding pocket. In contrast, a few inter-monomer NOEs to residues in the

hydrophobic "face" of the SBD shown in Fig. 10d and at the beta sheet at the "bottom" were observed, suggesting that the dimerization interaction may take place at these locations. Despite this unnatural (?) dimerization of the isolated beta basket, the fact remains that substrate binding/release causes major changes in its properties. This is in line with expectations for an allosteric protein. Apparently, a protein–protein interaction interface is only exposed in the apo state but not in the substrate-bound state. This is quite reminiscent of the fact that the SBD interacts with NBD in the apo state but not in the substrate-bound state. It is tempting to speculate that the unnatural dimerization of the isolated SBD without LID fortuitously mimics the interaction of the SBD with the NBD. However, if such is true, why was this unnatural dimerization not seen for the beta domain extended with helices A and B [79]?

Perhaps the combined results point to the following mechanism. (1) In the SBD apo-state, there exists a patch which is poised for protein–protein interactions. (2) Without NBD and LID, the patch interacts to form unnatural homo-dimers. (3) *Without* NBD but *with* LID, the patch is covered by the LID. (4) With LID and with NBD, the NBD displaces the LID from the patch because NBD has a high affinity for that patch (or NBD-SBD linker; see below).

This hypothesis would suggest that the internal substrate-binding allostery of isolated SBD is different from the internal substrate-binding allostery of the SBD in presence of NBD. The following supports such a view. While the isolated DnaK (387–552, L542Y, L543E) showed little difference in hydrogen exchange rates between apo and substrate-bound states [79], widespread changes in amide proton protection were seen upon ADP/ATP exchange for the SBD in the two-domain construct DnaK(1–552, L542Y, L543E) [65]. In particular, Thr 420 and V436 are more exposed in the ATP state, whereas H422 is protected in that state.

These findings correspond closely to those of Mayer and co-workers [118] who mapped the differences in amide proton exchange of DnaK(T199A) between ADP and ATP state using proteolysis and mass spectrometry. ATP hydrolysis in DnaK (T199A) is greatly reduced, but allosteric communication with the SBD is maintained. Figure 11 shows that the SBD is dramatically destabilized in the ATP/apo state, just as was found for the isolated beta basket without substrate [74]. Noteworthy is that stretch 413–437 and the edge strand of the lower beta sheet become more exposed in the ATP state. The former area contains the mutation sites K414I [62] and P419A [91, 92] and N415G [93] which abolish or attenuate allosteric communications. Regretfully the resolution is not high enough to distinguish the loop from the strand. Substrate binding significantly reduced amide proton exchange in the beta domain, especially on the longer time scale. Regretfully, again, the resolution is too low to disclose whether global rigidification or just local rigidification around the peptide binding cleft occurs.

New amide proton exchange experiments [118] for wt-DnaK in the ATP-APO state show a gradient of deprotection towards loops 3,4 and 5,6 closely corresponding to the melting of the substrate-binding cleft in the isolated beta basket in the APO state [74].

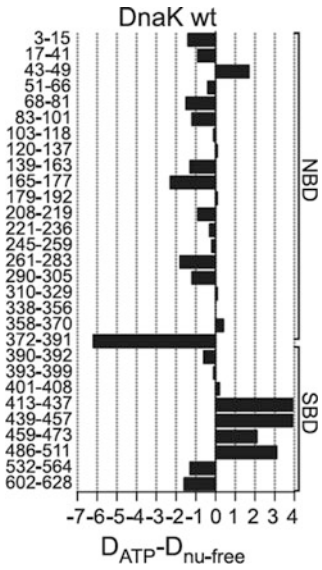

Fig. 11 Differences in amide-proton exchange for *E. coli* DnaK in the ATP and ADP state. Positive numbers indicate less protection in the ATP state. From [63]

Taken together, there is sufficient evidence from several sources to suggest that widespread conformational/dynamical change takes place in the SBD upon ligand binding and/or ATP/ADP binding. The results obtained for the construct containing both beta basket and helices A and B of the LID, which did not show such changes [79], appear surprising in this context, but do help in underlining the subtleties of NBD/beta/LID/linker/substrate interactions, and the need for further investigations.

9 Where Does the SBD Interact with the NBD in the ATP State?

As discussed above, we do not believe that any valid Hsp70 structures in which NBD and SBD dock have yet been described. In the previous section we hypothesized that a hydrophobic "face" of the SBD, may interact with the NBD in the NBD(ATP)-SBD(Apo) state.

There have been suggestions that the hydrophobic linker may interact with a hydrophobic patch that "faces" the NBD as seen in Fig. 10b [37, 78]. In this way, the NBD and SBD never interact directly – interaction is mediated by the linker from both sides. Presence of a hydrophobic site in the corresponding SBD area has been confirmed: NMR signals for L392, L397, and A413 disappeared while V394, T395, L484, and L507 weakened in the NMR spectrum of DnaK(386–561) due to interaction with a hydrophobic peptide labeled with paramagnetic label [78]. Significantly, L392 is part of the linker, while A413 is next to the mutation sites K414I [62] and N415G [93] that affect allostery. It was also noted that LID helix A is docked to the same hydrophobic patch [78]. Perhaps the NBD-SBD linker can displace the LID in the ATP form.

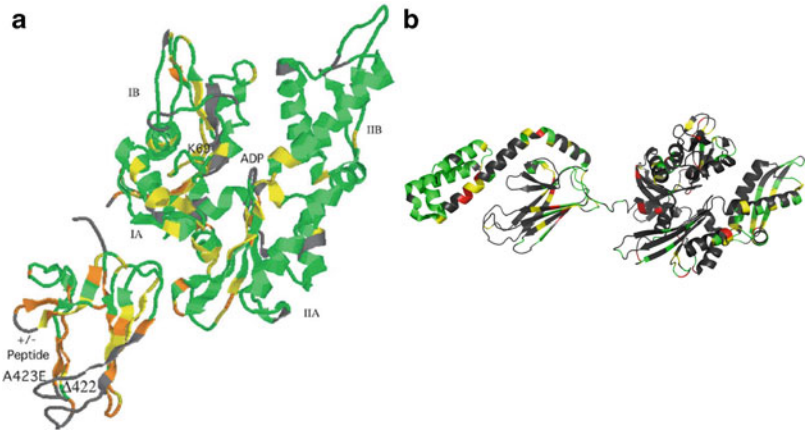

Fig. 12 Chemical shifts changes and two-domain allostery. (**a**) Chemical shift changes between the ADP-apo and ADP-NRLLLTG state in DnaK *T. Thermophilus* (1–501) From [64]. (**b**) Chemical shift changes between ADP-apo DnaK E. coli (1–605) and ATP-apo DnaK *E. coli* (1–605) (T199A/V436F) (Bertelsen and Zuiderweg, unpublished)

Table 3 Sequence homology of Hsp110 *S. cerv.* vs Hsc70 *H. sapiens*

	Identity (%)	Homology (%)		Identity (%)	Homology (%)
IA	35	61			
IB	30	55	Linker	12	32
IIA	44	76	Beta	10	20
IIB	42	67	LID	16	31
NBD	35	60	ALL	25	44

The precise mechanism by which the substrate binding is signaled to the loop that contains K414?, P419A and N415G is unknown. Perhaps the intrinsic flexibility of this loop as seen in substrate-free SBD [63, 74] allows a captured fit [119] of the NBD-SBD linker, while the rigidification of the entire domain upon ligand binding is sufficient to interfere with this process. This mechanism would be related to allostery by dynamic change alone, predicted by Cooper and Dryden [120], and experimentally confirmed by NMR studies for several systems [121–126].

On the other hand, there are also indications that beta strands 3, 6, 7, and 8 of the SBD are involved in contact: residues in these strands show dramatic chemical shift changes between the NBD(ADP)-SBD(apo) state and the NBD(ADP)-SBD(sub) state of *TTh* DnaK(1–501) [64] (see Fig. 12a). Similarly, chemical shifts in these strands were identified when comparing the NMR spectrum of DnaK(1–605) in the NBD(ADP)-SBD(sub) state with that of DnaK(1–605) T99A V436F in the NBD (ATP)-SBD(apo) states (Fig. 12b).

Surprisingly, no changes were observed in either of these cases for the residues in the Loop 2,3 facing the NBD, which contains all the mutation sites mentioned. Clearly, more work is still needed to understand fully the complete allosteric pathway in the SBD of the Hsp70s.

10 Relevance of Hsp70 Allostery

Structural and dynamical properties for the two "end-point" allosteric states are listed in Table 4. Some, but not all aspects of this table can be represented in a cartoon as shown in Fig. 13. It is truly amazing that so many differences exist, while the free energy of allostery is only a few kcal/mol as judged from the difference in substrate binding energy between these states (Table 2). The real conundrum, however, is that the corresponding small difference in substrate binding constants (~2 μM for the ATP state and 70 nM for the ADP state; see Table 1) can only discriminate between ligands in the concentration range of 200 nM: ten times more concentrated substrates would remain bound even to the ATP state, while ten times less concentrated substrates would not even bind to the ADP state. Such a concentration limitation seems awkward for a molecular machine that needs to refold a variety of proteins over a wide concentration range.

Maybe one should look at this differently. Classically, the argument is that the free energy of ATP hydrolysis is needed to unfold the misfolded proteins; in this view, little of the ATP hydrolysis energy remains to effect conformational changes in the Hsp70 themselves. However, ATP's free energy may not be (directly) needed for the unfolding task: the gain in hydrophobic interaction between substrate and SBD should at least partially compensate for the loss of energy associated with the loss of aggregation. In turn, the loss of the interaction energy upon release of the substrate is at least partially regained in the hydrophobic docking of NBD and SBD in the ATP state. In this view, considerable fractions of the 7–14 kcal/mol of ATP hydrolysis energy (depending on conditions) may be used to break the NBD-SBD interface and be the cause of the major conformational changes seen. In this view, substrate binding to the ADP state does not need to be tighter than substrate binding to the ATP state. This hypothesis also explains how substrate could efficiently bind to the low-affinity open ATP state at the start of the chaperone cycle, while it is efficiently released from this same state at the end of the cycle. Indeed, all that is needed is that the chaperone is brought into contact with the substrate (with help of DnaJ, see below) and retains its substrate long enough to allow unfolding by Brownian motion, referred to as "entropic pulling" [52], with the possible assistance of multiple copies of DnaK or DnaJ (transiently) binding to the same target (see Fig. 2 and [127] and see below). Opening of the substrate binding cleft at the end of the cycle is then sufficient to let the unfolded protein diffuse away. In this sense, the "thermodynamic" allostery would play only a minor role in the functional cycle. One may quantify this as a mixed thermodynamic/kinetic mechanism as follows. Substrate binding occurs with the high association rates of the DnaK-ATP state and dissociates with the slow dissociation rate of the ADP state. Such a *non-equilibrium* K_D is in the order of 1 nM (k_{on}(DnaK-ATP) ~ 1×10^6 M^{-1} s^{-1}, k_{off}(DnaK-ADP) ~ 0.001 s^{-1}; see Table 1). This "affinity" is high enough to bind even low-abundant proteins. Upon nucleotide exchange the K_D reverts to that of the ATP state, i.e., it increases 1,000-fold. Potentially, NEFs can even compete for the bound substrate (see below), further reducing effective substrate affinity. Viewed in this mixed thermodynamic/kinetic way, the Hsp70s could successfully operate on substrates in a concentration range between 1 and 1,000 nM.

Table 4 Summary of allosteric changes

	Nucleotide binding cleft	IA-IIA cleft	NBD dynamics	Linker	SBD	SBD dynamics	LID
NBD(ATP)-SBD(apo)	Closed	Open	Rigid	Docked	Docked	Millisecond/microsecond time scale[a]	Released
NBD(ADP)-SBD(sub)	Open	Closed	Second/decisecond time scale[b]	Mobile	Not docked	Rigid	Docked

[a]Extensive NMR line broadening observed
[b]Multiple NMR peaks in slow exchange observed

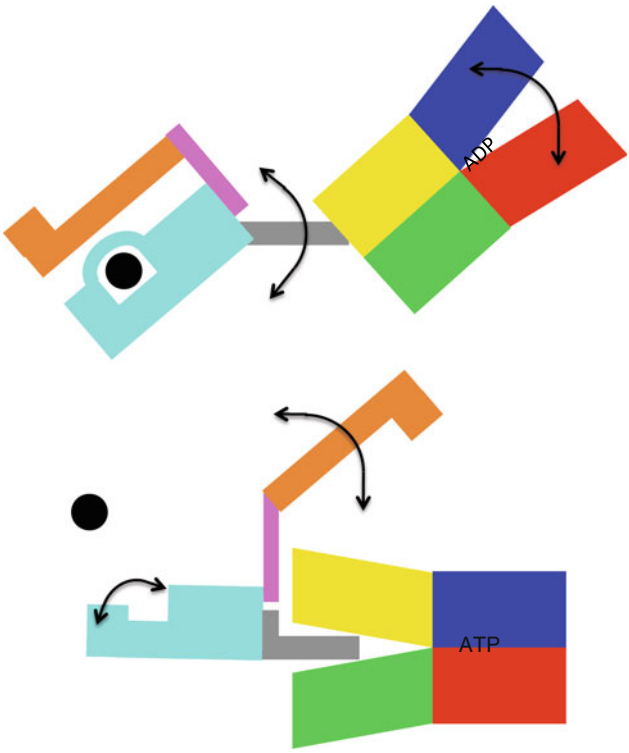

Fig. 13 Cartoon representation of the allosteric changes between the ADP.sub state (*top*) and ATP-apo state (*bottom*). Color coding is (as in Fig. 1): NBD subdomain IA, *yellow*; IB, *blue*; IIA, *green*; IIB, *red*; linker, *gray*; beta domain, *cyan*; LID-helix-A, *magenta*; Lid, *orange*. Relative domain orientations of NBD, SBD and LID in the top cartoon are representative of reality (see Fig. 1). The relative domain orientations of those domains in the bottom cartoon are based on the hypotheses reviewed herein. Also see Table 4

The kinetics of the Hsp70 chaperone system is complex. It involves substrate on-off processes, nucleotide on-off processes, lid opening and closing, ATP hydrolysis, and conformational changes. In addition, co-factors such as DnaJ and GrpE bind and release and affect the rates mentioned above. It is not the purpose of this chapter to review the large body of literature on this subject. We note that Witt and coworkers [97, 101, 128–131], Christen and co-workers [132–135], and Bukau and co-workers [56, 61, 136] have contributed much to this field.

11 The Role of the NEFs in Allostery

Nucleotide exchange factors enhance the exchange of ADP for ATP up to 1,000-fold [133, 137]. At the present time, four very different NEFs have been co-crystallized with Hsp70 NBDs: GrpE [71], BAG-1 [110], BAG-2 [138],

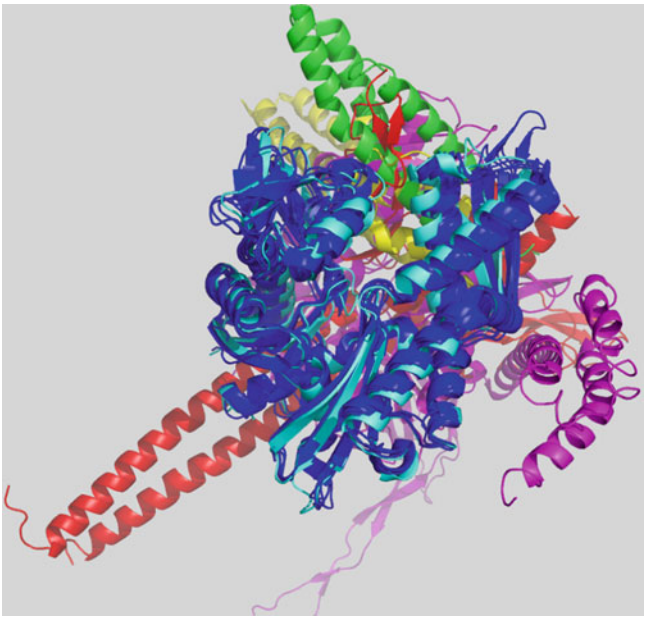

Fig. 14 NBD-NEF complexes. The NBDs were superposed and all colored *blue*. GrpE (1DKG) in *red*; Hsp110 (3C7N) in *magenta*, BAG-1 (1HX1) in *green*; BAG-2 (3CQX) in *yellow*. The NBD of Hsc70 without NEF (3HSC) is shown in *cyan*

Hsp110 [80, 139] (see Fig. 14). A partial structure is available for exchange factor HSPBP [111, 140]. While the binding interfaces between the factors and the Hsp70 are vastly different, all Hsp70 NBDs in the different complexes have in common that the nucleotide binding cleft is opened wider than in isolated Hsp70 NBD crystal structures. These observations clearly account for enhanced access and egress of the nucleotide. Initially the NEFs were thought to open actively the NBD cleft in an induced-fit mechanism [71, 110]. However, in light of the wide variety of NEFs which all achieve the same effect, it is more reasonable to assume that NEFS capture (transient) opening fluctuations of the NBD. This is in line with the recent solution NMR data that show that the nucleotide binding cleft in the isolated NBD in the ADP state is considerably more widely open than in the ATP state [82]. Such a "captured fit" would also provide a mechanism for GrpE to interact exclusively with the (dynamic) ADP-like state, and not with the static closed ATP state; the latter would be a wasteful and undesirable interaction.

The bacterial NEF, GrpE, has a remarkable structure. It is a hammer-like dimer, which (also in solution [141]) interacts with a monomeric Hsp70. The interaction of the NBD occurs mostly by the head of the hammer. Upon inspection of the crystal structure of the complex, the authors suggested [71] that the shaft might interact with the SBD (which was absent in the complex). Interestingly, the simple exercise of superposing the common NBD in the crystal structure of DnaK(NBD)-GrpE [71] with the solution structure of wt-DnaK in the ADP-sub form [38] places the end of

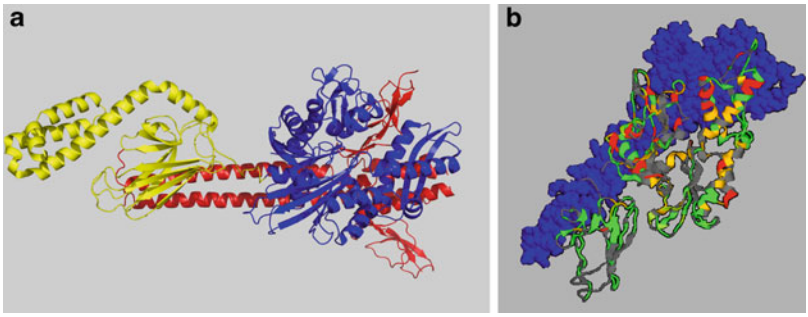

Fig. 15 Hypothetical GrpE-DnaK complexes. (**a**) Model of a functional *E. coli* DnaK-GrpE complex based on the structures of DnaK ADP.NRLLTG (2KHO) and DnaK-NBD + GrpE 40–197 (1DKG.pdb) in which the NBDs were superposed. GrpE is in *red*. The GrpE N-terminus (residue 40) is at the *left*. (**b**) Chemical shifts occurring on DnaK *T. Thermophilus* (1–501) upon addition of GrpE *T. Thermophilus*. Model composed as in Fig. 15a (Deep and Zuiderweg, unpublished)

the GRPE shaft in immediate vicinity of the SBD cleft (see Fig. 15a). GrpE residues 1–37, which would extend even further towards the SBD cleft, are not visible in the crystal. It is intriguing that a hydrophobic sequence ^{17}Ile-Ile-Met^{19} exists in this otherwise hydrophilic area of GrpE. We speculate that these residues may be responsible for the demonstrated competition of the GrpE N-terminus with substrate [142]. Indeed, the affinity of Hsp70 for substrate in the ATP state is actually not that much lower than that in the ADP state (see Table 2) and assistance to remove substrate from the ATP state is likely necessary.

Our lab has collected chemical shift evidence showing interaction of the GrpE shaft with the SBD for a two-domain construct of DnaK *T. thermophilus* and the N-terminus of GrpE *T. thermophilus* (S. Deep and E.R.P. Zuiderweg, unpublished; see Fig. 15b). Folding/unfolding transitions in the GrpE N-terminus have been shown to act as a thermostat for the DnaK activity [141]. This hypothesis does not seem valid for eukaryotes. BAG proteins, the NEFs of Hsc70, do have extended, likely unfolded areas at the N-terminus, but, according to the crystal structure of the Hsc70–BAG1 domain complex, this area would not be in the vicinity of the SBD.

12 The Role of DnaJ in Allostery

The human genome codes for 50 J-proteins are subdivided into three classes: DnaJA, DnaJB, and DnaJC (see Table 5). The J-proteins are also referred to as Hsp40. Like Hsp70s, DnaJs also bind to stretches of exposed hydrophobic residues in client proteins. DnaJ *E. coli* [143] and DnaK *E. coli* [144] substrate specificities are similar, and both prefer hydrophobic sequences. However, DnaJ can also bind to synthetic D-amino acid peptides [145]. This strongly suggests that DnaJ does not make hydrogen bonds in the peptide backbone of its client, but instead interacts

Table 5 DnaJ nomenclature and structure. The sequence numbers are for YdJ1 (yeast)

Type	Example	J-domain (1–70)	GF region (71–110)	SBD(116–145 and 208–255)	Zn-domain (146–206)	GM region	SBD-duplicate (260–340)	Dimer helix (350–360)	Extended Tail (370–409)
DNAJA (Type I)	DnaJ E. coli Ydj1 yeast HDJ-2 human	Present	Present	Present	Present		Present	Present	Present
DNAJB (Type II)	HDJ-1 human Sis1 yeast	Present	Present	Present		Present	Present	Present	
DNAJC (Type III)	pyJ polio virus	Present							

mainly with hydrophobic sidechains and is more forgiving in the substrate's local structure.

The most commonly [45] but not universally [42] held view is that DnaJ apportions the clients to DnaK which is in the ATP-apo state with an open SBD. After or during the process of client transfer, DnaK hydrolyzes ATP and assumes the ADP-(sub) state. However, the chaperone activity of DnaK in luciferase refolding was maximal at a DnaJ concentration 100-fold lower [45, 46] than the typical K_D for DnaJ substrate interaction (around 1 μM, see above). Moreover, it had been discovered that the maximum enhancement of DnaK ATPase activity by DnaJ occurs at a different molecular to that for optimal refolding [117]. These facts suggest a more "catalytic" and transient role for DnaJ once DnaK has acquired client (see below).

The four human type A J-proteins show strong homology to *E. coli* DnaJ, and show a complex domain topology (see Table 5 and Fig. 17). They contain an N-terminal J-domain, a glycine/phenylalanine-rich region, a Zn-finger domain, a substrate binding domain, a copy of a substrate binding domain, and a variable C-terminal domain. The N-terminal 73-residue J-domain is the most conserved, and its structure has been determined for several homologs in the context of truncation mutants (1–70 to 1–108) [100, 129, 130]. The structure is essentially an anti-parallel two-helix bundle with two small adjacent helical elements. (see Fig. 16). The J-domain alone is sufficient to stimulate ATPase activity of Hsp70 [125]. There is a conserved HPD sequence located in a flexible loop connecting the main helices II and III. Mutations in the HPD motif and in positively charged residues of helix II of the J domain abolish functional interactions with partner Hsp70s [126, 150]. This identified the J-domain as the domain that recognizes DnaK. Indeed, it was found by NMR that J(1–75) interacts with wt-DnaK in the ADP state and also with the isolated DnaK NBD [151]. The K_D for this interaction was around 10 μM. This K_D value may seem to be too weak to be of physiological relevance. However, as will be outlined below, DnaJ is a "poly-dentate" ligand for DnaK to which the J-domain interaction is only one of the determinants. Helix II of DnaJ is most involved in the interaction with DnaK [151]. This helix contains several conserved Lys and Arg residues, which are sensitive to mutation [126, 150]. It has therefore been suggested that the interaction between the J-domain and DnaK is electrostatic in nature [151]. Only small perturbations were found for the NMR chemical shifts of the HPD loop [151]. Recent studies of our group confirmed these findings – there are *no* changes for the NMR chemical shifts of the HPD loop [152]. These results are surprising in the light of the mutational sensitivity of these residues [126, 150]. Mutations in the HPD loop do not affect the interaction with the ADP state, but do strongly diminish the affinity of the J-domain for ATP state of DnaK [153]. At present it is not known if the HPD loop is directly involved in the interaction with DnaK, or if it stabilizes the interaction-competent J-domain conformation.

A crystal structure is available for YDJ1(110–337) [147], a DNAJA protein. It shows two highly homologous beta domains. Substrate is bound in a hydrophobic surface cleft of the first beta domain. The Zn-Cys domain is seen to be an insert in the first beta domain (see Fig. 17a).

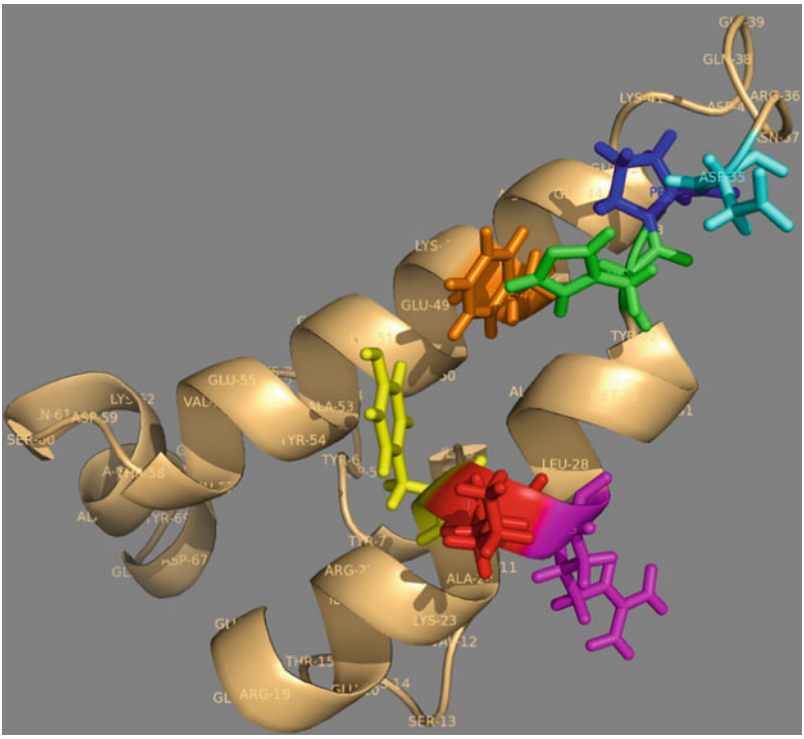

Fig. 16 The solution structure of *E. coli* DnaJ(2–76) in context of DnaJ(2–108) (1XBL) [148]. The mutationally sensitive [149] residues Y25 (*yellow*), K26 (*red*), R26 (*magenta*), H33 (*green*), P34 (*blue*), D35 (*cyan*), and F47 (*orange*) are highlighted

The Gly/Phe-rich region (residues 75–110) connects the J-domain with the C-terminal domains. A NMR solution investigation of DnaJ(1–108) [154] showed that the GF-region was dynamic and disordered. The role of the Gly/Phe-rich region is likely to allow flexibility in relative position and orientation of the J-recognition domain and DnaJ's substrate binding domain. The flexibility would increase the probability of substrate transfer to the DnaK SBD (or simultaneous substrate binding) while the J-domain binds to the DnaK NBD.

However, why does the G-F domain contain phenylalanines and not serines or threonines? In addition, why do G-F region mutations of DnaJ residues ^{90}FSDIFGDVFG^{100} affect DnaJ function [155]? Recently our lab obtained evidence [152] that the G-F domain interacts with DnaK's SBD substrate binding cleft in the absence of other substrate. That is, the G-F region is the second site of a DnaJ poly-dentate interaction. Figure 18 illustrates our way of thinking about the J-K complex. Because of the multi-dentate interactions many binding modes are possible, while the individual interaction determinants are not of very high affinity (1–10 μM).

Gross and co-workers carried out SPR measurements with different DnaK and DnaJ constructs. The key findings of their first paper in this area [156] are that DnaK

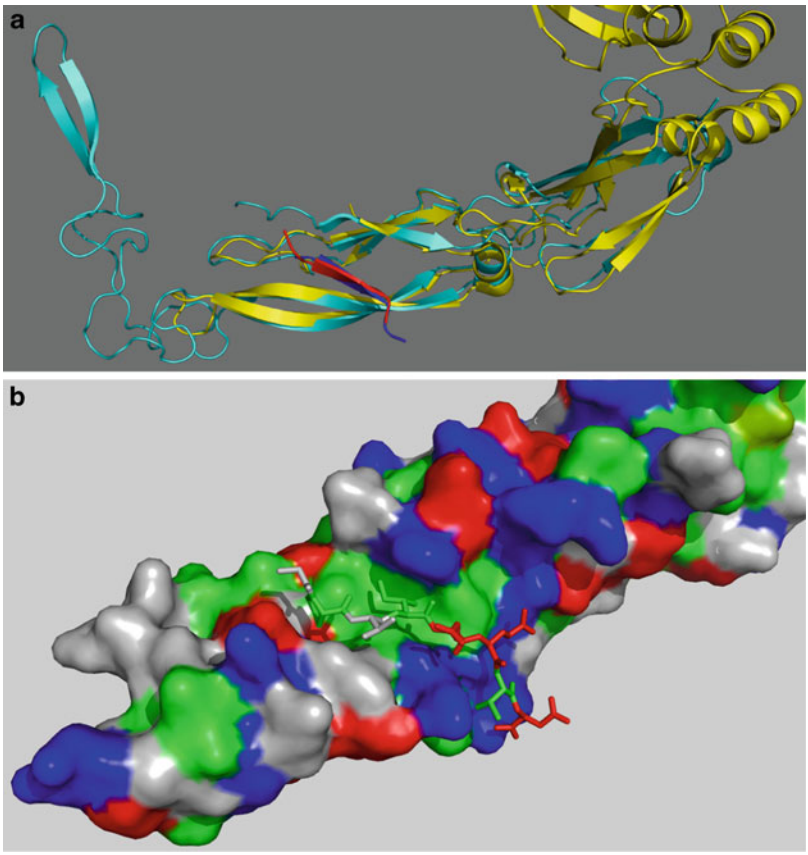

Fig. 17 (**a**) Overlay of a crystal structure of the peptide-binding and dimerization domain of human HDJ1 [146] in *yellow*, with that of yeast YDJ1 [147], in *cyan*. The HDJ1 substrate (GPTIEEVD) is in *red*, the YDJ1 substrate (GWLYEIS) is in *blue*. The CA positions in the SBD (193–240 and 205–252 for HDJ1 and YDJ1, respectively) were superposed. YDJ1's Zn domain is at the left, HDJ1's dimerization helices are at the *right* (the latter were deleted in the crystallization construct of YDJ1). (**b**) Detail of the hydrophobic cleft of HDJ1, composed of residues M183, I185, L204, I206, F220, I235, and F237 and ligand GPTIEEVD

mutants in the NBD (R167A, N170A, and T173D) and the SBD (G400D and G539D) individually reduce the wt-DnaJ binding tenfold. Since these mutations occur on both NBD and SBD, this result also shows that DnaJ is poly-dentate. The key findings of their other work in this area [157] are that DnaJ does not bind to DnaK(1–403) (NBD) or to DnaK(386–638) (SBD). Similarly, while DnaJ(1–108) binds almost as well as wt-DnaJ, DnaJ(1–75) does not bind. In the context of SPR, this indicates $K_D > 1$ μM. These results are consistent with the fact that the binding constants of the individual determinants are indeed around 10 μM. Others have shown bidentate interaction as well. Laufen et al. [106] showed that DnaJ was inefficient in stimulation of ATP hydrolysis by a DnaK mutant with defects in substrate binding, suggesting synergistic action of DnaJ and substrate. Others [158, 159] show that DnaJ(1–70) required either the GF-rich region or a peptide substrate provided in trans to strongly enhance DnaK's

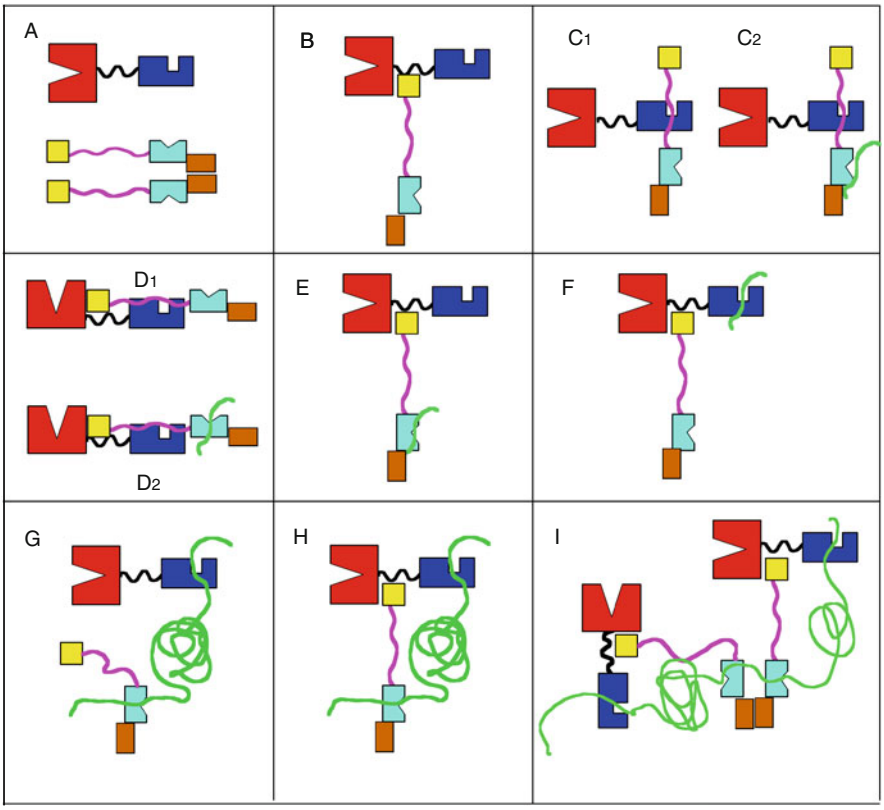

Fig. 18 Hypothetical binding modes between DnaK (*red*: NBD; *blue*: SBD), DnaJ (*yellow*: J-domain; *magenta*: G–F; *cyan*: SBD; *brown*: dimerization domain and substrate (*green*) in the ADP state

ATPase activity. At high concentrations, DnaJ itself serves as substrate for DnaK in a process considered to be unphysiological, where it stimulates ATP hydrolysis by DnaK > 1,000-fold [106].

A major and not yet resolved question in the field is whether DnaJ interacts more strongly with DnaK in the ADP or in the ATP state. Pierpaoli et al. [160] obtained a weak K_D value of >2 μM for the binding of DnaJ to DnaK.ATP and a strong K_D of 0.14 μM for the binding of DnaJ to a preformed 1:1 complex of DnaK and acrodylan-labeled CLLLSAPRR in the presence of ADP [160]. However, these results are contradicted by the following studies. Landry and co-workers have made a fusion of DnaJ (1–78) to CLLLSAPRR [153]. This J-fusion bound much more tightly to DnaK in the presence of ATP (0.2 nM) than in the absence of nucleotide (30 nM). A later paper of the same group using the same construct and using NMR spectroscopy to monitor binding to several DnaK constructs in different nucleotide states confirmed their earlier observations [161]. SPR experiments by Gross and co-workers [157] strongly suggest that wt-DnaJ binds tightly to the ATP state ($K_D = 70$ nM) but does not bind to DnaK in the ADP state (i.e., $K_D > 1$ μM).

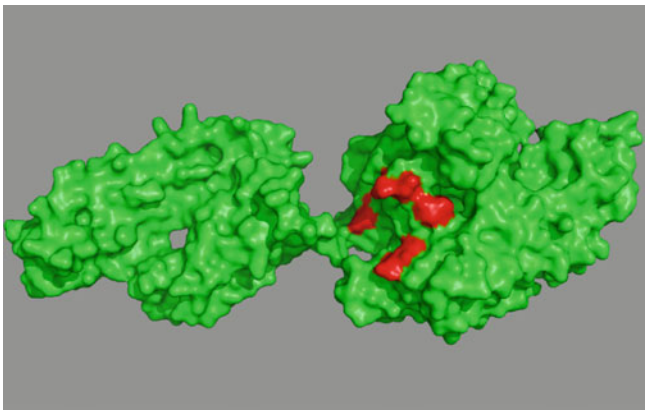

Fig. 19 The location of residues on *E. coli* DnaK that affect DnaK–DnaJ interaction as deduced from mutagenesis experiments (see text)

Single molecule fluorescence studies show that the yeast J protein Mdj1 is stably bound to yeast Hsp70 Ssc1 in the ATP state and dissociates upon ATP hydrolysis [96]. We have recently obtained results using NMR showing that DnaJ(1–70) binds at least ten times more tightly to DnaK(ATP-apo) than to the DnaK(ADP-sub). The majority of results thus suggest that DnaJ is poised to dissociate from DnaK once substrate is delivered.

While it is becoming clear how DnaJ interacts with DnaK, and how substrate and substrate-binding cleft are involved, it is much less clear which precise residues on the DnaK NBD interact with the J-domain. The DnaK mutations $YND_{145,147,148}AAA$ [86], $EV_{217,218}AA$ [86], and $R_{167}A$ [156] on the DnaK NBD domain weaken J–K interaction. All of these residues are found around the cleft area between subdomains IA and IIA of the NBD (see Fig. 19). However, mutations of these residues also affect the allosteric mechanism of DnaK itself, and it is unclear how the two effects intermingle. The mutant R167A is most interesting. Suh and co-workers [156] showed by SPR that the R167A mutant on DnaK could rescue the interaction of DnaJ D35N with DnaK. The effects were not dramatic (it "rescues" a K_D of 300 nM to a K_D of 100 nM). The R167H mutant had exactly the same rescuing capabilities as R167A. Potentially, Arg167 becomes buried in the complex with DnaJ. Such burial would be unfavorable if it is not compensated by buried negative charge in its vicinity. Hence, when the compensatory negative charge (D35) is mutated out, one must also mutate out burial of the positive charge to regain binding. The smallness of the effect argues for rather weak or remote D35 – R167 interaction. The SPR data strongly suggest that the J-domain interacts with NBD at a location that is now believed to be also the interaction site between the SBD and the NBD [38]. The interaction likely helps to establish or stabilize the DnaK state in which NBD and SBD do not interact.

A co-crystal structure of the NBD of Hsc70 with a J-domain of auxilin has been advanced [107]. The two proteins were covalently linked through disulfide chemistry between an Asp-Cys mutant at the equivalent location of Asp35 of DnaJ and an

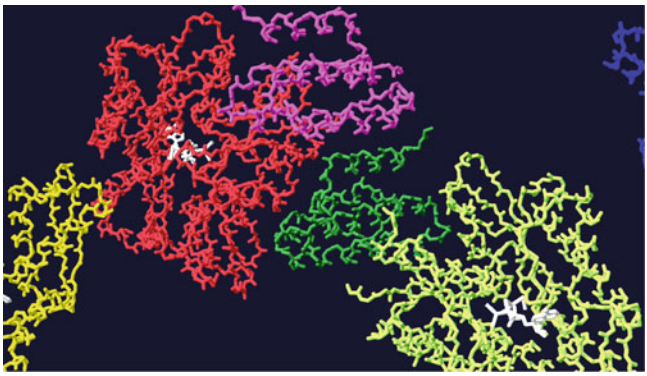

Fig. 20 Crystal contacts in the covalent adduct of human Auxilin (DnaJ homolog) and the NBD human Hsc70 [107]. The NBD and J-domain of the PDB-deposited adduct are in *light* and *dark green*, respectively. ADP is in *white*. The NBD and J-domain of the neighbor in the crystal are in *red* and *magenta*, respectively. The *green*" J-domain has a 372-Å^2 interface with its disulfide-linked Hsc70 NBD partner (*light green*). However, a symmetry-related NBD (*red*) has a 582 Å^2 interface with the same "*green*" J-domain (using www.ebi.ac.uk/msd-srv/prot_int/pistart.html). This figure was prepared using the Swiss PDB viewer

Arg-Cys mutant at the equivalent location of R167 in DnaK, as inspired by the work of Suh et al. [156]. This complex could potentially represent state E in Fig. 18. However, the complex is in the ADP state, and it is known from other work that the HPD loop is not involved in DnaJ–DnaK interaction in that state [152, 153]. In addition to questions about the validity of forcing the structure to a pre-determined pose by disulfide linking, the structure of this adduct is also rather suspect because crystal contacts between the J-domain of one "complex" with the NBD of another "complex" must affect the relative J-K orientations in the adduct (see Fig. 20).

Recently, using solution NMR, we obtained the three-dimensional conformation for a noncovalent Hsp70-DnaJ complex in the ADP state, loaded with substrate peptide [152]. The solution structure, which contained NBD, SBD, LID, substrate, and DnaJ(1–70), is completely different from the crystal structure of the adduct [107] (see Fig. 21). We establish that the J-domain (residues 1–70) binds with its positively charged helix II, which contains conserved residues that are critical to the interaction, as determined by mutagenesis [162], to a negatively charged area, ^{206}EIDEVDGEKTFEVLAT^{221} in the Hsp70 nucleotide-binding domain. In the crystal structure [107], this helix is not in the interface. The interface in the crystal (helix III) is not involved in contact in solution in the ADP state. The solution complex shows an unusual "tethered" binding mode which is stoichiometric and saturable, but which has a dynamic interface.

Recently, NMR data were published that suggest that DnaK residues 215–220 interact with the NBD-SBD linker in the ATP state but not in the ADP state [83]. It is significant that we [152] found that the J domain interacts with DnaK residues that contain this site, suggesting that its presence interferes with the docking of the linker, promoting the ADP conformation. This provides the long-awaited structural evidence for understanding how the J proteins regulate Hsp70 allostery.

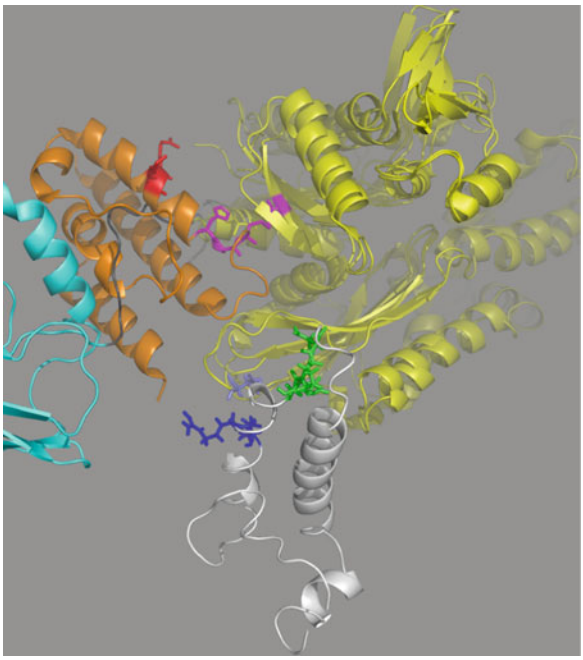

Fig. 21 The crystal structure [107] of the covalent adduct of Auxilin-J-domain (*orange*) and the NBD of human Hsc70 (*yellow*) superposed on the solution conformation [154] for the non-covalent complex of DnaJ-J-domain (*white*), DnaK NBD (*yellow*), NBD-SBD linker (*black*) and DnaK SBD (*cyan*). On Auxilin, the HPD loop and its covalent link to the NBD are in *purple* and the positive residues on helix II are *red*. On DnaJ, the HPD loop is *green*, and the positive residues on helix II are *blue*. Val210, in the center of the DnaK interface, is in *blue-gray*

13 Hsp70-Allosteric Effectors as Drugs

Consistent with its key role in protein homeostasis, Hsp70 chaperones have been implicated in numerous diseases. The various disease pathologies can be associated with "too much" Hsp70 activity (recycling of a toxic substrate) or with "too little" activity (failure to act on misfolded substrates). Thus, disease might arise from disruption of the delicately balanced proteostasis in either direction [163]. We will describe here just two disease classes, cancer and tauopathies, in which there is "too much" Hsp70 activity, so that one can conceivably aid in the therapy of these diseases by inhibiting Hsp70s.

All known tumors express elevated levels of Hsp70s [14]. One hypothesis is that the physiopathological features of the tumor microenvironment (low glucose, pH, and oxygen) mimic stress conditions [18, 19]. Alternatively, conformationally unstable oncoproteins may elicit a stress response [28, 164–167]. In cancer cells, Hsp70 stabilizes pro-survival factors [15–17] and inhibit cell death pathways [19, 22–26, 168, 169]. In addition, Hsp70 may prevent translocation of the apoptotic enhancer BAX from the cytosol to the mitochondria [170]. Hsp70 can also stabilize lysosomal membranes to inhibit the release of cathepsins and other enzymes which can induce cell death [171]. Hsp70 also plays roles in post-mitochondrial signaling pathways by antagonizing release of apoptogenic factors, such as cytochrome *c* and AIF [170]. Furthermore, Hsp70 can bind to and block the activity of APAF1 to avert the formation of the apoptosome and subsequent activation of caspase

enzymes [172]. Finally, Hsp70 also directly participates in oncogenic transformation [19]. One of the likely responsible mechanisms is the interaction of mitochondrial Hsp70 (mt-Hsp70) with mutant and wild-type tumor suppressor proteins, such as p53 [28, 166, 167, 173–175], and Rb107 [176]. The malignant transformation has been explained, in part, by the inactivation of p53 tumor suppressor protein by mt-Hsp70 [27]. In particular, wild-type p53 and mt-Hsp70 co-localize in the cytoplasm in several human cancers (undifferentiated neuroblastoma, retinoblastoma, colorectal and hepatocellular carcinomas, and glioblastoma) [28]. Together these observations support a model in which Hsp70 expression is anti-apoptotic and required for cancer cell viability. In addition, high expression of Hsp70 also confers resistance to chemotherapy, radiation, and hyperthermia therapy in breast cancer [18, 177]. Together, these observations suggest that Hsp70 is an important, potential drug target in cancer.

In support of these ideas, knockdown of Hsp70 chaperone expression [178, 179] or inhibition by small molecules [180] is lethal to cancer cell lines. For example, Hsp70 inhibitors generated by the Wipf and Brodsky groups have anti-proliferative activity against lung cancer cells [181] and Hsp70 inhibitors synthesized by the biotechnology company, Vernalis, have potent activity against cancer cells [182]. Moreover, a natural product, epigallocatechin gallate, interacts with Hsp70 [183] and triggers apoptosis in tumor cells [183]. MKT-077, a cationic rhodacyanine dye analog, which binds to Hsp70 [184], has activity against CX-1 colon carcinoma cells ($IC_{50} \sim 7\ \mu M$), but has no effect on normal epithelial cells [180]. Mechanistic studies indicated that MTK-077 inhibits the deleterious interaction of mt-Hsp70 with p53 by binding to the mt-Hsp70 NBD [167, 185]. These studies on MKT-077 generated significant excitement about this compound and it was advanced to phase I clinical trials [186]. However, MKT-077 was found to be nephrotoxic.

Many neurodegenerative disorders, such as Alzheimer's and Parkinson's diseases, are characterized by abnormal protein misfolding and accumulation [187–189]. In these disorders, misfolded proteins are not properly cleared by the chaperone/quality control system and, subsequently, they self-associate into cytotoxic oligomers. Diseases such as Alzheimer's are also characterized, besides beta plaques, by aberrant accumulation of hyperphosphorylated tau, called tau-tangles [29, 190–192]. Clearance of tau-tangles is being recognized as therapeutic to Alzheimer-affected neuronal cells [193]. Hsp70s participate in the clearance of tau-tangles through a mechanism that is in the process of being uncovered [194]. A key finding pertaining to this mechanism is that inhibitors of Hsp70 lead to a rapid increase in tau ubiquitination and proteasome-dependent degradation in tau-overexpressing HeLa cells [195]. Conversely, activators of Hsp70 led to a decrease proteasome-dependent degradation of tau. Thus, it seems that inhibition of Hsp70 is a potential target for helping the clearance of tau and a first step towards a therapy of CNS disorders.

As evident throughout this review, Hsp70s are highly allosteric enzymes that engage in a number of critical protein–protein interactions. Thus, Hsp70s proteins must be very druggable [196] because they offer so many opportunities for interference (Fig. 22). The most obvious sites for designing inhibitors are the primary

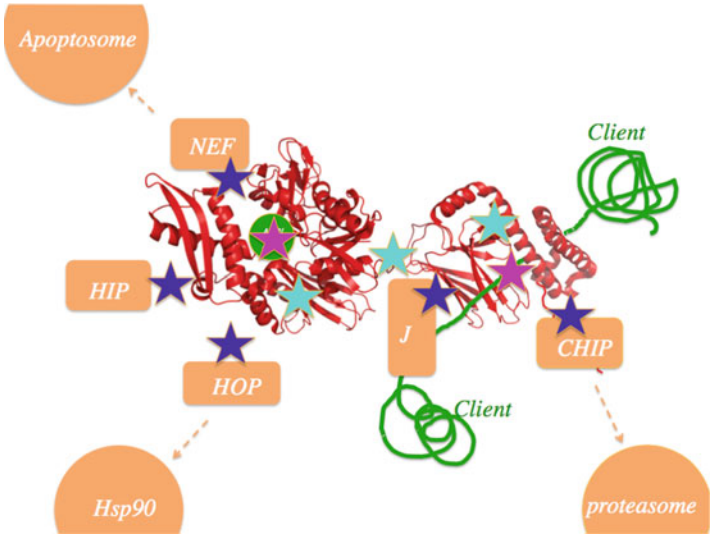

Fig. 22 Potential sites for interference with the Hsp70 chaperone function. *Purple*: primary sites, *cyan*: allosteric sites, *blue*: co-chaperone interaction sites

ATP and substrate-binding pockets. Such deep clefts are often associated with favorable progress in drug discovery campaigns. In fact, both of these binding sites have been explored [197, 198] and some of the resulting compounds have promising anti-cancer and anti-bacterial activity. However, these pockets have a number of features that make them challenging. For example, the nucleotide-binding cassette of Hsp70s is highly conserved, creating problems in selectivity. Similarly, the substrate-binding cleft of the Hsp70s is designed to be promiscuous and capable of binding many hydrophobic sequences; thus, it is expected to be difficult to generate soluble, selective compounds for that region. Another potential problem with these strategies is that they would be expected to "lock" Hsp70s into a specific structure in the ensemble. Namely, competitive ATP-competitive inhibitors might lock the protein into the ATP-bound form, while substrate-based inhibitors would favor the substrate-bound form. As discussed in this review, there are many other states of Hsp70 and these might also be linked to aspects of disease. Thus, one can also imagine directing Hsp70 function in new ways by targeting its interactions with DnaJ co-chaperones or nucleotide exchange factors [3]. Hsp70s also interact with HIP [199], HOP [200], and CHIP [201], and some specialized factors such as ZIM (for mt-Hsp70) [202]. In theory, competing with these contacts or even enhancing their recruitment may be another, parallel avenue for modulating the activity and structure of Hsp70s. The potential advantage of this approach is that the activity of the Hsp70 complex might be "tuned" to achieve the desired outcomes.

In theory, compounds with activities at allosteric and protein–protein sites might either directly interfere with co-chaperone interactions or they might recognize allosteric differences and perturb the allosteric equilibrium between states of

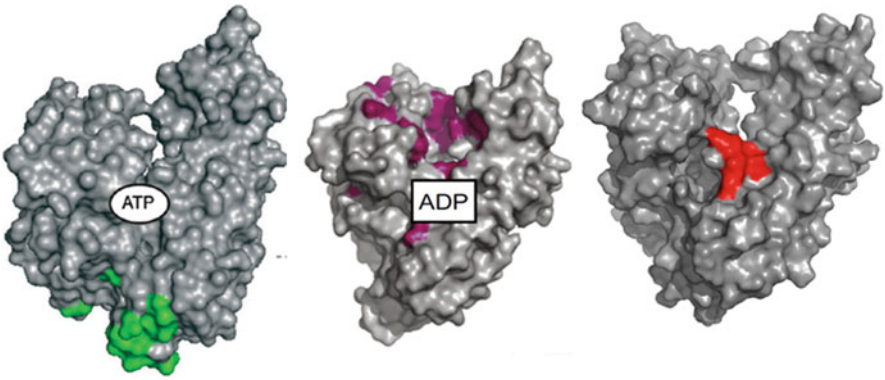

Fig. 23 The NMR-determined binding sites of recently discovered Hsp70 inhibitors. *Left*, 115-7C [203]; *middle*, myricetin [204]; *right*, MKT-077 [205]. Note that neither compound binds to an Hsp70 primary site, hence the compounds affect Hsp70 function by affecting allostery or co-chaperone interaction

Hsp70. Consistent with this idea, we recently discovered one class of DnaK inhibitors that functions by directly competing with the J protein interaction [203] (see Fig. 23a) and another class of compounds, including the flavonoid myricetin, which bind to a site on DnaK that is >30 Å from the DnaJ binding site to block this interaction allosterically [204] (Fig. 23b). These studies suggest that Hsp70s, such as DnaK, do indeed have multiple opportunities for pharmacologic intervention, including at sites that might not be anticipated from cursory examination of the structures.

Many of the emerging methods for targeting Hsp70 are likely to take advantage of the allostery in this target. For example, compounds that can recognize allosteric differences and perturb the allosteric equilibrium between the states should also modulate Hsp70s function. To illustrate this idea, we recently discovered that the anti-cancer compound MKT-077 is an allosteric inhibitor of Hsp70. MKT-077 [184, 206] was originally considered as a potential therapy for the treatment of breast cancer [207]. Later it was suggested that MKT-077 kills cancer cells by selectively inhibiting mt-Hsp70 [187]. However, the mechanism of MKT-077 wasn't clear and its potential binding site of Hsp70s was unknown. Based on the high homology between mt-Hsp70 and other Hsp70s, we reasoned that MKT-077 may also bind to cytosolic homologs, such as Hsc70 and Hsp70. Consistent with this idea, MKT-077 binds with an affinity of approximately 10 μM to human Hsc70 NBD (determined by NMR [205]). This value is remarkably close to the $IC_{50} \sim 7$ μM for MKT-077 activity against CX-1 colon carcinoma cells [180]. Also consistent with its cytosolic actions, MKT-077 clears tau in a dose-dependent manner in HeLa cells [205]. This activity may be therapeutically important because other compounds that reduce tau accumulation through Hsp70s recover cognitive function in mouse models of Alzheimer's disease [208].

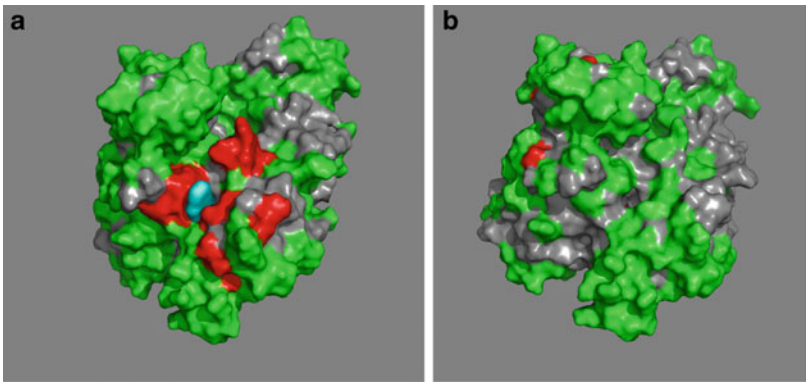

Fig. 24 (**a**) Chemical shifts seen [205] for the interaction of MKT-077 (*cyan*) with human Hsc70 in the ADP state. (**b**) Chemical shifts seen [205] for the interaction of MKT-077 with human Hsc70 in the AMP-PNP state

To help development of more potent MKT-077 derivatives, we investigated where the compound binds to Hsc70 [205]. The first finding was that MKT-077 binds to the Hsc70 ADP state, but that no binding to the ATP state could be detected (i.e., $K_D > 100$ μM) (Fig. 24). Thus, we hypothesized that MKT-077 might trap Hsp70 in the ADP-bound, high-affinity form. This hypothesis was supported by partial proteolysis findings, which suggested that MKT-077 stabilizes the ADP-bound conformation of full length Hsp70s. Although the mechanisms linking this allosteric switch to the degradation of tau is not yet clear, it seems possible that the long-lived Hsp70-ADP-tau complex becomes a good target for CHIP, an E3 ubiquitin ligase that binds Hsp70s. If so, then this "stalled" complex would favor the polyubiquitination and degradation of Hsp70-bound tau [201, 209].

How does MKT-077 distinguish between the NBD ADP and ATP state? It turns out that MKT-077 binds to a pocket that is close, but not identical, to the nucleotide-binding site (see Fig. 24). According to our earlier studies of the NBD of DnaK *T. Thermophilus*, ADP and AMPPNP cause significant changes in NBD subunit orientations [82], which affects the area where the MKT-077 pocket is located. However, in that study we did not carry out a high resolution structure determination. Rather, we suggested that the nucleotide-induced changes were not unlike those seen between crystal structures of Hsp70 in nucleotide-bound form (a representative of the ATP state) and those of Hsc70 bound to nucleotide exchange factors, (more representative of the ADP state). In Fig. 25 we show the difference between these crystal structures. Indeed, only in the ADP state is there a pocket available that can accommodate MKT-077. The pocket is smaller in the ATP state. Therefore, MKT-077 is an allosteric effector, and acts not unlike 2,3-DPG which down-regulates hemoglobin oxygen affinity by binding to a non-heme site that is open in the T-state and closed in the R-state [210]

Subsequently, we modeled the binding of MKT-077 on the conformation of Hsc70 NBD as seen in a complex containing NEF. The NMR chemical shift

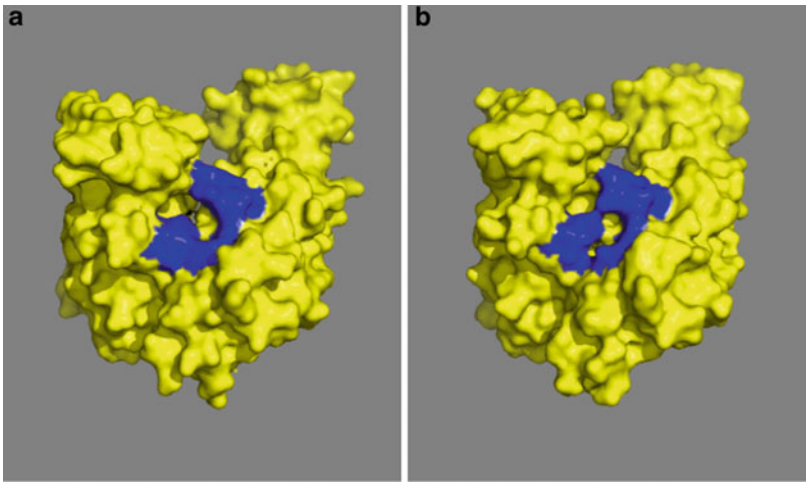

Fig. 25 (**a**) The MKT-077 binding site [205] (*blue*) projected on human Hsc70 NBD in the open state (complexed with NEF; 3C7N.pdb) (**b**). The MKT-077 binding site (*blue*) projected on Hsc70 NBD in the closed state (3HSC.pdb)

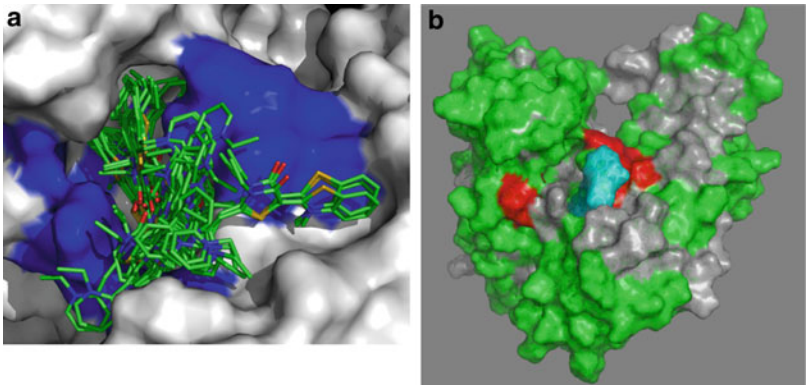

Fig. 26 The MKT-077 Hsc70 NBD interaction in detail [205]. (**a**) Collection of poses for the binding of MKT077 to Hsc70 (3C7N.pdb) obtained from NMR restrained AUTODOCK. *Blue*: NMR shifts. (**b**) Final best binding pose of MKT077 (*cyan*) on Hsc70 (3C7N.pdb) obtained with AMBER. *Green*: no shifts; *red*: shifts; *gray*: undecided

perturbations were used to constrain the search box in the AUTODOCK [211] docking program. AUTODOCK produced four families of binding poses that were energetically equivalent, but which differed as much as having different rings of MKT-077 inside or outside the pocket (Fig. 26a). We decided to carry out AMBER molecular dynamics [212] simulated annealing computations using Hsc70 in explicit water, starting with representatives of the four different AUTODOCK families. After equilibrium was reached, we evaluated the AMBER binding energy using the MM-GB/PBSA protocol [213]. As a result, one particular family of poses

stood out. This pose is shown in Fig. 26b. It forms the basis for our further drug development endeavors.

Together, these results, while quite preliminary, suggest that Hsp70s may be targets for cancer and CNS disorders through a variety of direct and allosteric mechanisms. Hopefully, a larger battery of Hsp70 inhibitors with defined mechanisms-of-action will become available and these reagents will, in turn, allow new insights into the roles of Hsp70s in disease.

14 Outlook

The Hsp70/DnaJ/NEF system is complicated and subtle. Different scientific disciplines uncover seemingly unrelated and sometimes contradictory facts about the system. Clearly, much more research is required to uncover all aspects of the Hsp70/DnaJ/NEF system. In addition, the Hsp70s interact with many co-factors such as HIP, HOP, and CHIP. In most cases not even structures of such complexes are known, let alone the subtleties of the energetics and dynamics of these interactions. We hope that support for many more years of Hsp70 research will be forthcoming. It should be well worth it, given the fact that disregulation of Hsp70s is involved in diseases that affect much of humanity.

Acknowledgements Support from NIH grants GM63027-S02 (ERPZ, AA), NS059690 (AR, ERPZ and JEG) is gratefully acknowledged. An anonymous reviewer is gratefully acknowledged for suggesting many improvements to the manuscript.

References

1. Hightower LE (1991) Heat-shock, stress proteins, chaperones, and proteotoxicity. Cell 66:191–197
2. Marques C, Guo W, Pereira P, Taylor A, Patterson C, Evans PC, Shang F (2006) The triage of damaged proteins: degradation by the ubiquitin-proteasome pathway or repair by molecular chaperones. FASEB J 20:741–743
3. Bukau B, Weissman J, Horwich A (2006) Molecular chaperones and protein quality control. Cell 125:443–451
4. Sfatos CD, Gutin AM, Abkevich VI, Shakhnovich EI (1996) Simulations of chaperone-assisted folding. Biochemistry 35:334–339
5. Gupta RS (1998) Protein phylogenies and signature sequences: a reappraisal of evolutionary relationships among archaebacteria, eubacteria, and eukaryotes. Microbiol Mol Biol Rev 62:1435–1491
6. Zylicz M, Wawrzynow A (2001) Insights into the function of Hsp70 chaperones. IUBMB Life 51:283–287
7. Qian S-B, McDonough H, Boellmann F, Cyr DM, Patterson C (2006) CHIP-mediated stress recovery by sequential ubiquitination of substrates and Hsp70. Nature 440:551–555
8. Majeski AE, Dice JF (2004) Mechanisms of chaperone-mediated autophagy. Int J Biochem Cell Biol 36:2435–2444

9. Craig EA, Huang P, Aron R, Andrew A (2006) The diverse roles of J-proteins, the obligate Hsp70 co-chaperone. Rev Physiol Biochem Pharmacol 156:1–21
10. Tzankov S, Wong MJ, Shi K, Nassif C, Young JC (2008) Functional divergence between co-chaperones of Hsc70. J Biol Chem 283:27100–27109
11. Chappell TG, Konforti BB, Schmid SL, Rothman JE (1987) The ATPase core of a clathrin uncoating protein. J Biol Chem 262:746–751
12. Brinker A, Scheufler C, Von Der Mulbe F, Fleckenstein B, Herrmann C, Jung G, Moarefi I, Hartl FU (2002) Ligand discrimination by TPR domains. Relevance and selectivity of EEVD-recognition in Hsp70 x Hop x Hsp90 complexes. J Biol Chem 277:19265–19275
13. Wells AD, Rai SK, Salvato MS, Band H, Malkovsky M (1997) Restoration of MHC class I surface expression and endogenous antigen presentation by a molecular chaperone. Scand J Immunol 45:605–612
14. Shin BK, Wang H, Yim AM, Le Naour F, Brichory F, Jang JH, Zhao R, Puravs E, Tra J, Michael CW, Misek DE, Hanash SM (2003) Global profiling of the cell surface proteome of cancer cells uncovers an abundance of proteins with chaperone function. J Biol Chem 278:7607–7616
15. Nylandsted J, Brand K, Jaattela M (2000) Heat shock protein 70 is required for the survival of cancer cells. Ann N Y Acad Sci 926:122–125
16. Kaul Z, Yaguchi T, Kaul SC, Hirano T, Wadhwa R, Taira K (2003) Mortalin imaging in normal and cancer cells with quantum dot immuno-conjugates. Cell Res 13:503–507
17. Kaul SC, Yaguchi T, Taira K, Reddel RR, Wadhwa R (2003) Overexpressed mortalin (mot-2)/mthsp70/GRP75 and hTERT cooperate to extend the in vitro lifespan of human fibroblasts. Exp Cell Res 286:96–101
18. Ciocca DR, Calderwood SK (2005) Heat shock proteins in cancer: diagnostic, prognostic, predictive, and treatment implications. Cell Stress Chaperones 10:86–103
19. Garrido C, Brunet M, Didelot C, Zermati Y, Schmitt E, Kroemer G (2006) Heat shock proteins 27 and 70: anti-apoptotic proteins with tumorigenic properties. Cell Cycle 5:2592–2601
20. Soti C, Csermely P (2002) Chaperones and aging: role in neurodegeneration and in other civilizational diseases. Neurochem Int 41:383–389
21. Soti C, Csermely P (2002) Chaperones come of age. Cell Stress Chaperones 7:186–190
22. Abarzua F, Sakaguchi M, Tanimoto R, Sonegawa H, Li DW, Edamura K, Kobayashi T, Watanabe M, Kashiwakura Y, Kaku H, Saika T, Nakamura K, Nasu Y, Kumon H, Huh NH (2007) Heat shock proteins play a crucial role in tumor-specific apoptosis by REIC/Dkk-3. Int J Mol Med 20:37–43
23. Lanneau D, Brunet M, Frisan E, Solary E, Fontenay M, Garrido C (2008) Heat shock proteins: essential proteins for apoptosis regulation. J Cell Mol Med 12:743–761
24. Calderwood SK, Ciocca DR (2008) Heat shock proteins: stress proteins with Janus-like properties in cancer. Int J Hyperthermia 24:31–39
25. Beere HM, Wolf BB, Cain K, Mosser DD, Mahboubi A, Kuwana T, Tailor P, Morimoto RI, Cohen GM, Green DR (2000) Heat-shock protein 70 inhibits apoptosis by preventing recruitment of procaspase-9 to the Apaf-1 apoptosome. Nat Cell Biol 2:469–475
26. Garrido C, Schmitt E, Cande C, Vahsen N, Parcellier A, Kroemer G (2003) Hsp27 and Hsp70: potentially oncogenic apoptosis inhibitors. Cell Cycle 2:579–584
27. Kaul SC, Duncan EL, Englezou A, Takano S, Reddel RR, Mitsui Y, Wadhwa R (1998) Malignant transformation of NIH3T3 cells by overexpression of mot-2 protein. Oncogene 17:907–911
28. Walker C, Bottger S, Low B (2006) Mortalin-based cytoplasmic sequestration of p53 in a nonmammalian cancer model. Am J Pathol 168:1526–1530
29. Buee L, Bussiere T, Buee-Scherrer V, Delacourte A, Hof PR (2000) Tau protein isoforms, phosphorylation and role in neurodegenerative disorders. Brain Res Rev 33:95–130
30. Flaherty KM, Deluca-Flaherty C, McKay DB (1990) 3-Dimensional structure of the ATPase fragment of a 70 k heat-shock cognate protein. Nature 346:623–628

31. Bork P, Sander C, Valencia A (1992) An ATPase domain common to prokaryotic cell-cycle proteins, sugar kinases, actin, and Hsp70 heat-shock proteins. Proc Natl Acad Sci USA 89:7290–7294
32. O'Brien MC, Flaherty KM, McKay DB (1996) Lysine 71 of the chaperone protein Hsc70 Is essential for ATP hydrolysis. J Biol Chem 271:15874–15878
33. Wilbanks SM, DeLuca-Flaherty C, McKay DB (1994) Structural basis of the 70-kilodalton heat shock cognate protein ATP hydrolytic activity. I. Kinetic analyses of active site mutants. J Biol Chem 269:12893–12898
34. O'Brien MC, McKay DB (1995) How potassium affects the activity of the molecular chaperone Hsc70.I. Potassium is required for optimal ATPase activity. J Biol Chem 270:2247–2250
35. Vogel M, Mayer MP, Bukau B (2006) Allosteric regulation of Hsp70 chaperones involves a conserved interdomain linker. J Biol Chem 281:38705–38711
36. Morshauser RC, Wang H, Flynn GC, Zuiderweg ER (1995) The peptide-binding domain of the chaperone protein Hsc70 has an unusual secondary structure topology. Biochemistry 34:6261–6266
37. Zhu XT, Zhao X, Burkholder WF, Gragerov A, Ogata CM, Gottesman ME, Hendrickson WA (1996) Structural analysis of substrate binding by the molecular chaperone DnaK. Science 272:1606–1614
38. Bertelsen EB, Chang L, Gestwicki JE, Zuiderweg ERP (2009) Solution conformation of wild-type E. coli Hsp70 (DnaK) chaperone complexed with ADP and substrate. Proc Natl Acad Sci USA 106:8471–8476
39. Smock RG, Blackburn ME, Gierasch LM (2011) Conserved, disordered C terminus of DnaK enhances cellular survival upon stress and DnaK in vitro chaperone activity. J Biol Chem 286:31821–31829
40. Pidoux AL, Armstrong J (1992) Analysis of the BIP gene and identification of an ER retention signal in S. Pombe. EMBO J 11:1583–1591
41. Bukau B, Horwich AL (1998) The Hsp70 and Hsp60 chaperone machines. Cell 92:351–366
42. Han WJ, Christen P (2003) Mechanism of the targeting action of DnaJ in the DnaK molecular chaperone system. J Biol Chem 278:19038–19043
43. Moreno-del Alamo M, Sanchez-Gorostiaga A, Serrano AM, Prieto A, Cuellar J, Martin-Benito J, Valpuesta JM, Giraldo R (2010) Structural analysis of the interactions between Hsp70 chaperones and the yeast DNA replication protein Orc4p. J Mol Biol 403:24–39
44. Mayer MP, Bukau B (2005) Hsp70 chaperones: cellular functions and molecular mechanism. Cell Mol Life Sci 62:670–684
45. Schroder H, Langer T, Hartl FU, Bukau B (1993) Dnak Dnaj and Grpe form a cellular chaperone machinery capable of repairing heat-induced protein damage. EMBO J 12:4137–4144
46. Ziemienowicz A, Skowyra D, Zeilstra-Ryalls J, Fayet O, Georgopoulos C, Zylicz M (1993) Both the Escherichia coli chaperone systems, GroEL/GroES and DnaK/DnaJ/GrpE, can reactivate heat-treated RNA polymerase. Different mechanisms for the same activity. J Biol Chem 268:25425–25431
47. Diamant S, Ben-Zvi AP, Bukau B, Goloubinoff P (2000) Size-dependent disaggregation of stable protein aggregates by the DnaK chaperone machinery. J Biol Chem 275:21107–21113
48. Hartl FU, Hayer-Hartl M (2002) Molecular chaperones in the cytosol: from nascent chain to folded protein. Science 295:1852–1858
49. Yam AY, Xia Y, Lin HTJ, Burlingame A, Gerstein M, Frydman J (2008) Defining the TRiC/CCT interactome links chaperonin function to stabilization of newly made proteins with complex topologies. Nat Struct Mol Biol 15:1255–1262
50. De los Rios P, Ben-Zvi A, Slutsky O, Azem A, Goloubinoff P (2006) Hsp70 chaperones accelerate protein translocation and the unfolding of stable protein aggregates by entropic pulling. Proc Natl Acad Sci USA 103:6166–6171
51. Sharma SK, De Los Rios P, Christen P, Lustig A, Goloubinoff P (2010) The kinetic parameters and energy cost of the Hsp70 chaperone as a polypeptide unfoldase. Nat Chem Biol 6:914–920

52. Goloubinoff P, De Los Rios P (2007) The mechanism of Hsp70 chaperones: (entropic) pulling the models together. Trends Biochem Sci 32:372–380
53. Szabo A, Langer T, Schroder H, Flanagan J, Bukau B, Hartl FU (1994) The ATP hydrolysis-dependent reaction cycle of the Escherichia coli Hsp70 system DnaK, DnaJ, and GrpE. Proc Natl Acad Sci USA 91:10345–10349
54. Mayer MP, Rudiger S, Bukau B (2000) Molecular basis for interactions of the DnaK chaperone with substrates. Biol Chem 381:877–885
55. Schmid D, Baici A, Gehring H, Christen P (1994) Kinetics of molecular chaperone action. Science 263:971–973
56. McCarty JS, Buchberger A, Reinstein J, Bukau B (1995) The role of ATP in the functional cycle of the DnaK chaperone system. J Mol Biol 249:126–137
57. Kim DH, Lee YJ, Corry PM (1992) Constitutive Hsp70-oligomerization and its dependence on ATP binding. J Cell Physiol 153:353–361
58. Chang L, Bertelsen EB, Wisen S, Larsen EM, Zuiderweg ERP, Gestwicki JE (2008) High-throughput screen for small molecules that modulate the ATPase activity of the molecular chaperone DnaK. Anal Biochem 372:167–176
59. Jayakumar J, Smolenski RT, Gray CC, Goodwin AT, Kalsi K, Amrani M, Yacoub MH (1998) Influence of heat stress on myocardial metabolism and functional recovery after cardioplegic arrest: a P-31 NMR study. Eur J Cardiothorac Surg 13:467–474
60. Theyssen H, Schuster HP, Packschies L, Bukau B, Reinstein J (1996) The second step of ATP binding to DnaK induces peptide release. J Mol Biol 263:657–670
61. Buchberger A, Theyssen H, Schroder H, McCarty JS, Virgallita G, Milkereit P, Reinstein J, Bukau B (1995) Nucleotide-induced conformational changes in the ATPase and substrate binding domains of the DnaK chaperone provide evidence for interdomain communication. J Biol Chem 270:16903–16910
62. Montgomery DL, Morimoto RI, Gierasch LM (1999) Mutations in the substrate binding domain of the Escherichia coli 70 kDa molecular chaperone, DnaK, which alter substrate affinity or interdomain coupling. J Mol Biol 286:915–932
63. Rist W, Graf C, Bukau B, Mayer MP (2006) Amide hydrogen exchange reveals conformational changes in hsp70 chaperones important for allosteric regulation. J Biol Chem 281:16493–16501
64. Revington M, Zhang Y, Yip GN, Kurochkin AV, Zuiderweg ER (2005) NMR investigations of allosteric processes in a two-domain Thermus thermophilus Hsp70 molecular chaperone. J Mol Biol 349:163–183
65. Swain JF, Dinler G, Sivendran R, Montgomery DL, Stotz M, Gierasch LM (2007) Hsp70 chaperone ligands control domain association via an allosteric mechanism mediated by the interdomain linker. Mol Cell 26:27–39
66. Bukau B, Walker GC (1989) Cellular defects caused by deletion of the Escherichia coli dnaK gene indicate roles for heat shock protein in normal metabolism. J Bacteriol 171:2337–2346
67. Georgopoulos CP (1977) New bacterial gene (Gropc) which affects lambda-DNA replication. Mol Gen Genet 151:35–39
68. Schlecht R, Erbse AH, Bukau B, Mayer MP (2011) Mechanics of Hsp70 chaperones enables differential interaction with client proteins. Nat Struct Mol Biol 18:345–351
69. Chang L, Thompson AD, Ung P, Carlson HA, Gestwicki JE (2010) Mutagenesis reveals the complex relationships between ATPase rate and the chaperone activities of Escherichia coli heat shock protein 70 (Hsp70/DnaK). J Biol Chem 285:21282–21291
70. Flaherty KM, Wilbanks SM, DeLuca-Flaherty C, McKay DB (1994) Structural basis of the 70-kilodalton heat shock cognate protein ATP hydrolytic activity. II. Structure of the active site with ADP or ATP bound to wild type and mutant ATPase fragment. J Biol Chem 269:12899–12907
71. Harrison CJ, Hayer-Hartl M, Di Liberto M, Hartl F, Kuriyan J (1997) Crystal structure of the nucleotide exchange factor GrpE bound to the ATPase domain of the molecular chaperone DnaK. Science 276:431–435

72. Osipiuk J, Walsh MA, Freeman BC, Morimoto RI, Joachimiak A (1999) Structure of a new crystal form of human Hsp70 ATPase domain. Acta Crystallogr D Biol Crystallogr 55:1105–1107
73. Morshauser RC, Hu W, Wang H, Pang Y, Flynn GC, Zuiderweg ER (1999) High-resolution solution structure of the 18 kDa substrate-binding domain of the mammalian chaperone protein Hsc70. J Mol Biol 289:1387–1403
74. Pellecchia M, Montgomery DL, Stevens SY, Vander Kooi CW, Feng HP, Gierasch LM, Zuiderweg ER (2000) Structural insights into substrate binding by the molecular chaperone DnaK. Nat Struct Biol 7:298–303
75. Bertelsen EB, Zhou H, Lowry DF, Flynn GC, Dahlquist FW (1999) Topology and dynamics of the 10 kDa C-terminal domain of DnaK in solution. Protein Sci 8:343–354
76. Jiang J, Prasad K, Lafer EM, Sousa R (2005) Structural basis of interdomain communication in the Hsc70 chaperone. Mol Cell 20:513–524
77. Chang YW, Sun YJ, Wang C, Hsiao CD (2008) Crystal structures of the 70-kDa heat shock proteins in domain disjoining conformation. J Biol Chem 283:15502–15511
78. Wang H, Pang Y, Kurochkin AV, Hu W, Flynn GC, Zuiderweg ERP (1998) The solution structure of the 21 kDa chaperone protein DnaK substrate binding domain: a preview of chaperone - protein interaction. Biochemistry 37:7929–7940
79. Swain JF, Schulz EG, Gierasch LM (2006) Direct comparison of a stable isolated Hsp70 substrate-binding domain in the empty and substrate-bound states. J Biol Chem 281:1605–1611
80. Liu Q, Hendrickson WA (2007) Insights into hsp70 chaperone activity from a crystal structure of the yeast Hsp110 Sse1. Cell 131:106–120
81. Zhang Y, Zuiderweg ER (2004) The 70-kDa heat shock protein chaperone nucleotide-binding domain in solution unveiled as a molecular machine that can reorient its functional subdomains. Proc Natl Acad Sci USA 101:10272–10277
82. Bhattacharya A, Kurochkin AV, Yip GN, Zhang Y, Bertelsen EB, Zuiderweg ER (2009) Allostery in Hsp70 chaperones is transduced by subdomain rotations. J Mol Biol 388:475–490
83. Zhuravleva A, Gierasch LM (2011) Allosteric signal transmission in the nucleotide-binding domain of 70-kDa heat shock protein (Hsp70) molecular chaperones. Proc Natl Acad Sci USA 108:6987–6992
84. Sousa MC, McKay DB (1998) The hydroxyl of threonine 13 of the bovine 70-kDa heat shock cognate protein is essential for transducing the ATP-induced conformational change. Biochemistry 37:15392–15399
85. O'Brien MC, McKay DB (1993) Threonine 204 of the chaperone protein Hsc70 influences the structure of the active site, but is not essential for ATP hydrolysis. J Biol Chem 268:24323–24329
86. Gassler CS, Buchberger A, Laufen T, Mayer MP, Schroder H, Valencia A, Bukau B (1998) Mutations in the DnaK chaperone affecting interaction with the DnaJ cochaperone. Proc Natl Acad Sci USA 95:15229–15234
87. Barthel TK, Zhang J, Walker GC (2001) ATPase-defective derivatives of Escherichia coli DnaK that behave differently with respect to ATP-induced conformational change and peptide release. J Bacteriol 183:5482–5490
88. Rudiger S, Mayer MP, Schneider-Mergener J, Bukau B (2000) Modulation of substrate specificity of the DnaK chaperone by alteration of a hydrophobic arch. J Mol Biol 304:245–251
89. Vogel M, Bukau B, Mayer MP (2006) Allosteric regulation of Hsp70 chaperones by a proline switch. Mol Cell 21:359–367
90. Han W, Christen P (2001) Mutations in the interdomain linker region of DnaK abolish the chaperone action of the DnaK/DnaJ/GrpE system. FEBS Lett 497:55–58
91. Burkholder WF, Zhao X, Zhu X, Hendrickson WA, Gragerov A, Gottesman ME (1996) Mutations in the C-terminal fragment of DnaK affecting peptide binding. Proc Natl Acad Sci USA 93:10632–10637

92. Voisine C, Craig EA, Zufall N, von Ahsen O, Pfanner N, Voos W (1999) The protein import motor of mitochondria: unfolding and trapping of preproteins are distinct and separable functions of matrix Hsp70. Cell 97:565–574
93. Smock RG, Rivoire O, Russ WP, Swain JF, Leibler S, Ranganathan R, Gierasch LM (2010) An interdomain sector mediating allostery in Hsp70 molecular chaperones. Mol Syst Biol 6:414
94. Shi L, Kataoka M, Fink AL (1996) Conformational characterization of DnaK and its complexes by small-angle X-ray scattering. Biochemistry 35:3297–3308
95. Wilbanks SM, Chen L, Tsuruta H, Hodgson KO, McKay DB (1995) Solution small-angle X-ray scattering study of the molecular chaperone Hsc70 and its subfragments. Biochemistry 34:12095–12106
96. Mapa K, Sikor M, Kudryavtsev V, Waegemann K, Kalinin S, Seidel CAM, Neupert W, Lamb DC, Mokranjac D (2010) The conformational dynamics of the mitochondrial Hsp70 chaperone. Mol Cell 38:89–100
97. Buczynski G, Slepenkov SV, Sehorn MG, Witt SN (2001) Characterization of a lidless form of the molecular chaperone DnaK: deletion of the lid increases peptide on- and off-rate constants. J Biol Chem 276:27231–27236
98. Slepenkov SV, Witt SN (2002) Kinetic analysis of interdomain coupling in a lidless variant of the molecular chaperone DnaK: DnaK's lid inhibits transition to the low affinity state. Biochemistry 41:12224–12235
99. Chesnokova LS, Slepenkov SV, Protasevich II, Sehorn MG, Brouillette CG, Witt SN (2003) Deletion of DnaK's lid strengthens binding to the nucleotide exchange factor, GrpE: a kinetic and thermodynamic analysis. Biochemistry 42:9028–9040
100. Slepenkov SV, Patchen B, Peterson KM, Witt SN (2003) Importance of the D and E helices of the molecular chaperone DnaK for ATP binding and substrate release. Biochemistry 42:5867–5876
101. Slepenkov SV, Witt SN (1998) Kinetics of the reactions of the Escherichia coli molecular chaperone DnaK with ATP: evidence that a three-step reaction precedes ATP hydrolysis. Biochemistry 37:1015–1024
102. Slepenkov SV, Witt SN (1998) Peptide-induced conformational changes in the molecular chaperone DnaK. Biochemistry 37:16749–16756
103. Slepenkov SV, Witt SN (2002) The unfolding story of the Escherichia coli Hsp70 DnaK: is DnaK a holdase or an unfoldase? Mol Microbiol 45:1197–1206
104. Slepenkov SV, Witt SN (2003) Detection of a concerted conformational change in the ATPase domain of DnaK triggered by peptide binding. FEBS Lett 539:100–104
105. Buchberger A, Valencia A, McMacken R, Sander C, Bukau B (1994) The chaperone function of DnaK requires the coupling of ATPase activity with substrate binding through residue E171. Embo J 13:1687–1695
106. Laufen T, Mayer MP, Beisel C, Klostermeier D, Mogk A, Reinstein J, Bukau B (1999) Mechanism of regulation of hsp70 chaperones by DnaJ cochaperones. Proc Natl Acad Sci USA 96:5452–5457
107. Jiang J, Maes EG, Taylor AB, Wang L, Hinck AP, Lafer EM, Sousa R (2007) Structural basis of J cochaperone binding and regulation of Hsp70. Mol Cell 28:422–433
108. Revington M, Holder TM, Zuiderweg ER (2004) NMR study of nucleotide-induced changes in the nucleotide binding domain of Thermus thermophilus Hsp70 chaperone DnaK: implications for the allosteric mechanism. J Biol Chem 279:33958–33967
109. Fischer MW, Losonczi JA, Weaver JL, Prestegard JH (1999) Domain orientation and dynamics in multidomain proteins from residual dipolar couplings. Biochemistry 38:9013–9022
110. Sondermann H, Scheufler C, Schneider C, Hohfeld J, Hartl FU, Moarefi I (2001) Structure of a Bag/Hsc70 complex: convergent functional evolution of Hsp70 nucleotide exchange factors. Science 291:1553–1557

111. Shomura Y, Dragovic Z, Chang HC, Tzvetkov N, Young JC, Brodsky JL, Guerriero V, Hartl FU, Bracher A (2005) Regulation of Hsp70 function by HspBP1: structural analysis reveals an alternate mechanism for Hsp70 nucleotide exchange. Mol Cell 17:367–379
112. Dragovic Z, Broadley SA, Shomura Y, Bracher A, Hartl FU (2006) Molecular chaperones of the Hsp110 family act as nucleotide exchange factors of Hsp70s. EMBO J 25:2519–2528
113. Arakawa A, Handa N, Ohsawa N, Shida M, Kigawa T, Hayashi F, Shirouzu M, Yokoyama S (2010) The C-terminal BAG domain of BAG5 induces conformational changes of the Hsp70 nucleotide-binding domain for ADP-ATP exchange. Structure 18:309–319
114. Stevens SY, Cai S, Pellecchia M, Zuiderweg ER (2003) The solution structure of the bacterial HSP70 chaperone protein domain DnaK(393-507) in complex with the peptide NRLLLTG. Protein Sci 12:2588–2596
115. Fernandez-Saiz V, Moro F, Arizmendi JM, Acebron SP, Muga A (2006) Ionic contacts at DnaK substrate binding domain involved in the allosteric regulation of lid dynamics. J Biol Chem 281:7479–7488
116. Banecki B, Zylicz M (1996) Real time kinetics of the DnaK/DnaJ/GrpE molecular chaperone machine action. J Biol Chem 271:6137–6143
117. Moro F, Fernandez V, Muga A (2003) Interdomain interaction through helices A and B of DnaK peptide binding domain. FEBS Lett 533:119–123
118. Mayer MP (2010) Gymnastics of molecular chaperones. Mol Cell 39:321–331
119. Zhang Q, Sun X, Watt ED, Al-Hashimi HM (2006) Resolving the motional modes that code for RNA adaptation. Science 311:653–656
120. Cooper A, Dryden DTF (1984) Allostery without conformational change - a plausible model. Eur Biophys J Biophys Lett 11:103–109
121. Lechtenberg BC, Johnson DJD, Freund SMV, Huntington JA (2010) NMR resonance assignments of thrombin reveal the conformational and dynamic effects of ligation. Proc Natl Acad Sci USA 107:14087–14092
122. Itoh K, Sasai M (2010) Entropic mechanism of large fluctuation in allosteric transition. Proc Natl Acad Sci USA 107:7775–7780
123. Tzeng SR, Kalodimos CG (2009) Dynamic activation of an allosteric regulatory protein. Nature 462:368–U139
124. Kern D, Zuiderweg ER (2003) The role of dynamics in allosteric regulation. Curr Opin Struct Biol 13:748–757
125. Stevens SY, Sanker S, Kent C, Zuiderweg ERP (2001) Delineation of the allosteric mechanism of a cytidylyltransferase exhibiting negative cooperativity. Nat Struct Biol 8:947–952
126. Maler L, Blankenship J, Rance M, Chazin WJ (2000) Site-site communication in the EF-hand Ca2+-binding protein calbindin D9k. Nat Struct Biol 7:245–250
127. Han WJ, Christen P (2004) cis-Effect of DnaJ on DnaK in ternary complexes with chimeric DnaK/DnaJ-binding peptides. FEBS Lett 563:146–150
128. Farr CD, Galiano FJ, Witt SN (1995) Large activation energy barriers to chaperone-peptide complex formation and dissociation. Biochemistry 34:15574–15582
129. Farr CD, Witt SN (1997) Kinetic evidence for peptide-induced oligomerization of the molecular chaperone DnaK at heat shock temperatures. Biochemistry 36:10793–10800
130. Farr CD, Slepenkov SV, Witt SN (1998) Visualization of a slow, ATP-induced structural transition in the bacterial molecular chaperone DnaK. J Biol Chem 273:9744–9748
131. Farr CD, Witt SN (1999) ATP lowers the activation enthalpy barriers to DnaK-peptide complex formation and dissociation. Cell Stress Chaperones 4:77–85
132. Varley P, Gronenborn AM, Christensen H, Wingfield PT, Pain RH, Clore GM (1993) Kinetics of folding of the all-beta sheet protein interleukin-1 beta. Science 260:1110–1113
133. Pierpaoli EV, Sandmeier E, Baici A, Schonfeld HJ, Gisler S, Christen P (1997) The power stroke of the DnaK/DnaJ/GrpE molecular chaperone system. J Mol Biol 269:757–768
134. Han WJ, Christen P (2003) Interdomain communication in the molecular chaperone DnaK. Biochem J 369:627–634

135. Siegenthaler RK, Christen P (2006) Tuning of DnaK chaperone action by nonnative protein sensor DnaJ and thermosensor GrpE. J Biol Chem 281:34448–34456
136. Goloubinoff P, Mogk A, Zvi AP, Tomoyasu T, Bukau B (1999) Sequential mechanism of solubilization and refolding of stable protein aggregates by a bichaperone network. Proc Natl Acad Sci USA 96:13732–13737
137. Packschies L, Theyssen H, Buchberger A, Bukau B, Goody RS, Reinstein J (1997) GrpE accelerates nucleotide exchange of the molecular chaperone DnaK with an associative displacement mechanism. Biochemistry 36:3417–3422
138. Xu Z, Page RC, Gomes MM, Kohli E, Nix JC, Herr AB, Patterson C, Misra S (2008) Structural basis of nucleotide exchange and client binding by the Hsp70 cochaperone Bag2. Nat Struct Mol Biol 15:1309–1317
139. Schuermann JP, Jiang JW, Cuellar J, Llorca O, Wang LP, Gimenez LE, Jin SP, Taylor AB, Demeler B, Morano KA, Hart PJ, Valpuesta JM, Lafer EM, Sousa R (2008) Structure of the Hsp110: Hsc70 nucleotide exchange machine. Mol Cell 31:232–243
140. Kabani M, McLellan C, Raynes DA, Guerriero V, Brodsky JL (2002) HspBP1, a homologue of the yeast Fes1 and Sls1 proteins, is an Hsc70 nucleotide exchange factor. FEBS Lett 531:339–342
141. Grimshaw JPA, Jelesarov I, Siegenthaler RK, Christen P (2003) Thermosensor action of GrpE - the DnaK chaperone system at heat shock temperatures. J Biol Chem 278:19048–19053
142. Brehmer D, Gassler C, Rist W, Mayer MP, Bukau B (2004) Influence of GrpE on DnaK-substrate interactions. J Biol Chem 279:27957–27964
143. Rudiger S, Schneider-Mergener J, Bukau B (2001) Its substrate specificity characterizes the DnaJ co-chaperone as a scanning factor for the DnaK chaperone. EMBO J 20:1042–1050
144. Rudiger S, Germeroth L, Schneider-Mergener J, Bukau B (1997) Substrate specificity of the DnaK chaperone determined by screening cellulose-bound peptide libraries. EMBO J 16:1501–1507
145. Feifel B, Schonfeld HJ, Christen P (1998) D-peptide ligands for the co-chaperone DnaJ. J Biol Chem 273:11999–12002
146. Suzuki H, Noguchi S, Arakawa H, Tokida T, Hashimoto M, Satow Y (2010) Peptide-binding sites as revealed by the crystal structures of the human Hsp40 Hdj1 C-terminal domain in complex with the octapeptide from human Hsp70. Biochemistry 49:8577–8584
147. Li JZ, Oian XG, Sha B (2003) The crystal structure of the yeast Hsp40 Ydj1 complexed with its peptide substrate. Structure 11:1475–1483
148. Pellecchia M, Szyperski T, Wall D, Georgopoulos C, Wuthrich K (1996) NMR structure of the J-domain and the Gly/Phe-rich region of the Escherichia coli DnaJ chaperone. J Mol Biol 260:236–250
149. Genevaux P, Fau-Schwager F, Fau K, Georgopoulos C, Kelley W (2002) Scanning mutagenesis identifies amino acid residues essential for the in vivo activity of the Escherichia coli DnaJ (Hsp40) J-domain. Genetics 162:1045–1053
150. Wall D, Zylicz M, Georgopoulos C (1994) The NH2-terminal 108 amino acids of the Escherichia coli DnaJ protein stimulate the ATPase activity of DnaK and are sufficient for lambda replication. J Biol Chem 269:5446–5451
151. Greene MK, Maskos K, Landry SJ (1998) Role of the J-domain in the cooperation of Hsp40 with Hsp70. Proc Natl Acad Sci USA 95:6108–6113
152. Ahmad A, Bhattacharya A, McDonald RA, Cordes M, Ellington B, Bertelsen EB, Zuiderweg ER (2011) Heat shock protein 70 kDa chaperone/DnaJ cochaperone complex employs an unusual dynamic interface. Proc Natl Acad Sci USA 108:18966–18971
153. Wittung-Stafshede P, Guidry J, Horne BE, Landry SJ (2003) The J-domain of Hsp40 couples ATP hydrolysis to substrate capture in Hsp70. Biochemistry 42:4937–4944
154. Huang K, Flanagan JM, Prestegard JH (1999) The influence of C-terminal extension on the structure of the "J-domain" in E. coli DnaJ. Protein Sci 8:203–214

155. Cajo GC, Horne BE, Kelley WL, Schwager F, Georgopoulos C, Genevaux P (2006) The role of the DIF motif of the DnaJ (Hsp40) co-chaperone in the regulation of the DnaK (Hsp70) chaperone cycle. J Biol Chem 281:12436–12444
156. Suh WC, Burkholder WF, Lu CZ, Zhao X, Gottesman ME, Gross CA (1998) Interaction of the Hsp70 molecular chaperone, DnaK, with its cochaperone DnaJ. Proc Natl Acad Sci USA 95:15223–15228
157. Suh WC, Lu CZ, Gross CA (1999) Structural features required for the interaction of the Hsp70 molecular chaperone DnaK with its cochaperone DnaJ. J Biol Chem 274:30534–30539
158. Wall D, Zylicz M, Georgopoulos C (1995) The conserved G/F motif of the DnaJ chaperone is necessary for the activation of the substrate binding properties of the DnaK chaperone. J Biol Chem 270:2139–2144
159. Karzai AW, McMacken R (1996) A bipartite signaling mechanism involved in DnaJ-mediated activation of the Escherichia coli DnaK protein. J Biol Chem 271:11236–11246
160. Pierpaoli EV, Sandmeier E, Schonfeld HJ, Christen P (1998) Control of the DnaK chaperone cycle by substoichiometric concentrations of the co-chaperones DnaJ and GrpE. J Biol Chem 273:6643–6649
161. Horne BE, Li TF, Genevaux P, Georgopoulos C, Landry SJ (2010) The Hsp40 J-domain stimulates Hsp70 when tethered by the client to the ATPase domain. J Biol Chem 285:21679–21688
162. Yochem J, Uchida H, Sunshine M, Saito H, Georgopoulos CP, Feiss M (1978) Genetic-analysis of 2 genes, DnaJ and DnaK, necessary for Escherichia-coli and Bacteriophage-lambda DNA-eeplication. Mol Gen Genet 164:9–14
163. Patury S, Miyata Y, Gestwicki JE (2009) Pharmacological targeting of the Hsp70 chaperone. Curr Top Med Chem 9:1337–1351
164. Nihei T, Sato N, Takahashi S, Ishikawa M, Sagae S, Kudo R, Kikuchi K, Inoue A (1993) Demonstration of selective protein complexes of p53 with 73 kDa heat shock cognate protein, but not with 72 kDa heat shock protein in human tumor cells. Cancer Lett 73:181–189
165. Fourie AM, Hupp TR, Lane DP, Sang BC, Barbosa MS, Sambrook JF, Gething MJ (1997) HSP70 binding sites in the tumor suppressor protein p53. J Biol Chem 272:19471–19479
166. Zylicz M, King FW, Wawrzynow A (2001) Hsp70 interactions with the p53 tumour suppressor protein. EMBO J 20:4634–4638
167. Wadhwa R, Yaguchi T, Hasan MK, Mitsui Y, Reddel RR, Kaul SC (2002) Hsp70 family member, mot-2/mthsp70/GRP75, binds to the cytoplasmic sequestration domain of the p53 protein. Exp Cell Res 274:246–253
168. Bienemann AS, Lee YB, Howarth J, Uney JB (2008) Hsp70 suppresses apoptosis in sympathetic neurones by preventing the activation of c-Jun. J Neurochem 104:271–278
169. Hui-Qing X, Jian-da Z, Xin-Min N, Yan-Zhong Z, Cheng-Qun L, Quan-Yong H, Yi X, Babu Pokharel P, Shao-Hua W, Dan X (2008) HSP70 inhibits burn serum-induced apoptosis of cardiomyocytes via mitochondrial and membrane death receptor pathways. J Burn Care Res 29:512–518
170. Guo F, Sigua C, Bali P, George P, Fiskus W, Scuto A, Annavarapu S, Mouttaki A, Sondarva G, Wei S, Wu J, Djeu J, Bhalla K (2005) Mechanistic role of heat shock protein 70 in Bcr-Abl-mediated resistance to apoptosis in human acute leukemia cells. Blood 105:1246–1255
171. Gyrd-Hansen M, Nylandsted J, Jaattela M (2004) Heat shock protein 70 promotes cancer cell viability by safeguarding lysosomal integrity. Cell Cycle 3:1484–1485
172. Didelot C, Lanneau D, Brunet M, Joly AL, De Thonel A, Chiosis G, Garrido C (2007) Anti-cancer therapeutic approaches based on intracellular and extracellular heat shock proteins. Curr Med Chem 14:2839–2847
173. Wadhwa R, Takano S, Robert M, Yoshida A, Nomura H, Reddel RR, Mitsui Y, Kaul SC (1998) Inactivation of tumor suppressor p53 by mot-2, a hsp70 family member. J Biol Chem 273:29586–29591

174. Lehman TA, Bennett WP, Metcalf RA, Welsh JA, Ecker J, Modali RV, Ullrich S, Romano JW, Appella E, Testa JR et al (1991) p53 mutations, ras mutations, and p53-heat shock 70 protein complexes in human lung carcinoma cell lines. Cancer Res 51:4090–4096
175. King FW, Wawrzynow A, Hohfeld J, Zylicz M (2001) Co-chaperones Bag-1, Hop and Hsp40 regulate Hsc70 and Hsp90 interactions with wild-type or mutant p53. EMBO J 20:6297–6305
176. Lane DP, Midgley C, Hupp T (1993) Tumour suppressor genes and molecular chaperones. Philos Trans R Soc Lond B Biol Sci 339:369–372, discussion 372-3
177. Vargas-Roig LM, Fanelli MA, López LA, Gago FE, Tello O, Aznar JC, Ciocca DR (1997) Heat shock proteins and cell proliferation in human breast cancer biopsy samples. Cancer Detect Prev 21:441–451
178. Nylandsted J, Wick W, Hirt UA, Brand K, Rohde M, Leist M, Weller M, Jaattela M (2002) Eradication of glioblastoma, and breast and colon carcinoma xenografts by Hsp70 depletion. Cancer Res 62:7139–7142
179. Wadhwa R, Takano S, Taira K, Kaul SC (2004) Reduction in mortalin level by its antisense expression causes senescence-like growth arrest in human immortalized cells. J Gene Med 6:439–444
180. Modica-Napolitano JS, Koya K, Weisberg E, Brunelli BT, Li Y, Chen LB (1996) Selective damage to carcinoma mitochondria by the rhodacyanine MKT-077. Cancer Res 56:544–550
181. Rodina A, Vilenchik M, Moulick K, Aguirre J, Kim J, Chiang A, Litz J, Clement CC, Kang Y, She Y, Wu N, Felts S, Wipf P, Massague J, Jiang X, Brodsky JL, Krystal GW, Chiosis G (2007) Selective compounds define Hsp90 as a major inhibitor of apoptosis in small-cell lung cancer. Nat Chem Biol 3:498–507
182. Massey AJ, Wood M (2010) A novel, small molecule inhibitor of Hsc70/Hsp70 potentiates Hsp90 inhibitor induced apoptosis in HCT116 colon carcinoma cells. Cancer Chemother Pharmacol 66:535–545
183. Ermakova SP, Kang BS, Choi BY, Choi HS, Schuster TF, Ma WY, Bode AM, Dong Z (2006) (-)-Epigallocatechin gallate overcomes resistance to etoposide-induced cell death by targeting the molecular chaperone glucose-regulated protein 78. Cancer Res 66:9260–9269
184. Wadhwa R, Sugihara T, Yoshida A, Nomura H, Reddel RR, Simpson R, Maruta H, Kaul SC (2000) Selective toxicity of MKT-077 to cancer cells is mediated by its binding to the hsp70 family protein mot-2 and reactivation of p53 function. Cancer Res 60:6818–6821
185. Wadhwa R, Takano S, Mitsui Y, Kaul SC (1999) NIH 3 T3 cells malignantly transformed by mot-2 show inactivation and cytoplasmic sequestration of the p53 protein. Cell Res 9:261–269
186. Britten CD, Rowinsky EK, Baker SD, Weiss GR, Smith L, Stephenson J, Rothenberg M, Smetzer L, Cramer J, Collins W, Von Hoff DD, Eckhardt SG (2000) A phase I and pharmacokinetic study of the mitochondrial-specific rhodacyanine dye analog MKT 077. Clin Cancer Res 6:42–49
187. Koo EH, Lansbury PT, Kelly JW (1999) Amyloid diseases: abnormal protein aggregation in neurodegeneration. Proc Natl Acad Sci USA 96:9989–9990
188. Caughey B, Lansbury PT (2003) Protofibrils, pores, fibrils, and neurodegeneration: separating the responsible protein aggregates from the innocent bystanders. Annu Rev Neurosci 26:267–298
189. Selkoe DJ (2003) Folding proteins in fatal ways. Nature 426:900–904
190. Avila J, Lucas JJ, Perez M, Hernandez F (2004) Role of tau protein in both physiological and pathological conditions. Physiol Rev 84:361–384
191. Bramblett GT, Goedert M, Jakes R, Merrick SE, Trojanowski JQ, Lee VMY (1993) Abnormal tau-phosphorylation at ser(396) in Alzheimers disease recapitulates development and contributes to reduced microtubule binding. Neuron 10:1089–1099
192. Geschwind DH (2003) Tau phosphorylation, tangles, and neurodegeneration: the chicken or the egg? Neuron 40:457–460
193. Boutajangout A, Quartermain D, Sigurdsson EM (2010) Immunotherapy targeting pathological tau prevents cognitive decline in a new tangle mouse model. J Neurosci 30:16559–16566

194. Dou F, Netzer WJ, Tanemura K, Li F, Hartl FU, Takashima A, Gouras GK, Greengard P, Xu H (2003) Chaperones increase association of tau protein with microtubules. Proc Natl Acad Sci USA 100:721–726
195. Jinwal UK, Miyata Y, Koren J 3rd, Jones JR, Trotter JH, Chang L, O'Leary J, Morgan D, Lee DC, Shults CL, Rousaki A, Weeber EJ, Zuiderweg ER, Gestwicki JE, Dickey CA (2009) Chemical manipulation of hsp70 ATPase activity regulates tau stability. J Neurosci 29:12079–12088
196. Powers MV, Jones K, Barillari C, Westwood I, van Montfort RLM, Workman P (2010) Targeting HSP70: the second potentially druggable heat shock protein and molecular chaperone? Cell Cycle 9:1542–1550
197. Williamson DS, Borgognoni J, Clay A, Daniels Z, Dokurno P, Drysdale MJ, Foloppe N, Francis GL, Graham CJ, Howes R, Macias AT, Murray JB, Parsons R, Shaw T, Surgenor AE, Terry L, Wang YK, Wood M, Massey AJ (2009) Novel adenosine-derived inhibitors of 70 kDa heat shock protein, discovered through structure-based design. J Med Chem 52:1510–1513
198. Kragol G, Lovas S, Varadi G, Condie BA, Hoffmann R, Otvos L (2001) The antibacterial peptide pyrrhocoricin inhibits the ATPase actions of DnaK and prevents chaperone-assisted protein folding. Biochemistry 40:3016–3026
199. Hohfeld J, Minami Y, Hartl F-U (1995) Hip, a novel cochaperone involved in the eukaryotic Hsc70/Hsp40 reaction cycle. Cell 83:589–598
200. Johnson BD, Schumacher RJ, Ross ED, Toft DO (1998) Hop modulates Hsp70/Hsp90 interactions in protein folding. J Biol Chem 273:3679–3686
201. Connell P, Ballinger CA, Jiang J, Wu Y, Thompson LJ, Hohfeld J, Patterson C (2001) The co-chaperone CHIP regulates protein triage decisions mediated by heat-shock proteins. Nat Cell Biol 3:93–96
202. Burri L, Vascotto K, Fredersdorf S, Tiedt R, Hall MN, Lithgow T (2004) Zim17, a novel zinc finger protein essential for protein import into mitochondria. J Biol Chem 279:50243–50249
203. Wisen S, Bertelsen EB, Thompson AD, Patury S, Ung P, Chang L, Evans CG, Walter GM, Wipf P, Carlson HA, Brodsky JL, Zuiderweg ERP, Gestwicki JE (2010) Binding of a small molecule at a protein-protein interface regulates the chaperone activity of Hsp70-Hsp40. ACS Chem Biol 5:611–622
204. Chang L, Miyata Y, Ung PM, Bertelsen EB, McQuade TJ, Carlson HA, Zuiderweg ER, Gestwicki JE (2011) Chemical screens against a reconstituted multiprotein complex: myricetin blocks DnaJ regulation of DnaK through an allosteric mechanism. Chem Biol 18:210–221
205. Rousaki A, Miyata Y, Jinwal UK, Dickey CA, Gestwicki JE, Zuiderweg ER (2011) Allosteric drugs: the interaction of antitumor compound MKT-077 with human Hsp70 chaperones. J Mol Biol 411:614–632
206. Tikoo A, Shakri R, Connolly L, Hirokawa Y, Shishido T, Bowers B, Ye LH, Kohama K, Simpson RJ, Maruta H (2000) Treatment of ras-induced cancers by the F-actin-bundling drug MKT-077. Cancer J 6:162–168
207. Koya K, Li Y, Wang H, Ukai T, Tatsuta N, Kawakami M, Shishido, Chen LB (1996) MKT-077, a novel rhodacyanine dye in clinical trials, exhibits anticarcinoma activity in preclinical studies based on selective mitochondrial accumulation. Cancer Res 56:538–543
208. O'Leary JC, Li QY, Marinec P, Blair LJ, Congdon EE, Johnson AG, Jinwal UK, Koren J, Jones JR, Kraft C, Peters M, Abisambra JF, Duff KE, Weeber EJ, Gestwicki JE, Dickey CA (2010) Phenothiazine-mediated rescue of cognition in tau transgenic mice requires neuroprotection and reduced soluble tau burden. Mol Neurodegener 5:45
209. Dickey CA, Koren J, Zhang YJ, Xu YF, Jinwal UK, Birnbaum MJ, Monks B, Sun M, Cheng AQ, Pattersonl C, Bailey RM, Dunmore J, Soresh S, Leon C, Morgan D, Petrucelli L (2008) Akt and CHIP coregulate tau degradation through coordinated interactions. Proc Natl Acad Sci USA 105:3622–3627

210. Arnone A, Perutz MF (1974) Structure of inositol hexaphosphate-human deoxyhemoglobin complex. Nature 249:34–36
211. Morris G, Goodsell D, Pique M, Lindstrom W, Huey R, Forli S, Hart W, Halliday S, Belew R, Olson A (2010) AutoDock Version 4.2
212. Case DA, Cheatham TE 3rd, Darden T, Gohlke H, Luo R, Merz KM Jr, Onufriev A, Simmerling C, Wang B, Woods RJ (2005) The Amber biomolecular simulation programs. J Comput Chem 26:1668–1688
213. Fogolari F, Brigo A, Molinari H (2003) Protocol for MM/PBSA molecular dynamics simulations of proteins. Biophys J 85:159–166

Top Curr Chem (2013) 328: 155–240
DOI: 10.1007/128_2012_356

Published online: 6 September 2012

Hsp90: Structure and Function

Sophie E. Jackson

Abstract Hsp90 is a highly abundant and ubiquitous molecular chaperone which plays an essential role in many cellular processes including cell cycle control, cell survival, hormone and other signalling pathways. It is important for the cell's response to stress and is a key player in maintaining cellular homeostasis. In the last ten years, it has become a major therapeutic target for cancer, and there has also been increasing interest in it as a therapeutic target in neurodegenerative disorders, and in the development of anti-virals and anti-protozoan infections. The focus of this review is the structural and mechanistic studies which have been performed in order to understand how this important chaperone acts on a wide variety of different proteins (its client proteins) and cellular processes. As with many of the other classes of molecular chaperone, Hsp90 has a critical ATPase activity, and ATP binding and hydrolysis known to modulate the conformational dynamics of the protein. It also uses a host of cochaperones which not only regulate the ATPase activity and conformational dynamics but which also mediate interactions with Hsp90 client proteins. The system is also regulated by post-translational modifications including phosphorylation and acetylation. This review discusses all these aspects of Hsp90 structure and function.

Keywords Acetylation · ATPase · Cochaperone · Conformational dynamics · Geldanamycin · Grp94 · Hsp90 · HtpG · Phosphorylation · Radicicol · TRAP-1

S.E. Jackson (✉)
Department of Chemistry, Lensfield Road, Cambridge CB2 1EW, UK
e-mail: sej13@cam.ac.uk

Contents

1 Introduction

Hsp90 is a highly abundant and ubiquitous molecular chaperone which plays an essential role in many cellular processes including cell cycle control, cell survival, hormone and other signalling pathways [1–5]. It is important for the cell's response to stress and is a key player in maintaining cellular homeostasis [6–10]. In the last 10 years, it has become a major therapeutic target for cancer [11] and there has also been increasing interest in it as a therapeutic target in neurodegenerative disorders [12, 13] and in the development of anti-virals [14] and anti-protozoan infections [15].

The focus of this review is the structural and mechanistic studies which have been performed in order to understand how this important chaperone acts on a wide variety of different proteins and cellular processes. The review begins with some background on the biological activity of Hsp90 including its homologues which are found in different cellular compartments and other organisms.

2 Biological Activity and Client Proteins

Hsp90 is required for the correct maturation and activation of a number of key cellular proteins and protein complexes. The proteins on which it acts are collectively called "clients" and many of them play important roles in signal transduction pathways. The number of potential clients of Hsp90 has increased dramatically in recent years and an up-to-date list of the known "interactors" which are not cochaperones can be downloaded from the website run by the Picard group in Geneva (http://www.picard.ch/downloads/Hsp90interactors.pdf). In addition, a recent review summarises a great number of studies that have been carried out in order to gain information on the Hsp90 interactome which includes cochaperones as well as client proteins [16].

Many Hsp90 clients are either kinases or transcription factors, and this includes the kinases Akt, cdk4/6, B-Raf, Plk1, src as well as other tyrosine kinases, and steroid receptors (including the oestrogen, gluco-corticoid and mineralo-corticoid, androgen, progesterone receptors), heat shock factor 1 (HSF1), p53, v-erb A to name just a few. Other client proteins are from structurally and functionally very diverse families – some ribosomal proteins, many viral polymerases and coat proteins, telomerase, the NLR protein in plants, and other proteins associated with neurodegenerative disorders such as tau and α-synuclein. How Hsp90 recognises such a wide range of different clients remains one of the major unsolved questions in the field. Given the number of clients that are either up-regulated or mutated in cancers, it is unsurprising that Hsp90 is now the target of many cancer therapeutic drugs, and this is discussed in more detail later in the review. Recently, a genome-wide study in *S. cerevisiae* suggested that up to 10% of all proteins required Hsp90 for their function, although, in this case, many may be through an indirect mechanism, i.e. their activity is regulated by an Hsp90 client [17, 18].

The glucocorticoid receptor (GR) was the first protein to be shown to be a client of Hsp90 back in the 1980s [19]. Now, it is known that many steroid receptors (SRs) require Hsp90 for their maturation and activation including oestrogen (ER), progesterone (PR), androgen (AR) and mineralocorticoid (MR) [20–23]. In addition, other members of the extended nuclear hormone receptor superfamily also are dependent upon Hsp90 including peroxisome proliferator-activated receptors (PPARs), a ryl hydrocarbon receptor (AhR), constitutive androstane receptor (CAR) pregnane receptor (PXR) and vitamin D receptors (VDR) [3, 4, 24–29].

As with many molecular chaperones, Hsp90 does not act alone but has a host of cochaperones which regulate its activity and confer specificity on the machinery

(see http://www.picard.ch/downloads/Hsp90interactors.pdf and a recent review [30]). Many of the first cochaperones were discovered as they were essential for the full activation of SRs and this includes p23, FKBP51/52 and recently FKBPL, Cyp40 and PP5. For an excellent review which focuses more on the biology of Hsp90 and cochaperones in steroid receptor function, in particular on how mouse models have been used to elucidate the roles of the different Hsp90 isoforms and cochaperones, see the recent review by Sanchez [31].

A long-standing model for how Hsp90 and cochaperones cooperate in the folding and maturation of steroid receptors is shown in Fig. 1b [29, 32]. In this model the newly synthesized receptor first interacts with the Hsp40/Hsp70 chaperones and then the receptor is efficiently transferred to Hsp90 by the action of Hop which can simultaneously bind to both Hsp70 and Hsp90. It is thought that at this stage the Hsp90 is in a nucleotide free state and an open conformation. The next step is the binding of ATP, the closure of the structure and dimerisation of the N-terminal domains of Hsp90, the release of Hop and/or the Hsp70 chaperone machinery followed by the binding of other cochaperones such as p23, FKBP51/52 or Cyp40. For more information on the role of ATP binding, hydrolysis and conformational dynamics of Hsp90 see later sections of this review. Binding of an Hsp90 inhibitor such as geldanamycin (GA), which binds to the ATP-binding site and prevents nucleotide binding, results in blocking of the cycle and subsequent degradation of the receptor [33–35].

In addition to the role of Hsp90 in the assembly of active steroid receptor complexes, it is also required for the correct assembly of many other key cellular complexes including telomere complexes, snoRP (small nucleolar ribonucleoproteins), RNA polII, PIKK (phosphatidylinositol 3-kinase-related protein kinase), the kinetochore, RISC (RNA-inducing silencing complex) and the 26S proteosome, reviewed in [36].

The Hsp90 family is highly conserved, being found in organisms in all kingdoms of life except archaea [37, 38]. In addition, there are four Hsp90 homologues in different cellular compartments [39]. The Hsp90 family can be subdivided into five subfamilies: cytosolic Hsp90s, ER-localized Grp94, mitochondrial TRAP1, chloroplast HSP90 and bacterial HtpG. In contrast to the eukaryotic Hsp90s, HtpG is not essential under non-stress conditions but does have some effect on growth at high temperatures [40]. Different members of the Hsp90 family have different cellular functions as outlined below and in later sections.

The function of Hsp90 in yeast has been studied extensively [41] and it is known that expression of at least one isoform is necessary for viability, and that, although it is possible to reduce the levels of cytosolic Hsp90 considerably to levels 5–10% that of normal, the yeast cells show a temperature-sensitive phenotype under these conditions [42]. *S. cerevisiae* has been used in many in vivo studies (see many of the references herein and also work from the Lindquist and Piper groups amongst others). Mouse knockouts have also been used to study the function of Hsp90 in vivo. In the case of Hsp90β, which is constitutively expressed, knockout in mice results in embryonic lethality. In contrast, knockout of the inducible isoform Hsp90α results in viable mice which are phenotypically normal except that the males

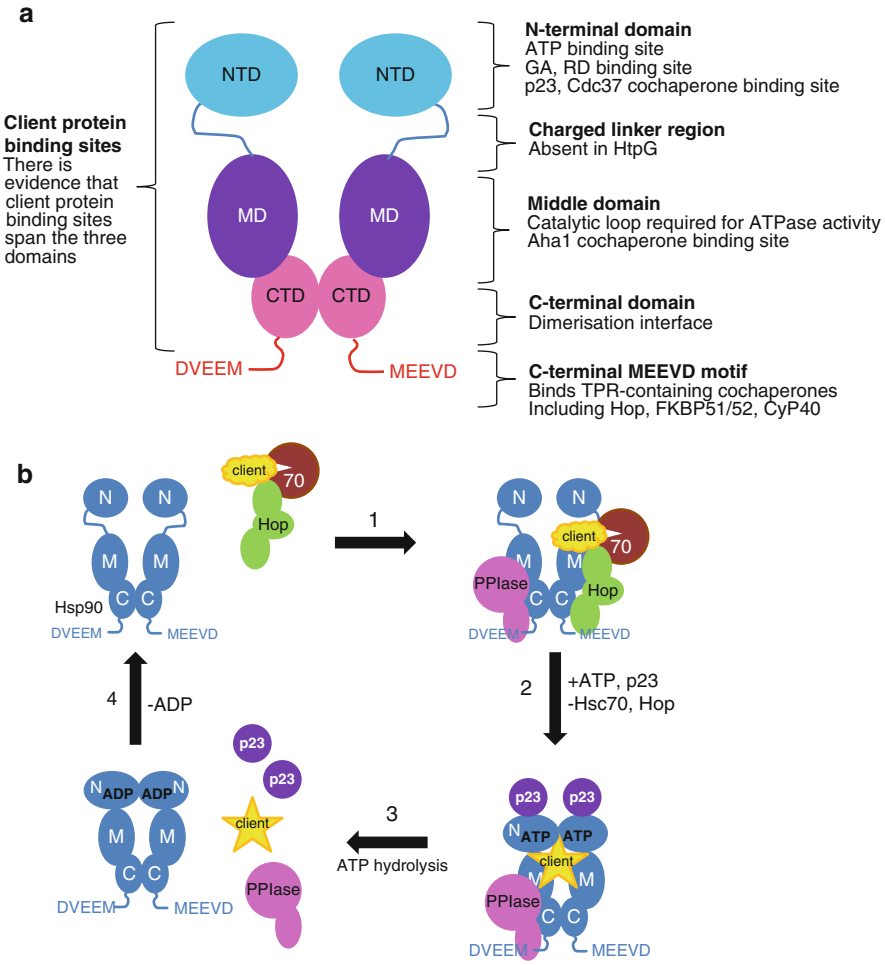

Fig. 1 Structure and mechanism of Hsp90. (**a**) Structural domains in the Hsp90 dimer. *NTD* is the N-terminal domain which binds ATP, GA, RD and other small molecule inhibitors and which also binds co-chaperones and potentially client proteins. This is followed by an unstructured highly charged linker region which is absent in HtpG. *MD* is the middle domain which contains a catalytic arginine required for the ATPase activity, binds to co-chaperones and is thought to be the major client-protein binding site. *CTD* is the C-terminal domain which contains the major dimerisation interface which makes Hsp90 a constitutive dimer. At the C-terminus is a highly conserved MEEVD motif which binds to TPR-containing co-chaperones. (**b**) Model proposed for the activation of steroid receptor client proteins (*yellow*) by the Hsp90 machinery. Hsp90 is shown in *blue*, Hsp70 in *dark red*, co-chaperones include Hop (*green*), high molecular weight PPIases such as FKBP51, FKBP52 or CyP40 (*pink*) and the small acidic protein p23 (*purple*)

are sterile [43]. In other organisms, either Hsp90 or one of its homologues have also been shown to be very important – Grp94 is essential in *Drosophila* [44], TRAP1 is essential for mitochondrial function (see later sections for further details), and

chloroplast Hsp90 function is necessary for the correct biogenesis of chloroplasts in *Arabidopsis thaliana* [45]. Only the *E. coli* homologue HtpG is not essential for viability; however, reduced HtpG function still results in mild growth defects and is needed for thermotolerance in cyanobacteria [46–48]. Other model organisms, including non-mammalian metazoan model systems, have also been employed such as *C. elegans*, *D. melonagaster* and *Danio rerio* (zebrafish) and the function of Hsp90 in these organisms is described in a recent review article [49].

The biological activity and function of Hsp90 and its homologues/paralogues is crucially dependent on both its ATPase activity and its conformational dynamics. The latter includes both structural changes within a single domain as well as changes in the conformation of Hsp90's three structural domains relative to each other. The following section describes in detail the structural studies on Hsp90 and its relatives that have been undertaken in order to understand better the mechanism of action of this critical molecular chaperone.

3 Structural Studies of the Hsp90 Molecular Chaperone Machinery

Hsp90 and its paralogues/homologues have three structural domains – an N-terminal domain (NTD) which contains the ATP binding site, which is connected to a middle domain (MD) through a variable charged linker, and a C-terminal domain (CTD) which is responsible for Hsp90 being a dimer. At the C-terminus there is another unstructured region which ends with a highly conserved MEEVD motif (Fig. 1a). The charged linker region is intrinsically disordered and therefore no detailed structural studies have been made. Whereas it was originally thought to act simply as a spacer between the NTD and middle domains, thereby allowing the necessary conformational rearrangements on nucleotide, cochaperone and potentially client protein binding, it has recently been shown that the sequence of this linker region can modulate the activity of Hsp90 in vivo [50]. In eukaryotes the charged linker contains unique regulatory sites, thereby acting as a "rheostat", finely tuning the Hsp90 chaperone machine [50].

3.1 High-Resolution X-Ray Crystal Structures of Hsp90

3.1.1 Structures of Isolated Domains

The first high-resolution crystal structures of a domain of Hsp90 to be solved were of the N-terminal domain of yeast and human Hsp90 both in their apo states as well as in complexes with nucleotides or inhibitors [51–55]. The overall structure of the NTD is an α/β sandwich in which a pocket extends from the buried face of the anti-

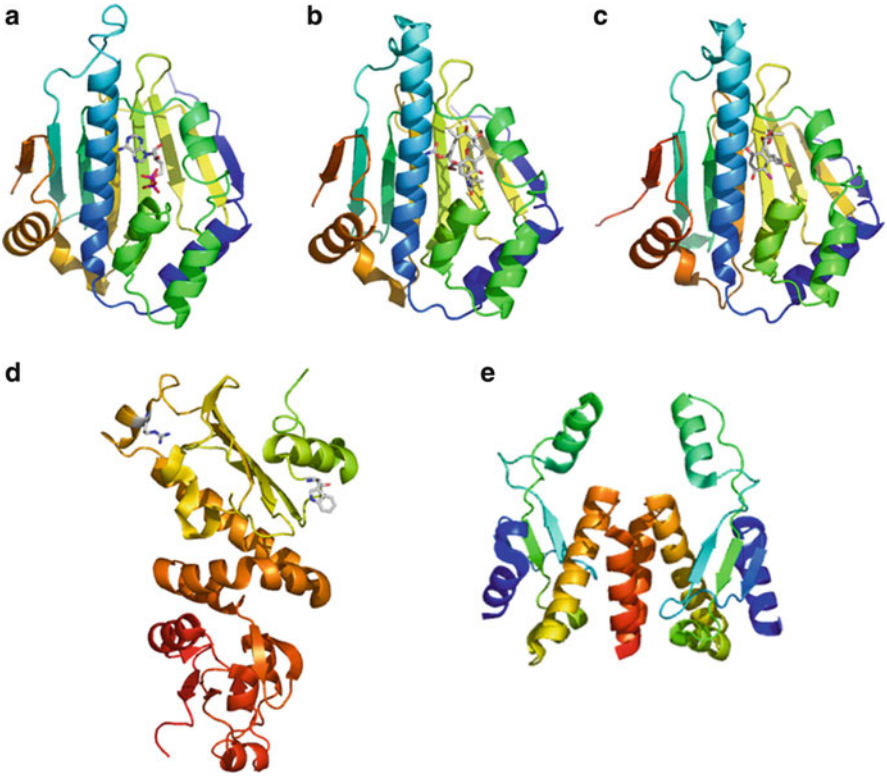

Fig. 2 Crystal structures of isolated domains of Hsp90s. (**a**) Structure of the N-terminal domain of human Hsp90 with ADP bound (pdb code: 1BYQ). The ribbon is coloured *dark blue* to *red* from N-terminus to C-terminus, ADP is shown as a stick model. (**b**) Structure of the N-terminal domain of human Hsp90 with geldanamycin (GA) bound (pdb code: 1YET). The ribbon is coloured *dark blue* to *red* from N-terminus to C-terminus, GA is shown as a stick model. (**c**) Structure of the N-terminal domain of yeast Hsp90 with Radicicol (RD) bound (pdb code: 1BGQ). The ribbon is coloured *dark blue* to *red* from N-terminus to C-terminus, RD is shown as a stick model. (**d**) Crystal structure of the middle domain of yeast Hsp90 (pdb code:1HK7), the side chains of residues Phe300 and Arg380 are shown in stick models. The ribbon is coloured from N-terminus (*yellow*/*green*) to C-terminus (*red*). (**e**) Crystal structure of the dimeric C-terminal domain of the *E. coli* HtpG (pdb code: 1SF8). The ribbons of the two chains are coloured the same from *dark blue* (N-terminus) to *red* (C-terminus). The dimerisation interface forms a four-helical bundle (α-helices coloured in *orange* and *red*)

parallel β-sheet to the surface which forms the nucleotide-binding site (Fig. 2a–c). The structures of the NTDs with nucleotide bound confirmed that Hsp90 is an ATP-binding protein and therefore likely has ATPase activity (Fig. 2a) [51–53], something which had up to that point been controversial due to the fact that the basal ATPase activity is very low. The structure allowed the identification of the key catalytic residues and subsequent mutagenesis studies further confirmed the ATPase activity. Structures with the natural products geldanamycin (GA) and radicicol (RD)

established that these inhibit the function of Hsp90 by binding to the ATP-binding pocket and therefore act as competitive inhibitors of the essential ATPase activity of Hsp90 [54, 55]. These structures also revealed that these inhibitors bind in a very similar way to the nucleotide (which binds in an unusual kinked conformation) both in terms of shape complementarity and also conservation of key interactions including those with a tightly bound water molecule (Fig. 2b, c). There are now numerous crystal structures of the NTDs of human and yeast Hsp90 complexed with a variety of different inhibitors, as well as the NTDs of Hsp90s from other organisms including *Leishmania major*, *Plasmodium falciparum* and *Trypansoma brucei*, in addition to the NTDs from the Hsp90 homologues, Grp94 and HtpG; see Table 1.

The structure of the middle domain of yeast Hsp90 was the next to be solved in 2003, and it comprises two structural subdomains – a large α/β/α domain at the N-terminal end which is linked to a smaller α/β/α domain through a series of short helices (Fig. 2d) [58]. The structure revealed a hydrophobic patch containing an exposed tryptophan (Trp300 in the *S. cerevisaie* Hsp82) and an amphipathic protrusion, which were proposed to be important for client protein binding. This domain also contains a critical catalytic loop with a highly conserved Arg residue essential for the ATPase activity. In the structure of the isolated domain, it is in a structured short α-helical region which differs from the structure in the full-length protein (Figs. 2d and 3e). The structure of the isolated middle domain of HtpG has also been solved and is very similar [73]. Shortly after the publication of this structure, the structure of the remaining C-terminal domain from HtpG was reported [59]. The CTD is a homodimer of two small mixed α/β domains, where the dimer interface is formed by two α-helices which pack together to form a four-helical bundle (Fig. 2e) [59]. These high-resolution structures of all three domains of Hsp90 subsequently allowed the use of lower resolution structural techniques such as small-angle X-ray scattering (SAXS) and electron microscopy (EM) to obtain information on the conformations and dynamics of full-length Hsp90s.

3.1.2 Structures of Multi-domain Constructs of Hsp90

In 2005 the first structure of a multi-domain construct of an Hsp90 homologue was reported with the publication of the structure of the NTD and middle domain of HtpG [63]. Both the apo and ADP-bound states were solved and conformational changes on ADP binding observed. Perhaps more importantly, extensive interactions between the two domains were seen and although the primary binding site for ADP was clearly in the NTD as expected, there were also interactions with the middle domain. A comparison of the structure with structures known for other members of the GHKL ATPase superfamily demonstrated that there were likely to be large motions of the domains relative to each other around a hinge region, mechanistically now supported by many other studies; see the section on ATPase activity for further details. The structure of the middle and C-terminal domain of yeast Hsp90 was reported shortly afterwards at the same time as the structure of the full-length protein [71], and the structure of a construct of Grp94 comprising the

Table 1 Summary of the X-ray crystal structures of the individual domains of Hsp90

Construct	Organism	Nucleotide/inhibitor	Resolution (Angstrom)	Pdb code	Reference	Release year
NTD Hsp90	*S. cerevisiae*		2.10	1AH8	[52, 53]	1997 Orthorhombic
	S. cerevisiae		1.80	1AH6	[52, 53]	1997 Tetragonal
	Human	GA	1.90	1YET	[55]	1998
	Human		2.20	1YES	[55]	1998
	Human		1.65	1YER	[55]	1998
	S. cerevisiae	ADP	1.85	1AMW	[52, 53]	1998
	S. cerevisiae	ADP	2.00	1AM1	[52, 53]	1998
	S. cerevisiae	GA	2.50	1A4H	[52, 53]	1998
	Human	ADP/MG^{2+}	1.50	1BYQ	[51]	1998
	S. cerevisiae	RAD	2.50	1BGQ	[54]	1999
	Human	17-DMAG	1.75	1OSF	[56]	2003
NTD Grp94	Dog	NECA	1.75	1QY5	[57]	2003
NTD Grp94	Dog	RD	1.85	1QY8	[57]	2003
NTD Grp94	Dog	2-Chloro-dideoxy-adenosine	2.10	1QYE	[57]	2003
Middle domain Hsp90	*S. cerevisiae*		2.50	1HK7	[58]	2004
CTD HtpG	*E. coli*		2.60	1SF8	[59]	2004
NTD Alpha	Human	9-Butyl-8-(3,4,5-trimethoxybenzyl)-9H-purin-6-amine	1.90	1UY6	[60]	2004
NTD Alpha	Human	9-Butyl-8-(4-methoxybenzyl)-9H-purin-6-amine	1.90	1UY7	[60]	2004
NTD Alpha	Human	9-Butyl-8-(3-methoxybenzyl)-9H-purin-6-amine	1.98	1UY8	[60]	2004

(continued)

Table 1 (continued)

Construct	Organism	Nucleotide/inhibitor	Resolution (Angstrom)	Pdb code	Reference	Release year
NTD Alpha	Human	8-Benzo[1,3]dioxol-,5-ylmethyl-9-butyl-9H-purin-6-ylamine	2.00	1UY9	[60]	2004
NTD Alpha	Human	9-Butyl-8-(2,5-dimethoxy-benzyl)-9H-purin-6-ylamine	2.00	1UYC	[60]	2004
NTD Alpha	Human	9-Butyl-8-(2-chloro-3,4,5-trimethoxy-benzyl)-9H-purin-6-ylamine	2.20	1UYD	[60]	2004
NTD Alpha	Human	8-(2-Chloro-3,4,5-trimethoxy-benzyl)-9-pent-4-ylnyl-9H-purin-6-ylamine	2.00	1UYE	[60]	2004
NTD Alpha	Human	8-(2-Chloro-3,4,5-trimethoxy-benzyl)-2-fluoro-9-pent-4-ylnyl-9H-purin-6-ylamine	2.00	1UYF	[60]	2004
NTD Alpha	Human	8-(2,5-Dimethoxy-benzyl)-2-fluoro-9H-purin-6-ylamine	2.00	1UYG	[60]	2004
NTD Alpha	Human	9-Butyl-8-(2,5-dimethoxy-benzyl)-2-fluoro-9H-purin-6-ylamine	2.20	1UYH	[60]	2004
NTD Alpha	Human	8-(2,5-Dimethoxy-benzyl)-2-fluoro-9-pent-9H-purin-6-ylamine	2.20	1UYI	[60]	2004
NTD Alpha	Human	8-Benzo[1,3]dioxol-,5-ylmethyl-9-but yl-2-fluoro-9H-purin-6-ylamine	2.20	1UYK	[60]	2004
NTD beta	Human	9-Butyl-8-(3,4,5-trimethoxybenzyl)-9H-purin-6-amine (immormino, 2004)	2.45	1UYM	[60]	2004
NTD Grp94 Engineered 287–327 polyG	Dog	AMP	2.15	1TBW	[61]	2004
NTD Grp94 Engineered 287–327 polyG	Dog	ATP	2.20	1TC0	[61]	2004

NTD Grp94 Engineered 287–327 polyG	Dog	ADP	2.87	1TC6	[61]	2004
NTD Grp94	Dog	NECA	2.10	1UTO	[57]	2004
NTD Hsp90 Alpha	Human	4-(1,3-Benzodioxol-5-yl)-5-(5-ethyl-2,4-dihydroxyphenyl)-2H-pyrazole-3-carboxylic acid	2.12	1YC3	[62]	2005
NTD and Middle domain HtpG	*E. coli*	ADP	2.90	1Y4S	[63]	2005
NTD and Middle domain HtpG	*E. coli*		2.90	1Y4U	[63]	2005
NTD Grp94 287–327 GGGG	Dog	NECA	2.65	1YSZ	[64]	2005
NTD Grp94 287–327 GGGG Delta41	Dog	ADP	2.40	1YT0	[64]	2005
NTD Grp94 287–327 GGGG	Dog		2.20	1YT1	[64]	2005
NTD Grp94	Dog		3.25	1YT2	[64]	2005

(continued)

Table 1 (continued)

Construct	Organism	Nucleotide/inhibitor	Resolution (Angstrom)	Pdb code	Reference	Release year
NTD Hsp90 Alpha	Human	5-(5-Chloro-2,4-dihydroxyphenyl)-*n*-ethyl-4-(4-methoxyphenyl)-1H-pyrazole-3-carboxamide	2.05	2BSM	[65]	2005
NTD Hsp90 Alpha	Human	4-[4-(2,3-Dihydro-1,4-benzodioxin-6-yl)-3-methyl-1H-pyrazol-5-yl]-6-ethylbenzene-1,3-diol	1.90	2BT0	[65]	2005
NTD Grp94	Dog	*N*-propyl carboxyamido adenosine	2.30	1U0Y	[64]	2005
NTD Grp94	Dog	RAD	1.90	1U0Z	[64]	2005
NTD Hsp90	*S. Cerevisiae*	4-[4-(2,3-Dihydro-1,4-benzodioxin-6-yl)-3-methyl-1H-pyrazol-5-yl]-6-ethylbenzene-1,3-diol	1.60	2BRC	[66]	2005
NTD Hsp90	*S. cerevisiae*	4-(4-[4-(3-Aminopropoxy)phenyl]-1H-pyrazol-5-yl}-6-chlorobenzene-1,3-diol	2.00	2BRE	[66]	2005
NTD Hsp90 Alpha	Human	*N*-(4-acetylphenyl)-5-(5-chloro-2,4-dihydroxyphenyl)-1H-pyrazole-4-carboxamide	1.90	2BYH	[67]	2005
NTD Hsp90 Alpha	Human	3-(5-Chloro-2,4-dihydroxy-phenyl)-1H-pyrazole-4-carboxylic acid 4-sulfamoyl-benzylamide	1.60	2BYI	[67]	2005
NTD Hsp90 Alpha	Human	2,5-Dichloro-*n*-[4-hydroxy-3-(2-hydroxy-1-naphthyl)phenyl] benzenesulfonamide	1.90	2BZ5	[68]	2005
NTD Hsp90 Alpha	Human	4-[4-(2,3-Dihydro-1,4-benzodioxin-6-yl)-3-methyl-1H-pyrazol-5-yl]-6-ethylbenzene-1,3-diol	1.90	2CDD	[69]	2006
NTD Hsp90 Delta24	*S. cerevisiae*		1.94	2AKP	[70]	2006
NTD Hsp90 Alpha	Human	4-Chloro-6-(4-(4-[4-(methylsulfonyl)benzyl]piperazin-1-yl}-1H-pyrazol-5-yl)benzene-1,3-diol	2.70	2CCU	[69]	2006

NTD Hsp90 Alpha	Human	5-(5-Chloro-2,4-dihydroxyphenyl)-*n*-ethyl-4-piperazin-1-yl-1H-pyrazole-3-carboxamide	2.30	2CCT	[69]	2006
NTD Hsp90 Alpha	Human	4-Chloro-6-(4-piperazin-1-yl-1H-pyrazol-5-yl)benzene-1,3-diol	1.79	2CCS	[69]	2006
Middle and CTD	*S. cerevisiae*		3.00	2CGE	[71]	2006
NTD Hsp90	*S. cerevisiae*	2-(3-Amino-2,5,6-trimethoxyphenyl)ethyl 5-chloro-2,4-dihydroxybenzoate	1.65	1ZWH		2006
NTD Hsp90	*S. cerevisiae*	8-(6-Bromo-benzo[1,3]dioxol-5-ylsulfanyl)-9-(3-isopropylamino-propyl)-adenine	1.90	1ZW9		2006
NTD Hsp90 Alpha	Human	2-Fluoro-8-[(6-iodo-1,3-benzodioxol-5-yl)methyl]-9-[3-(isopropylamino)propyl]-9H-purin-6-amine	2.00	2H55	[72]	2006
NTD Hsp90 Alpha	Human	8-[(6-Iodo-1,3-benzodioxol-5-yl)thio]-9-[3-(isopropylamino) propyl]-9H-purin-6-amine	2.10	2FWZ	[72]	2006
NTD Hsp90 Alpha	Human	8-(6-Bromo-benzo[1,3]dioxol-5-ylsulfanyl)-9-(3-isopropylamino-propyl)-adenine	2.10	2FWY	[72]	2006
NTD Grp94 287–327 GGGG 168–169 KS–AA	Dog	GA	1.90	2ESA		2006
NTD Grp94 287–327 GGGG	Dog		2.35	2EXL		2006

(continued)

Table 1 (continued)

Construct	Organism	Nucleotide/inhibitor	Resolution (Angstrom)	Pdb code	Reference	Release year
Middle domain HtpG	*E. coli*		1.90	2GQ0	[73]	2006
NTD HtpG	*E. coli*	ADP	1.65	2IOR	[73]	2006
NTD Hsp90	*S. cerevisiae*	(5*Z*)-13-chloro-14,16-dihydroxy-3,4,7,8,9,10-hexahydro-1H-2-benzoxacyclotetradecine-1,11(12H)-dione	2.20	2CGF	[74]	2006
NTD Hsp90	*S. cerevisiae*	(5*E*)-14-chloro-15,17-dihydroxy-4,7,8,9,10,11-hexahydro-2-benzoxacyclopentadecine-1,12(3H,13H)-dione	1.50	2IWX	[74]	2006
NTD Hsp90	*S. cerevisiae*	(5*E*)-12-chloro-13,15-dihydroxy-4,7,8,9-tetrahydro-2-benzoxacyclotridecine-1,10(3H,11H)-dione	2.80	2IWU	[74]	2006
NTD Hsp90	*S. cerevisiae*	(5*Z*)-12-chloro-13,15-dihydroxy-4,7,8,9-tetrahydro-2-benzoxacyclotridecine-1,10(3H,11H)-dione	2.70	2IWS	[74]	2006
NTD Grp94 287–327 GGGG	Dog	2-(3-Amino-2,5,6-trimethoxyphenyl)ethyl 5-chloro-2,4-dihydroxybenzoate	1.95	2FYP		2007
NTDHsp90	*S. cerevisiae*	Methyl 3-chloro-2-(3-[(2,5-dihydroxy-4-methoxyphenyl)amino]-3-oxopropyl}-4,6-dihydroxybenzoate	2.00	2FXS		2007
NTD Grp94 287–327 GGGG	Dog	*N*-propyl carboxyamido adenosine	1.50	2GQP		2007
NTD Grp94 287–327 GGGG	Dog	Methyl 3-chloro-2-(3-[(2,5-dihydroxy-4-methoxyphenyl)amino]-3-oxopropyl}-4,6-dihydroxybenzoate	2.30	2GFD		2007
NTD Grp94 287–327 GGGG	Dog	5-(5-Chloro-2,4-dihydroxyphenyl)-*n*-ethyl-4-(4-methoxyphenyl) isoxazole-3-carboxamide	1.90	2UWD		2007
	Dog	(2*S*,3*S*,4*R*,5*R*)-5-(6-amino-2-iodo-9H-purin-9-yl)-*n*-ethyl-3,4-dihydroxytetrahydrofuran-2-carboxamide	1.80	2H8M		2007

NTD Grp94 287–327 GGGG						
NTD Grp94 287–327 GGGG	Dog	5′-*N*-[(2-amino)ethyl carboxamido] adenosine	2.30	2HCH		2007
NTD Grp94 287–327 GGGG	Dog	5′-*N*-(2-hydroxyl)ethyl carboxyamido adenosine	2.30	2HG1		2007
NTD and middle domain Grp94 287–327 GGGG	Dog		3.40	2O1W	[75]	2007
Middle and CTD domain Grp94	Dog		3.20	2O1T	[75]	2007
NTD Hsp90 Alpha	Human	5-(5-Chloro-2,4-dihydroxyphenyl)-*n*-ethyl-4-[4-(morpholin-4-ylmethyl)phenyl]isoxazole-3-carboxamide	2.50	2VCJ	[76]	2007
NTD Hsp90 Alpha	Human	5-[2,4-Dihydroxy-5-(1-methylethyl)phenyl]-*n*-ethyl-4-[4-(morpholin-4-ylmethyl)phenyl]isoxazole-3-carboxamide	2.00	2VCI	[76]	2007
NTD Hsp90 Alpha	Human	2-[(2-Methoxyethyl)amino]-4-(4-oxo-1,2,3,4-tetrahydro-9H-carbazol-9-yl)benzamide	1.74	3D0B	[77]	2008
NTD Hsp90	*S. cerevisiae*	Macbecin	2.40	2VWC	[78]	2008
NTD Hsp90 Alpha	Human	3-((2-[(2-Amino-6-methylpyrimidin-4-yl)ethynyl]benzyl} amino)-1,3-oxazol-2(3H)-one	1.80	2QG2	[79]	2008
NTD Hsp90 Alpha	Human	4-Methyl-6-(trifluoromethyl)pyrimidin-2-amine-3*E*)-3-[(phenylamino)methylidene]dihydrofuran-2(3H)-one	1.68	2QFO	[79]	2008

(continued)

Table 1 (continued)

Construct	Organism	Nucleotide/inhibitor	Resolution (Angstrom)	Pdb code	Reference	Release year
NTD Hsp90 Alpha	Human	6-(3-Bromo-2-naphthyl)-1,3,5-triazine-2,4-diamine	3.10	2QF6	[79]	2008
NTD Hsp90 Alpha	Human	4-Chloro-6-(5-[(2-morpholin-4-ylethyl)amino]-1,2-benzisoxazol-3-yl}benzene-1,3-diol	1.60	3BMY		2008
NTD Hsp90 Alpha	Human	4-Bromo-6-(6-hydroxy-1,2-benzisoxazol-3-yl)benzene-1,3-diol	1.60	3BMY	[80]	2008
NTD Hsp90 Alpha	Human	Pyrimidin-2-amine	1.95	2JJC		2008
NTD Hsp90 K98A, K99A	*S. cerevisiae*	GA	1.60	3C11		2008
NTD Hsp90 K98A, K99A	*S. cerevisiae*		1.90	3C0E		2008
NTD Hsp90	*S. cerevisiae*	(4*E*,8*S*,9*R*,10*E*,12*S*,13*R*,14*S*,16*R*)-13,20-dihydroxy-14-methoxy-4,8,10,12,16-pentamethyl-3-oxo-2-azabicyclo[16.3.1]docosa-1(22),4,10,18,20-pentaen-9-yl carbamate	1.90	2VW5	[81, 82]	2008
NTD Hsp90 Alpha	Human	4-([(2*R*)-2-(2-methylphenyl)pyrrolidin-1-yl]carbonyl}benzene-1,3-diol	2.00	3EKR	[83]	2008
NTD Hsp90 Alpha	Human	2-(1H-pyrrol-1-ylcarbonyl)benzene-1,3,5-triol	1.55	3EKO	[83]	2008
NTD Hsp90 LI-IV mutant	*S. cerevisiae*	RD	1.60	2WER	[84]	2009

NTD Hsp90 LI-IV mutant	*S. cerevisiae*	GA	2.20	2WEQ	[84]	2009
NTD Hsp90 LI-IV mutant	*S. cerevisiae*	ADP	2.20	2WEP	[84, 85]	2009
NTD Hsp90 Alpha	Human	4-Methyl-7,8-dihydro-5H-thiopyrano[4,3-d]pyrimidin-2-amine	1.90	3FT5	[85]	2009
NTD Hsp90	*Leishmania major*	Phosphoaminophosphonic acid-adenylate ester	2.00	3H80		2009
CTD Hsp90	*Leishmania major*		2.50	3HJC		2009
NTD Hsp90 Alpha	Human	(5*E*,7*S*)-2-amino-7-(4-fluoro-2-pyridin-3-ylphenyl)-4-methyl-7,8-dihydroquinazolin-5(6H)-one oxime	2.00	3FT8	[85, 86]	2009
NTD Hsp90 Alpha	Human	Ethyl (4-(3-[2,4-dihydroxy-5-(1-methylethyl)phenyl]-5-sulfanyl-4H-1,2,4-triazol-4-yl}benzyl)carbamate	1.59	3HHU	[86]	2009
NTD Hsp90 Alpha	Human	2-Amino-4-[2,4-dichloro-5-(2-pyrrolidin-1-ylethoxy)phenyl]-*n*-ethylthieno[2,3-d]pyrimidine-6-carboxamide	2.50	2WI7	[87]	2009
NTD Hsp90 Alpha	Human	2-Amino-4-(2,4-dichlorophenyl)-n-ethylthieno[2,3-d] pyrimidine-6-carboxamide	2.18	2WI6	[87]	2009
NTD Hsp90 Alpha	Human	3,6-Diamino-5-cyano-4-(4-ethoxyphenyl)thieno[2,3-b]pyridine-2-carboxamide	2.10	2WI5	[87]	2009
NTD Hsp90 Alpha	Human	4-(2,4-Dichlorophenyl)-5-phenyldiazenyl-pyrimidin-2-amine	2.40	2WI4	[87]	2009

(continued)

Table 1 (continued)

Construct	Organism	Nucleotide/inhibitor	Resolution (Angstrom)	Pdb code	Reference	Release year
NTD Hsp90 Alpha	Human	4-Methyl-6-(methylsulfanyl)-1,3,5-triazin-2-amine	1.90	2WI3	[87]	2009
NTD Hsp90 Alpha	Human	4-Methyl-6-(methylsulfanyl)-1,3,5-triazin-2-amine	2.09	2WI2	[87]	2009
NTD Hsp90 Alpha	Human	4-(2-Methoxyethoxy)-6-methylpyrimidin-2-amine	2.30	2WI1	[87]	2009
NTD Hsp90	*Plasmodium falciparum*	AMP phosphoramidate	2.01	3IED		2009
NTD Hsp90 Alpha	Human	(1*S*,2*R*)-1-[(5-chloro-2,4-dihydroxyphenyl)carbonyl]-2-(4-[(3,3-difluoropyrrolidin-1-yl)methyl]phenyl}pyrrolidinium	1.95	3HEK	[88]	2009
NTD Hsp90 Alpha	Human	Methyl 5-furan-2-yl-3-methyl-1H-pyrazole-4-carboxylate	1.90	3HYY		2010
NTD Hsp90 Alpha	Human	4-(1,3-Dihydro-2H-isoindol-2-ylcarbonyl)benzene-1,3-diol	2.10	3K99	[89]	2010
NTD Hsp90 Alpha	Human	(1*R*)-2-[(5-chloro-2,4-dihydroxyphenyl)carbonyl]-*n*-ethyl-2,3-dihydro-1H-isoindole-1-carboxamide	2.40	3K98	[89]	2010
NTD Hsp90 Alpha	Human	4-Chloro-6-([(2*R*)-2-(2-methylphenyl)pyrrolidin-1-yl]carbonyl}benzene-1,3-diol	1.95	3K97	[89]	2010

NTD Hsp90 Alpha	Human	*N*-[4-(5-furan-2-yl-3-methyl-1H-pyrazol-4-yl)butyl]-*n*-methyl-7H-purin-6-amine	1.90	3HZ5		2010
NTD Hsp90 Alpha	Human	Methyl 5-furan-2-yl-3-methyl-1H-pyrazole-4-carboxylate *N*,*N*-dimethyl-7H-purin-6-amine	2.30	3HZ1		2010
NTD Hsp90 Alpha	Human	*N*,*N*-dimethyl-7H-purin-6-amine	2.30	3HYZ		2010
NTD Hsp90 Alpha	Human	Methyl 5-furan-2-yl-3-methyl-1H-pyrazole-4-carboxylate	1.90	3HYY		2010
NTD Hsp90 Alpha	Human	2-[(3,4,5-Trimethoxyphenyl)amino]-4-(2,6,6-trimethyl-4-oxo-4,5,6,7-tetrahydro-1H-indol-1-yl)benzamide	1.90	3MNR	[90]	2010
NTD Hsp90 Alpha	Human	(2,4-Dihydroxy-5-propan-2-yl-phenyl)-[5-[(4-methylpiperazin-1-yl)methyl]isoindol-2-yl]methanone	1.66	2XJX	[91–93]	2010
NTD Hsp90 Alpha	Human	1,3-Dihydroisoindol-2-yl-(6-hydroxy-3,3-dimethyl-1,2-dihydroindol-5-yl)methanone	1.90	2XJJ	[91–93]	2010
NTD Hsp90 Alpha	Human	1,3-Dihydroisoindol-2-yl-(2-hydroxy-4-methoxy-5-propan-2-yl-phenyl)methanone	2.25	2XJG	[91–93]	2010
NTD Hsp90	*S. cerevisiae*	(5*Z*)-13-chloro-14,16-dihydroxy-1,11-dioxo-3,4,7,8,9,10,11,12-octahydro-1H-2-benzoxacyclotetradecine-6-carbaldehyde	2.20	2XD6	[94]	2010
NTD Hsp90 Alpha	Human	4-(1,3-Dihydro-2H-isoindol-2-ylcarbonyl)-6-(1-methylethyl) benzene-1,3-diol	1.90	2XAB	[91–93]	2010

(continued)

Table 1 (continued)

Construct	Organism	Nucleotide/inhibitor	Resolution (Angstrom)	Pdb code	Reference	Release year
NTD Hsp90	*Trypanasoma brucei*	6-Chloro-9-[(4-methoxy-3,5-dimethylpyridin-2-yl)methyl]-9H-purin-2-amine	2.00	3O6O		2010
NTD Hsp90 Deletion mutant 212–301)/GGG	*Plasmodium falciparum*	ADP	2.30	3K60	[95]	2010
NTD Hsp90 Alpha	Human	(5*E*,9*E*,11*E*)-14,16-dihydroxy-3,4,7,8-tetrahydro-1H-2-benzoxacyclotetradecine-1,11(12H)-dione 11-[o-(2-oxo-2-piperidin-1-ylethyl)oxime]	1.75	3INX	[96]	2010
NTD Hsp90 Alpha	Human	(5E,9E,11E)-13-chloro-14,16-dihydroxy-3,4,7,8-tetrahydro-1H-2-benzoxacyclotetradecine-1,11(12H)-dione 11-[o-(2-oxo-2-piperidin-1-ylethyl)oxime]	1.95	3INW	[96]	2010
NTD Hsp90 Alpha	Human	ADP	1.95	2XK2	[91–93]	2010
NTD Hsp90 Alpha	Human	2-*tert*-Butyl-4-(1,3-dihydro-2H-isoindol-2-ylcarbonyl)phenol	2.80	2XHX	[91–93]	2010
NTD Hsp90 Alpha	Human	(3-*tert*-Butyl-4-hydroxyphenyl)morpholin-4-yl-methanone	2.27	2XHT	[91–93]	2010
NTD Hsp90 Alpha	Human	4-Chloro-6-[2,4-dichloro-5-(2-morpholin-4-ylethoxy)phenyl] pyrimidin-2-amine	2.20	2XHR	[91–93]	2010
NTD Hsp90 Alpha	Human	4-Chloro-6-(2-methoxyphenyl)pyrimidin-2-amine	2.42	2XDX	[91–93]	2010

NTD Hsp90 Alpha	Human	1-Chloro-4-methylphthalazine Pyrimidin-2-amine	1.74	2XDU	[91–93]	2010
NTD Hsp90 Alpha	Human	1-Chloro-4-methylphthalazine	1.97	2XDS	[91–93]	2010
NTD Hsp90 Alpha	Human	2-Methyl-4-diethylamide-phenol	1.98	2XDL	[91–93]	2010
NTD Hsp90 Alpha	Human	2-Amino-4-pyridyl-pyrimidine	1.97	2XDK	[91–93]	2010
NTD Hsp90	*Trypanasoma brucei*	4-[6,6-Dimethyl-4-oxo-3-(trifluoromethyl)-4,5,6,7-tetrahydro-1H-indazol-1-yl]-2-[(*cis*-4-hydroxycyclohexyl)amino] benzamide	2.60	3OPD		2010
NTD Hsp90	*Trypanasoma brucei*	2-Amino-4-(2,4-dichloro-5-[2-(diethylamino)ethoxy]phenyl}-*n*-ethylthieno[2,3-d]pyrimidine-6-carboxamide	2.15	3OMU		2010

middle and C-terminal domains was also reported at the same time as the structure for full-length Grp94 [75]. The structures of full-length Hsp90, Grp94 and HtpG are discussed in the next two sections.

3.1.3 Structures of Full-Length Hsp90 and Its Homologues

The first structure of a full-length construct of Hsp90 was published in 2006 by the Pearl group [71]. In order to crystallise the inherently highly dynamic chaperone, they engineered yeast Hsp90 such that it lacked the highly charged linker region between the N-terminal and middle domains and contained the Ala107Asn mutation known to increase the ATPase activity by increasing N-terminal dimerisation. Using this construct, in the presence of the non-hydrolysable ATP analogue AMP–PNP and a domain of yeast p23 (sba1) which binds and stabilises the ATP-bound state, crystals were obtained which diffracted well. Thus, they were able to trap Hsp90 in a closed state in which the N-terminal domains were dimerised (Fig. 3). The structure showed extensive interactions both between the domains within each monomer and also between the two monomers (Fig. 3a). Of particular note are the facts that the NTD connects to the middle domain through a β-strand (from the middle domain) which forms part of the anti-parallel β-sheet in the NTD, and an extended loop from the middle domain interacts with an α-helix at the start of the CTD. The amphipathic loop observed in the structure of the isolated middle domain points towards the inner face of the dimeric structure, and there is a helical segment in the CTD which also points towards the N-termini of the protein and is involved in some monomer:monomer interactions (this segment was observed in the structure of the isolated CTD of HtpG but adopts a different orientation [59]). In addition to this structure, the structure of a construct consisting of only the middle and C-terminal domains was also solved, allowing comparison of the two and thus some of the changes on ATP binding to be inferred. The CTD dimerisation interface is effectively the same in both structures; however, there are changes in the middle domain:CTD interface and the relative positions of the two middle domains – they are considerably closer in the AMP–PNP/p23-bound structure of the full-length protein, the consequence of this being that there is little room for a client protein in the region between the two middle domains (Fig. 3a). The structure of the full-length protein showed extensive interactions between the two NTDs and significant differences in structure between each NTD and that observed in the isolated domain (Figs. 2a and 3b–d). In particular, the N-terminal β-strands undergo domain swapping and form interactions with the NTD of the other chain (Fig. 3b). This is accompanied with a movement of α-helix 1 and a large movement in the ATP-binding lid region which moves around a hinge created by two critical glycine residues to fold over the nucleotide-binding pocket (Fig. 3c). This conformational change exposes a hydrophobic patch on the lid, creating an interface for N-terminal domain dimerisation (Fig. 3d). The structure elegantly explained the effects of a number of temperature-sensitive mutants which had been shown to have increased or decreased ATPase activity [41, 97]. The γ-phosphate of AMP–PNP was shown

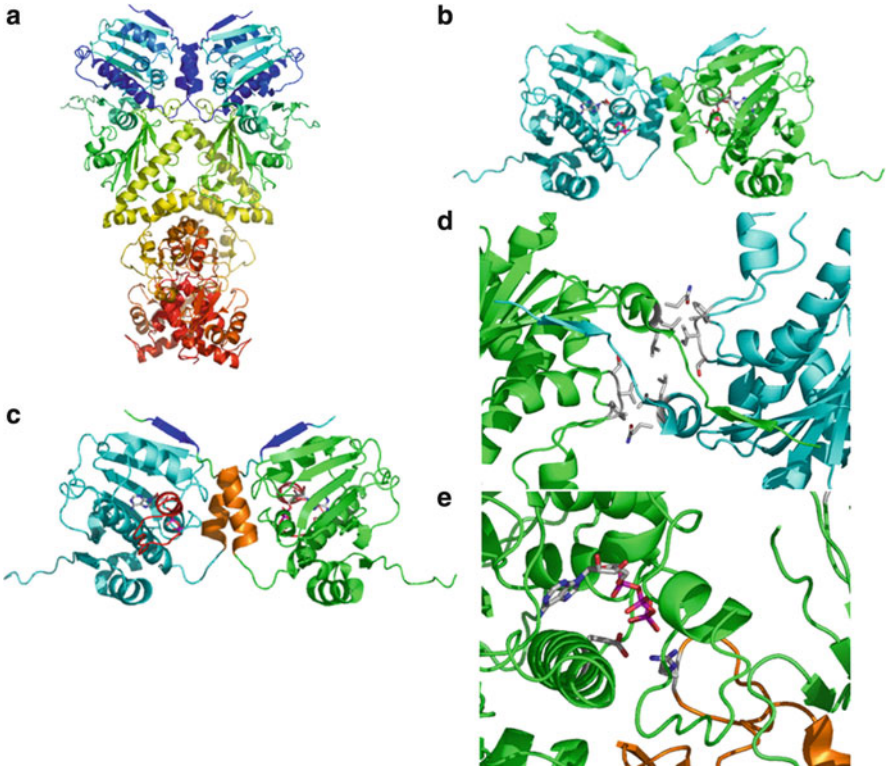

Fig. 3 Crystal structure of full-length yeast Hsp90 complexed with p23 and AMP–PNP. (**a**) The crystal structure of full-length yeast Hsp90 complexed with p23 (sba1) and AMP–PNP (pdb code: 2cg9). Shown are the ribbons for the two chains of the yeast Hsp90 homodimer coloured from N-terminus (*dark blue*) to the C-terminus (*red*). The NTD is coloured *dark blue/light blue*, the middle domain is coloured *green/yellow/light orange* and the CTD is coloured *dark orange/red*. (**b**). The dimerised NTDs of the full-length yeast Hsp90 complexed with p23 and AMP–PNP (structure shown in (*a*)). The two NTDs are coloured *green* and *light blue* and the AMP–PMP in each subunit is shown as a stick model. The domain swapping of β-strand1 from each subunit is shown. (**c**) The dimerised NTDs of the full-length yeast Hsp90 complexed with p23 and AMP–PNP [structure shown in (*a*)]. The two NTDs are coloured *green* and *light blue* and the AMP–PMP in each subunit is shown as stick models. β-Strand1 is coloured *dark blue*, α-helix1 is coloured *orange* and the ATP lid is coloured *red*. (**d**) Detail of the dimerisation interface of the two NTDs from the structure of the full-length yeast Hsp90 complexed with p23 and AMP–PNP [structure shown in (*a*)]. The two NTDs are coloured *green* and *light blue* and the side chains of residues Leu15, Gln14, Leu18, Thr95, Ile96, Ala97 and Phe 120 are shown as stick models. (**e**) Detail of the ATP-binding site from the structure of the full-length yeast Hsp90 complexed with p23 and AMP–PNP [structure shown in (*a*)]. Only one chain of the homodimer is shown. The NTD is coloured *green* and the middle domain is shown in *orange*. AMP–PNP binding to the ATP-binding site is shown as a stick model and the side chains of Glu33, a catalytic residue in the NTD, and Arg380, the catalytic arginine from the middle domain, are shown as stick models

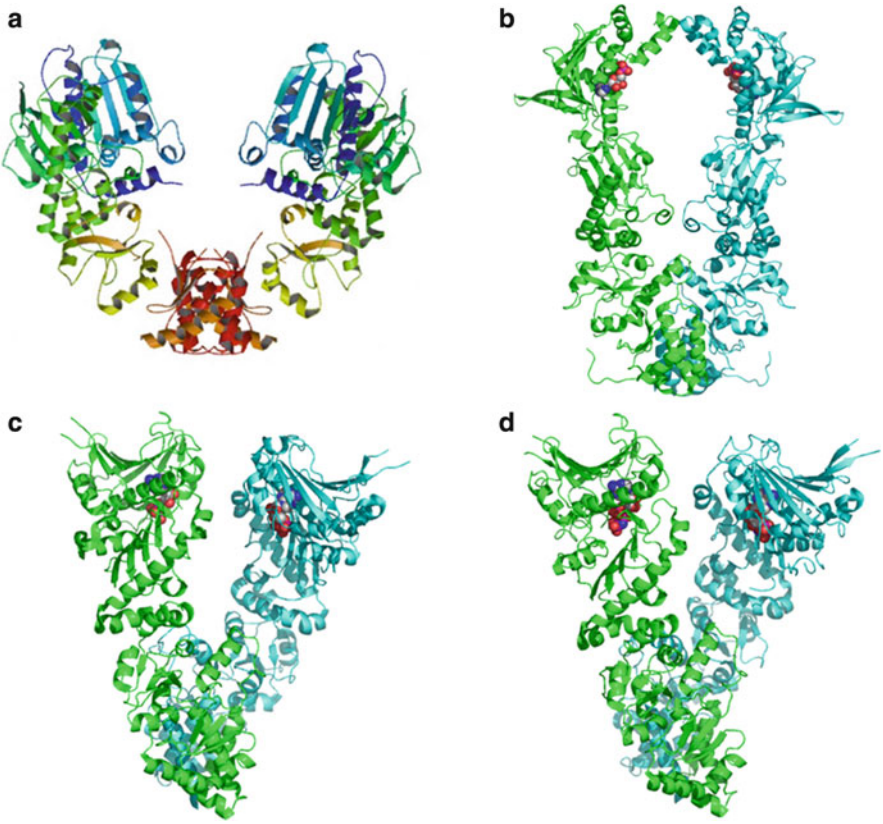

Fig. 4 Structures of full-length constructs of *E. coli* HtpG and dog Grp94. (**a**) Crystal structure of apo HtpG (pdb code: 2IOQ). The two chains in the homodimer are coloured *green* and *light blue*. (**b**) Crystal structure of HtpG complexed with ADP (pdb code: 2IOP). The two chains in the homodimer are coloured *green* and *light blue*. ADP is shown as a stick model. (**c**) Crystal structure of dog Grp94 in complex with ADP (pdb code: 2O1V). The two chains in the homodimer are coloured *green* and *light blue*. ADP is shown as a stick model. (**d**) Crystal structure of dog Grp94 in complex with AMP–PNP (pdb code: 2O1U). The two chains in the homodimer are coloured *green* and *light blue*. AMP–PNP is shown as a stick model

to interact with the catalytic arginine in the middle domain, confirming the role of this critical residue (Fig. 3e).

In contrast to the relatively compact structure of yeast Hsp90 complexed with AMP–PNP and p23, the crystal structure of the apo form of full-length HtpG is much more open, adopting a V-like conformation (Fig. 4a) [73]. Overall, the structures of each of the three domains are very similar in this structure to those observed for the isolated domains and in the structure of full-length yHsp90; however, some differences were observed – particularly in the NTD (which were attributed to nucleotide binding) and in the helical segment that protrudes out from the CTD [73]. In the structure of apo HtpG, this region is disordered but is predicted

to point towards the central cleft in the middle of the dimer where client proteins may bind. In all three domains there are hydrophobic patches which are exposed in apo HtpG, suggesting potential binding sites for client proteins. It was proposed that apo HtpG is the state with which clients initially interact and it is flexible in order to accommodate a range of different client proteins [73]. Extensive domain:domain interactions between the N-terminal and middle domains were observed, whilst in contrast the interactions between the middle and C-terminal domains were much less [73]. These observations were used to propose that in HtpG most of the conformational flexibility observed in the EM and SAXS studies (see later sections) are due to movements of the middle domain relative to the CTD.

The ATP lid in HtpG comprises a helix–loop–helix motif similar to that in the eukaryotic Hsp90s; however, it is longer and shifted in position. In the apo state, the lid is positioned in such a way as to block nucleotide binding (an autoinhibitory mechanism that has also been observed in yeast Hsp90 [70]), and the structures solved in this study suggest that there must be a structural rearrangement of the NTD relative to the middle domain in order to allow the closure of the lid after nucleotide binds [73]. A crystal structure of the HtpG–ADP complex (Fig. 4b) revealed a conformation different to that observed for AMP–PNP [73]. However, as this complex crystallised as a dimer of dimers and the structure was dissimilar to that observed for the complex in EM, it remains a little uncertain as to whether the somewhat unusual conformation observed is due to crystallisation artefacts.

Shortly after the structure of full-length HtpG was reported, the crystal structures of two full-length Grp94-nucleotide complexes were solved [75]. ADP and AMP–PNP complexes of an engineered form of canine Grp94 (where the charged linker region was replaced with a GGGG sequence and an N-terminal region preceding the NTD was deleted) showed open structures where the dimer formed a twisted V conformation (Fig. 4c, d). The conformations that were observed were distinct from those observed for either yeast Hsp90 (Fig. 3a) or HtpG (Fig. 4a, b) and represent Grp94 in a catalytically incompetent state despite the bound AMP–PNP. Essentially, no differences were observed in the structures with either AMP–PNP or ADP bound, confirming earlier studies which showed that Grp94 doesn't discriminate greatly in its binding of nucleotides in contrast to other Hsp90s. Despite the open conformation observed for the Grp94:AMP–PNP complex, this study established that Grp94 does have ATPase activity. Based on the structures, the authors note that the existence of an open AMP–PNP-bound conformation suggests that ATP binding alone does not drive the chaperone into a catalytically active N-terminally dimerised state, something which has recently been established in kinetic experiments where it has been shown that nucleotide binding is only weakly coupled to conformational change for yeast Hsp90 [98]. These Grp94 structures also suggest a "primed" state in which the client protein binds initially to an open ATP-bound state prior to large scale conformational changes and ATP turnover, which are known to occur and be necessary for client protein maturation in the cytosolic Hsp90s. The Grp94–ADP structure differs from that of the HtpG–ADP complex solved using X-ray crystallography, but is not that dissimilar to the EM structures of the HtpG–ADP complex.

3.1.4 Structures of Cochaperones and Their Complexes with Hsp90

Despite the increasing number of high-resolution structures of full-length Hsp90s, there remains only one Hsp90–cochaperone complex for which there is a crystal structure of the cochaperone with the full-length protein. This is the yeast Hsp90–p23-AMP–PNP complex described above [71] in which two p23 molecules bind into broad grooves formed at the interface of the two NTDs of Hsp90 (Fig. 5a, b). The binding interface requires that the ATP lid has closed and the two NTDs dimerised which occurs only on ATP or AMP–PNP binding, consistent with the fact that the binding of p23 is ATP dependent for yeast Hsp90 (Fig. 5a, b). There are three main sites of interaction which in the NTDs include α-helix1 and a β-hairpin from one NTD and the ATP lid from the other NTD (Fig. 5a, b). Although the structure of the complex doesn't directly reveal how p23 inhibits the ATPase activity of Hsp90, it seems likely that it does so by stabilising the closed NTD-dimerised state, thereby preventing release of ADP and phosphate.

There are a number of complexes of domains of cochaperones with their Hsp90-binding domains (Table 3) and these have been very informative in terms of precisely defining how these cochaperones recognise and bind to Hsp90, and also how these cochaperones exert their effects, e.g. on the ATPase activity of Hsp90 (Table 2). The first of these structures was the N-terminal domain of Aha1 which was crystallised in complex with the middle domain of yeast Hsp90 [99, 100] (Fig. 5c). The NTD of Aha1 forms an elongated cylindrical structure in which an N-terminal and a C-terminal α-helix pack onto an anti-parallel β-sheet (Fig. 5c). The structure is similar to two other structures in the protein databank of a putative Aha1 from *Plasmodium falciparum* (Table 4). The structure of the NTD–yAha1–MD–yeast Hsp90 complex reveals how Aha1 binds to the middle domain: in addition to hydrophobic patches there are extensive polar interactions between the two molecules including hydrogen bonds and ion pairs (Fig. 5c), providing a structural basis for earlier observations that the binding of Aha1 to Hsp90 is sensitive to salt [101]. Most importantly, a comparison of the structures of the isolated middle domain of Hsp90 with that observed in complex with Aha1 provided a likely mechanism for the activation of the ATPase activity by Aha1. In the isolated middle domain there is a short helix (residues 372–386 in yeast Hsp90) which connects to a long helix (starting at residue 389) and in so doing maintains the catalytic loop containing Arg380 in a retracted conformation. Structural changes on Aha1 binding result in the long helix extending a few residues, thereby destabilising the short helix and releasing the catalytic loop (which can then interact with the ATP bound in the NTD of Hsp90).

Cdc37 is a kinase-specific cochaperone which has two structural domains – the NTD is known to bind the kinase client whilst the CTD binds to the NTD of Hsp90. A crystal structure of the core complex, i.e. the CTD of human Cdc37 and the NTD of yeast Hsp90, revealed an unusual structure for the cochaperone and how it binds and inactivates the ATPase activity of Hsp90 [102]. The CTD of Cdc37 comprises a six-helix bundle which connects to a smaller three-helix bundle via a long α-helix

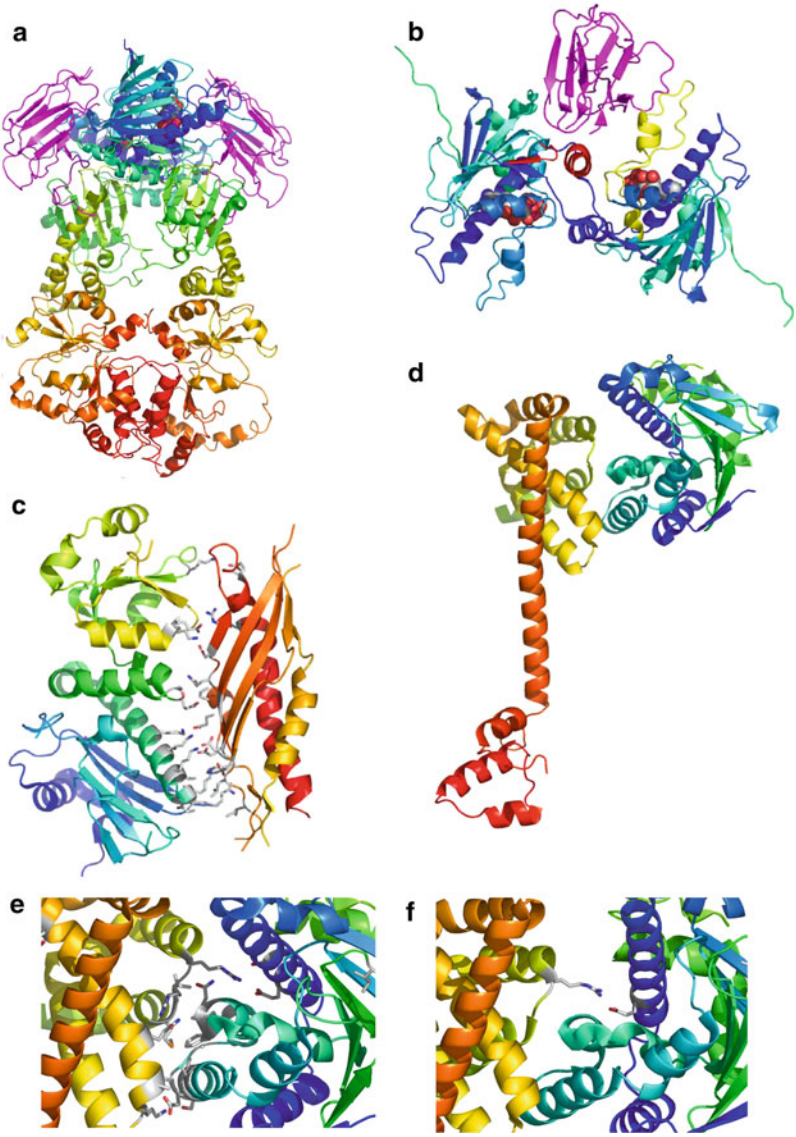

Fig. 5 Structure of Hsp90–cochaperone complexes. (**a**) Crystal structure of p23 (sba1) bound to the full-length yeast Hsp90–AMP–PNP complex (pdb code: 2CG9). The two chains of the Hsp90 dimer are coloured as follows: NTD (*dark blue* to *light blue*), the middle domain (*yellow*/*green* to *light orange*) and the CTD (*orange-red*). The two p23 molecules are coloured magenta and the AMP–PNP is coloured for each element and is shown in a space filling model. (**b**) The two N-terminal domains of Hsp90 shown coloured from N- to C-termini (*dark blue* to *turquoise*) complexed with one p23 shown in *magenta* (the other p23 which binds to the *bottom face* of the two NTDs is not shown for clarity) using the crystal structure of p23 (sba1) bound to the full-length yeast Hsp90–AMP–PNP complex (pdb code: 2CG9). The main interaction sites between p23 and the NTDs of Hsp90 are shown: in *red* is the first α-helix and a β-hairpin of one NTD, in *yellow* is

Table 2 Summary of the X-ray crystal structures of full-length Hsp90

Construct	Organism	Nucleotide	Resolution	Pdb code	Reference	Release year
Hsp90–Sba1 complex	*S. cerevisiae*	ATP	3.10	2CG9	[71]	2006
Hsp90 engineered lacking charged linker region						
Full-length HtpG	*E. coli*	Free	3.50	2IOQ	[73]	2006
Full-length HtpG4	*E. coli*	ADP	3.55	2IOP	[73]	2006
Full-length Grp94 287–327 GGGG	Dog	ADP	2.45	2O1V	[75]	2007
Full-length Grp94 287–327 GGGG	Dog	AMP–PNP	2.40	2O1U	[75]	2007

(Fig. 5d). The main interaction sites are located within the larger six-helix bundle domain which interacts with regions of the NTD of Hsp90 that are involved in the ATP-dependent dimerisation of the NTDs including the ATP lid (in which there are some conformational changes), as well as regions in the NTD which interact with the middle domain on dimerisation (Fig. 5e). Many of the interactions in the interface are hydrophobic in nature although there are a few key polar interactions (Fig. 5e). Cdc37 inhibits the ATPase activity in a number of different ways: (1) it inserts an arginine side chain into the ATP-binding pocket which interacts with the catalytic side chain of Glu33 (it doesn't prevent ATP or inhibitor binding but neutralises the otherwise nucleophilic Glu) (Fig. 5f), (2) it binds to the ATP lid preventing closure of the lid over the ATP-binding pocket and blocks access of critical residues in the middle domain to the active site, and (3) it binds and sits between the two NTDs, thereby holding them apart and preventing dimerisation (Fig. 5f).

A later study of the complex of the C-terminal region of human Cdc37 with the N-terminal domain of human Hsp90, which used the crystal structures of isolated domains and results of heteronuclear solution state NMR and docking algorithms to model the structure of the complex, generated a very similar conformation to that

Fig. 5 (continued) the ATP lid region from the other NTD. AMP–PNP is coloured according to element and is shown in a space filling model. (**c**) Crystal structure of the complex between the N-terminal domain of yAha1 and the middle domain of Hsp90 (pdb code: 1USU). The Hsp90 chain is shown on the *left* and it is coloured from N-terminus to C-terminus from *purple* to *yellow*, the Aha1 chain is on the *right* and is coloured from N-terminus to C-terminus from *yellow* to *red*. The side chains of the residues involved in forming the binding interface are shown as stick models. (**d**) Crystal structure of the CTD of human Cdc37 coloured from N-terminus (*green*/*yellow*) to C-terminus (*red*) complexed to the NTD of yeast Hsp90 coloured from N-terminus (*dark blue*) to C-terminus (*green*) (pdb code: 1US7). (**e**) Detail of the interface between the CTD of Cdc37 and the NTD of Hsp90 shown in (*d*). The side chains of the residues involved in the interaction are shown as stick models. (**f**) Detail of the interface between the CTD of Cdc37 and the NTD of Hsp90 shown in (*d*) illustrating how Arg167 from Cdc37 inserts and hydrogen bonds to the catalytic Glu33 in the active site in the NTD of Hsp90. Arg167 and Glu33 side chains are shown as stick models

Table 3 Summary of the crystal structures of the complexes formed between Hsp90 and cochaperones

Construct	Organism	Cochaperone	Resolution	Pdb code	Reference	Release year
Middle domain Hsp90	*S. cerevisiae*	NTD Aha1 (*S. cerevisiae*)	2.15	1USU	[99, 100]	2004
Middle domain Hsp90	*S. cerevisiae*	NTD Aha1 (*S. cerevisiae*)	2.70	1USV	[99, 100]	2004
NTD Hsp90	*S. cerevisiae*	C-domain of Cdc37 (human)	2.30	1US7	[102]	2004
NTD Hsp90-ADP	*Hordeum vulgare*	CS domain SGT1 (*Arabidopsis thaliana*)	3.30	2JKI	[81, 82]	2008
NTD Hsp90 Alpha	Human	Cdc37 148–276	NMR modelling	2K5B	[103]	2008
NTD Hsp90–ADP	*Hordeum vulgare*	CS domain SGT1 (*Arabidopsis thaliana*) CHORD 2 domain (RAR1) (*Arabidopsis thaliana*)	2.20	2XCM	[104]	2010

already observed in the crystal structure [103]. However, a few key features were different and are worthy of mention. First, the Cdc37 was found to be monomeric in this study as opposed to the dimer observed in the crystalline state. Second, the structure was found to be more compact, and third, a significantly greater area was found to be buried in the interface, suggesting a tighter complex was formed [103].

In plants, Hsp90 plays an important role in the function of the NLR receptor and innate immunity, an activity which requires two cochaperones – SGT1 and a CHORD-containing protein such as Rar1 [111]. Although SGT1 contains a TPR domain, it interacts with Hsp90 through its CS domain which, despite some similarity in structure to p23, binds at a different site in the NTD domain [81, 82]. The crystal structure of the complex between the NTD of barley Hsp90 (HvHsp90) and the CS domain of SGT1 from *Arabidobsis thaliana* has been solved in the presence of ADP (Fig. 6a, b). It clearly shows how the CS domain binds the NTD of Hsp90 away from the ATP lid region [81, 82]. The structure of the ternary complex formed between the NTD of HvHsp90, the CS domain from AtSGT1 and the $CHORD_{II}$ domain from AtRar1 has also been solved [104]. The CHORD domain comprises two structural lobes – the C-terminal region includes a three-stranded anti-parallel β-sheet with a short α-helix, whilst the N-terminal region is largely unstructured but does contain one β-strand which packs against the β-sheet, and there are two bound Zn^{2+} ions which help maintain structural stability (Fig. 6c). The ternary complex that is formed adopts a puckered ring structure with the three domains repeated in an a, b, c, a, b, c arrangement such that each protein domain only contacts one copy of the other domains

Table 4 Summary of the structures of cochaperones

Construct	Organism	Ligand	Resolution	Pdb code	Reference	Release year
TPR2A domain of Hop	Human	MEEVD peptide	1.90	1ELR	[105]	2000
SGT1 CS domain	Human		NMR	1RL1	[106]	2004
CTD FKBP52	Human	MEEVD	3.00	1QZZ	[107]	2004
CHIP U-BOX E3 ubiquitin ligase	Mouse	DTSRMEEVD	3.30	2C2L	[108]	2005
FKBP35 TPR domain	*Plasmodium falciparum*	MEEVD	1.63	2FBN	[109]	2006
PP5 TPR domain	Human	MEEVD	NMR	2BUG	[110]	2006
Cdc37 148–276	Human		1.88	2W0G	[103]	2008
Hop TPR2A	Human	GASSGPTIEEVD (C-terminus Hsc70)	2.05	3ESK		2009
Aha1 (putative) PFC0270W	*Plasmodium falciparum*		1.77	3N72		2010
Aha1 (putative) PFC0360W	*Plasmodium falciparum*		2.50	3NI8		2010

(Fig. 6d). The interface between the NTD of Hsp90 and the CS domain of SGT1 is essentially the same as in the binary complex, whilst the opposite face of the CS domain binds to the $CHORD_{II}$ domain. The interface centres on a hydrophobic patch which is surrounded by polar and solvent-bridged interactions. The $CHORD_{II}$ domain interacts with the NTD of Hsp90 through its C-terminal lobe which is at the opposite end of the CS-binding site. Both hydrophobic, polar and solvent mediated interactions are important. In addition to the main binding site, the $CHORD_{II}$ domain also interacts directly with the Mg–ADP bound in the NTD of Hsp90 (Fig. 6e). In this case, the side chain of His188 hydrogen bonds to the β phosphate of ADP, whilst the side chain of Asp189 interacts with two water molecules bound to the Mg^{2+} ion.

3.2 Solution-State Nuclear Magnetic Resonance Studies on Hsp90 Structure

Hsp90 is a challenging protein for NMR studies due to both its size (the dimer is 170 kDa) and its highly dynamic nature. Despite this, recent technological advances

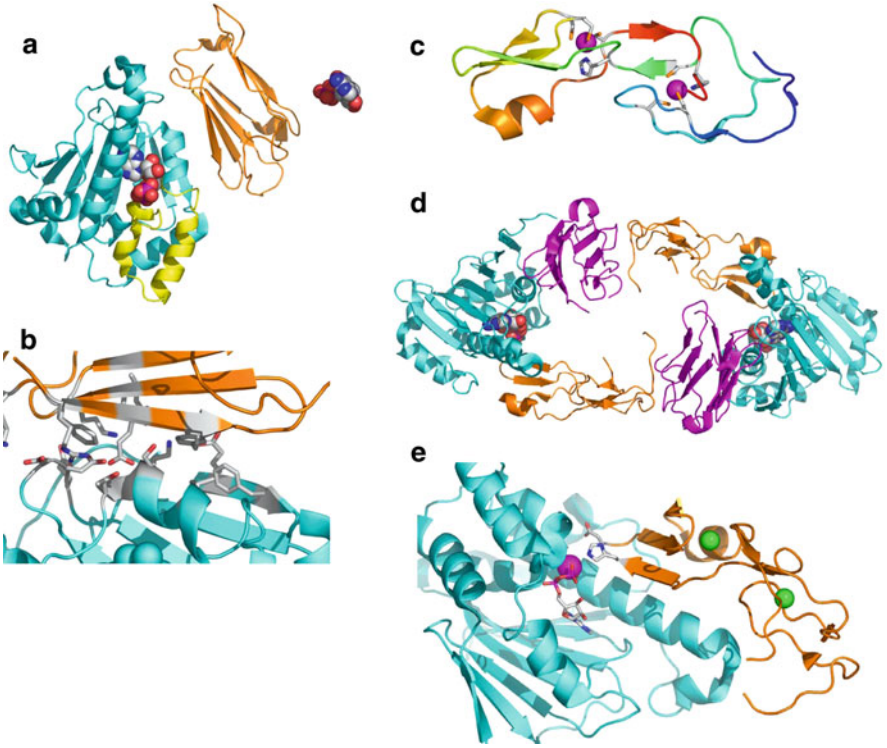

Fig. 6 Structure of Hsp90–cochaperone complexes: Hsp90–Sgt1–Rar1. (**a**) Structure of the NTD of HvHsp90 from barley complexed with the CS domain of SGT1 from *Arabidobsis thaliana* (pdb code: 2JKI). The NTD of Hsp90 is shown in *cyan* with the ATP lid highlighted in *yellow*, the CS domain of SGT1 is shown in *orange*. The ADP is shown as a space-filling model. (**b**) Detail of the structure of the interface between the NTD of Hsp90 and the CS domain of SGT1 shown in (*g*) (pdb code: 2JKI). The NTD of Hsp90 is shown in *cyan* and the CS domain of SGT1 is shown in *orange*. The side chains of the residues which line the interface are shown as stick models. (**c**) Structure of the $CHORD_{II}$ domain from Rar1 (pdb code: 2XCM). The chain is coloured from N-terminus (*dark blue*) to C-terminus (*red*), the Zn^{2+} ions are shown as magenta spheres, and the side chains that act as ligands of the zinc ions are shown as stick models. (**d**) Structure of the ternary complex formed between the NTD of HvHsp90, the CS domain of AtSGT1 and the $CHORD_{II}$ domain of AtRar1 (pdb code: 2XCM). The two NTDs of Hsp90 are coloured *cyan*, the CS domains are coloured *magenta* and the two CHORD domains are coloured *orange*. ADP bound in the NTD of Hsp90 is shown in space filling mode. (**e**) Structure of the complex formed between the NTD of HvHsp90 and the $CHORD_{II}$ domain of AtRar1 (pdb code: 2XCM). The NTD of Hsp90 is coloured *cyan*, and the $CHORD_{II}$ domain is coloured *orange*. ADP bound in the NTD of Hsp90 is shown in space filling mode. Mg^{2+} is shown as a *magenta sphere*, Zn^{2+} is shown as *green spheres*. The side chains of His188 and Asp189 in the $CHORD_{II}$ domain which interact with the Mg–ADP in the active site of Hsp90 are shown as stick models

in NMR spectroscopy have meant that high-resolution NMR studies have become feasible. In particular, the use of TROSY and CRINEPT methods has overcome the problems associated with size, perdeuteration of Hsp90 has reduced relaxation processes and increased sensitivity, and selective labelling techniques in

conjunction with protein engineering methods have solved some of the problems associated with spectral complexity and made assignment possible [112, 113]. In the past five years this has resulted in a number of NMR studies of both Hsp90, and its complexes with cochaperones and some substrate or client proteins, being published [112, 113].

The first NMR studies were on the three isolated domains – N-terminal domain [114–116], middle domain [117] and C-terminal domain [118]. In each case the $^{1}H–^{15}N$ spectra were fully or partially assigned. Selective isotope labelling with ^{13}C-labelled Ile, Leu and Val was used to simplify and then assign the $^{1}H–^{13}C$ spectrum of both full-length Hsp90β and α [119–122]. Comparison with the $^{1}H–^{13}C$ spectra of the isolated domains enabled resonances in the spectrum of the full-length spectrum to be assigned.

In addition to the studies of Hsp90 alone, NMR has also been used to study the complexes formed between Hsp90 and its cochaperones. HDX (hydrogen–deuterium exchange) methods have been used with ^{15}N-labelled Aha1 and the middle domain of Hsp90 to map the binding site [123]. The NMR results were consistent with previous crystal structures; however, the data also pointed towards a potential second binding site on the opposite side of Aha1 to that already known. Other studies have combined NMR with FRET (Förster Resonance Energy Transfer) to probe the interaction between full-length Hsp90 and Aha1 [124]. In this case, not only was the N-terminal domain of Aha1 shown to interact with Hsp90 but it was also demonstrated that the C-terminal domain of Aha1 is also involved [124]. These studies also identified a large hydrophobic groove on the surface of Hsp90 consistent with the crystal structure. NMR studies on the Hsp90–Cdc37 complex have already been described above [103]. Using ^{13}C-labelled Ile, the complex formed between Hsp90 and p23 has also been studied in solution using NMR. Here, the complex was shown to form by measuring the translational diffusion coefficient with DOSY-TROSY experiments [112, 113]. Analysis of the chemical shifts in Hsp90 on p23 binding showed that the primary binding site is the N-terminal domain of Hsp90 in agreement with the earlier crystal structure; however, the NMR also revealed that there are chemical shift changes in the middle domain which are attributed to long-range conformational changes in this domain on p23 binding to the NTD [119]. In addition, a subset of Hsp90 peaks was observed to undergo doubling on p23 binding, suggesting that an asymmetric complex of Hsp90–p23 may be formed in contrast to that observed in the crystal structure [119].

There is an excellent review of the NMR studies of Hsp90 by Rudiger and co-workers in the recent Special Issue on Hsp90 in *Biochimica & Biophysica Acta* [112, 113].

3.3 Other Structural Studies on Hsp90

The crystal structures of full-length homologues of Hsp90 have revealed that, whereas they all have identical domain architectures, they differ in their overall

conformation and the position of the three structural domains relative to each other. In order to understand further the conformations that the Hsp90 dimer adopts in solution, small-angle X-ray scattering (SAXS) and cryo-EM (electron microscopy) studies have been undertaken to try to establish the structure of the protein in solution in both apo and nucleotide-bound states.

3.3.1 Electron Microscopy Studies of Hsp90 Complexes

Although the dimer of Hsp90 is really too small for electron microscopy techniques to provide structural information, EM has been used very successfully on a number of Hsp90–cochaperone and client complexes. One of the most impressive studies to date, and a real tour-de-force, is the EM study of the complex formed between Hsp90–Cdc37 and the client kinase cdk4 [125]. Vaughan and co-workers used a baculovirus expression system to coexpress and purify an affinity tagged Hsp90–Cdc37–cdk4 complex, and used negative stain and single particle analysis and reconstruction to determine the structure of the complex (Fig. 7a). In this study, native state mass spectrometry established the stoichiometry of the complex to be an Hsp90 dimer bound to a single Cdc37 and one cdk4 molecule. This was in contrast with previous studies which had observed both $(Hsp90)_2(Cdc37)_2$ and $(Cdc37)_2$(cdk4) complexes, suggesting that, whilst cdk4 binds initially to the dimer of Cdc37, one Cdc37 dissociates from the complex on binding Hsp90 [125]. Two lobes of density were observed which were associated with cdk4 in the complex, suggesting that it binds in an extended conformation – one structural lobe interacting with the middle domain (close to a previously proposed client protein binding site – which would be Trp300 in yeast Hsp90) whilst the other lobe interacts with the NTD of Hsp90 and/or possibly the N-terminal region of Cdc37 [125]. The simultaneous binding of cdk4 to both middle and N-terminal domains of Hsp90 suggests a mechanism by which ATP binding or hydrolysis in the NTD may be coupled to conformational changes in the bound client, thus activating it [125].

More recently, cryo-EM single-particle reconstruction has been used to study the apo and nucleotide-bound forms of the three main Hsp90s studied – HtpG, yeast and human Hsp90 [126] (Fig. 7b, c). This study revealed three distinct conformational states for the apo, ATP and ADP-bound forms existing in equilibrium with each other and that the occupancy of the different states varies significantly between species. Importantly, for human Hsp90 the binding of nucleotide did not substantially shift the conformational equilibrium, the protein remaining in a dominantly extended conformation, in contrast to the results obtained for yeast Hsp90 and HtpG. Cross-linking experiments verified that all three Hsp90s can adopt both a closed ATP-bound and a compact ADP-bound state, but that these states were not necessarily the dominant species in solution in the absence of cross-linking [126].

Most recently, a 15-Å resolution cryo-EM structure of a human Hsp90–Hop complex was published, stable complexes being formed by engineering intermolecular disulphide bridges between Hsp90 and Hop and through the use of mild

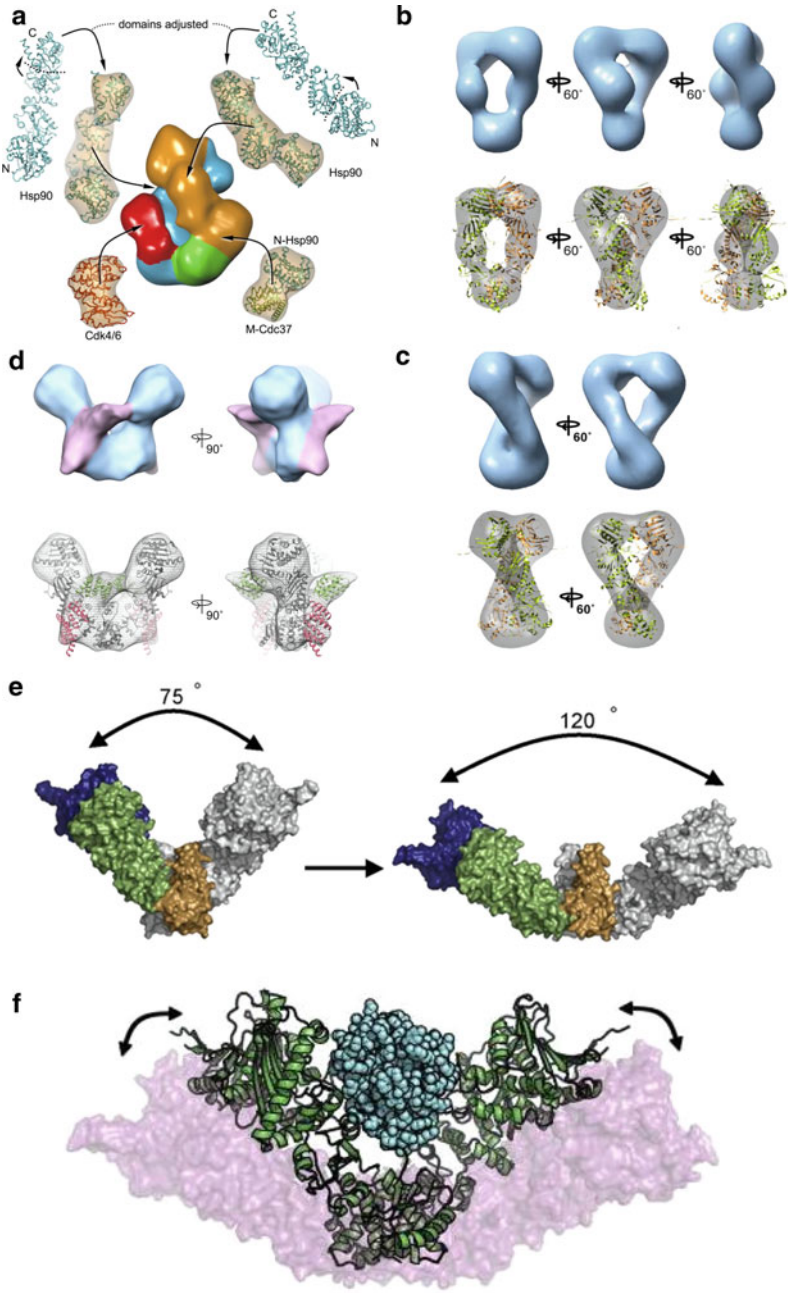

Fig. 7 Structures of Hsp90s from electron microscopy and small-angle X-ray scattering studies. (**a**) Structure of the Hsp90–Cdc37–cdk4 complex from EM studies. The two subunits of Hsp90 are shown in *light blue* and *gold*, the middle domain of Cdc37 is shown in green and the client cdk4 is shown in *red*. Adapted from [125]. (**b**) The *top panel* shows the density from an EM study of the

cross-linking conditions (Fig. 7d) [127]. A 2:2 complex is formed comprising the Hsp90 dimer and two molecules of Hop which do not interact with each other. Comparison of the structure with the different structures solved using X-ray diffraction, EM and SAXS revealed several important features of the complex. Hop induces conformational changes in Hsp90 relative to the apo state such that the angle between the middle domain and CTD is small, the NTD being rotated some 90° relative to the MD in the apo state, such that it the NTD:MD interface is similar to that observed in the closed ATP-bound state. Although this state has not undergone NTD dimerisation it appears primed for both ATP binding (as the nucleotide binding site is accessible in this form with high k_{on} and k_{off} values) and ATP hydrolysis. In the Hsp90–Hop complex, many hydrophobic patches are exposed and line the interdimer cleft likely forming the client protein binding sites. The primary binding site (and potentially the location of the C-terminal MEEVD motif of Hsp90) is thought to be near the MD:CTD interface. The structure reveals how Hop acts as an inhibitor of ATP hydrolysis, as it prevents the full rotation of the MD relative to the CTD needed for NTD dimerisation; TPR1 of Hop also sterically blocks dimerisation, it being positioned between the two Hsp90 monomers. Although the EM structure is of a 2:2 Hsp90:Hop complex, SEC-MALS experiments show that it is likely that the ternary $(Hsp90)_2$:Hop complex is the primary species in solution and a single Hsp70 is shown to bind to either the tetrameric or trimeric Hsp90:Hop complex.

3.3.2 Small-Angle X-Ray Scattering Studies

Early small-angle X-ray scattering (SAXS) studies on human Hsp90 and its complex with the cochaperone Cdc37 established the potential of the technique in studying the solution structure of both Hsp90 and its complexes [131]. Although shape reconstruction was not reported at the time (shape reconstruction from the SAXS data was undertaken but it was not possible to obtain a single converged structure – not surprising in light of the later studies which showed the

Fig. 7 (continued) HtpG–AMP–PNP complex, whilst the *bottom image* shows how this is similar to the crystal structure of yeast Hsp90 in complex with AMP–PNP and p23. Adapted from [126]. (**c**) The *top panel* shows the density from an EM study of the yeast Hsp90.AMP–PNP complex and the *lower panel* shows the crystal structure of yeast Hsp90–AMP–PNP–p23 complex (only the Hsp90 is shown) modelled into this density. Adapted from [126]. (**d**) EM structure of Hsp90–Hop complex. In the *top image*, the density from the EM studies corresponding to Hsp90 is shown in *light blue* and Hop in *pink*. In the *lower panel* the structures of Hsp90 (*grey*) and Hop (TPR1 and 2A are shown in *red* and *green*) are modelled in to the EM density. Adapted from [127]. (**e**) Structure of apo HtpG from crystal structure (*left*) and from rigid-body refinement of solution-state SAXS studies (*right*). Adapted from [128]. (**f**) Structure of the HtpG-Δ131Δ complex as determined by SAXS. The Δ131Δ is shown in *cyan*, the conformation of HtpG when bound to Δ131Δ is shown in *green*, and in shadow representation (*light red*) is the conformation of apo HtpG. It is worth noting that there is still a conformational equilibrium between the two states. Adapted from [129, 130]

conformational heterogeneity of this protein in solution), global structural parameters R_g and D_{max}, the radius of gyration and maximum diameter respectively, did provide important information on the structure of human Hsp90 in solution [131]. Binding of either a non-hydrolysable ATP analogue, AMP-PCP, or ADP, had little effect on the structural parameters, suggesting little if any conformational change, whilst in contrast binding of geldanamycin induced a compaction of the structure. At the time these results appeared to be at odds with the prevailing mechanism which had proposed that ATP binding induces a large conformational change and dimerisation of the N-terminal domains; however, it is now well established that ATP binding is only coupled weakly to conformational changes [98].

In 2008, a number of studies were published which used SAXS and cryo-EM methods to study the structure of Hsp90s in solution [132]. In the first study, the apo form of pig Hsp90 was shown to be in a conformational equilibrium between two open states different from any previously observed [133]. Analysis of the data revealed that the differences in conformation were due to large movements in the N-terminal domain and middle domains around two flexible hinge regions [133]. A SAXS study of HtpG which used more advanced molecular modelling methods revealed that there are multiple conformations of the protein which co-exist in solution and which differ from the crystal structures (Fig. 7e) [128]. The apo form adopts a more extended conformation than in the crystal, and binding of AMP–PNP results in a conformational equilibrium between this extended state and a more compact structure which resembles the closed state observed for an engineered variant of yeast Hsp90. This study highlighted the dynamic nature of HtpG and the conformational heterogeneity that exists in solution [128].

SAXS in conjunction with rigid body modelling has been used to study the nucleotide-free states of yeast and human Hsp90s, as well as mouse Grp94. All three proteins were shown to adopt an extended, chair-like conformation distinct from the extended conformation observed for HtpG. For Grp94, binding of AMP–PNP caused a small shift towards the more compact structure observed in the crystalline state; however, even here the extended state remained the dominant species. In contrast to the crystal structures of Grp94, this SAXS study provided evidence that Grp94 adopts conformational states similar to other eukaryotic Hsp90s [134, 135].

SAXS has also been used to show that the equilibrium between open and closed forms of the Hsp90 dimer can be altered by changing solution conditions including pH and osmolytes [134–136]. SAXS and EM studies on the apo form of HtpG showed that the previously established equilibrium between open and closed states (the closed state being similar to that observed in the crystal structure of full-length Grp94 in which the structure is compact but the N-terminal domains are not dimerised) can be influenced by pH. Protein engineering studies showed that this pH dependence was due to histidine residues (interestingly these histidines are not conserved and the pH dependent conformational state appears to occur only in the bacterial homologue HtpG). Aggregation assays with citrate synthase were used to demonstrate that the closed state had a higher general chaperone activity that the

open state [134, 135]. Osmolytes such as TMAO (trimethylamine N-oxide) can induce significant changes to the open/closed equilibrium favouring the more compact closed state. The effect is significant on the apo form of HtpG but there is little effect on the AMP–PMP-bound state, presumably as it already adopts a more compact structure. Similar results were obtained for the apo forms of yeast and human Hsp90 [136].

It is now clear from all the structural studies – X-ray crystallography, NMR, electron microscopy and NMR – that Hsp90 is a highly dynamic protein which can adopt a wide range of different conformations, many of which are in equilibria with each other. These conformations are influenced by a number of different factors including cochaperone binding and the nucleotide status of the binding site in the N-terminal domain. The conformational dynamics are important for the ATPase activity of Hsp90 and this is discussed in more detail in the next section.

4 ATPase Activity

4.1 Hsp90 Has ATPase Activity

Early on in the field there was some controversy over whether Hsp90 was an ATP-binding protein with ATPase activity or not, this almost certainly being exacerbated by the fact that its affinity for ATP is quite low and the intrinsic ATPase activity very low compared to many other ATPases [137–144]. However, by 1998, it had been established that the yeast and *E. coli* variants of this chaperone, like many other chaperones, did bind and hydrolyse ATP [139, 145] and that this activity was essential for the function of Hsp90 in vivo [139]. In these cases the Hsp90-specific inhibitor geldanamycin was used to demonstrate that the ATPase activity detected was from Hsp90 and not some contaminant. These studies also established that geldanamycin is a competitive inhibitor of the ATPase activity. Later, human Hsp90 was also shown to have ATPase activity although the intrinsic ATPase level is even lower than that of yeast Hsp90 [146, 147]. Inhibition of the ATPase activity of Hsp90 has been used extensively in the study of potential drugs targeting this chaperone and has been used in a number of high throughput assays [148, 149].

The N-terminal domain of Hsp90 is structurally similar to the ATP-binding domain of MutL and DNA gyrase. On the basis of this similarity a “molecular clamp” model for the ATPase activity of Hsp90 was proposed and tested [150]. In this model, the binding of ATP in the N-terminal domains drives a conformational change and dimerisation of these two domains to form a closed state which then undergoes ATP hydrolysis (Fig. 1b). In support of this model, these studies demonstrated reduced ATPase activity of a truncation mutant of yeast Hsp90 lacking the C-terminal dimerisation domain but showed that on addition of AMP–PNP some dimerisation could be detected, a result of the dimerisation of

the NTDs. In addition, a series of temperature-sensitive mutants were studied and a correlation between the ATPase activity and the extent of N-terminal dimerisation observed [150]. This model proposed that the NTD dimerisation was directly coupled to ATP binding.

Another study on the ATPase activity of yeast Hsp90 published in the same year provided more mechanistic detail and established that ATP binds in a two-step mechanism, ATP hydrolysis is rate limiting, the isolated NTD has little ATPase activity and that the C-terminal domain is essential for trapping the bound ATP such that it is committed to hydrolysis and for maximal ATP turnover rates [151]. A follow-on study by the same group used the fact that it is possible to make heterodimers of yeast Hsp90 containing one wild-type and one mutant subunit simply by mixing two different homodimers [152]. A heterodimer lacking one of the two NTDs showed low ATPase activity; however, a heterodimer with an NTD that was unable to bind ATP showed wild-type levels of activity, establishing that, although interactions between the two NTDs are necessary for activation and ATP hydrolysis, ATP does not need to be bound in both subunits [152].

A later study on human Hsp90 also undertook a detailed kinetic analysis of ATP binding and hydrolysis [153]. The results showed that there is a fast initial formation of a weak diffusion-collision complex between Hsp90 and ATP which is followed by a conformational change and then subsequent ATP hydrolysis which was shown to be the slow, likely rate-limiting step [153]. However, no cooperativity was observed either for ATP binding or hydrolysis (consistent with the study on yeast Hsp90 discussed above in which a single ATPase active subunit was needed for wild-type activity levels [152]), nor was there any protein concentration dependence for the ATPase activity of a monomeric C-terminal deletion construct, both of which are predicted from the molecular clamp model [153].

The mechanism of ATP hydrolysis by Hsp90 is now well understood, and it is known that, in addition to the ATP binding site in the N-terminal domain, an arginine residue on a "catalytic" loop located in the middle domain, also plays an essential role [58, 154].

It is now known that the "basic" mechanism of the ATPase cycle of Hsp90 is similar for Hsp90s from all cellular compartments and organisms [155]. However, it is also now established that there is relatively weak coupling between ATP binding and large scale conformational changes [98], which likely explains the differing results obtained in different studies.

4.2 Regulation of the ATPase Activity

It is now well established that the ATPase activity of Hsp90 is highly regulated by cochaperone binding, post-translational modification and even client-protein binding. The effect of a number of cochaperones on the ATPase activity has been studied in detail and, together with structural work (see earlier sections), the mechanisms by which the cochaperones up-regulate or down-regulate the activity

is clear. The effect of the cochaperone Hop (Sti1 in yeast) on ATP binding and hydrolysis in Hsp90 was one of the first to be studied. It inhibits the ATPase activity both in the yeast system [156] and the human system [146, 147]. Although there have been differing reports of both its oligomeric state and stoichiometry of binding to Hsp90 (it has been found to be a dimer [156, 157] and a monomer [158] in solution, and bind to Hsp90 with stoichiometries of either 1:2 or 2:2 (Hop:Hsp90) [127, 156, 157, 159–162]), it has recently been shown that binding of only one Hop molecule to the Hsp90 dimer is needed to inhibit fully the ATPase activity [160–162]. A recent cryo-EM structure of the Hsp90–Hop complex reveals how Hop acts as an inhibitor of ATP hydrolysis, as it prevents the full rotation of the MD relative to the CTD needed for NTD dimerisation. One of the TPR domains also sterically blocks NTD dimerisation, it being positioned between the two Hsp90 monomers (Fig. 7d); see EM section for more details [127].

In contrast to Hop, which is made up of three TPR (tetra-tricopeptide repeat) domains, one of which binds to the C-terminal MEEVD motif of Hsp90, other TPR-containing cochaperones which bind to the same motif have rather little effect on the intrinsic ATPase activity. This includes the high molecular weight peptidyl prolyl isomerases such as FKBP51, FKBP52 and Cyp40. Cpr6 (the yeast homologue of human Cyp40) has been shown to have little effect on the intrinsic ATPase activity of yeast Hsp90, but it can displace Hop, thereby increasing the activity of a Hop-inhibited Hsp90 [156]. In addition, human FKBP52 was shown to have little effect on the intrinsic ATPase activity of human Hsp90 [146, 147].

The small acidic cochaperone p23 (sba1 in yeast), on the other hand, inhibits the ATPase activity in both the human [146, 147] and yeast [163, 164] systems. These studies suggested that the highest affinity state for the binding of p23 is the ATP-bound NTD dimerised state of Hsp90, and in subsequent structural studies p23 was used to stabilise this closed form of Hsp90 and this binding mode was confirmed [71] (Fig. 5a, b). Although there is some evidence from mass spectrometric analysis that complexes of one p23 bound to the Hsp90 dimer can exist [165], other studies have shown that two molecules of p23 bind to the dimer [164], and this is indeed clearly the case in the crystal structure [71] (Fig. 5a, b). Although the structure of the complex doesn't directly reveal how p23 inhibits the ATPase activity of Hsp90, it seems likely that it does so by stabilising the closed NTD-dimerised state, thereby preventing release of ADP and phosphate.

The kinase-specific cochaperone Cdc37 has also been shown to inhibit ATP turnover, thereby arresting the ATPase cycle during client protein loading [166]. As with Hop, this inhibition can be reversed by the binding of Cpr6 (Cyp40) which displaces Cdc37. Cdc37 can form a stable complex with the GA-bound form of Hsp90 [166]. The structural basis for the inhibition has been established and the crystal structure of the core interaction between the C-terminal domain of Cdc37 and the N-terminal domain of Hsp90 has been solved [102] (Fig. 5d–f). Cdc37 binds as a dimer to surfaces of the NTDs which are involved in the NTD dimerisation and also associates with residues in the middle domain of Hsp90 which are known to play a role in the ATPase activity. Essentially, Cdc37 fixes the ATP lid in an open conformation and inserts an arginine into the ATP binding

pocket, thus preventing catalysis. The binding of a dimer of Cdc37 to the N-terminal domains of Hsp90 has also been established in the human system using SAXS and other biochemical techniques [131].

The first cochaperone to be identified which significantly stimulates the ATPase activity of Hsp90 was Aha1, a member of a ubiquitous class of stress regulated proteins required for the activation of clients such as v-src [101]. In fact, the first case of enhancement of the intrinsically low ATPase activity of Hsp90 was by a client protein, the hormone-binding domain of the glucocorticoid receptor, which established that the ATPase activity could be both down-regulated and up-regulated [146, 147]. Aha1 and its relative Hch1 bind to the middle domain of Hsp90 and were shown to be necessary for the activation of a heterologously expressed v-src and become crucial for cell viability under stress conditions [167]. The structural basis for the stimulation of the Hsp90 ATPase activity by Aha1 is known and the crystal structure of a complex between the N-terminal domain of Aha1 (which binds to the central segment of Hsp90) and the middle domain of Hsp90 has been solved (Fig. 5c). Aha1 promotes a conformational change in the catalytic loop in the middle domain, releasing the catalytic arginine and enabling its interaction with the gamma phosphate of ATP [99, 100]. Competition experiments which studied the binding of numerous cochaperones to Hsp90 have come up with some conflicting results with regard to which cochaperones can bind to the Hsp90–Aha1 complex; one study showed that Aha1 competes with Hop and Cdc37 but not CyP40 whilst another study suggested that Aha1 and Cdc37 were able to bind to Hsp90 simultaneously [163, 168]. Recently, a strategy employing NMR techniques demonstrated that only one Aha1 molecule was required per Hsp90 dimer in order to stimulate fully the ATPase activity and that it did so by binding to sites in the middle and N-terminal domains sequentially, the binding inducing the otherwise unfavoured N-terminally dimerised state [124]. One of the most interesting aspects of this study was that the activation by Aha1 is asymmetric, leading to the idea that in this complex one Hsp90 subunit could be used for conformational regulation of the ATPase activity whilst the other could be used for client protein processing [124]. Aha1 has been shown to play a role in the stability of the CFTR (cystic fibrosis transmembrane receptor) and down-regulation of Aha1 rescues the ΔF508 CF-associated mutant form of CFTR [169]. Mutations in Aha1 which impair its ability to bind to Hsp90 and stimulate its ATPase activity have been shown to modulate the folding and trafficking of wild-type and ΔF508 CFTR [170].

In addition to the cochaperones, the ATPase activity of Hsp90 is also regulated by binding of client proteins as well as post-translational modification. In the case of clients, the ligand-binding domain of the glucocorticoid receptor was shown to be able to stimulate the ATPase rate up to 200-fold, and this effect was specific – other partially or fully unfolded proteins having no effect [146, 147]. Post-translational modification is also beginning to emerge as a powerful regulator of ATPase activity and this is discussed in more detail in the later section on post-translational modifications.

5 In Vitro Studies of Hsp90 with Client Proteins

One of the Holy Grails of research in the Hsp90 field in the last decade has been to obtain structural information on the binding of client proteins. This has always been a technically challenging problem due to the inherent difficulties in forming Hsp90-client protein complexes. However, the Pearl group overcame this in style and published a beautiful cryo-EM structure of the Hsp90–Cdc37–cdk4 complex (see EM section for further details). In addition to this, a number of other studies have addressed this very important issue.

p53 has long been known to be a client of Hsp90 and it has been established that the interaction is largely with the DNA-binding domain (DBD) of p53. Although the complex formed between Hsp90 and p53 DBD is large (approximately 200 kDa), advanced NMR techniques have been used to obtain structural information, particularly on the state of p53 DBD when bound to Hsp90 [171]. In this case, transverse relaxation-optimised NMR spectroscopy combined with cross-correlated relaxation enhanced polarisation (CRINEPT-TROSY) on a ^{15}N-labelled sample of p53 DBD was used to study the system and the results suggested that p53 was largely unfolded when bound to Hsp90 lacking α-helical or β-sheet structure [171].

In a more recent study using similar techniques, it was concluded that the p53 DBD changed its structure on binding to Hsp90 and it was proposed to bind to the chaperone in a molten-globule like state. This conclusion was based on the fact that the intensity of many of the NMR peaks decreased on complex formation, particularly those in the central β-sheet region of the DBD [120–122]. Hydrogen–deuterium exchange experiments supported this loosening of structure on Hsp90 binding [120–122]. However, other recent NMR studies have concluded that Hsp90 interacts with native p53 DBD, see the next paragraph for more details [118]. It remains unclear whether the differences in these three studies are due to different experimental conditions, particularly ionic strength and different Hsp90s, or whether the differences come from interpretation of the data – in each study the conclusions rely heavily on the interpretation given to the disappearance of crosspeaks on binding of p53 to Hsp90 [112, 113]. It is not yet clear where on Hsp90 p53 binds; in some NMR studies, resonances affected by the client protein binding were located throughout the structure [120–122], whilst other studies have suggested that a negatively charged pentapeptide DEDEE located near the C-terminus of Hsp90 is involved, in addition to residues in the middle domain [118].

Another recent study of the interaction between Hsp90 and p53 DBD combined both NMR, fluorescence polarisation and analytical ultracentrifugation to obtain important information both on the structure of the Hsp90-bound DBD as well as the interaction sites in Hsp90 [118]. In contrast to the previous NMR studies, this study suggested that p53 binds in a native-like conformation to Hsp90 and concluded that the loss of NMR signals from p53 observed in earlier studies was likely due to the size of the complex formed as well as chemical exchange processes. They clearly demonstrated that the main binding site is at the C-terminus of Hsp90 in an unstructured region which is highly acidic, containing an EDEDE motif. This is

the first time a client protein has been shown to interact with the CTD. However, they also observed binding sites in the middle domain and NTD, the former comprising another patch of negatively charged residues. Thus it appears that Hsp90 binds to the DBD of p53 in a manner similar to that of DNA; however, as the binding to DNA is considerably stronger, DNA can displace Hsp90 from p53. By mutating the binding sites that had been identified in the NMR experiments, it was also shown that all of these sites are needed for the full chaperoning of p53 by Hsp90; thus the interaction surfaces show cooperative behaviour.

Recently the Agard group has used SAXS, FRET and NMR measurements to study the binding of a partially folded fragment of staphylococcal nuclease (Δ131Δ) to Hsp90 [129, 130]. Although Δ131Δ is not a true client of Hsp90, this is one of the few structural studies of an Hsp90-partially folded substrate protein complex. The SAXS data showed that the structure of apo Hsp90 becomes more compact on binding Δ131Δ and the interaction is stronger in the presence of AMP–PNP. Fluorescence-based assays showed that Δ131Δ accelerated the rate of dimerisation of the N-terminal domains and thus increased the ATPase activity. NMR was used to show that Hsp90 binds to a structured region in Δ131Δ, and the interaction occurs via the middle domain of Hsp90, binding triggering a conformational change in the chaperone [129, 130].

6 Post-translational Modifications

It is now well established that post-translational modifications play an important role in regulating and modifying the activity of Hsp90 as well as some of its cochaperones [172, 173]. Acetylation and phosphorylation have both been shown to affect the function of Hsp90 by a number of different mechanisms including effects on the ATPase activity, the binding of cochaperones and the binding of client proteins. In addition to these post-translational modifications, Hsp90 can also be ubiquitinated although less is known about this particular covalent modification, the focus of most studies usually being on the ubiquitination and subsequent degradation of Hsp90 client proteins. There is also evidence that, in addition to the regulatory post-translational modifications, Hsp90 can react with various cellular small molecule nucleophiles, such as reactive aldehydes produced as a result of oxidative damage to lipids, and it has been hypothesized that these lead to Hsp90 malfunction which may play a role in some disease states [174]. The next sections outline what is known about the different post-translational modifications.

6.1 Acetylation

Inhibitors of histone deacetylases (HDACs) are known to induce Hsp90 acetylation, thereby inhibiting its activity [175, 176]. One acetylation site has been identified in

the middle domain (Lys294 of yeast Hsp90) and it has been shown that the acetylation status affects both client protein and cochaperone binding [172, 173]. Mutants of Lys294 in yeast Hsp90 which are incapable of being acetylated show reduced viability in yeast, demonstrating the importance of the post-translational modification in Hsp90 function in vivo [172, 173]. Two other studies have shown the importance of Hsp90 acetylation for the maturation of the glucocorticoid receptor (GR) in vivo, again inactivation of HDACs using small molecule inhibitors leading to Hsp90 hyperacetylation, dissociation of the cochaperone p23 and reduced ligand binding by the GR. Similar results were found in HDAC6 deficient cell lines [177, 178].

A recent study has established the effect of the small molecule HDAC6 inhibitor carbamazepine on the cellular levels of the Hsp90 client protein, Her2. Treatment of cells with carbamazepine results in decreased levels of Her2 consistent with disruption of Hsp90 function [179]. Androgen receptor (AR) activity has also been shown to be affected by HDAC6 inhibition, thus suggesting that steroid receptors in general may require dynamic Hsp90 acetylation/deacetylation to attain their full function [180]. A mass spectrometric study on Hsp90 from *Plasmodium falciparum* has also revealed an acetylation site which overlaps with the Aha1 and p23 binding sites [181] suggesting that acetylation is a generic method for regulating the activity of Hsp90 particularly towards a subset of client proteins.

6.2 Phosphorylation

Hsp90 has been known to be phosphorylated under certain conditions, for example, when in complex with the P2X(7) receptor, for some time [182]. However, some of the enzymes responsible for phosphorylation and the effect of phosphorylation on the structure and function of Hsp90 have only recently begun to be established. C-src phosphorylates Hsp90 on Tyr300 (yeast) and in doing so stimulates the association of the client eNOS with Hsp90 and thus NO release [183].

The most detailed studies of Hsp90 phosphorylation have been undertaken in a collaboration between by the Neckers, Pearl and Piper groups. They have shown that yeast $Swe1^{Wee1}$, itself an Hsp90 client protein, phosphorylates a conserved tyrosine (Tyr24 in yeast Hsp90) [184, 185]. As Swe1 is a cell cycle protein this means that the phosphorylation of Tyr24 is also cell cycle regulated. To date, no phosphatase has been identified which can dephosphorylate Tyr24 and there is some evidence that it phosphorylates a nuclear form of Hsp90 which is then transported to the cytosol where it can be ubiquitinated and degraded [184, 185]. Phosphorylation modulates the chaperoning activity of yeast Hsp90 with respect to specific client proteins including v-src and other kinases in addition to heat shock factor 1 (HSF1). Tyr24 is located in the N-terminal α-helix which is known to play a role in N-terminal domain dimerisation and therefore the ATPase activity. A non-phosphorylatable mutant was shown to have normal ATPase activity, be sufficient for yeast viability and be able to chaperone the glucocorticoid or

androgen receptors (GR and AR). In contrast, phosphorylation mimic mutants Y24E or Y24D were not viable in yeast and recombinant forms of these mutants had minimal ATPase activity in in vitro assays and failed to undergo N-terminal dimerisation on binding AMP–PNP [184, 185]. Importantly, deletion of Swe1 resulted in increased sensitivity of the yeast strain to Hsp90 inhibition by geldanamycin [184, 185]. These results suggested that phosphorylation of Hsp90 has an effect on a distinct set of client proteins. A follow-up paper demonstrated that Tyr24 phosphorylation of Hsp90 by Swe1 is important for the association of the protein with the chaperone and therefore its cellular stability [184, 185]. This study also established that Hsp90 phosphorylation is important for proper cell cycle regulation [184, 185].

Recently it was shown that casein kinase 2 phosphorylates a conserved threonine (Thr22 in yeast Hsp90), also located in the N-terminal α-helix which plays a role in N-terminal domain dimerisation, in both in vitro and in vivo experiments [186]. A non-phosphorylatable (T22A) and a phosphomimetic mutant (T22E) were made and characterised in vitro and in vivo. Whilst the T22A showed ATPase activity similar to wild type, the T22E mutant had reduced activity consistent with the results which showed that it had a lower tendency for N-terminal dimerisation on binding AMP–PNP. Interestingly, the two mutants showed different levels of chaperoning activity with respect to specific client proteins in yeast. Neither mutant was able to chaperone fully some kinase clients including v-src, ste11 and Mpk1/Slt2, suggesting that dynamic phosphorylation is needed in these cases. In contrast, the T22E mutant showed a greater ability to chaperone the GR, whilst T22A showed reduced levels of GR activity in the yeast assay. The T22E mutant was also more able to chaperone CFTR. The T22E mutant also showed reduced interaction with the cochaperone Cdc37 and completely abolished the interaction with Aha1. Overexpression of Aha1 restored the chaperoning ability of both the T22A and T22E mutants with respect to the client v-src but reduced the activity of the client GR. These results suggest that phosphorylation of Thr22 in α-helix1 allows Hsp90 to discriminate between different client proteins and may facilitate the chaperoning of a specific set of clients. There is an excellent commentary on this paper, which provides some of the structural background to the effect of the two mutations, in the same issue of *Molecular Cell* [187] and in excellent recent review articles [188, 189].

In another study, phosphorylation of Thr90 in Hsp90α by protein kinase A was shown to affect both the binding of ATP and the binding of cochaperones such as Aha1, p23, PP5 and CHIP (which are increased by the phosphorylation) as well as Hsp70, Hop and Cdc37 (whose binding is decreased by the phosphorylation) [190]. The binding of a number of client proteins, including src, Akt and PKCγ, was also impaired. Interestingly, the amount of Hsp90 phosphorylated at Thr90 is significantly elevated in proliferating cells [190].

In addition, phosphorylation of cochaperones such as Cdc37 has also been shown to affect the function of the Hsp90 machinery [191]. In this case, Ser13 of a mammalian Cdc37 can be phosphorylated by casein kinase II, and mutation of this

residue to either a non-phosphorylatable side chain (Ala) or phosphorylation mimic (Glu) affected binding to Hsp90-client protein complexes [191].

6.3 Ubiquitination and Other Post-translational Modifications

Recent studies in vitro have established that the cochaperone CHIP can mediate the ubiquitination of Hsp90 on a number of lysine residues including Lys 107, 204, 219, 275, 284, 347, 399, 477, 481, 538, 550, 607 and 623 [34, 35]. These lysines are clustered either in the C-terminus of the protein or in the N-terminal domain or the region of the middle domain which lies close to the ATP-binding site. Polyubiquitin chains with K6, K11, K48 and K63 linkages were all shown to form during these in vitro ubiquitination experiments [34, 35]. These interesting results suggest that ubiquitination may play a role in regulating Hps90 function in vivo; however, further work is needed to confirm that these modifications take place in a cellular environment.

Biological electrophiles such as α,β-unsaturated aldehydes produced from oxidative metabolism of either endogenous cellular components such as lipids, or exogenous compounds, can also modify Hsp90 [174]. For example, 4-hydroxynonenal (HNE) can form adducts with Hsp90 and this has been associated with changes in gene expression, particularly an up-regulation of genes controlled by heat shock factor 1 (HSF1) which is presumably released from Hsp90 subsequent to modification. Hsp70 may also be involved and amongst many other genes BAG3 expression is induced, this protein promoting cell survival [174]. Thus Hsp90 may play a role in protecting cells against electrophile-induced cell death.

7 Hsp90 Homologues in Other Cellular Compartments and Organisms

7.1 Grp94: A Homologue of Hsp90 in the Endoplasmic Reticulum

Grp94 (glucose-regulated protein 94) is the Hsp90-like protein in the lumen of the endoplasmic reticulum (ER) and the sarcoplasmic reticulum of muscle cells; it is also known as gp96 and endoplasmin [192]. Recently, many similarities with the cytosolic Hsp90s have been established, including the ability to bind and hydrolyse ATP [75, 193], an activity which has been shown to be essential in vivo [194], binding the natural product inhibitors of Hsp90 geldanamycin [195] and radiciol [57]. However, there are some striking differences with the cytosolic Hsp90s – Grp94 has a distinct set of client proteins [192], all of which are disulphide bonded, and in contrast to Hsp90 it is a major calcium binding protein in the ER [196].

Grp94 is targeted to the ER through a 21-residue N-terminal signal sequence which is cleaved after translocation, and it is retained in the ER by a C-terminal KDEL motif. There are some reports that a minor fraction of Grp94 might be cytosolic, and there is even a suggestion that, in some specific cases, it may be extracellular. It was first identified as a protein which was up-regulated under low glucose conditions (hence its name) [197, 198], but unlike cytosolic Hsp90 it is not induced by high temperatures [199] or other stresses but by ER stress only [192, 197, 198]. Grp94 is therefore is a well-established hallmark of the UPR (unfolded protein response) in the ER [192].

As with the cytosolic Hsp90s, Grp94 is known to be post-translationally modified, the best characterised modification being glycosylation of Asn196 [200]. However, the functional consequences of this post-translation modification have yet to be established. There is also some evidence that it can be phosphorylated on Ser/Thr sites by casein kinase II [201, 202], or on tyrosines by src kinase fyn [203]. Further work is needed to confirm these studies and to rationalise how cytosolic kinases can act on an ER protein (it may be the small pool of cytosolic Grp94 that undergoes phosphorylation). It is interesting to speculate whether Grp94 could be acetylated (as are cytosolic Hsp90s) as the Lys is conserved and it has recently been suggested that there are ER lysine acetyltransferases [204].

Structurally, Grp94 is very similar to Hsp90, and it has three major structural domains – the NTD, middle domain and CTD (Fig. 4c–d). However, the first 50 residues in Grp94 are different from the cytosolic Hsp90s in terms of both length and sequence. The NTD is similar to that of Hsp90 and it can bind to GA and RD; however, they bind with slightly different orientations [57, 61, 75]. The most significant difference is the lid region where in Grp94 there is a five-residue insertion between the two helices [57, 61, 75].

A noticeable difference is in the charged linker region, which in Grp94 is shorter than in the Hsp90s and contains distinct regions which are rich in acidic residues (Asp and Glu) and form some of Grp94's many Ca^{2+} binding sites, and also a lysine-rich region. Grp94 has long been known to be a low-affinity, high-capacity calcium binding protein, with four moderate-affinity binding sites (K_d are approximately 2 μM) and possibly 11 low-affinity binding sites (K_d are approximately 600 μM) [196, 205]. Ca^{2+} binding is known to induce conformational change and modulate at least some of Grp94's functions including its peptide-binding activity [205].

The middle and C-terminal domain of Grp94 are very similar to Hsp90 apart from the fact that Grp94 forms a tighter dimerisation interface. In addition, it has a 55-residue C-terminal extension which contains many acidic groups and which lacks the C-terminal MEEVD motif (having the KDEL ER-retention motif instead). It has been shown that Grp94 is highly dynamic and adopts multiple conformations like Hsp90, which include an extended chair-like conformation, a more closed conformation and a twisted V-like conformation which is even more compact [57, 61, 64, 75].

As an ER protein, Grp94 has a distinct set of client proteins which are all disulphide bonded and it is therefore a rather selective chaperone. Clients include members of the immunoglobulin (Ig) family, either folding intermediates of unassembled MHC class II proteins or Ig heavy or light chains, BSDL, toll-like receptors (TLR), platelet glycoprotein Ib–IX–V complexes, thyroglobulin and insulin-like growth factors [192]. Like Hsp90, Grp94 clients range in the structures and functions they perform – some are monomeric, some oligomeric, some are single-domain proteins, others are multi-domain, whilst some are all alpha and others are comprised entirely of β-sheets [192].

Grp94 is known to play a role in ER stress, and is up-regulated under these conditions; as with Hsp90, Grp94 is found up-regulated in many tumours and is a potential biomarker [206, 207]. There is some evidence that Grp94 works with BiP (the ER Hsp70 homologue) [208, 209]. However, very few other Grp94 cochaperones have yet to be identified. None of the cochaperones identified for cytosolic Hsp90s have been found in the ER, and those proteins which have been identified as putative Grp94 cochaperones have very different structures and possible functions. These include CNPY3 which is necessary for the correct folding of TLRs [210–212], ANSA-1 which has been shown to associate with Grp94 using yeast two-hybrid and GST pulldown assays and which is involved in insulin secretion [213, 214], and OS-9 which is part of the machinery which targets misfolded proteins for ER-associated degradation [215]. Grp94 plays a role in quality control and it has been shown that mutant forms of α1-antitrypsin which would normally be degraded by the ERAD machinery do not occur in the absence of the chaperone [216]. OS-9, a putative Grp94 cochaperone, has also been shown to be involved.

One major difference with Hsp90s is the response to nucleotide binding – Grp94 binds ATP and ADP and both nucleotides induce the same conformational change resulting in a twisted V-like conformation (Fig. 4c, d) [75]. Strikingly, the lid region in the N-terminal domain opens upon nucleotide binding rather than closing it, as is the case for Hsp90 [61, 64, 193]. Grp94 still requires dimerisation of the NTDs for ATP hydrolysis and therefore considerable rotation of both the NTD relative to the middle domain, and middle domain relative to the CTD, is required in order to achieve this. As nucleotide does not induce NTD dimerisation, it has been proposed that binding of the client may induce the conformational changes required.

7.2 TRAP-1: A Homologue of Hsp90 in Mitochondria

TRAP-1, tumour necrosis factor receptor-associated protein 1, is the mitochondrial homologue of Hsp90 and accumulates predominantly in the mitochondrial matrix although some may also be in the intermembrane space [217]. It has been shown to be involved in a number of signalling networks which are important for both organelle integrity and cellular homeostasis [218]. It is deregulated in both cancer and neurodegenerative disorders and its activity is essential for mitochrondrial

integrity, oxidative cell death, organelle-compartmentalised protein folding, as well as transcriptional responses to proteotoxic stress [219]. It shares 34% identity (60% similarity) with cytosolic Hsp90 [220] and up to six variants have been predicted. Unsurprisingly, given the sequence similarity, it shares many properties with Hsp90 – it is an ATPase, the activity being inhibited by geldanamycin and radicicol [218]. It is induced upon heat shock (up to 200-fold), and ATP binding (which is higher affinity compared with Hsp90) shifts the conformational equilibria towards the closed state; however, the ATP is not committed to hydrolysis [221]. In contrast with Hsp90, it does not contain a C-terminal MEEVD motif, doesn't bind cochaperones such as p23 or Hop, and can't substitute for cytosolic Hsp90 with respect to progesterone receptor activation [218].

Levels of TRAP-1 are consistently elevated in a number of cancers [222], and in tumour cells it is associated with the matrix peptidyl prolyl isomerise cyclophilin D, CypD, which is a component of the permeability transition pore (PTP) known to be involved in mitochondrial apoptosis [224]. It has been suggested that CypD is a TRAP-1 client protein and it has been proposed that both are part of a stress-responsive cytoprotective mechanism which is up-regulated following oncogene expression [225–227]. Inhibition of TRAP-1 has also become established as a potential strategy for developing cancer therapeutics, and although many of the classic Hsp90 inhibitors do not accumulate in mitochondria, the synthetic peptidomimetic Shepherdin does [222, 228]. Recently, geldanamycin inhibitors have been fused to mitochondriotropic moieties to make Gamitrinibs (GA-mitochondrial matrix inhibitors) which have been shown to accumulate rapidly in mitochondria and induce collapse of mitochondrial integrity and PTP opening [229]. Gamitrinibs are proving to be promising potential anti-cancer agents [230, 231].

TRAP-1 has also been associated with neurodegenerative diseases such as Parkinson's disease (PD). In this case, PTEN-induced Putative Kinase (PINK-1) mutation, which is associated with PD, has been shown to be cytoprotective and this action is known to require TRAP-1. PINK-1 phosphorylates TRAP-1, illustrating that like Hsp90 its activity is controlled by post-translational modification, and the phosphorylated TRAP-1 prevents mitochondrial dysfunction and oxidative stress induced apoptosis [227].

7.3 Extracellular Hsp90

Over the last decade there has been much debate over whether there is an extracellular Hsp90 (eHsp90) be it cell-surface bound, cell released or a cell secreted form. Although reports of extracellular Hsp90 have appeared in the literature for several decades, it was thought that this might simply be an artefact of Hsp90 released from a small proportion of dead cells. However, it is now clear that there are extracellular forms and that they are involved in a number of important processes including cell

motility and wound healing [160–162]. It is the Hsp90α isoform that has been found outside the cell, and whilst quiescent cells do not secrete it, many stresses including reactive oxygen species, heat, hypoxia, irradiation and tissue injury release cytokines, induce its secretion. The induced secretion of eHsp90 in normal cells can be compared to its constitutive secretion in tumour cells. The exact mechanism by which it gets secreted is not known but it may involve a non-classical exosomal protein secretory pathway.

eHsp90α has been shown to promote cell motility. DMAG-N-oxide, a cell-impermeable geldanamycin derivative, was shown in a number of studies [232, 233] to reduce tumour cell invasion and it has been proposed that the downstream targets of eHsp90 may be matrix metalloproteases (MMPs). The mechanism of action of eHsp90 is clearly different from that of its cytosolic counterparts and it has been shown that its ATPase activity is not necessary for its function in cell motility. Instead, its activity has been shown to be associated with a fragment (F-5) comprising residues 236–350 which is located between the linker region and the middle domain [234, 235]. This fragment is just as efficient at promoting cell migration and wound healing as the full-length protein. This 115-amino acid region has been highly conserved. This seems at odds with the results on cell impermeable GA derivatives which are known to bind to and inhibit the ATPase activity in the N-terminal domain. However, it is currently thought that binding of this inhibitor results in the F-5 region becoming inaccessible and that this is, critical to its change in activity, rather than ATPase inhibition.

7.4 Plant Hsp90s

Plants have seven different Hsp90s including four cytosolic isoforms, a mitochrondrial Hsp90, an ER Hsp90 and an Hsp90 in chloroplasts [236]. Plants also contain many of the known cochaperones including p23, Aha1, Hop, FKBPs and PP5 [236]. Hsp90 is known to play a very important role in buffering genetic variation in plants [237–239], a function which has also been shown in yeast and in *Drosophila* [240, 241]. Although this is a fascinating aspect of Hsp90 function in vivo, its discussion is beyond the scope of this review and interested readers are directed to some of the original and recent literature in this area [6, 238–240, 242–246].

Plant Hsp90s are known to play many different roles but perhaps the one that has been most well characterised is the role in plant innate immune response, which involves the immune sensing NLR (nucleotide-binding domain and leucine rich repeat containing proteins) [247]. Two cochaperones RAR1 and SGT1 are known to function with Hsp90 in order to chaperone the NLR proteins which are therefore clients of the Hsp90 system [248]. SGT1 contains a TPR domain, a CS domain and an SGS domain, and, despite the presence of a TPR domain, it binds to the N-terminal domain of Hsp90 primarily through its CS domain; however, the

interaction is weak in the absence of RAR1 [104]. The CS domain also interacts with RAR1 whilst the SGS is proposed to bind to the client NLR proteins. RAR1 contains two similar CHORD domains (cysteine and histidine rich domains which bind to Zn^{2+}). The two CHORD domains of RAR1 interact with the N-terminal domain of one Hsp90 and the N-terminal/middle domain of the other monomer whilst the CS domain of SGT1 interacts with one of the RAR1 CHORD domains and an N-terminal domain of Hsp90 [104]. A model of the stable ternary complex formed is shown in Fig. 6d. SGT1 is known to bind to the NLR proteins which are chaperoned by the system. Some of the structures of the key complexes are known and these are discussed in further detail in the structure section of this review.

8 Cochaperones

Since the early days of Hsp90 research, it has been known that this chaperone does not act alone but has a host of cochaperones which vary depending upon cellular compartment, organism and client protein [37]. The cochaperones of cytosolic Hsp90 include p23, Hop, FKBP51 and 52, CyP40, PP5, Cdc37, SGT-1, CHIP and Aha1 [30, 37, 249]. See http://www.picard.ch/downloads/Hsp90interactors.pdf for a comprehensive list.

8.1 p23

The small acidic cochaperone p23 was first identified in complex with Hsp90 and steroid receptors back in the early 1990s [250, 251]. It is known to bind to the N-terminal domains of Hsp90 and preferentially to the ATP-bound state, thereby stabilising the N-terminally dimerised form of the chaperone (Fig. 5a, b) [71]. However, it has also been shown to bind to apo Hsp90, albeit more weakly [165]. It inhibits the ATPase activity of the chaperone [146, 147, 163, 164] and, although the exact mechanism by which it does so is unknown, it is likely that it may simply prevent release of ADP and phosphate [71]. The structure of p23 both free and bound to an Hsp90–AMP–PNP complex are known (Fig. 5a, b) [71, 252]. p23 promotes the hormone-binding activity of many SRs and prevents their degradation; however, it can be either stimulatory or inhibitory [31]. In addition to its functions with Hsp90, it has also recently been shown to have other activities [253], and is also known to play a role in the maintenance of telomeres [254]. The role of Hsp90 and p23 in the maintenance of telomeres is an important one but beyond the scope of this review. Interested readers are directed towards a recent review in this area [255].

8.2 High Molecular Weight PPIases

Another group of cochaperones associated with Hsp90 and steroid receptors are the high molecular weight PPIases (peptidyl prolyl isomerases) FKBP51, FKBP52 and CyP40 [3, 4, 29, 256]. These cochaperones contain multiple domains including a TPR (tetratricopeptide repeating unit) domain, for which the primary binding site is the C-terminal MEEVD motif of Hsp90 (for a recent review on the binding of TPR domains to Hsp90 see reference [257]) and a FKBP-like or cyclophilin-like domain which may have peptidyl-prolyl isomerase activity. This activity is required for the activation of some SRs, such as AR [258], but not others, e.g. GR. In general, FKBP52 is a positive regulator of SR action (with the possible exception of the ER) [259–262], whilst FKBP51 tends to have inhibitory effects despite being structurally very similar (again there is an exception here with AR where it is stimulatory) [263]. Interestingly, whilst some FKBP52 knockout mice are embryonically lethal, others grow into healthy adults; however, in these cases both male and female have reduced fertility. FKBP51, on the other hand, appears to play no role in male fertility but is a positive regulator of androgen-mediated growth of prostate cancer [264, 265]. Recently, FKBP51 has also been shown to have a role in the neuroendocrine control of behaviour and has been associated with post-traumatic stress disorder and depression [266, 267]. In addition, FKBP51 has been shown to have a role in the regulation of tau and is therefore associated with a number of neurodegenerative disorders [268]. See the later section on Hsp90 as a target against neurodegenerative diseases for more details.

The structure of bovine CyP40 has been solved in two different crystal forms and in one form is very similar to that of cyclophilin A [269]. It is known that yeast CyP40 has little effect on the intrinsic ATPase activity of yeast Hsp90 [156]. However, it can displace other cochaperones such as Hop, thereby increasing the activity of a Hop-inhibited Hsp90 [156]. It has not been as extensively studied as FKBP51 and 52; however, recently Cpr7 (the yeast homologue of CyP40) has been shown to be required for activity of both ERα and GR in an engineered yeast system [256]. There are parallels with the functions of FKBP51 and 52, and it has been proposed that this cochaperone makes a direct contact with the ligand-binding domain of the Hsp90-bound steroid receptors, thereby stabilising an optimal conformation for receptor activity [256]. Very recent work has also established a role for CyP40 in HSP90-mediated assembly of the RISC complex in plants [190].

8.3 PP5

Protein phosphatase 5, PP5, contains a TPR-binding domain [270] as well as a phosphatase domain and can bind to Hsp90 through its C-terminal MEEVD motif, thus competing with the high molecular weight PPIases and Hop for binding sites [110]. It has been shown to bind to Hsp90 in the presence of both GR

[271, 272] and ER [31], and is known to be involved in the regulation of tau [273]. PP5 is found in a range of organisms and recent work has shown it is required for Hsp90 function during proteotoxic stresses in *Trypanosoma brucei* [274]. A number of reviews of PP5 structure and function provide further details; in particular [275] gives important background on the cellular signalling pathways and the range of cellular processes on which PP5 acts; [276] discusses the role of PP5 in the regulation of stress-induced signalling networks and cancer; see also an early review by Chinkers [277].

8.4 Cdc37

Cdc37 is an Hsp90 cochaperone required for the correct activation of many cellular kinases [278]. Much is known about the structure and function of Cdc37; see previous sections [278]. Cdc37 has been shown to bind to the N-terminal domain of Hsp90 as illustrated in Fig. 5d–f [102]. Cdc37 is thought to interact directly with the client kinases, thereby recruiting them to the Hsp90 machinery. Pulse-chase and immunoprecipitation experiments have established that Cdc37 binds to the kinases either during or shortly after translation, thereby protecting them against proteasomal degradation [279, 280]. It is an essential protein and is itself oncogenic when over-expressed making the Hsp90–Cdc37 complex and important therapeutic target [278]. In addition to its function as an Hsp90 cochaperone, there is evidence that Cdc37 also has Hsp90-independent activities, and is able to support yeast growth and protein folding without its Hsp90-binding domain [281]. Consistent with this, recent genomic and proteomic studies in yeast have shown that, whereas a relatively small population of the cellular kinome requires Hsp90, many more kinases require Cdc37 [282].

8.5 Hop

Hop, Hsp70–Hsp90 organising protein, comprises three TPR domains – TPR1, 2A and 2B. Extensive structural and functional work has been done on this important cochaperone, which is known to bind simultaneously to both Hsp70 and Hsp90, thereby acting as an adaptor protein, mediating the transfer of client proteins from the Hsp70 machinery to the Hsp90 system (Fig. 1b). Hop binds to the C-terminal MEEVD motif of Hsp90 [283], but in addition to this primary binding site it is now known that there are other interaction sites elsewhere on Hsp90 [157, 285]. There is evidence that the binding of Hop to Hsp90 induces structural changes both in Hsp90 and in Hop itself [127, 157]. Hop is known to stimulate the ATPase activity of Hsp70 and inhibit the ATPase activity of Hsp90, thereby facilitating the transfer of clients [284]. A recent study from the Buchner group has dissected the roles of the different TPR domains as well as the two DP domains of Hop with respect to Hsp70

and Hsp90 binding, ATPase inhibition and client activation [285]. They propose a model in which TPR2A and 2B are bound to the CTD and middle domains of Hsp90, the domains being separated by a rigid linker region which orients the two domains such that the peptide-binding pockets point in opposite directions, enabling simultaneous binding to both Hsp70 and Hsp90. They show that both the DP21 and DP2 domains have α-helical structure and that DP2 plays a critical role in client activation (in this case GR activation), and propose that it may either (1) interact directly with the client protein or (2) promote the conformational changes required for client protein transfer from Hsp70 to Hsp90 [285]. As with other Hsp90 cochaperones, there is some evidence that Hop has a number of biological activities [283].

8.6 Aha1

Aha1, activator of Hsp90 ATPase activity, and Hch1 (the two homologues of Aha1 in yeast) were first identified as multi-copy suppressors of an inactive mutant of Hsp90 in yeast, restoring wild-type like growth rates [286]. It is now well established that Aha1, as its name suggests, stimulates the ATPase activity of Hsp90 [101, 167]. The mechanism was revealed in crystallographic studies which showed that binding of Aha1 to the middle domain of Hsp90 results in a conformational change which repositions the catalytic loop in the middle domain, and the catalytic arginine in particular, such that it is optimal for hydrolysis of the ATP in the N-terminal domain; see previous sections for more detail [99, 100]. Aha1 has been shown to have an important role in the correct trafficking and folding of the cystic fibrosis transmembrane conductance regulator (CFTR) in vivo. siRNA silencing of Aha1 leads to the rescue of the disease-associated ΔF508 CFTR mutant [169]. More recently, mutations in Aha1 which abrogate its binding to Hsp90 and therefore its stimulation of the ATPase activity have been shown to impair the ability of Hsp90 to chaperone both mutant and wild-type CFTR [170]. This study proposes that the dwell time of the client protein (in this case CFTR) on Hsp90 is crucial in determining its fate [170].

8.7 SGT1

The role of SGT1 has best been characterised in the plant innate immune system regulatory response [287]. Here, it acts as a cochaperone of Hsp90 to mediate and stabilise NLR (nucleotide-binding domain and leucine-rich repeat containing) proteins, which are the pathogen-sensing systems in both plants and mammals [248]. The NLR proteins need to be correctly folded and maintained in a state which will recognise pathogens [288, 289]. See also the structural section and the section on plant Hsp90s in this review for further details.

8.8 CHIP

CHIP, carboxyl-terminus of Hsc70 interacting protein, was originally identified as a co-chaperone of Hsc70 but has now been shown to bind to both Hsc70 and Hsp90 through its TPR domain. In addition to the TPR domain, it has a U-box domain which has a ubiquitin ligase activity and an intervening charged domain [290]. Its interaction with Hsc70 and Hsp90 results in client protein ubiquitylation and degradation by the proteasome [291]. CHIP has been shown to regulate the cellular levels and activity of tau, whose misfolding is associated with Alzheimer's disease [273], and it has also been linked with Parkinson's disease, a neurodegenerative movement disorder that is caused by the loss of dopaminergic neurons, and also associated with cellular abnormalities in proteostasis. Consistent with this, CHIP has been shown to modulate neuronal death [13]. It has also been associated with other disease states such as cancer [291].

A model has recently been proposed for how the Hsp90/Hsc70/CHIP machinery may act to triage proteins and determine which should be targeted for degradation. The model highlights a potential role of the chaperone machinery in dealing with proteins which have undergone oxidative damage [292].

8.9 General

The evolution of the Hsp90 and cochaperone machinery has been studied by Johnson and co-workers who have studied the types and number of chaperones/cochaperones from a number of different species and they find considerable variation [37]. Comparison of the genomes of 19 disparate eukaryotic organisms came up with the surprising result that no single cochaperone was found in all; however, a subset comprising Hop, PP5, Aha1, p23 and Sgt1, were present in the majority of the species (16/19) [38]. They concluded that the varied composition of the Hsp90 molecular chaperone machinery in both different cellular compartments and organisms reflects the adaptability of the system, enabling the machinery to act on a wide variety of different clients. This also helps explain why the Hsp90 system is hijacked by many cancer cells, viruses and pathogens; see later sections. Johnson also speculated on why some of the major cochaperones such as Cdc37 were not present in all species despite the fact that kinases were [37]. In this case, she proposes that either the kinases are in dependent upon Hsp90 for their activity or a different cochaperone may play a similar role [37].

8.10 Hsp90–Cochaperone Complexes

Many of the initial studies on cochaperones focused on the binary complexes formed between Hsp90 and the cochaperone, establishing affinity, stoichiometry,

mode of binding and affect on ATPase activity; see previous sections. However, it has long been proposed that not only can Hsp90 form a variety of multi-component complexes with clients and cochaperones, but that these complexes are highly dynamic (Fig. 1b). Recently a number of studies have begun to investigate such complexes and in so doing are beginning to address the important question of which cochaperones can simultaneously bind to Hsp90 and which complexes may exist in vivo. A variety of biochemical and biophysical methods have been used to probe the formation of these complexes including immunoprecipitation (IP), analytical ultracentrifugation (AUC) and FRET-based fluorescence assays [160–162], native-state mass spectrometry [159], as well as native gels, dynamic light scattering and electron microscopy [293].

The Buchner group have been one of the first to publish detailed studies on multi-cochaperone–Hsp90 complexes [160–162]. In their study they first established that only one Hop molecule was sufficient to completely inhibit the ATPase activity of Hsp90, suggesting the possibility that only one Hop bound, leaving a C-terminal MEEVD motif available for the binding of another cochaperone. Subsequent isolation of complexes from yeast cell lysates using an engineered Sti1 (the yeast homologue of Hop) variant provided evidence that a ternary complex between Hsp90-Sti1 and Cpr6 (a high-molecular weight PPIase in yeast) could form [160–162]. Interestingly, this study found no evidence for p23 or Aha1 in the same complex. Further experiments using an engineered Cpr6 variant revealed the same complex and also suggested that Hsc70 could be found in this complex (there was some evidence that Aha1 might also bind to the Hsp90-Cpr6 complex but that this was much weaker). These experiments were followed up with in vitro biophysical assays using FRET of dye-labelled chaperones and cochaperones and AUC using purified proteins and these demonstrated that an asymmetric ternary complex consisting of the Hsp90 dimer bound to a monomer of both Hop and FKBP52 can be formed under physiological conditions [160–162]. This study also demonstrated that p23 and AMP–PNP can act synergistically to disrupt the ternary complex formed and displace Sti1, but p23 alone has little effect. Both yeast and human Hsp90 and cochaperones homologues were studied and similar results obtained, thus demonstrating that the general mechanisms of the Hsp90 cycle are conserved [160–162].

Similar results were produced by a study by Bernal and co-workers [293]. In their study, albeit using somewhat indirect methods, they established that ternary complexes of Hsp90–Hop and FKBP52 could form using native-gels, DLS and EM to look at binding [293]. In this case, they speculated that an $(Hsp90)_2$–FKBP52–$(p23)_2$–$(Hop)_2$ could also exist, although it is hard to see how this might be, given there are only two MEEVD TPR-binding sites in the Hsp90 dimer.

Recently, native-state mass spectrometry has been used to observe directly the multitude of complexes that Hsp90 can form with its cochaperones [159]. This approach not only allowed the direct detection of the different complexes in solution but also generated a set of binding constants for all the complexes under the same experimental conditions [159]. These experiments also established that an

asymmetric ternary complex between Hsp90–Hop and FKBP52 can form and that it is not only prevalent but also very stable [159].

Both the Li et al. and Ebong et al. studies establish that the Hsp90 dimer:Hop monomer is likely the most relevant complex in vivo given cellular concentrations of the chaperones and cochaperones, and that statistically it is more likely that a high molecular weight PPIase such as FKBP52 binds to the additional MEEVD motif than another molecule of Hop. Thus, the asymmetric ternary complex is therefore likely to play a crucial role in vivo. These results also suggest that ternary complexes of Hsp90 with two different HMW PPIases may also form, and there is some evidence for this from rabbit reticulocyte lysates [294] although they have yet to be observed in reconstituted complexes formed in vitro.

9 Hsp90 as a Drug Target

9.1 Hsp90 as a Cancer Target

9.1.1 Small Molecule Inhibitors of the N-Terminal ATP-Binding Domain

Many Hsp90 clients are known to be involved in multiple oncogenic pathways and Hsp90 is now a well-established target of anti-tumour and anti-proliferative drugs [295]. Two natural products, geldanamycin, a benzoquinone ansamycin isolated from *Streptomyces hygroscopicus* (Fig. 8a) and radiciol, a macrocyclic lactone antibiotic from the fungus *Monosporium bonorden* (Fig. 8d) have both been shown to have anti-proliferative activity and target the ATP-binding site in the N-terminal domain of Hsp90, thereby inhibiting the essential ATPase activity and function of the chaperone [52–54, 143]. Inhibition of Hsp90 causes client proteins to undergo ubiquitination and subsequent degradation by the proteasome [30, 292, 307]. Initial studies on geldanamycin derivatives validated Hsp90 as a cancer target and numerous studies have now been undertaken by both academic laboratories and pharmaceutical companies to develop further small molecule inhibitors of Hsp90 as therapeutic agents [295]. Extensive work has been put into optimising the pharmokinetic, pharmocodynamic and toxicological properties of these potential drugs [295].

Geldanamycin (GA) was first identified in a screen aimed at identifying molecules capable of reversing the phenotype of v-src transformed cells [296]. It has been shown to inhibit the ATPase activity of Hsp90 by competing with ATP for the ATP-binding site in the N-terminal domain (Fig. 2b) [52, 53]. GA itself has poor solubility, limited in vivo stability and it is hepatotoxic, making it a poor drug candidate [308]. However, substituents at the C_{17} position (a non-essential methoxy group) (Fig. 8a) have improved properties. In particular, substitution with an allylamino group, to produce 17-AAG (17-allyl-17-demethoxygeldanamycin) (Fig. 8b), resulted in an improved toxicity profile [297] and 17-AAG has undergone extensive clinical trials. Although some of these proved to be of limited success,

recently better formulations and delivery methods have proved encouraging. In particular, combination therapies of 17-AAG with other chemotherapeutic drugs and radiotherapy have shown considerable success. In general, treatment with Hsp90 inhibitors sensitises cells to the toxic effects of both chemotherapy and radiotherapy. Substitution at C_{17} has also produced another derivative, 17-DMAG (17-desmethoxy-17 *N*,*N*′-dimethylaminoethylamino geldanamycin) (Fig. 8c), which has improved water solubility and oral bioavailability whilst retaining good anti-tumour activity [56]. IPI-504 (the water soluble hydroquinone hydrochloride salt of 17-AAG), also known as retaspimycin, has been shown to have improved pharmacokinetics and toxicity; in addition, IPI-493 a primary active, long-lived metabolite of 17-AAG [298, 299] (Fig. 8d) has been trialled but shown to have poor pharmaceutical properties.

Although the macrocyclic lactone radicicol (RD) was identified very early as having anti-proliferative activity and targeting Hsp90, it has never been developed as a therapeutic agent as it was quickly established that it was not stable in serum and had no in vivo activity because of the reactive epoxide and unsaturated carbonyl (Fig. 8e) [300]. However, it contains a resorcinol moiety which has been found in a number of other Hsp90 molecules that are in, or entering, clinical trials. These were discovered by a variety of techniques including high throughput screening and fragment-based drug discovery, not by modification of RD itself. This includes triazole derivatives STA-9090 (Ganetesib) developed by Synta, the isoxazole derivative NVP-AUY922/VER2296 developed by Cancer Research UK [301, 302], KW-2478 discovered by Kyowa Hakko Kirin Pharma [298, 299], AT-13387 developed using a fragment-based approach by Astex Therapeutics [93] and SNX-5422, a pyrazole containing molecule, developed by Serenex [301]; for structures see Fig. 8.

The first reported synthetic Hsp90 inhibitor was PU3 (Fig. 8i), developed by the Chiosis group and based on a purine scaffold and incorporating the features observed in the binding of ATP to Hsp90, most importantly a bent conformation [303, 304]. It has been extensively optimised in terms of its pharmaceutical properties, and a large number of such purine-based inhibitors are now in clinical trials [303, 304]. This includes CNF 2024/BIIB021 discovered and developed by Conforma Therapeutics and subsequently Biogen [298, 299], MPC-3100 developed by Myrexis/Myriad Pharmaceuticals [305], Debio 0932 (CUDC305) developed by Curis and Debiopharm and PU-H71, an inhibitor developed at Memorial Sloan Kettering by the Chiosis group [306]. For structures see Fig. 8j–n.

Peptidomimetics have also been developed which bind to the N-terminal domain of Hsp90, thereby inhibiting ATP binding and hydrolysis. Shepherdin is an example which was modelled on the basis of the binding of the protein survivin to Hsp90 [228], survivin being an anti-apoptotic and mitotic regulator [309]. Shepherdin has been shown to destabilise Hsp90 clients and induce tumour cell death [228], and to be well tolerated and inhibit human tumour growth in mice [228].

There are some features of Hsp90 inhibition that make it a particularly good target. For reasons, some of which are still unclear, cancer cells have a higher sensitivity to Hsp90 inhibition than normal cells and there is a preferential accumulation of the inhibitors in tumour cells [310–312]. It has been proposed that this

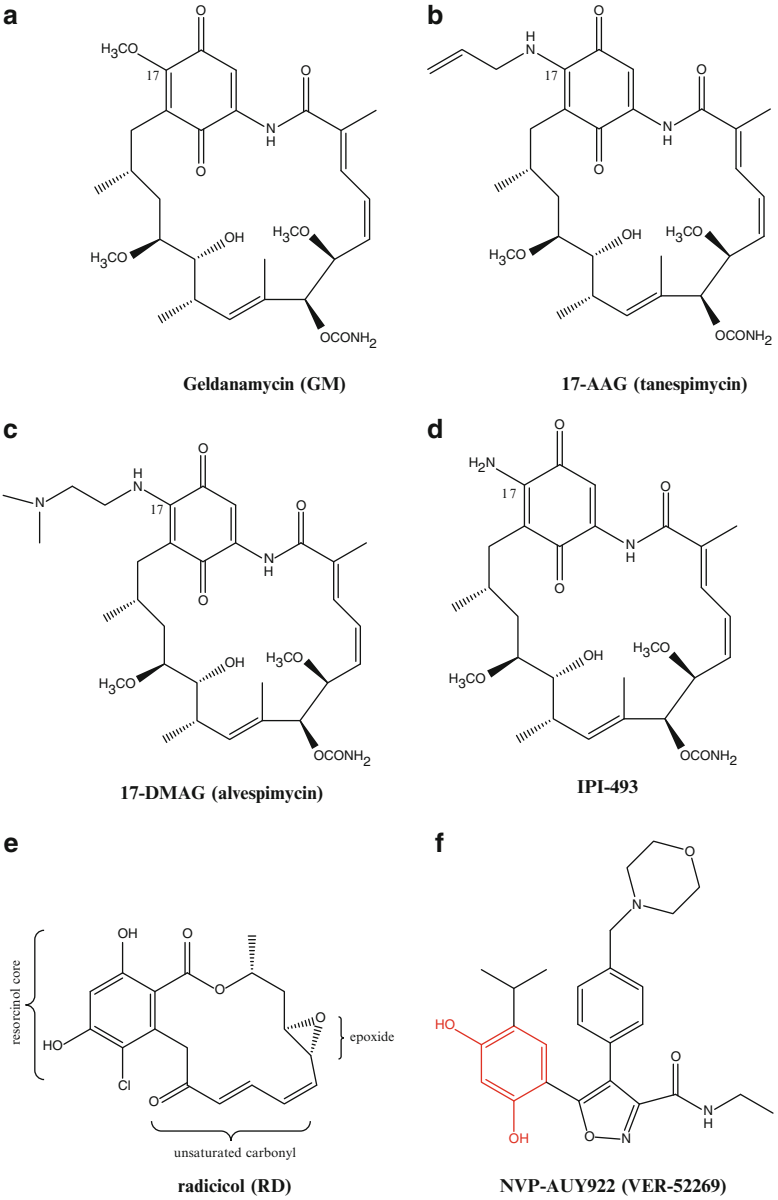

Fig. 8 (continued)

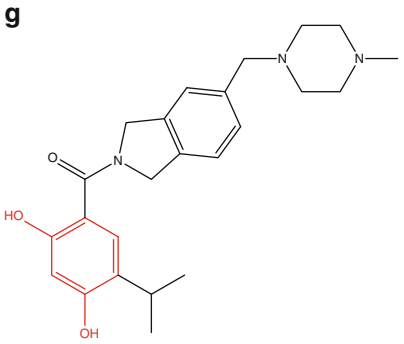

AT-13387

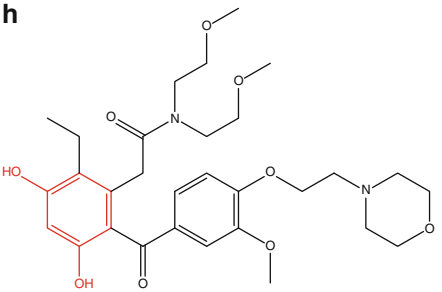

KW-2478

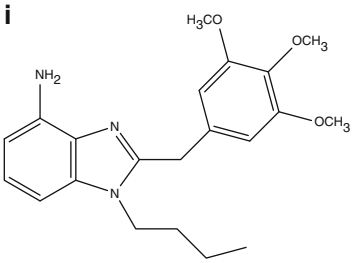

Purine scaffold (PU3)

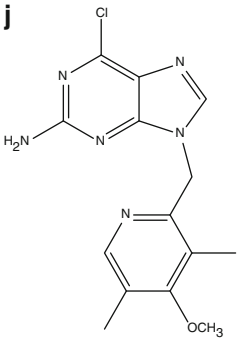

CNF2024/BIIB021

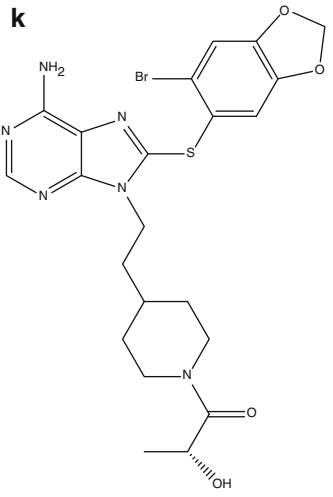

MPC-3100

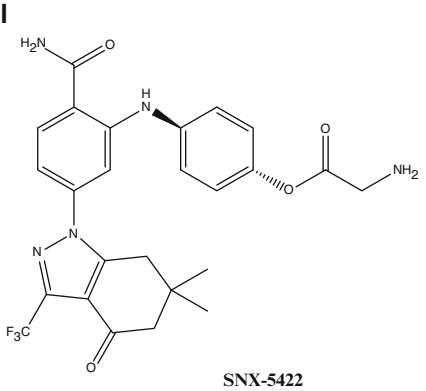

SNX-5422

Fig. 8 (continued)

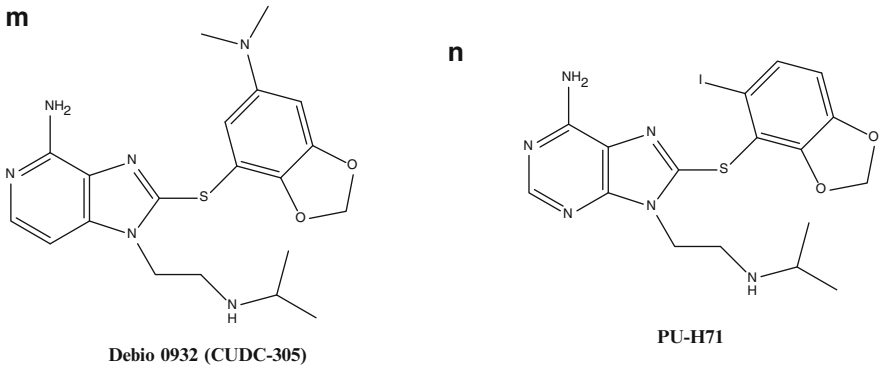

Fig. 8 Small molecule inhibitors of Hsp90 which bind to the ATP-binding site in the N-terminal domain and which are, or have been, in clinical trials. (**a–d**) Structures of geldanamycin (*GM*) [296] and its derivatives including (**a**) GM [296] (**b**) 17-AAG [297], (**c**) 17-DMAG [56] and (**d**) IPI-493 which is a primary active, long-lived metabolite of 17-AAG [298, 299]. (**e**) Structure of the macrocyclic lactone radicicol (*RD*) [300]. (**f**) Structure of an isoxazole derivative NVP-AUY922/VER2296 containing a resorcinol moiety (highlighted in *red*) developed by Cancer Research UK [301, 302]. (**g**) Structure of AT-13387 developed using a fragment-based approach by Astex Therapeutics and containing a resorcinol moiety (highlighted in *red*) [93]. (**h**) Structure of KW-2478. (**i**) Structure of the first synthetic Hsp90 inhibitor PU3, based on a purine scaffold [303, 304]. (**j**) Structure of the purine-based inhibitor CNF 2024/BIIB021 [298, 299]. (**k**) Structure of the purine-based inhibitor MPC-3100 [305]. (**l**) Structure of SNX-5422 a pyrazole containing inhibitor [301]. (**m**) Structure of Debio 0932. (**n**) Structure of PU-H71 [306]

may, in part, be due to the fact that Hsp90 in cancer cells is to a significant degree tied up in large multichaperone–client protein complexes, and it has been suggested that these complexes have a higher affinity for the inhibitors than the Hsp90 in normal cells, in which a much smaller fraction is associated with co-chaperones and clients [310]. Although this work has come in for some criticism, many groups finding it difficult to reproduce the results, recent studies also suggest that there are distinct differences in the complexes that Hsp90 forms in cancer vs normal cells.

9.1.2 Alternative Modes of Hsp90 Inhibition by Small Molecule Inhibitors

A number of other small molecules have also been discovered which interact with and disrupt the activity of Hsp90 but which do not bind to the ATP-binding site in the N-terminal domain [313]. There is growing interest in these as modulators of Hsp90 activity which can either be used in in vivo studies of Hsp90 function or as potential therapeutics. Novobiocin is a coumarin antibiotic (Fig. 9a) which can be isolated from strains of *Streptomyces* [318] and which has long been known to bind to the C-terminal domain of Hsp90, albeit weakly [314]. In addition to its potent activity against Gram-negative bacteria [318], novobiocin has also been shown to have anti-tumour activity against breast cancer cells. It does not affect the ATPase activity of Hsp90 but binds to a site in the C-terminal domain [319] which results in

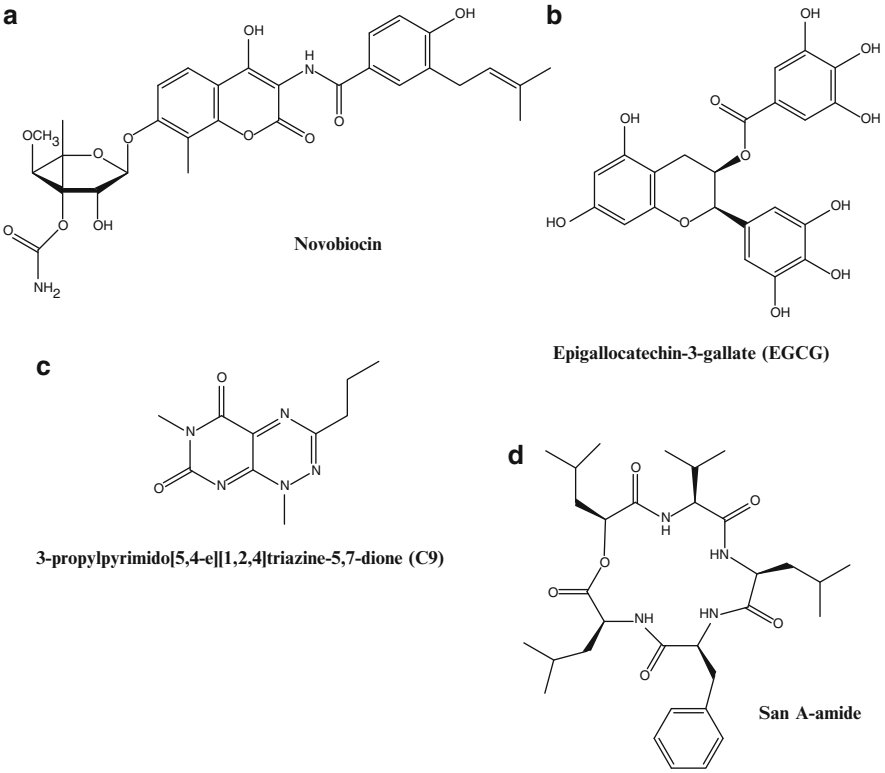

Fig. 9 Small molecular inhibitors of Hsp90 function which do not bind to the N-terminal ATP-binding site. (**a**) Structure of novobiocin, a coumarin antibiotic from *Streptomyces* [314]. (**b**) Structure of epigallocatechin-3-gallate (EGCG), a polyphenolic component of green tea [315]. (**c**) Structure of C9 (3-propylpyrimido[5,4-*e*][1,2,4]triazine-5,7-dione) which disrupts binding of the cochaperone Hop and shows activity in breast cancer cell lines [316]. (**d**) Structure of sansalvarnide A-amide (San A-amide) which allosterically disrupts the binding of proteins to the C-terminal domain of Hsp90 [317]

disruption of cochaperone binding and degradation of clients. Numerous studies have undertaken structure–activity relationships (SAR) on novobiocin derivatives and have developed compounds with 1,000-fold greater efficacy than novobiocin itself [320–327].

Epigallocatechin-3-gallate (EGCG) (Fig. 9b), one of the polyphenolic components of green tea, has also been shown to bind to the C-terminal domain of Hsp90, disrupt its function and inhibit the activity of some of its clients including telomerase, some kinases and AhR [315]. In addition, there is also evidence that cisplatin can bind to the C-terminal domain of Hsp90 and it has been proposed that some of the anti-cancer activity of cisplatin may be due to Hsp90 inhibition [328].

The studies described above identified known natural products or anti-cancer agents as inhibitors of Hsp90 function and established that they acted through

a mechanism which involves binding to the C-terminal domain. Regan and co-workers have recently used a novel approach to select and develop molecules which block binding of TPR-domain cochaperones including Hop to Hsp90 and so inhibit the activity of Hsp90. Their first study used AlphaScreen technology to set up a high-throughput screen (HTS) for compounds that disrupt the interaction between Hsp90 and Hop [329]. Using this approach, compounds were identified that were active in vivo against a number of different cancer cell lines, and which resulted in a decrease in the levels of Hsp90 clients such as Her2 (associated with breast cancer), consistent with the action of the well established inhibitors which bind to the ATP binding site [330]. In addition, they designed and engineered TPR proteins which bind to the C-terminal MEEVD motif of Hsp90 with higher affinities than Hop itself, thus acting as competitive inhibitors of Hop binding and reducing Hsp90 function in vivo [331]. These proteins were also active against a breast cancer cell line and also reduced levels of Her2 [331]. One of the compounds from the AlphaScreen HTS, 3-propylpyrimido[5,4-*e*][1,2,4]triazine-5,7-dione, also known as C9 (Fig. 9c), was recently shown to be effective in killing a number of different breast cancer cell lines [316]. Of particular interest in this study was the fact that C9 does not up-regulate the expression of Hsp70, which occurs with the ATP-binding site inhibitors and which partially counteracts the beneficial effects of Hsp90 inhibition [316].

Sansalvarnide A-amide (San A-amide) is another example of a small molecule inhibitor of Hsp90 action that specifically binds to a region encompassing both N-terminal and middle domains of Hsp90. It has been shown to disrupt allosterically the binding of proteins to the C-terminal domain of Hsp90, thus disrupting function and thereby affecting a subset of cancer-related pathways [317].

Hsp90 as a cancer target is, of course, a huge topic in its own right and much of the research that has been done in this area is beyond the scope of this review. Interested readers are directed towards some of the many recent reviews on this subject [298, 299, 303, 304, 332–335].

9.2 Hsp90 as a Target of Anti-viral Drugs

It is now well established that Hsp90 is required for the correct folding, maturation and assembly of many viral proteins and that the replication of many viruses is hypersensitive to Hsp90 inhibition [14, 336]. Viral client proteins of Hsp90 includes a large number of viral polymerases from both DNA and RNA viruses, such as DHBV (duck hepatitis virus), influenza virus A, HSV-1 (herpes simplex virus type 1) and FHV (Nodaviridae flock house virus). Hsp90 is also required for the activity of other viral proteins such as the large T antigen of SV40, a protease and helicase form HCV (hepatitis C virus), as well as viral capsid proteins; see the recent review by Frydman and co-workers for further details [14]. In the case of capsid proteins, it is thought that Hsp90 is required as these clients need to be metastable, that is they must be sufficiently stable to withstand harsh extracellular conditions at the same time as needing to disassemble once inside cells. It has also

already been shown that inhibition of Hsp90 with classic inhibitors such as geldanamycin and radicicol reduces viral activity and that they act broadly on a wide range of different viruses. In addition, and perhaps of crucial importance, is the emerging recognition that inhibition of host Hsp90 results in anti-viral activity in which the virus cannot develop drug resistance [337]. The results of many studies highlight the potential of Hsp90 inhibitors as antiviral agents [14, 336].

9.3 Hsp90 as a Therapeutic Target for Neurodegenerative Diseases

In recent years there has been increasing interest in Hsp90 as a target for a number of other disease states including many neurodegenerative disorders. Neurodegenerative diseases such as Alzheimer's disease (AD), Parkinson's disease (PD) and other dementias are characterised by the accumulation of both soluble, oligomeric forms of specific proteins and aggregated sometimes amyloid-like insoluble fibrils [338]. In many cases, molecular chaperones including Hsp90 are found to co-localise in the aggregates either with the Alzheimer's-associated Aβ plaques, the neurofibrillar tangles (NFTs) formed by phosphorylated tau, or in Parkinson's disease in the Lewy bodies formed by α-synuclein [339, 340].

Proteomics techniques have begun to identify the changes in protein expression and the post-translational modifications in the brains of people affected by Alzheimer's disease and a recent study has identified that Hsp90 levels are significantly increased in the hippocampus of AD brains [341], whilst other studies have shown that the levels of phosphorylated Hsp90 are reduced in PD brains [342, 343].

9.3.1 Hsp90 and Tau

Clinical evidence for a potential role of Hsp90 in neurodegenerative diseases, and tauopathies in particular, has come from a number of studies. It has been demonstrated that the expression of Hsp90 is altered in AD brains compared to normal controls [344] and that there is an inverse correlation between the levels of many Hsps including Hsp90 and the amount of NFTs in human brains showing varying degrees of NFT formation [345]. In addition, earlier studies using mouse models established an inverse relationship between accumulated tau and the levels of both Hsp70 and Hsp90 in transgenic mice [346, 347]. These studies also demonstrated that increasing the level of the chaperones in cell culture resulted in an increase in tau solubility and binding to microtubules, as well as decreased phosphorylation of tau, with opposite effects resulting from depletion of Hsp70 or Hsp90 [346, 347]. Both of the chaperones were shown to facilitate degradation of tau, especially mutant tau [346, 347].

Early studies using a high-throughput screen identified inhibitors of Hsp90 which significantly reduced the levels of soluble tau in vivo [348]. At the time, this was attributed to the fact that inhibition of Hsp90 up-regulates the cellular heat shock response through Hsp90 binding to and repressing HSF1, the major cellular heat shock transcription factor. Although the induction of many molecular chaperones through the heat shock response may be one mechanism by which Hsp90 inhibitors show neuroprotective properties (and this has been shown for derivatives of novobiocin) [349–351], it is now clear that other pathways may also be important. In a follow-up study, Dickey and co-workers established that Hsp90 inhibitors lead to the selective clearance of tau phosphorylated at proline-linked Ser and Thr sites such as pS202/T205 and pS396/S404 and also conformationally altered tau [352]. These studies also showed that the clearance was due to degradation via the proteasome. Interestingly, other forms of phosphorylated tau (such as at S262/S356) were minimally perturbed by Hsp90 inhibitors. Further studies have confirmed the earlier work and shown that Hsp90 inhibitors can eliminate aggregated forms of tau in both cellular and mouse models of tauopathies, and have shown that the effects might be mediated by changes in stability of the tau kinase p35, an Hsp90 client [353]. This mechanism has also been suggested for another tau kinase which is a client of Hsp90 – GSK3β [354, 355] as well as Akt which is an Hsp90 client and also known to regulate tau biology. In this case, the possible mechanism by which Hsp90 inhibition leads to the clearance of tau is complex – Akt is known to regulate the Hsp90.CHIP complex, the expression of CHIP, as well as potentially acting as a competitive binder for the Hsp90.CHIP complex, or itself it may act on a tau kinase [356].

Clearly there are effects of Hsp90 inhibition on tauopathies which are independent of the heat shock response, and this has been shown in both cellular and mouse models. In these studies the effects were dependent upon the Hsp90 co-chaperone CHIP, a ubiquitin E3 ligase [357]. In addition to the cochaperone CHIP, the cochaperone FKBP51 has also been shown to play a role in tauopathies [358]. FKBP51 prevents the clearance of tau and also regulates its phosphorylation status, an action which is mediated by the PPIase domain of FKBP51, as well as stabilising the interaction of tau with microtubules [358]. FKBP51 enhances the association of tau with Hsp90 but interaction with FKBP51 is independent of Hsp90 and a model has been proposed in which the Hsp90-FKBP51 complex isomerises tau, thereby altering its phosphorylation state (tau has a number of proline-directed phosphorylation sites where the phosphorylation depends upon whether the prolyl peptide bonds is *cis* or *trans*). These studies have established a central role of Hsp90 in both Alzheimer's disease and other tauopathies.

A number of studies have linked Hsp90 function with both tau and also α-synuclein, another amyloidogenic protein whose misfolding has been associated with Parkinson's disease (PD). In one study, the two proteins were found to interact directly and α-synuclein was shown to induce the fibrillisation of tau [359]. Interestingly, the interaction was abolished by the P301L mutation in tau and the interaction restored by the induction of Hsp70 and Hsp90 [359]. A later study found tau in inclusions of α-synuclein supporting the idea that this protein can induce the

aggregation of tau [360]. The next section discusses the link between Hsp90 and α-synuclein in more detail.

9.3.2 Hsp90 and α-Synuclein

Studies have shown that Hsp90 is the predominant molecular chaperone found in Lewy bodies, of which α-synuclein is a major component, as well as other inclusions associated with PD, and the levels of Hsp90 are the most predominantly increased in PD brains [361]. Mouse and cell culture studies have found the same [361]. In addition, yeast screens for suppressors of α-synuclein toxicity identified 40 genes of which Hsp90 was one of the top five [362]. Interestingly, this study also showed that Hsp90 (as well as some of the other genes identified) failed to protect against A30P or A35T mutant forms of α-synuclein and only had protective activity towards the wild-type protein [362].

The exact mechanism(s) by which Hsp90 exerts its protective effects relating to α-synuclein aggregation, toxicity and PD are unknown; however, a number of cellular processes may be involved including the clearance of α-synuclein by different degradative pathways. α-Synuclein has been shown to be degraded by chaperone-mediated autophagy (CMA) in which Hsp90 plays a central role [363]. In addition, clearance of misfolded proteins associated with PD can also occur through the formation of an aggresome, and inhibition of Hsp90 (as well as inhibition of the proteasome) has been shown to increase the targeting of such proteins to this inclusion body [364]. Thus, Hsp90 may play a key role in the degradation of α-synuclein, thereby alleviating the toxicity associated with its accumulation and misfolding/aggregation.

A more direct link between Hsp90 and the aggregation of α-synuclein has also been established by in vitro studies which show that Hsp90 can directly affect (both increase and decrease) the fibrillisation of wild-type α-synuclein, the effect depending upon whether ATP is present or not [365]. This is an interesting study, and a similar study on the aggregation kinetics of A53T α-synuclein in the author's laboratory has shown that Hsp90 also inhibits the aggregation and fibril formation of this mutant form, but, in contrast to the other study, under no conditions was Hsp90 found to promote fibril formation (Daturpalli and Jackson, unpublished results).

An extracellular form of α-synuclein has recently been proposed whose secretion depends upon the Hsp90 client protein, Rab11a [366, 367]. Inhibition of Hsp90 therefore prevents the secretion of α-synuclein, the extra-cellular form of which has been proposed to exert toxic effects [368].

In addition to its effect on α-synuclein, Hsp90 may also play a role in the function and activity of other PD-related proteins. Similar to its role with tau, the Hsp90-CHIP complex has been implicated in the degradation of another mutant protein associated with PD, LRRK2 [369], showing that the cellular levels of many of the proteins that misfold and which are associated with neurodegenerative disorders are regulated by Hsp90 complexes.

In contrast to the role of Hsp90 in cancer, much less is known about its role in neurodegenerative disorders. However, there are some excellent recent reviews on Hsp90 and Parkinson's disease and interested readers are directed towards these [13, 370–373].

9.3.3 Hsp90 and Amyloid in General

In addition to tau and α-synuclein, numerous other peptides and proteins can aggregate to form oligomers and fibrils which are also associated with different disease states; this includes amyloid-beta (Aβ), a short 40-residue or 42-residue peptide which forms amyloid plaques in Alzheimer's disease [338], transthyretin which results in another amyloidosis disease [374, 375] and huntingtin in Huntington's disease [376] amongst many others. Hsp90 and its homologues have also been implicated in the aggregation of these systems.

There is growing evidence that Hsp90 controls the amount of soluble Aβ in both in vitro and in vivo experiments. Hsp90 has been shown to affect Aβ aggregation in vitro at sub-stoichiometric concentrations [377], and results of this study suggest that it induces structural changes in the oligomers but not the fibrillar form of the peptide [377]. These results have also recently been confirmed in the author's laboratory (Kjaergaard, Daturpalli and Jackson, unpublished results). Hsp90, as well as Hsp32 and Hsp70, have been shown to increase phagocytosis and clearance of $A\beta_{1-42}$ peptides in in vitro microglial culture, and intrahippocampal injection of $A\beta_{1-42}$ resulted in microglial accumulation whilst Hsp90 significantly reduced the amounts of $A\beta_{1-42}$ and increased the production of cytokines, suggesting that Hsp90 may facilitate the clearance of $A\beta_{1-42}$ in vivo [378]. Other studies have shown that the levels of Hsp90 are increased in both the cellular and membranous fractions of AD brains, and Hsp90 co-localises with amyloid plaques [379]. Hsp90, together with Hsp60 and Hsp70, have both, alone and in combination, been shown to protect cells against intracellular Aβ stress through maintenance of mitochrondrial oxidative phosphorylation and the function of tricarboxylic acid cycle enzymes [380]. Rapid screening assays have been developed and designed to identify potential small molecule drugs which can protect cells against Aβ toxicity. A number of Hsp90 inhibitors have been screened in this way and novobiocin analogues shown to be effective without being toxic [350, 351]. Treatment of mammalian cells with geldanamycin at nanomolar concentrations induces expression of Hsp40, Hsp70 and Hsp90 and inhibits the aggregation of huntingtin [381].

Other homologues of Hsp90, including the ER resident Grp94, have also been shown to play a potential role in amyloidosis diseases. Grp94 was shown to be up-regulated during the expression of mutant forms of transthyretin [382]. In an interesting recent development, it has been shown that the Hsp90–cochaperone p23 can itself form amyloid-like fibrillar structures when treated with the small molecule celastrol which is known to inhibit the Hsp90 machinery [383]. In a different study, celastrol was shown to reduce Aβ pathology in transgenic mice [384].

These studies all suggest that Hsp90 as well as its cochaperones control the proteostasis of numerous peptides and proteins which are amyloidogenic and linked with disease states. Several good reviews have been published on Hsp90 and neurodegenerative diseases and interested readers are directed to the references [385–389].

9.4 Hsp90 as a Therapeutic Target Against Protozoan Infections

In recent years there has been increasing interest in targeting Hsp90 in diseases other than cancer [390]. Hsp90 is known to affect important cellular transformations of intracellular protozoan parasites and human pathogens including *Trypanosoma* (strains of which are responsible for Chagas' disease and sleeping sickness), *Leishmania* (strains of which cause leishmanasis), *Toxoplasma*, and *Plasmodium* (strains of which cause malaria). These parasites have evolved a relatively expanded or diverse complement of genes encoding molecular chaperones, presumably resulting from the fact that these parasites have to survive potentially hostile environments and their life cycles can involve multiple changes in environmental conditions including changes in temperature, pH, oxidative stress as well as desiccation [15]. For example, in *L. major* there are 17 copies of Hsp90 genes (many of which encode proteins with nearly identical sequences), and *Leishmania* also have a single copy of Grp94 which is thought to play a role in virulence [391]. In *L. donovani* it is estimated that Hsp90 constitutes some 3% of total protein content in the promastigotes stage [392]. There is also plenty of evidence for a plethora of Hsp90 cochaperones in *Leishmania* [391].

In *Trypanosoma cruzi* (the causative agent of Chagas' disease), there is a major cytosolic Hsp90 along with six homologous genes, three genes encoding Grp94 homologues and two genes encoding TRAP1 homologues [391]. Geldanamycin has been shown to cause growth arrest in *T. cruzi*; it is thought by preventing the maturation of proteins involved in epimastigote differentiation [393]. In mouse models of *Trypanasoma evansi*, treatment with inhibitors such as GA and 17-DMAG have been shown to be effective in attenuating parasite growth and prolonging survival [181].

Five *Plasmodium* species cause malaria, the most severe being *P. falciparum* and its genome contains 95 molecular chaperones of which there are 4 Hsp90s [394, 395]. PfHsp90 has been shown to be essential for the development of the parasite, and treatment with GA or 17-DMAG has been shown to be effective in attenuating parasite growth and prolonging survival [181]. PfHsp90 has been implicated in a number of processes on which the parasites are reliant: it has been associated with ferriprotoporphyrin, a product of haem metabolism (the parasite gets much of its nutrients from the digestion of haemoglobin). PfHsp90 is also thought to play a role in chromatin remodelling (this class of parasite relies heavily on epigenetic regulation as it has few transcription factors), and also drug resistance through a potential interaction with a putative PgP-like ABC transporter.

In *P. falciparum*, some Hsp90 cochaperones have also been demonstrated to play important cellular roles; Pf p23, for example, has been shown to be involved in DNA metabolism. Hsp90 in *P. falciparum* (PfHsp90) plays a critical role in regulating ring to trophozoite stage transition in the parasite [396]. There are significant sequence differences between human and PfHsp90 (about 40% sequence identity) making it an attractive and potentially tractable target for the generation of specific inhibitors [390].

Toxoplasma gondii is a parasite which normally affects only domestic and wild cats; however, it is an opportunistic infection in immune-compromised individuals, e.g. those who have HIV/AIDS. Heat shock proteins in general and Hsp90 have been implicated in the development and pathogenesis of this parasite [397–400]. Inhibition of TgHsp90 by GA has been shown to reduce growth in the tachzygote stage in the parasitic life cycle [400]. A number of Hsp90–cochaperone complexes have been identified in *T. gondii* and, along with genome data of 19 obligate parasites, suggest these species have complex networks of chaperones similar to higher eukaryotes [3, 4]. It is thought that the exact distribution of Hsp90 cochaperones may vary across species. In these cases, Hsp90 and many other molecular chaperones are key in triggering important stage transitions during their life cycles [15].

For a recent review of the role of molecular chaperones in the development and pathogenesis of intracellular protozoan parasites and as a potential drug target against such parasitic diseases see reviews [15, 401].

10 Final Comments

When I first started writing this chapter I already knew it would be a formidable task to try and summarise and review all the literature on Hsp90 from recent years. A quick search in PubMed reveals at least 1,365 papers published on this topic in 2011 alone. I will undoubtedly have missed out many excellent research papers and in attempting to review the field I have, of course, focussed on those areas which reflect my own interests. In those sections of the review where I have only been able to give the briefest of summaries, I hope to have provided references to recent reviews which will allow the interested reader to go further.

I don't think it could be clearer what an important protein Hsp90 is and in how many different cellular processes it plays a critical role. Despite the major advances in the field in the last 10 years, many of which have been discussed here, there remain key fundamental questions on how the molecular chaperone machine centred around Hsp90 works. In particular, we have only just begun to investigate the diversity of complexes that can be formed by Hsp90, its cochaperones and clients and we have to establish exactly which are relevant in vivo and exactly what role they play in the assembly and activation of clients. Perhaps more importantly, we are far from understanding what is happening to the client proteins as they interact with the Hsp90 machinery and progress through the reaction cycle, and

why certain proteins with very differing structures and functions require the action of this complex chaperone apparatus.

Acknowledgements I would like to thank my research group and collaborators (both past and present) for many interesting and informative discussions over the years. In addition, I'd like to thank everyone in the Hsp90 community, particularly Prof. Johannes Buchner and Prof. Didier Picard for providing us with many fantastic meetings in beautiful locations. Finally, I would like to dedicate this review to my father, who sadly passed away whilst I was writing it. Without his love and support over many years I am sure I would not have got this far.

References

1. Burrows F, Zhang H et al (2004) Hsp90 activation and cell cycle regulation. Cell Cycle 3(12):1530–1536
2. Pearl LH, Prodromou C (2000) Structure and in vivo function of Hsp90. Curr Opin Struct Biol 10(1):46–51
3. Echeverria PC, Picard D (2010) Molecular chaperones, essential partners of steroid hormone receptors for activity and mobility. Biochim Biophys Acta 1803(6):641–649
4. Echeverria PC, Figueras MJ et al (2010) The Hsp90 co-chaperone p23 of toxoplasma gondii: identification, functional analysis and dynamic interactome determination. Mol Biochem Parasitol 172(2):129–140
5. Seo NS, Lee SK et al (2008) The HSP90-SGT1-RAR1 molecular chaperone complex: a core modulator in plant immunity. J Plant Biol 51(1):1–10
6. Taipale M, Jarosz DF et al (2010) HSP90 at the hub of protein homeostasis: emerging mechanistic insights. Nat Rev Mol Cell Biol 11(7):515–528
7. Balch WE, Morimoto RI et al (2008) Adapting proteostasis for disease intervention. Science 319(5865):916–919
8. Gidalevitz T, Prahlad V et al (2011) The stress of protein misfolding: from single cells to multicellular organisms. Cold Spring Harb Perspect Biol 3(6)
9. Powers ET, Morimoto RI et al (2009) Biological and chemical approaches to diseases of proteostasis deficiency. Annu Rev Biochem 78:959–991
10. Voisine C, Pedersen JS et al (2010) Chaperone networks: tipping the balance in protein folding diseases. Neurobiol Dis 40(1):12–20
11. Neckers L, Workman P (2012) Hsp90 molecular chaperone inhibitors: are we there yet? Clin Cancer Res 18(1):64–76
12. Miyata Y, Koren J et al (2011) Molecular chaperones and regulation of tau quality control: strategies for drug discovery in tauopathies. Future Med Chem 3(12):1523–1537
13. Kalia SK, Kalia LV et al (2010) Molecular chaperones as rational drug targets for Parkinson's disease therapeutics. CNS Neurol Disord Drug Targets 9(6):741–753
14. Geller R, Taguwa S et al (2012) Broad action of Hsp90 as a host chaperone required for viral replication. Biophys Biochim Acta 1823:698–706
15. Shonhai A, Maier AG et al (2011) Intracellular protozoan parasites of humans: the role of molecular chaperones in development and pathogenesis. Protein Pept Lett 18(2):143–157
16. Hartson SD, Matts RL (2012) Approaches for defining the Hsp90-dependent proteome. Biophys Biochim Acta 1823:656–667
17. Zhao RM, Davey M et al (2005) Navigating the chaperone network: an integrative map of physical and genetic interactions mediated by the Hsp90 chaperone. Cell 120(5):715–727
18. McClellan AJ, Xia Y et al (2007) Diverse cellular functions of the Hsp90 molecular chaperone uncovered using systems approaches. Cell 131(1):121–135
19. Sanchez ER, Toft DO et al (1985) Evidence that the 90-kDa phosphoprotein associated with the untransformed L-cell glucocorticoid receptor is a murine heat-shock protein. J Biol Chem 260(23):2398–2401

20. Catelli MG, Binart N et al (1985) The common 90-kD protein-component of non-transformed 8S steroid-receptors is a heat-shock protein. EMBO J 4(12):3131–3135
21. Picard D (2006) Chaperoning steroid hormone action. Trends Endocrinol Metab 17(6):229–235
22. Pratt WB, Toft DO (1997) Steroid receptor interactions with heat shock protein and immunophilin chaperones. Endocr Rev 18(3):306–360
23. Schuh S, Yonemoto W et al (1985) A 90,000-dalton binding-protein common to both steroid-receptors and the Rous-sarcoma virus transforming protein, PP60V-SRC. J Biol Chem 260(26):4292–4296
24. Sumanasekera WK, Tien ES et al (2003) Heat shock protein-90 (Hsp90) acts as a repressor of peroxisome proliferator-activated receptor-alpha (PPAR alpha) and PPAR beta activity. Biochemistry 42(36):10726–10735
25. Chen HS, Singh SS et al (1997) The Ah receptor is a sensitive target of geldanamycin-induced protein turnover. Arch Biochem Biophys 348(1):190–198
26. Yoshinari K, Kobayashi K et al (2003) Identification of the nuclear receptor CAR:HSP90 complex in mouse liver and recruitment of protein phosphatase 2A in response to phenobarbital. FEBS Lett 548(1–3):17–20
27. Squires EJ, Sueyoshi T et al (2004) Cytoplasmic localization of pregnane X receptor and ligand-dependent nuclear translocation in mouse liver. J Biol Chem 279(47):49307–49314
28. Angelo G, Lamon-Fava S et al (2008) Heat shock protein 90 beta: a novel mediator of vitamin D action. Biochem Biophys Res Commun 367(3):578–583
29. Smith DF, Toft DO (2008) The intersection of steroid receptors with molecular chaperones: observations and questions. Mol Endocrinol 22(10):2229–2240
30. Zuehlke A, Johnson JL (2010) Hsp90 and co-chaperones twist the functions of diverse client proteins. Biopolymers 93(3):211–217
31. Sanchez ER (2012) Chaperoning steroidal physiology: lessons from mouse genetic models of Hsp90 and its cochaperones. Biophys Biochim Acta 1823:722–729
32. Pratt WB, Galigniana MD et al (2004) Role of molecular chaperones in steroid receptor action. Essays Biochem 40:41–58
33. Tillotson B, Slocum K et al (2010) Hsp90 (Heat Shock Protein 90) inhibitor occupancy is a direct determinant of client protein degradation and tumor growth arrest in vivo. J Biol Chem 285(51):39835–39843
34. Kundrat L, Regan L (2010) Balance between folding and degradation for Hsp90-dependent client proteins: a key role for CHIP. Biochemistry 49(35):7428–7438
35. Kundrat L, Regan L (2010) Identification of residues on Hsp70 and Hsp90 ubiquitinated by the cochaperone CHIP. J Mol Biol 395(3):587–594
36. Makhnevych T, Houry WA (2012) The role of Hsp90 in protein complex assembly. Biophys Biochim Acta 1823:674–682
37. Johnson JL (2012) Evolution and function of diverse Hsp90 homologs and cochaperone proteins. Biophys Biochim Acta 1823:607–613
38. Johnson JL, Brown C (2009) Plasticity of the Hsp90 chaperone machine in divergent eukaryotic organisms. Cell Stress Chaperones 14(1):83–94
39. Stechmann A, Cavalier-Smith T (2004) Evolutionary origins of Hsp90 chaperones and a deep paralogy in their bacterial ancestors. J Eukaryot Microbiol 51(3):364–373
40. Lund PA (2001) Microbial molecular chaperones. Adv Microb Physiol 44(44):93–140
41. Nathan DF, Vos MH et al (1997) In vivo functions of the *Saccharomyces cerevisiae* Hsp90 chaperone. Proc Natl Acad Sci USA 94(24):12949–12956
42. Picard D, Khursheed B et al (1990) Reduced levels of HSP90 compromise steroid-receptor action in vivo. Nature 348(6297):166–168
43. Grad I, Cederroth CR et al (2010) The molecular chaperone Hsp90 alpha is required for meiotic progression of spermatocytes beyond pachytene in the mouse. PLoS One 5(12)

44. Maynard JC, Pham T et al (2010) Gp93, the Drosophila GRP94 ortholog, is required for gut epithelial homeostasis and nutrient assimilation-coupled growth control. Dev Biol 339(2):295–306
45. Cao DS, Froehlich JE et al (2003) The chlorate-resistant and photomorphogenesis-defective mutant cr88 encodes a chloroplast-targeted HSP90. Plant J 33(1):107–118
46. Saito M, Watanabe S et al (2008) Interaction of the molecular chaperone HtpG with uroporphyrinogen decarboxylase in the cyanobacterium Synechococcus elongatus PCC 7942. Biosci Biotechnol Biochem 72(5):1394–1397
47. Sato T, Minagawa S et al (2010) HtpG, the prokaryotic homologue of Hsp90, stabilizes a phycobilisome protein in the cyanobacterium Synechococcus elongatus PCC 7942. Mol Microbiol 76(3):576–589
48. Thomas JG, Baneyx F (2000) ClpB and HtpG facilitate de novo protein folding in stressed Escherichia coli cells. Mol Microbiol 36(6):1360–1370
49. Haslbeck V, Kaiser CJO et al (2011) Hsp90 in non-mammalian metazoan model systems. Biophys Biochim Acta
50. Tsutsumi S, Mollapour M et al (2012) Charged linker sequence modulates eukaryotic heat shock protein 90 (Hsp90) chaperone activity. Proc Natl Acad Sci USA 109:2937–2942
51. Obermann WMJ, Sondermann H et al (1998) In vivo function of Hsp90 is dependent on ATP binding and ATP hydrolysis. J Cell Biol 143(4):901–910
52. Prodromou C, Roe SM et al (1997) Identification and structural characterization of the ATP/ADP-binding site in the Hsp90 molecular chaperone. CeN 90(1):65–75
53. Prodromou C, Roe SM et al (1997) A molecular clamp in the crystal structure of the N-terminal domain of the yeast Hsp90 chaperone. Nat Struct Biol 4(6):477–482
54. Roe SM, Prodromou C et al (1999) Structural basis for inhibition of the Hsp90 molecular chaperone by the antitumor antibiotics radicicol and geldanamycin. J Med Chem 42(2):260–266
55. Stebbins CE, Russo AA et al (1997) Crystal structure of an Hsp90-geldanamycin complex: targeting of a protein chaperone by an antitumor agent. CeN 89(2):239–250
56. Jez JM, Chen JCH et al (2003) Crystal structure and molecular modeling of 17-DMAG in complex with human Hsp90. Chem Biol 10(4):361–368
57. Soldano KL, Jivan A et al (2003) Structure of the N-terminal domain of GRP94 – basis for ligand specificity and regulation. J Biol Chem 278(48):48330–48338
58. Meyer P, Prodromou C et al (2003) Structural and functional analysis of the middle segment of Hsp90: implications for ATP hydrolysis and client protein and cochaperone interactions. Mol Cell 11(3):647–658
59. Harris SF, Shiau AK et al (2004) The crystal structure of the carboxy-terminal dimerization domain of htpG, the Escherichia coli Hsp90, reveals a potential substrate binding site. Structure 12(6):1087–1097
60. Wright L, Barril X et al (2004) Structure-activity relationships in purine-based inhibitor binding to HSP90 isoforms. Chem Biol 11(6):775–785
61. Immormino RM, Dollins DE et al (2004) Ligand-induced conformational shift in the N-terminal domain of GRP94, an Hsp90 chaperone. J Biol Chem 279(44):46162–46171
62. Kreusch A, Han SL et al (2005) Crystal structures of human HSP90 alpha-complexed with dihydroxyphenylpyrazoles. Bioorg Med Chem Lett 15(5):1475–1478
63. Huai Q, Wang HC et al (2005) Structures of the N-terminal and middle domains of E-coli Hsp90 and conformation changes upon ADP binding. Structure 13(4):579–590
64. Dollins DE, Immormino RM et al (2005) Structure of unliganded GRP94, the endoplasmic reticulum Hsp90 – basis for nucleotide-induced conformational change. J Biol Chem 280(34):30438–30447
65. Dymock BW, Barril X et al (2005) Novel, potent small-molecule inhibitors of the molecular chaperone Hsp90 discovered through structure-based design. J Med Chem 48(13):4212–4215

66. Cheung KMJ, Matthews TP et al (2005) The identification, synthesis, protein crystal structure and in vitro biochemical evaluation of a new 3,4-diarylpyrazole class of Hsp90 inhibitors. Bioorg Med Chem Lett 15(14):3338–3343
67. Brough PA, Barril X et al (2005) 3-(5-Chloro-2,4-dihydroxyphenyl)-pyrazole-4-carboxamides as inhibitors of the Hsp90 molecular chaperone. Bioorg Med Chem Lett 15(23):5197–5201
68. Barril X, Brough P et al (2005) Structure-based discovery of a new class of Hsp90 inhibitors. Bioorg Med Chem Lett 15(23):5187–5191
69. Barril X, Beswick MC et al (2006) 4-Amino derivatives of the Hsp90 inhibitor CCT018159. Bioorg Med Chem Lett 16(9):2543–2548
70. Richter K, Moser S et al (2006) Intrinsic inhibition of the Hsp90 ATPase activity. J Biol Chem 281(16):11301–11311
71. Ali MMU, Roe SM et al (2006) Crystal structure of an Hsp90-nucleotide-p23 Sba1 closed chaperone complex. Nature 440(7087):1013–1017
72. Immormino RM, Kang YL et al (2006) Structural and quantum chemical studies of 8-aryl-sulfanyl adenine class Hsp90 inhibitors. J Med Chem 49(16):4953–4960
73. Shiau AK, Harris SF et al (2006) Structural analysis of E-coli hsp90 reveals dramatic nucleotide-dependent conformational rearrangements. Cell 127(2):329–340
74. Proisy N, Sharp SY et al (2006) Inhibition of Hsp90 with synthesis macrolactones: synthesis and structural and biological evaluation of ring and conformational analogs of radicicol. Chem Biol 13(11):1203–1215
75. Dollins DE, Warren JJ et al (2007) Structures of GRP94-nucleotide complexes reveal mechanistic differences between the Hsp90 chaperones. Mol Cell 28(1):41–56
76. Brough PA, Aherne W et al (2008) 4,5-Diarylisoxazole HSP90 chaperone inhibitors: potential therapeutic agents for the treatment of cancer. J Med Chem 51(2):196–218
77. Barta TE, Veal JM et al (2008) Discovery of benzamide tetrahydro-4H-carbazol-4-ones as novel small molecule inhibitors of Hsp90. Bioorg Med Chem Lett 18(12):3517–3521
78. Martin CJ, Gaisser S et al (2008) Molecular characterization of macbecin as an Hsp90 inhibitor. J Med Chem 51(9):2853–2857
79. Huth JR, Park C et al (2007) Discovery and design of novel HSP90 inhibitors using multiple fragment-based design strategies. Chem Biol Drug Des 70(1):1–12
80. Gopalsamy A, Shi MX et al (2008) Discovery of benzisoxazoles as potent inhibitors of chaperone heat shock protein 90. J Med Chem 51(3):373–375
81. Zhang MH, Boter M et al (2008) Structural and functional coupling of Hsp90-and Sgt1-centred multi-protein complexes. EMBO J 27(20):2789–2798
82. Zhang MQ, Gaisser S et al (2008) Optimizing natural products by biosynthetic engineering: discovery of nonquinone Hsp90 inhibitors. J Med Chem 51(18):5494–5497
83. Kung PP, Funk L et al (2008) Dihydroxylphenyl amides as inhibitors of the Hsp90 molecular chaperone. Bioorg Med Chem Lett 18(23):6273–6278
84. Prodromou C (2009) Strategies for stalling malignancy: targeting cancer's addiction to Hsp90. Curr Top Med Chem 9(15):1352–1368
85. Barker JJ, Barker O et al (2009) Fragment-based identification of Hsp90 inhibitors. ChemMedChem 4(6):963–966
86. Feldman RI, Mintzer B et al (2009) Potent triazolothione inhibitor of heat-shock protein-90. Chem Biol Drug Des 74(1):43–50
87. Brough PA, Barril X et al (2009) Combining hit identification strategies: fragment-based and in silico approaches to orally active 2-aminothieno 2,3-d pyrimidine inhibitors of the Hsp90 molecular chaperone. J Med Chem 52(15):4794–4809
88. Cho-Schultz S, Patten MJ et al (2009) Solution-phase parallel synthesis of Hsp90 inhibitors. J Comb Chem 11(5):860–874
89. Kung PP, Huang BW et al (2010) Dihydroxyphenylisoindoline amides as orally bioavailable inhibitors of the heat shock protein 90 (Hsp90) molecular chaperone. J Med Chem 53(1):499–503

90. Fadden P, Huang KH et al (2010) Application of chemoproteomics to drug discovery: identification of a clinical candidate targeting Hsp90. Chem Biol 17(7):686–694
91. Murray CW, Blundell TL (2010) Structural biology in fragment-based drug design. Curr Opin Struct Biol 20(4):497–507
92. Murray CW, Carr MG et al (2010) Fragment-based drug discovery applied to Hsp90. Discovery of two lead series with high ligand efficiency. J Med Chem 53(16):5942–5955
93. Woodhead AJ, Angove H et al (2010) Discovery of (2,4-dihydroxy-5-isopropylphenyl)- 5-(4-methylpiperazin-1-ylmethyl)-1,3- dihydroisoindol-2-yl methanone (AT13387), a novel inhibitor of the molecular chaperone Hsp90 by fragment based drug design. J Med Chem 53(16):5956–5969
94. Day JEH, Sharp SY et al (2010) Inhibition of Hsp90 with resorcylic acid macrolactones: synthesis and binding studies. Chemistry-A Eur J 16(34):10366–10372
95. Corbett KD, Berger JM (2010) Structure of the ATP-binding domain of Plasmodium falciparum Hsp90. Proteins Struct Funct Bioinformatics 78(13):2738–2744
96. Barluenga S, Fontaine JG et al (2009) Inhibition of HSP90 with pochoximes: SAR and structure-based insights. Chembiochem 10(17):2753–2759
97. Nathan DF, Lindquist S (1995) Mutational analysis of HSP90 function – interactions with a steroid-receptor and a protein-kinase. Mol Cell Biol 15(7):3917–3925
98. Mickler M, Hessling M et al (2009) The large conformational changes of Hsp90 are only weakly coupled to ATP hydrolysis. Nat Struct Mol Biol 16:281–286
99. Meyer P, Prodromou C et al (2004) Structural basis for recruitment of the ATPase activator Aha1 to the Hsp90 chaperone machinery. EMBO J 23(6):1402–1410, 511
100. Meyer P, Prodromou C et al (2004) Structural basis for recruitment of the ATPase activator Aha1 to the Hsp90 chaperone machinery. EMBO J 23(3):511–519
101. Panaretou B, Siligardi G et al (2002) Activation of the ATPase activity of Hsp90 by the stress-regulated cochaperone Aha1. Mol Cell 10(6):1307–1318
102. Roe SM, Ali MMU et al (2004) The mechanism of Hsp90 regulation by the protein kinase-specific cochaperone p50(cdc37). Cell 116(1):87–98
103. Sreeramulu S, Jonker HRA et al (2009) The human Cdc37 center dot Hsp90 complex studied by heteronuclear NMR spectroscopy. J Biol Chem 284(6):3885–3896
104. Zhang MH, Kadota Y et al (2010) Structural basis for assembly of Hsp90-Sgt1-CH0RD protein complexes: implications for chaperoning of NLR innate immunity receptors. Mol Cell 39(2):269–281
105. Scheufler C, Brinker A et al (2000) Structure of TPR domain-peptide complexes: critical elements in the assembly of the Hsp70-Hsp90 multichaperone machine. Cell 101(2):199–210
106. Lee YT, Jacob J et al (2004) Human Sgt1 binds HSP90 through the CHORD-Sgt1 domain and not the tetratricopeptide repeat domain. J Biol Chem 279(16):16511–16517
107. Wu BL, Li PY et al (2004) 3D structure of human FK506-binding protein 52: implications for the assembly of the glucocorticoid receptor/Hsp90/immunophilin heterocomplex. Proc Natl Acad Sci USA 101(22):8348–8353
108. Zhang MH, Windheim M et al (2005) Chaperoned ubiquitylation – crystal structures of the CHIPU box E3 ubiquitin ligase and a CHIP-Ubc13-Uev1a complex. Mol Cell 20(4):525–538
109. Alag R, Bharatham N et al (2009) Crystallographic structure of the tetratricopeptide repeat domain of Plasmodium falciparum FKBP35 and its molecular interaction with Hsp90 C-terminal pentapeptide. Protein Sci 18(10):2115–2124
110. Cliff MJ, Harris R et al (2006) Conformational diversity in the TPR domain-mediated interaction of protein phosphatase 5 with Hsp90. Structure 14(3):415–426
111. Shirasu K, Schulze-Lefert P (2003) Complex formation, promiscuity and multi-functionality: protein interactions in disease-resistance pathways. Trends Plant Sci 8(6):252–258
112. Didenko T, Boelens R et al (2011) 3D DOSY-TROSY to determine the translational diffusion coefficient of large protein complexes. Protein Eng Des Sel 24(1–2):99–103
113. Didenko T, Duarte AMS et al (2012) Hsp90 structure and function studied by NMR spectroscopy. Biophys Biochim Acta 1823:636–647

114. Dehner A, Furrer J et al (2003) NMR chemical shift perturbation study of the N-terminal domain of Hsp90 upon binding of ADR AMP-PNP, geldanamycin, and radicicol. Chembiochem 4(9):870–877
115. Jacobs DM, Langer T et al (2006) NMR backbone assignment of the N-terminal domain of human HSP90. J Biomol NMR 36:52
116. Salek RM, Williams MA et al (2002) Letter to the editor: backbone resonance assignments of the 25kD N-terminal ATPase domain from the Hsp90 chaperone. J Biomol NMR 23(4):327–328
117. Martinez-Yamout MA, Venkitakrishnan RP et al (2006) Localization of sites of interaction between p23 and Hsp90 in solution. J Biol Chem 281(20):14457–14464
118. Hagn F, Lagleder S et al (2011) Structural analysis of the interaction between Hsp90 and the tumor suppressor protein p53. Nat Struct Mol Biol 18:1086–1093
119. Karagoz GE, Duarte AMS et al (2011) N-terminal domain of human Hsp90 triggers binding to the cochaperone p23. Proc Natl Acad Sci USA 108(2):580–585
120. Park MS, Chu FX et al (2011) Identification of cyclophilin-40-interacting proteins reveals potential cellular function of cyclophilin-40. Anal Biochem 410(2):257–265
121. Park SJ, Borin BN et al (2011) The client protein p53 adopts a molten globule-like state in the presence of Hsp90. Nat Struct Mol Biol 18(5):537–541
122. Park SJ, Kostic M et al (2011) Dynamic interaction of Hsp90 with its client protein p53. J Mol Biol 411(1):158–173
123. Dyson HJ, Kostic M et al (2008) Hydrogen-deuterium exchange strategy for delineation of contact sites in protein complexes. FEBS Lett 582(10):1495–1500
124. Retzlaff M, Hagn F et al (2010) Asymmetric activation of the Hsp90 dimer by its cochaperone Aha1. Mol Cell 37(3):344–354
125. Vaughan CK, Gohlke U et al (2006) Structure of an Hsp90-Cdc37-Cdk4 complex. Mol Cell 23(5):697–707
126. Southworth DR, Agard DA (2008) Species-dependent ensembles of conserved conformational states define the Hsp90 chaperone ATPase cycle. Mol Cell 32(5):631–640
127. Southworth DR, Agard DA (2011) Client-loading conformation of the Hsp90 molecular chaperone revealed in the cryo-EM structure of the human Hsp90:Hop complex. Mol Cell 42(6):771–781
128. Krukenberg KA, Forster F et al (2008) Multiple conformations of E-coli Hsp90 in solution: insights into the conformational dynamics of Hsp90. Structure 16(5):755–765
129. Street TO, Lavery LA et al (2011) Substrate binding drives large-scale conformational changes in the Hsp90 molecular chaperone. Mol Cell 42:96–105
130. Street TO, Lavery LA et al (2012) Cross-monomer substrate contacts reposition the Hsp90 N-terminal domain and prime the chaperone activity. J Mol Biol 415:3–15
131. Zhang W, Hirshberg M et al (2004) Biochemical and structural studies of the interaction of Cdc37 with Hsp90. J Mol Biol 340(4):891–907
132. Krukenberg KA, Street TO et al (2011) Conformational dynamics of the molecular chaperone Hsp90. Q Rev Biophys 44(2):229–255
133. Bron P, Giudice E et al (2008) Apo-Hsp90 coexists in two open conformational states in solution. Biol Cell 100(7):413–425
134. Krukenberg KA, Bottcher UMK et al (2009) Grp94, the endoplasmic reticulum Hsp90, has a similar solution conformation to cytosolic Hsp90 in the absence of nucleotide. Protein Sci 18(9):1815–1827
135. Krukenberg KA, Southworth DR et al (2009) pH-dependent conformational changes in bacterial Hsp90 reveal a Grp94-like conformation at pH 6 that is highly active in suppression of citrate synthase aggregation. J Mol Biol 390(2):278–291
136. Street TO, Krukenberg KA et al (2010) Osmolyte-induced conformational changes in the Hsp90 molecular chaperone. Protein Sci 19(1):57–65
137. Jakob U, Scheibel T et al (1996) Assessment of the ATP binding properties of Hsp90. J Biol Chem 271(17):10035–10041

138. Scheibel T, Neuhofen S et al (1997) ATP-binding properties of human Hsp90. J Biol Chem 272(30):18608–18613
139. Panaretou B, Prodromou C et al (1998) ATP binding and hydrolysis are essential to the function of the Hsp90 molecular chaperone in vivo. EMBO J 17(16):4829–4836
140. Nadeau K, Das A et al (1993) HSP90 chaperonins possess atpase activity and bind heat-shock transcription factors and peptidyl prolyl isomerases. J Biol Chem 268(2):1479–1487
141. Nardai G, Schnaider T et al (1996) Characterization of the 90 kDa heat shock protein (HSP90)-associated ATP/GTPase. J Biosci 21(2):179–190
142. Sullivan W, Stensgard B et al (1997) Nucleotides and two functional states of hsp90. J Biol Chem 272(12):8007–8012
143. Grenert JP, Sullivan WP et al (1997) The amino-terminal domain of heat shock protein 90 (hsp90) that binds geldanamycin is an ATP/ADP switch domain that regulates hsp90 conformation. J Biol Chem 272(38):23843–23850
144. Soti C, Csermely P (1998) Characterization of the nucleotide binding properties of the 90 kDa heat shock protein (Hsp90). J Biosci 23(4):347–352
145. Scheibel T, Weikl T et al (1998) Two chaperone sites in Hsp90 differing in substrate specificity and ATP dependence. Proc Natl Acad Sci USA 95(4):1495–1499
146. McLaughlin SH, Jackson SE (2002) Folding and stability of the ligand-binding domain of the glucocorticoid receptor. Protein Sci 11(8):1926–1936
147. McLaughlin SH, Smith HW et al (2002) Stimulation of the weak ATPase activity of human Hsp90 by a client protein. J Mol Biol 315(4):787–798
148. Rowlands M, McAndrew C et al (2010) Detection of the ATPase activity of the molecular chaperones Hsp90 and Hsp72 using the transcreener (TM) AdP assay kit. J Biomol Screen 15(3):279–286
149. Rowlands MG, Newbatt YM et al (2004) High-throughput screening assay for inhibitors of heat-shock protein 90 ATPase activity. Anal Biochem 327(2):176–183
150. Prodromou C, Panaretou B et al (2000) The ATPase cycle of Hsp90 drives a molecular 'clamp' via transient dimerization of the N-terminal domains. EMBO J 19(16):4383–4392
151. Weikl T, Muschler P et al (2000) C-terminal regions of Hsp90 are important for trapping the nucleotide during the ATPase cycle. J Mol Biol 303(4):583–592
152. Richter K, Muschler P et al (2001) Coordinated ATP hydrolysis by the Hsp90 dimer. J Biol Chem 276(36):33689–33696
153. McLaughlin SH, Ventouras LA et al (2004) Independent ATPase activity of Hsp90 subunits creates a flexible assembly platform. J Mol Biol 344(3):813–826
154. Prodromou C, Pearl LH (2003) Structure and functional relationships of Hsp90. Curr Cancer Drug Targets 3(5):301–323
155. Vaughan CK, Piper PW et al (2009) A common conformationally coupled ATPase mechanism for yeast and human cytoplasmic HSP90s. FEBS J 276(1):199–209
156. Prodromou C, Siligardi G et al (1999) Regulation of Hsp90 ATPase activity by tetratricopeptide repeat (TPR)-domain co-chaperones. EMBO J 18(3):754–762
157. Onuoha SC, Couistock ET et al (2008) Structural studies on the co-chaperone hop and its complexes with Hsp90. J Mol Biol 379(4):732–744
158. Yi F, Doudevski I et al (2010) HOP is a monomer: investigation of the oligomeric state of the co-chaperone HOP. Protein Sci 19(1):19–25
159. Ebong II, Morgner NM et al (2011) Heterogeneity and dynamics in the assembly of the Hsp90 chaperone complexes. Proc Natl Acad Sci USA 108:17939–17944
160. Li J, Richter K et al (2011) Mixed Hsp90-cochaperone complexes are important for the progression of the reaction cycle. Nat Struct Mol Biol 18(1):61–66
161. Li L, Lou Z et al (2011) The role of FKBP5 in cancer aetiology and chemoresistance. Br J Cancer 104(1):19–23
162. Li W, Sahu D et al (2012) Secreted heat shock protein-90 (Hsp90) in wound healing and cancer. Biophys Biochim Acta 1823:730–741

163. Siligardi G, Hu B et al (2004) Co-chaperone regulation of conformational switching in the Hsp90 ATPase cycle. J Biol Chem 279(50):51989–51998
164. Richter K, Walter S et al (2004) The co-chaperone Sba1 connects the ATPase reaction of Hsp90 to the progression of the chaperone cycle. J Mol Biol 342(5):1403–1413
165. McLaughlin SH, Sobott F et al (2006) The co-chaperone p23 arrests the Hsp90 ATPase cycle to trap client proteins. J Mol Biol 356(3):746–758
166. Siligardi G, Panaretou B et al (2002) Regulation of Hsp90 ATPase activity by the co-chaperone Cdc37p/p50(cdc97). J Biol Chem 277(23):20151–20159
167. Lotz GP, Lin HY et al (2003) Aha1 binds to the middle domain of Hsp90, contributes to client protein activation, and stimulates the ATPase activity of the molecular chaperone. J Biol Chem 278(19):17228–17235
168. Harst A, Lin HY et al (2005) Aha1 competes with Hop, p50 and p23 for binding to the molecular chaperone Hsp90 and contributes to kinase and hormone receptor activation. Biochem J 387:789–796
169. Wang XD, Venable J et al (2006) Hsp90 cochaperone Aha1 downregulation rescues misfolding of CFTR in cystic fibrosis. CeN 127(4):803–815
170. Koulov AV, LaPointe P et al (2010) Biological and structural basis for Aha1 regulation of Hsp90 ATPase activity in maintaining proteostasis in the human disease cystic fibrosis. Mol Biol Cell 21(6):871–884
171. Rudiger S, Freund SMV et al (2002) CRINEPT-TROSY NMR reveals p53 core domain bound in an unfolded form to the chaperone Hsp90. Proc Natl Acad Sci USA 99(17):11085–11090
172. Scroggins BT, Neckers L (2007) Post-translational modification of heat-shock protein 90: impact on chaperone function. Expert Opin Drug Discov 2(10):1403–1414
173. Scroggins BT, Robzyk K et al (2007) An acetylation site in the middle domain of Hsp90 regulates chaperone function. Mol Cell 25(1):151–159
174. Jacobs AT, Marnett LJ (2010) Systems analysis of protein modification and cellular responses induced by electrophile stress. Acc Chem Res 43(5):673–683
175. Aoyagi S, Archer TK (2005) Modulating molecular chaperone Hsp90 functions through reversible acetylation. Trends Cell Biol 15(11):565–567
176. Mollapour M, Neckers L (2012) Post-translational modifications of Hsp90 and their contributions to chaperone regulation. Biochim Biophys Acta 1823:648–655
177. Kovacs JJ, Murphy PJM et al (2005) HDAC6 regulates Hsp90 acetylation and chaperone-dependent activation of glucocorticoid receptor. Mol Cell 18(5):601–607
178. Murphy PJM, Morishima Y et al (2005) Regulation of the dynamics of hsp90 action on the glucocorticoid receptor by acetylation/deacetylation of the chaperone. J Biol Chem 280 (40):33792–33799
179. Meng Q, Chen X et al (2011) Carbamazepine promotes Her-2 protein degradation in breast cancer cells by modulating HDAC6 activity and acetylation of Hsp90. Mol Cell Biochem 348 (1–2):165–171
180. Ai J, Wang Y et al (2009) HDAC6 regulates androgen receptor hypersensitivity and nuclear localization via modulating Hsp90 acetylation in castration-resistant prostate cancer. Mol Endocrinol 23(12):1963–1972
181. Pallavi R, Roy N et al (2010) Heat shock protein 90 as a drug target against protozoan infections biochemical characterization of hsp90 from Plasmodium falciparum and Trypanosoma evansi and evaluation of its inhibitor as a candidate drug. J Biol Chem 285(49):37964–37975
182. Adinolfi E, Kim M et al (2003) Tyrosine phosphorylation of HSP90 within the P2X(7) receptor complex negatively regulates P2X(7) receptors. J Biol Chem 278(39):37344–37351
183. Duval M, Le Boeuf F et al (2007) Src-mediated phosphorylation of hsp90 in response to vascular endothelial growth factor (VEGF) is required for VEGF receptor-2 signaling to endothelial NO synthase. Mol Biol Cell 18(11):4659–4668

184. Mollapour M, Tsutsumi S et al (2010) Swe1(Wee1)-dependent tyrosine phosphorylation of Hsp90 regulates distinct facets of chaperone function. Mol Cell 37(3):333–343
185. Mollapour M, Tsutsumi S et al (2010) Hsp90 phosphorylation, Wee1, and the cell cycle. Cell Cycle 9(12):2310–2316
186. Mollapour M, Neckers L (2011) Detecting HSP90 phosphorylation. Methods Mol Biol 787:67–74 (Clifton, NJ)
187. Schmid S, Hugel T (2011) Regulatory post-translational modifications in Hsp90 can be compensated by cochaperone Aha1. Mol Cell 41:619–620
188. Mollapour M, Tsutsumi S et al (2011) Casein kinase 2 phosphorylation of Hsp90 threonine 22 modulates chaperone function and drug sensitivity. Oncotarget 2(5):407–417
189. Mollapour M, Tsutsumi S et al (2011) Threonine22 phosphorylation attenuates Hsp90 interaction with cochaerones and affects its chaperone activity. Mol Cell 41:672–681
190. Iki T, Yoshikawa M et al (2011) Cyclophilin 40 facilitates HSP90-mediated RISC assembly in plants. EMBO J 31(2):267–278
191. Shao JY, Prince T et al (2003) Phosphorylation of serine 13 is required for the proper function of the Hsp90 co-chaperone, Cdc37. J Biol Chem 278(40):38117–38120
192. Marzec M, Eletto D et al (2012) Grp94: an Hsp90-like protein specialized for protein folding and quality control in the endoplasmic reticulum. Biochim Biophys Acta 1823:774–787
193. Frey S, Leskovar A et al (2007) The ATPase cycle of the endoplasmic chaperone Grp94. J Biol Chem 282:35612–35620
194. Ostrovsky O, Makarewich CA et al (2009) An essential role for ATP binding and hydrolysis in the chaperone activity of GRP94 in cells. Proc Natl Acad Sci USA 106:11600–11605
195. Immormino RM, Metzger LE et al (2009) Different poses for ligand and chaperone in inhibitor-bound Hsp90 and GRP94: implications for paralog-specific drug design. J Mol Biol 388:1033–1042
196. Van PN, Peter F et al (1989) Four intracisternal calcium-binding glycoproteins from rat-liver microsomes with high-affinity for calcium – no indication for calsequestrin-like proteins in inositol 1,4,5-trisphosphate-sensitive calcium sequestering rat-liver vesicles. J Biol Chem 264(29):17494–17501
197. Lee AS (1981) The accumulation of 3 specific proteins related to glucose-regulated proteins in a temperature-sensitive hamster mutant-cell line K12. J Cell Physiol 106(1):119–125
198. Shiu RPC, Pouyssegur J et al (1977) Glucose depletion accounts for induction of 2 transformation-sensitive membrane proteins in rous-sarcoma virus-transformed chick-embryo fibroblasts – (glucose starvation membrane proteins). Proc Natl Acad Sci USA 74(9):3840–3844
199. Subjeck JR, Shyy TT (1986) Stress protein systems of mammalian-cells. Am J Physiol 250(1):C1–C17
200. Qu DF, Mazzarella RA et al (1994) Analysis of the structure and synthesis of GRP94, an abundant stress protein of the endoplasmic-reticulum. DNA Cell Biol 13(2):117–124
201. Riera M, Roher N et al (1999) Association of protein kinase CK2 with eukaryotic translation initiation factor eIF-2 and with grp94/endoplasmin. Mol Cell Biochem 191(1–2):97–104
202. Trujillo R, Miro F et al (1997) Substrates for protein kinase CK2 in insulin receptor preparations from rat liver membranes: identification of a 210-kDa protein substrate as the dimeric form of endoplasmin. Arch Biochem Biophys 344(1):18–28
203. Frasson M, Vitadello M et al (2009) Grp94 is Tyr-phosphorylated by Fyn in the lumen of the endoplasmic reticulum and translocates to golgi in differentiating myoblasts. Biochim Biophys Acta 1793(2):239–252
204. Ko MH, Puglielli L (2009) Two endoplasmic reticulum (ER)/ER Golgi intermediate compartment-based lysine acetyltransferases post-translationally regulate BACE1 levels. J Biol Chem 284(4):2482–2492
205. Biswas C, Ostrovsky O et al (2007) The peptide-binding activity of GRP94 is regulated by calcium. Biochem J 405:233–241
206. Ma YJ, Hendershot LM (2004) The role of the unfolded protein response in tumour development: friend or foe? Nat Rev Cancer 4(12):966–977

207. Ni M, Lee AS (2007) ER chaperones in mammalian development and human diseases. FEBS Lett 581(19):3641–3651
208. Melnick J, Argon Y (1995) Molecular chaperones and the biosynthesis of antigen receptors. Immunol Today 16(5):243–250
209. Melnick J, Dul JL et al (1994) Sequential interaction of the chaperones BIP and GRP94 with immunoglobulin-chains in the endoplasmic-reticulum. Nature 370(6488):373–375
210. Liu B, Yang Y et al (2010) Folding of toll-like receptors by the HSP90 paralogue gp96 requires a substrate-specific cochaperone. Nat Commun 1:79
211. Liu F, Gao YG et al (2010) A survey of lambda repressor fragments from two-state to downhill folding. J Mol Biol 397(3):789–798
212. Wakabayashi Y, Kobayashi M et al (2006) A protein associated with toll-like receptor 4 (PRAT4A) regulates cell surface expression of TLR4. J Immunol 177(3):1772–1779
213. Kao G, Nordenson C et al (2007) ASNA-1 positively regulates insulin secretion in C-elegans and mammalian cells. Cell 128(3):577–587
214. Stefanovic S, Hegde RS (2007) Identification of a targeting factor for posttranslational membrane protein insertion into the ER. Cell 128(6):1147–1159
215. Bhamidipati A, Denic V et al (2005) Exploration of the topological requirements of ERAD identifies Yos9p as a lectin sensor of misfolded glycoproteins in the ER lumen. Mol Cell 19(6):741–751
216. Christianson JC, Shaler TA et al (2008) OS-9 and GRP94 deliver mutant alpha 1-antitrypsin to the Hrd1-SEL1L ubiquitin ligase complex for ERAD. Nat Cell Biol 10(3):272–282
217. Cechetto JD, Gupta RS (2000) Immunoelectron microscopy provides evidence that tumor necrosis factor receptor-associated protein 1 (TRAP-1) is a mitochondrial protein which also localizes at specific extramitochondrial sites. Exp Cell Res 260(1):30–39
218. Felts SJ, Owen BAL et al (2000) The hsp90-related protein TRAP1 is a mitochondrial protein with distinct functional properties. J Biol Chem 275(5):3305–3312
219. Altieri DC, Stein GS et al (2012) TRAP-1, the mitochondrial Hsp90. Biochimica et Biophysica Acta 1823:767–773
220. Song HY, Dunbar JD et al (1995) Identification of a protein with homology to HSP90 that binds the type-1 tumor-necrosis-factor receptor. J Biol Chem 270(8):3574–3581
221. Leskovar A, Wegele H et al (2008) The ATPase cycle of the mitochondrial Hsp90 analog trap1. J Biol Chem 283(17):11677–11688
222. Kang BH, Plescia J et al (2007) Regulation of tumor cell mitochondrial homeostasis by an organelle-specific Hsp90 chaperone network. Cell 131(2):257–270
223. Kang BH, Plescia J et al (2009) Combinatorial drug design targeting multiple cancer signaling networks controlled by mitochondrial Hsp90. J Clin Invest 119(3):454–464
224. Green DR, Kroemer G (2004) The pathophysiology of mitochondrial cell death. Science 305(5684):626–629
225. Hua GQ, Zhang QX et al (2007) Heat shock protein 75 (TRAP1) antagonizes reactive oxygen species generation and protects cells from granzyme M-mediated apoptosis. J Biol Chem 282(28):20553–20560
226. Masuda Y, Shima G et al (2004) Involvement of tumor necrosis factor receptor-associated protein 1 (TRAP1) in apoptosis induced by beta-hydroxyisovalerylshikonin. J Biol Chem 279(41):42503–42515
227. Pridgeon JW, Olzmann JA et al (2007) PINK1 protects against oxidative stress by phosphorylating mitochondrial chaperone TRAP1. PLoS Biol 5(7):1494–1503
228. Plescia J, Salz W et al (2005) Rational design of shepherdin, a novel anticancer agent. Cancer Cell 7(5):457–468
229. Kang BH, Altieri DC (2009) Compartmentalized cancer drug discovery targeting mitochondrial Hsp90 chaperones. Oncogene 28(42):3681–3688
230. Kang BH, Siegelin MD et al (2010) Preclinical characterization of mitochondria-targeted small molecule Hsp90 inhibitors, gamitrinibs, in advanced prostate cancer. Clin Cancer Res 16(19):4779–4788

231. Kang BH, Tavecchio M et al (2011) Targeted inhibition of mitochondrial Hsp90 suppresses localised and metastatic prostate cancer growth in a genetic mouse model of disease. Br J Cancer 104(4):629–634
232. Eustace BK, Sakurai T et al (2004) Functional proteomic screens reveal an essential extracellular role for hsp90 alpha in cancer cell invasiveness. Nat Cell Biol 6(6):507–514
233. Tsutsumi S, Scroggins B et al (2008) A small molecule cell-impermeant Hsp90 antagonist inhibits tumor cell motility and invasion. Oncogene 27(17):2478–2487
234. Cheng CF, Fan JH et al (2008) Transforming growth factor alpha (TGF alpha)-stimulated secretion of HSP90 alpha: using the receptor LRF-1/CD91 to promote human skin cell migration against a TGF beta-rich environment during wound healing. Mol Cell Biol 28(10):3344–3358
235. Cheng CF, Sahu D et al (2011) A fragment of secreted Hsp90 alpha carries properties that enable it to accelerate effectively both acute and diabetic wound healing in mice. J Clin Invest 121(11):4348–4361
236. Kadota Y, Shirasu K (2012) The HSP90 complex of plants. Biophys Biochim Acta 1823:689–697
237. Sangster TA, Queitsch C (2005) The HSP90 chaperone complex, an emerging force in plant development and phenotypic plasticity. Curr Opin Plant Biol 8(1):86–92
238. Sangster TA, Salathia N et al (2008) HSP90-buffered genetic variation is common in Arabidopsis thaliana. Proc Natl Acad Sci USA 105(8):2969–2974
239. Sangster TA, Salathia N et al (2008) HSP90 affects the expression of genetic variation and developmental stability in quantitative traits. Proc Natl Acad Sci USA 105(8):2963–2968
240. Jarosz DF, Lindquist S (2010) Hsp90 and environmental stress transform the adaptive value of natural genetic variation. Science 330(6012):1820–1824
241. Gangaraju VK, Yin H et al (2011) Drosophila Piwi functions in Hsp90-mediated suppression of phenotypic variation. Nat Genet 43(2):153–158
242. Cowen LE, Lindquist S (2005) Hsp90 potentiates the rapid evotution of new traits: drug resistance in diverse fungi. Science 309(5744):2185–2189
243. Queitsch C, Sangster TA et al (2002) Hsp90 as a capacitor of phenotypic variation. Nature 417(6889):618–624
244. Rutherford SL, Lindquist S (1998) Hsp90 as a capacitor for morphological evolution. Nature 396(6709):336–342
245. Sangster TA, Bahrami A et al (2007) Phenotypic diversity and altered environmental plasticity in Arabidopsis thaliana with reduced Hsp90 levels. PLoS One 2(7)
246. Sangster TA, Lindquist S et al (2004) Under cover: causes, effects and implications of Hsp90-mediated genetic capacitance. Bioessays 26(4):348–362
247. Maekawa T, Kufer TA et al (2011) NLR functions in plant and animal immune systems: so far and yet so close. Nat Immunol 12(9):818–826
248. Kadota Y, Shirasu K et al (2010) NLR sensors meet at the SGT1-HSP90 crossroad. Trends Biochem Sci 35(4):199–207
249. Cox MB, Johnson JL (2011) The role of p23, Hop, immunophilins, and other co-chaperones in regulating Hsp90 function. Methods Mol Biol 787:45–66 (Clifton, NJ)
250. Smith DF, Faber LE et al (1990) Purification of unactivated progesterone-receptor and identification of novel receptor-associated proteins. J Biol Chem 265(7):3996–4003
251. Bresnick EH, Dalman FC et al (1990) Direct stoichiometric evidence that the untransformed MR 300 000, 9S, glucocorticoid receptor is a core unit derived from a larger heteromeric complex. Biochemistry 29(2):520–527
252. Weaver AJ, Sullivan WP et al (2000) Crystal structure and activity of human p23, a heat shock protein 90 co-chaperone. J Biol Chem 275(30):23045–23052
253. Tanioka T, Nakatani Y et al (2000) Molecular identification of cytosolic prostaglandin E-2 synthase that is functionally coupled with cyclooxygenase-1 in immediate prostaglandin E-2 biosynthesis. J Biol Chem 275(42):32775–32782

254. Toogun OA, Zeiger W et al (2007) The p23 molecular chaperone promotes functional telomerase complexes through DNA dissociation. Proc Natl Acad Sci USA 104(14):5765–5770
255. DeZwaan DC, Freeman BC (2010) HSP90 manages the ends. Trends Biochem Sci 35(7):384–391
256. Ratajczak T, Ward BK et al (2009) Cyclophilin 40: an Hsp90-cochaperone associated with apo-steroid receptors. Int J Biochem Cell Biol 41(8–9):1652–1655
257. Allan RK, Ratajczak T (2011) Versatile TPR domains accommodate different modes of target protein recognition and function. Cell Stress Chaperones 16(4):353–367
258. Cheung-Flynn J, Prapapanich V et al (2005) Physiological role for the cochaperone FKBP52 in androgen receptor signaling. Mol Endocrinol 19(6):1654–1666
259. Riggs DL, Roberts PJ et al (2003) The Hsp90-binding peptidylprolyl isomerase FKBP52 potentiates glucocorticoid signaling in vivo. EMBO J 22(5):1158–1167
260. Wochnik GM, Ruegg J et al (2005) FK506-binding proteins 51 and 52 differentially regulate dynein interaction and nuclear translocation of the glucocorticoid receptor in mammalian cells. J Biol Chem 280(6):4609–4616
261. Davies TH, Ning YM et al (2005) Differential control of glucocorticoid receptor hormone-binding function by tetratricopeptide repeat (TPR) proteins and the immunosuppressive ligand FK506. Biochemistry 44(6):2030–2038
262. Yang ZC, Wolf IM et al (2006) FK506-binding protein 52 is essential to uterine reproductive physiology controlled by the progesterone receptor A isoform. Mol Endocrinol 20(11):2682–2710
263. Stechschulte LA, Sanchez ER (2011) FKBP51-a selective modulator of glucocorticoid and androgen sensitivity. Curr Opin Pharmacol 11(4):332–337
264. Periyasamy S, Hinds T et al (2010) FKBP51 and Cyp40 are positive regulators of androgen-dependent prostate cancer cell growth and the targets of FK506 and cyclosporin A. Oncogene 29(11):1691–1701
265. Ni L, Yang CS et al (2010) FKBP51 Promotes assembly of the Hsp90 chaperone complex and regulates androgen receptor signaling in prostate cancer cells. Mol Cell Biol 30(5):1243–1253
266. Hartmann J, Wagner KV et al (2012) The involvement of FK506-binding protein 51 (FKBP5) in the behavioral and neuroendocrine effects of chronic social defeat stress. Neuropharmacology 62(1):332–339
267. Touma C, Gassen NC et al (2011) FK506 binding protein 5 shapes stress responsiveness: modulation of neuroendocrine reactivity and coping behavior. Biol Psychiatry 70(10):928–936
268. Koren J, Jinwal UK et al (2011) Bending tau into shape: the emerging role of peptidyl-prolyl isomerases in tauopathies. Mol Neurobiol 44(1):65–70
269. Taylor P, Dornan J et al (2001) Two structures of cyclophilin 40: folding and fidelity in the TPR domains. Structure 9(5):431–438
270. Das AK, Cohen PTW et al (1998) The structure of the tetratricopeptide repeats of protein phosphatase 5: implications for TPR-mediated protein-protein interactions. EMBO J 17(5):1192–1199
271. Chen MS, Silverstein AM et al (1996) The tetratricopeptide repeat domain of protein phosphatase 5 mediates binding to glucocorticoid receptor heterocomplexes and acts as a dominant negative mutant. J Biol Chem 271(50):32315–32320
272. Silverstein AM, Galigniana MD et al (1997) Protein phosphatase 5 is a major component of glucocorticoid receptor hsp90 complexes with properties of an FK506-binding immunophilin. J Biol Chem 272(26):16224–16230
273. Salminen A, Ojala J et al (2011) Hsp90 regulates tau pathology through co-chaperone complexes in Alzheimer's disease. Prog Neurobiol 93:99–110
274. Jones C, Anderson S et al (2008) Protein phosphatase 5 is required for Hsp90 function during proteotoxic stresses in Trypanosoma brucei. Parasitol Res 102(5):835–844
275. Hinds TD, Sanchez ER (2008) Protein phosphatase 5. Int J Biochem Cell Biol 40(11):2358–2362

276. Golden T, Swingle M et al (2008) The role of serine/threonine protein phosphatase type 5 (PP5) in the regulation of stress-induced signaling networks and cancer. Cancer Metastasis Rev 27(2):169–178
277. Chinkers M (2001) Protein phosphatase 5 in signal transduction. Trends Endocrinol Metab 12(1):28–32
278. Pearl LH (2005) Hsp90 and Cdc37 – a chaperone cancer conspiracy. Curr Opin Genet Dev 15(1):55–61
279. Caplan AJ, Mandal AK et al (2007) Molecular chaperones and protein kinase quality control. Trends Cell Biol 17(2):87–92
280. Mandal AK, Theodoraki MA et al (2011) Role of molecular chaperones in biogenesis of the protein kinome. Methods Mol Biol 787:75–81 (Clifton, NJ)
281. MacLean M, Picard D (2003) Cdc37 goes beyond Hsp90 and kinases. Cell Stress Chaperones 8(2):114–119
282. Karnitz LM, Felts SJ (2007) Cdc37 regulation of the kinome: when to hold 'em and when to fold' em. Sci Signal Transduct Knowl Environ 385:pe22
283. Odunuga OO, Longshaw VM et al (2004) Hop: more than an Hsp70/Hsp90 adaptor protein. Bioessays 26:1058–1068
284. Wegele H, Wandinger SK et al (2006) Substrate transfer from the chaperone Hsp70 to Hsp90. J Mol Biol 356(3):802–811
285. Schmid AB, Lagleder S et al (2012) The architecture of functional modules in the Hsp90 co-chaperone Sti1/Hop. EMBO J 31:1506–1517
286. Nathan DF, Vos MH et al (1999) Identification of SSF1, CNS1, and HCH1 as multicopy suppressors of a Saccharomyces cerevisiae Hsp90 loss-of-function mutation. Proc Natl Acad Sci USA 96(4):1409–1414
287. Muskett P, Parker J (2003) Role of SGT1 in the regulation of plant R gene signalling. Microbes Infect 5(11):969–976
288. Shirasu K (2009) The HSP90-SGT1 chaperone complex for NLR immune sensors. Annu Rev Plant Biol 60:139–164
289. Ye ZM, Ting JPY (2008) NLR, the nucleotide-binding domain leucine-rich repeat containing gene family. Curr Opin Immunol 20(1):3–9
290. Murata S, Chiba T et al (2003) CHIP: a quality-control E3 ligase collaborating with molecular chaperones. Int J Biochem Cell Biol 35(5):572–578
291. McDonough H, Patterson C (2003) CHIP: a link between the chaperone and proteasome systems. Cell Stress Chaperones 8(4):303–308
292. Pratt WB, Morishima Y et al (2010) Proposal for a role of the Hsp90/Hsp70-based chaperone machinery in making triage decisions when proteins undergo oxidative and toxic damage. Exp Biol Med 235(3):278–289
293. Hildenbrand ZL, Molugu SK et al (2011) Hsp90 can accommodate the simultaneous binding of the FKBP52 and Hop proteins. Oncotarget 2:43–58
294. OwensGrillo JK, Czar MJ et al (1996) A model of protein targeting mediated by immunophilins and other proteins that bind to hsp90 via tetratricopeptide repeat domains. J Biol Chem 271(23):13468–13475
295. Jhaveri K, Taldone T et al (2012) Advances in the clinical development of heat shock protein 90 (Hsp90) inhibitors in cancers. Biochim Biophys Acta 1823:742–755
296. Whitesell L, Shifrin SD et al (1992) Benzoquinonoid ansamycins possess selective tumoricidal activity unrelated to SRC kinase inhibition. Cancer Res 52(7):1721–1728
297. Schulte TW, Neckers L (1998) The benzoquinone ansamycin 17-allylamino-17-demethoxy-geldanamycin binds to HSP90 and shares important biologic activities with geldanamycin. Cancer Chemother Pharmacol 42(4):273–279
298. Kim DJ, Kim HS et al (2009) Crystal structure of thermotoga maritima SPOUT superfamily RNA methyltransferase Tm1570 in complex with S-adenosyl-L-methionine. Proteins Struct Funct Bioinformatics 74(1):245–249

299. Kim YS, Alarcon SV et al (2009) Update on Hsp90 inhibitors in clinical trial. Curr Top Med Chem 9(15):1479–1492
300. Johnson VA, Singh EK et al (2010) Macrocyclic inhibitors of Hsp90. Curr Top Med Chem 10(14):1380–1402
301. Taldone T, Gozman A et al (2008) Targeting Hsp90: small-molecule inhibitors and their clinical development. Curr Opin Pharmacol 8(4):370–374
302. Talele TT, Khedkar SA et al (2010) Successful applications of computer aided drug discovery: moving drugs from concept to the clinic. Curr Top Med Chem 10(1):127–141
303. Taldone T, Chiosis G (2009) Purine-scaffold Hsp90 inhibitors. Curr Top Med Chem 9(15):1436–1446
304. Taldone T, Chiosis G (2009) Purine-scaffold Hsp90 inhibitors. Curr Topics
305. Porter JR, Fritz CC et al (2010) Discovery and development of Hsp90 inhibitors: a promising pathway for cancer therapy. Curr Opin Chem Biol 14(3):412–420
306. Taldone T, Zatorska D et al (2011) Design, synthesis, and evaluation of small molecule Hsp90 probes. Bioorg Med Chem 19(8):2603–2614
307. Pearl LH, Prodromou C et al (2008) The Hsp90 molecular chaperone: an open and shut case for treatment. Biochem J 410:439–453
308. Neckers L (2006) Chaperoning oncogenes: Hsp90 as a target of geldanamycin. Handb Exp Pharmacol 172:259–277
309. Fortugno P, Beltrami E et al (2003) Regulation of survivin function by Hsp90. Proc Natl Acad Sci USA 100(24):13791–13796
310. Kamal A, Thao L et al (2003) A high-affinity conformation of Hsp90 confers tumour selectivity on Hsp90 inhibitors. Nature 425(6956):407–410
311. Moulick K, Ahn JH et al (2011) Affinity-based proteomics reveal cancer-specific networks coordinated by Hsp90. Nat Chem Biol 7(11):818–826
312. Vilenchik M, Solit D et al (2004) Targeting wide-range oncogenic transformation via PU24FCI, a specific inhibitor of tumor Hsp90. Chem Biol 11(6):787–797
313. Brandt GEL, Blagg BSJ (2009) Alternate strategies of Hsp90 modulation for the treatment of cancer and other diseases. Curr Top Med Chem 9(15):1447–1461
314. Donnelly A, Blagg BSJ (2008) Novobiocin and additional inhibitors of the Hsp90 C-terminal nucleotide-binding pocket. Curr Med Chem 15(26):2702–2717
315. Palermo CM, Westlake CA et al (2005) Epigallocatechin gallate inhibits aryl hydrocarbon receptor gene transcription through an indirect mechanism involving binding to a 90 kDa heat shock protein. Biochemistry 44(13):5041–5052
316. Pimienta G, Herbert KM et al (2011) A compound that inhibits the HOP-Hsp90 complex formation and has unique killing effects in breast cancer cell lines. Mol Pharm 8(6):2252–2261
317. Vasko RC, Rodriguez RA et al (2010) Mechanistic studies of sansalvamide a-amide: an allosteric modulator of Hsp90. ACS Med Chem Lett 1(1):4–8
318. Heide L (2009) The aminocoumarins: biosynthesis and biology. Nat Prod Rep 26(10):1241–1250
319. Marcu MG, Schulte TW et al (2000) Novobiocin and related coumarins and depletion of heat shock protein 90-dependent signaling proteins. J Natl Cancer Inst 92(3):242–248
320. Burlison JA, Blagg BSJ (2006) Synthesis and evaluation of coumermycin A1 analogues that inhibit the Hsp90 protein folding machinery. Org Lett 8(21):4855–4858
321. Yu XM, Shen G et al (2005) Hsp90 inhibitors identified from a library of novobiocin analogues. J Am Chem Soc 127(37):12778–12779
322. Burlison JA, Avila C et al (2008) Development of novobiocin analogues that manifest anti-proliferative activity against several cancer cell lines. J Org Chem 73(6):2130–2137
323. Burlison JA, Neckers L et al (2006) Novobiocin: redesigning a DNA gyrase inhibitor for selective inhibition of Hsp90. J Am Chem Soc 128(48):15529–15536
324. Huang Y-T, Blagg BSJ (2007) A library of noviosylated coumarin analogues. J Org Chem 72(10):3609–3613

325. Huang JR, Craggs TD et al (2007) Stable intermediate states and high energy barriers in the unfolding of GFP. J Mol Biol 370(2):356–371
326. Le Bras G, Radanyi C et al (2007) New novobiocin analogues as antiproliferative agents in breast cancer cells and potential inhibitors of heat shock protein 90. J Med Chem 50(24):6189–6200
327. Radanyi C, Le Bras G et al (2008) Synthesis and biological activity of simplified denoviose-coumarins related to novobiocin as potent inhibitors of heat-shock protein 90 (hsp90). Bioorg Med Chem Lett 18(7):2495–2498
328. Soti C, Racz A et al (2002) A nucleotide-dependent molecular switch controls ATP binding at the C-terminal domain of Hsp90 – N-terminal nucleotide binding unmasks a C-terminal binding pocket. J Biol Chem 277(9):7066–7075
329. Yi F, Zhu P et al (2009) An alphascreen (TM)-based high-throughput screen to identify inhibitors of Hsp90-cochaperone interaction. J Biomol Screen 14(3):273–281
330. Yi F, Regan L (2008) A novel class of small molecule inhibitors of Hsp90. ACS Chem Biol 3(10):645–654
331. Cortajarena AL, Yi F et al (2008) Designed TPR modules as novel anticancer agents. ACS Chem Biol 3(3):161–166
332. Patel HJ, Modi S et al (2011) Advances in the discovery and development of heat-shock protein 90 inhibitors for cancer treatment. Expert Opin Drug Discov 6(5):559–587
333. Trepel J, Mollapour M et al (2010) Targeting the dynamic HSP90 complex in cancer. Nat Rev Cancer 10(8):537–549
334. Tsutsumi S, Beebe K et al (2009) Impact of heat-shock protein 90 on cancer metastasis. Future Oncol 5(5):679–688
335. Tsutsumi S, Mollapour M et al (2009) Hsp90 charged-linker truncation reverses the functional consequences of weakened hydrophobic contacts in the N domain. Nat Struct Mol Biol 16(11):1141–1147
336. Nagy PD, Wang RY et al (2011) Emerging picture of host chaperone and cyclophilin roles in RNA virus replication. Virology 411(2):374–382
337. Geller R, Vignuzzi M et al (2007) Evolutionary constraints on chaperone-mediated folding provide an antiviral approach refractory to development of drug resistance. Genes Dev 21(2):195–205
338. Luheshi LM, Dobson CM (2009) Bridging the gap: from protein misfolding to protein misfolding diseases. FEBS Lett 583(16):2581–2586
339. Ramirez-Alvarado M, Kelly JW et al (2010) Protein misfolding diseases: current and emerging principles and therapies. Wiley series in protein and peptide science. Wiley
340. Owen JB, Di Domenico F et al (2009) Proteomics-determined differences in the concanavalin-a-fractionated proteome of hippocampus and inferior parietal lobule in subjects with Alzheimer's disease and mild cognitive impairment: implications for progression of AD. J Proteome Res 8(2):471–482
341. Kulathingal J, Ko LW et al (2009) Proteomic profiling of phosphoproteins and glycoproteins responsive to wild-type alpha-synuclein accumulation and aggregation. Biochim Biophys Acta 1794(2):211–224
342. Kulathingal J, Ko L-W et al (2009) Proteomic profiling of phosphoproteins and glycoproteins responsive to wild-type alpha-synuclein accumulation and aggregation. Biochim Biophys Acta 1794(2):211–224
343. Yokota T, Mishra M et al (2006) Brain site-specific gene expression analysis in Alzheimer's disease patients. Eur J Clin Invest 36(11):820–830
344. Sahara N, Maeda S et al (2007) Molecular chaperone-mediated Tau protein metabolism counteracts the formation of granular Tau oligomers in human brain. J Neurosci Res 85:3098–3108
345. Dou F, Netzer WJ et al (2003) Heat shock proteins reduce aggregation and facilitate degradation of tau protein. Mol Mech Epochal Therap Ischemic Stroke Dementia 1252:383–393

346. Dou F, Netzer WJ et al (2003) Chaperones increase association of tau protein with microtubules. Proc Natl Acad Sci USA 100(2):721–726
347. Dickey CA, Eriksen J et al (2005) Development of a high throughput drug screening assay for the detection of changes in tau levels – proof of concept with HSP90 inhibitors. Curr Alzheimer Res 2(2):231–238
348. Ansar S, Burlison JA et al (2007) A non-toxic Hsp90 inhibitor protects neurons from Abeta-induced toxicity. Bioorg Med Chem Lett 17(7):1984–1990
349. Lu J, den Dulk-Ras A et al (2009) Agrobacterium tumefaciens VirC2 enhances T-DNA transfer and virulence through its C-terminal ribbon-helix-helix DNA-binding fold. Proc Natl Acad Sci USA 106(24):9643–9648
350. Lu Y, Ansar S et al (2009) Neuroprotective activity and evaluation of Hsp90 inhibitors in an immortalized neuronal cell line. Bioorg Med Chem 17(4):1709–1715
351. Dickey CA, Dunmore J et al (2006) HSP induction mediates selective clearance of tau phosphorylated at proline-directed Ser/Thr sites but not KXGS (MARK) sites. Faseb J 20(2):753–755
352. Luo WJ, Dou F et al (2007) Roles of heat-shock protein 90 in maintaining and facilitating the neurodegenerative phenotype in tauopathies. Proc Natl Acad Sci USA 104(22):9511–9516
353. Dou F, Chang XY et al (2007) Hsp90 maintains the stability and function of the tau phosphorylating kinase GSK3 beta. Int J Mol Sci 8(1):51–60
354. Tortosa E, Santa-Maria I et al (2009) Binding of Hsp90 to Tau promotes a conformational change and aggregation of Tau protein. J Alzheimers Dis 17(2):319–325
355. Dickey CA, Koren J et al (2008) Akt and CHIP coregulate tau degradation through coordinated interactions. Proc Natl Acad Sci USA 105(9):3622–3627
356. Dickey CA, Kamal A et al (2007) The high-affinity HSP90-CHIP complex recognizes and selectively degrades phosphorylated tau client proteins. J Clin Invest 117(3):648–658
357. Jinwal UK, Koren J et al (2010) The Hsp90 cochaperone, FKBP51, increases Tau stability and polymerizes microtubules. J Neurosci 30(2):591–599
358. Benussi L, Ghidoni R et al (2005) Interaction between tau and alpha-synuclein proteins is impaired in the presence of P301L tau mutation. Exp Cell Res 308(1):78–84
359. Riedel M, Goldbaum O et al (2009) Alpha-synuclein promotes the recruitment of Tau to protein inclusions in oligodendroglial cells: effects of oxidative and proteolytic stress. J Mol Neurosci 39(1–2):226–234
360. Uryu K, Richter-Landsberg C et al (2006) Convergence of heat shock protein 90 with ubiquitin in filamentous alpha-synuclein inclusions of alpha-synucleinopathies. Am J Pathol 168(3):947–961
361. Liang J, Clark-Dixon C et al (2008) Novel suppressors of alpha-synuclein toxicity identified using yeast. Hum Mol Genet 17(23):3784–3795
362. Koga H, Cuervo AM (2011) Chaperone-mediated autophagy dysfunction in the pathogenesis of neurodegeneration. Neurobiol Dis 43(1):29–37
363. Zaarur N, Meriin AB et al (2008) Triggering aggresome formation – dissecting aggresome-targeting and aggregation signals in synphilin 1. J Biol Chem 283(41):27575–27584
364. Falsone SF, Kungl AJ et al (2009) The molecular chaperone Hsp90 modulates intermediate steps of amyloid assembly of the Parkinson-related protein alpha-synuclein. J Biol Chem 284(45):31190–31199
365. Liu J, Chen S et al (2009) Rab11a and HSP90 regulate recycling of extracellular alpha-synuclein. Mov Disord 24:S39–S40
366. Liu J, Zhang JP et al (2009) Rab11a and HSP90 regulate recycling of extracellular alpha-synuclein. J Neurosci 29(5):1480–1485
367. Lee SJ, Lim HS et al (2011) Protein aggregate spreading in neurodegenerative diseases: problems and perspectives. Neurosci Res 70(4):339–348
368. Ko HS, Bailey R et al (2009) CHIP regulates leucine-rich repeat kinase-2 ubiquitination, degradation, and toxicity. Proc Natl Acad Sci USA 106(8):2897–2902

369. Hinault MP, Ben-Zvi A et al (2006) Chaperones and proteases – cellular fold-controlling factors of proteins in neurodegenerative diseases and aging. J Mol Neurosci 30(3):249–265
370. McNaught KSP, Olanow CW (2006) Protein aggregation in the pathogenesis of familial and sporadic Parkinson's disease. Neurobiol Aging 27(4):530–545
371. Olanow CW, McNaught KS (2006) Ubiquitin-proteasome system and Parkinson's disease. Mov Disord 21(11):1806–1823
372. Adachi H, Katsuno M et al (2009) Heat shock proteins in neurodegenerative diseases: pathogenic roles and therapeutic implications. Int J Hyperthermia 25(8):647–654
373. Connelly S, Choi S et al (2010) Structure-based design of kinetic stabilizers that ameliorate the transthyretin amyloidoses. Curr Opin Struct Biol 20(1):54–62
374. Sekijima Y, Kelly JW et al (2008) Pathogenesis of and therapeutic strategies to ameliorate the transthyretin amyloidoses. Curr Pharm Des 14(30):3219–3230
375. Kubota H, Kitamura A et al (2011) Analyzing the aggregation of polyglutamine-expansion proteins and its modulation by molecular chaperones. Methods 53(3):267–274
376. Evans CG, Wisen S et al (2006) Heat shock proteins 70 and 90 inhibit early stages of amyloid beta-(1–42) aggregation in vitro. J Biol Chem 281(44):33182–33191
377. Takata K, Kitamura Y et al (2003) Heat shock protein-90-induced microglial clearance of exogenous amyloid-beta(1–42) in rat hippocampus in vivo. Neurosci Lett 344(2):87–90
378. Kakimura J, Kitamura Y et al (2002) Microglial activation and amyloid-beta clearance induced by exogenous heat-shock proteins. FASEB J 16(2):601–603
379. Veereshwarayya V, Kumar P et al (2006) Differential effects of mitochondrial heat shock protein 60 and related molecular chaperones to prevent intracellular beta-amyloid-induced inhibition of complex IV and limit apoptosis. J Biol Chem 281(40):29468–29478
380. Sittler A, Lurz R et al (2001) Geldanamycin activates a heat shock response and inhibits huntingtin aggregation in a cell culture model of Huntington's disease. Hum Mol Genet 10(12):1307–1315
381. Sato T, Susuki S et al (2007) Endoplasmic reticulum quality control regulates the fate of transthyretin variants in the cell. EMBO J 26(10):2501–2512
382. Chadli A, Felts SJ et al (2010) Celastrol inhibits Hsp90 chaperoning of steroid receptors by inducing fibrillization of the Co-chaperone p23. J Biol Chem 285(6):4224–4231
383. Paris D, Ganey NJ et al (2010) Reduction of beta-amyloid pathology by celastrol in a transgenic mouse model of Alzheimer's disease. J Neuroinflammation 7:17
384. Chiosis G, Kang YL et al (2008) Discovery and development of purine-scaffold Hsp90 inhibitors. Expert Opin Drug Discov 3(1):99–114
385. Luo WJ, Rodina A et al (2008) Heat shock protein 90: translation from cancer to Alzheimer's disease treatment? BMC Neurosci 9:Suppl 2. S7 Review
386. Koren J, Jinwal UK et al (2009) Chaperone signalling complexes in Alzheimer's disease. J Cell Mol Med 13(4):619–630
387. DeTure M, Hicks C et al (2010) Targeting heat shock proteins in tauopathies. Curr Alzheimer Res 7(8):677–684
388. Luo WJ, Sun WL et al (2010) Heat shock protein 90 in neurodegenerative diseases. Mol Neurodegeneration 5
389. Neckers L, Tatu U (2008) Molecular chaperones in pathogen virulence: emerging new targets for therapy. Cell Host Microbe 4(6):519–527
390. Folgueira C, Requena JM (2007) A postgenomic view of the heat shock proteins in kinetoplastids. FEMS Microbiol Rev 31(4):359–377
391. Bente M, Harder S et al (2003) Developmentally induced changes of the proteome in the protozoan parasite Leishmania donovani. Proteomics 3(9):1811–1829
392. Graefe SEB, Wiesgigl M et al (2002) Inhibition of HSP90 in trypanosoma cruzi induces a stress response but no stage differentiation. Eukaryot Cell 1(6):936–943
393. Pesce ER, Cockburn IL et al (2010) Malaria heat shock proteins: drug targets that chaperone other drug targets. Infect Disord Drug Targets 10(3):147–157

394. Acharya P, Kumar R et al (2007) Chaperoning a cellular upheaval in malaria: heat shock proteins in Plasmodium falciparum. Mol Biochem Parasitol 153(2):85–94
395. Wiser MF (2003) A Plasmodium homologue of cochaperone p23 and its differential expression during the replicative cycle of the malaria parasite. Parasitol Res 90(2):166–170
396. Vonlaufen N, Kanzok SM et al (2008) Stress response pathways in protozoan parasites. Cell Microbiol 10(12):2387–2399
397. Ahn HJ, Kim HW et al (2003) Crystal structure of tRNA(m(1)G37)methyltransferase: insights into tRNA recognition. EMBO J 22(11):2593–2603
398. Ahn HJ, Kim S et al (2003) Molecular cloning of the 82-kDa heat shock protein (HSP90) of Toxoplasma gondii associated with the entry into and growth in host cells. Biochem Biophys Res Commun 311(3):654–659
399. Echeverria PC, Matrajt M et al (2005) Toxoplasma gondii Hsp90 is a potential drug target whose expression and subcellular localization are developmentally regulated. J Mol Biol 350(4):723–734
400. Roy N, Nageshan RK et al (2012) Heat shock protein 90 from neglected protozoan parasites. Biophys Biochim Acta 1823:707–711
401. Abisambra JF, Blair LJ et al (2010) Functionally intact Hsp27 links Tau aggregate disassembly to neuroprotection. Cell Transplant 19(3):329–329

Top Curr Chem (2013) 328: 241–268
DOI: 10.1007/128_2011_262

Published online: 11 November 2011

Extracellular Chaperones

Rebecca A. Dabbs, Amy R. Wyatt, Justin J. Yerbury, Heath Ecroyd, and Mark R. Wilson

Abstract The maintenance of the levels and correct folding state of proteins (proteostasis) is a fundamental prerequisite for life. Life has evolved complex mechanisms to maintain proteostasis and many of these that operate inside cells are now well understood. The same cannot yet be said of corresponding processes in extracellular fluids of the human body, where inappropriate protein aggregation is known to underpin many serious diseases such as Alzheimer's disease, type II diabetes and prion diseases. Recent research has uncovered a growing family of abundant extracellular chaperones in body fluids which appear to selectively bind to exposed regions of hydrophobicity on misfolded proteins to inhibit their toxicity and prevent them from aggregating to form insoluble deposits. These extracellular chaperones are also implicated in clearing the soluble, stabilized misfolded proteins from body fluids via receptor-mediated endocytosis for subsequent lysosomal degradation. Recent work also raises the possibility that extracellular chaperones may play roles in modulating the immune response. Future work will better define the in vivo functions of extracellular chaperones in proteostasis and immunology and pave the way for the development of new treatments for serious diseases.

Keywords Clearance • Extracellular chaperones • Extracellular proteostasis • Immune response • Protein misfolding diseases • Receptor-mediated endocytosis

R.A. Dabbs (✉), A.R. Wyatt, J.J. Yerbury, H. Ecroyd, and M.R. Wilson
School of Biological Sciences, University of Wollongong, Northfields Avenue, Wollongong, NSW, 2522, Australia
e-mail: mrw@uow.edu.au

Contents

1 Introduction

It has been estimated that about 400 g of protein are synthesized and degraded each day in the human body. Individual proteins are degraded at extremely varied rates, with half-lives ranging from several minutes to many hours. Intracellularly, this variation in half-life has been attributed to differences in the intrinsic stability of proteins and the recognition of non-native structures by highly selective and precisely regulated protein quality control systems. Molecular chaperones have been identified as key players in orchestrating the control of protein folding, but almost all previous studies have been restricted to a focus on intracellular events. The average 70 kg human contains 15 L of extracellular fluids, including 5 L of blood. Although the concentration of proteins is lower in extracellular than intracellular fluids (6% in plasma and 2% in interstitial fluid, 30% in cytosol), extracellular conditions are more oxidizing [1]. In addition, uniquely, extracellular fluids are continuously subjected to shear stress (e.g., the pumping of fluids around the body) which is known to induce protein unfolding and aggregation [2]. The relatively harsh extracellular conditions suggest that mechanisms to sense and control the folding state of extracellular proteins are likely to be essential for the maintenance of human (and other large animal) life.

Uncontrolled protein unfolding or misfolding and the consequent accumulation of protein aggregates are implicated in the pathology of many diseases collectively known as Protein Deposition Diseases (PDD). PDDs are typically late-onset [3], suggesting that the underlying cause of the disease may be disruption or overwhelming of protein folding quality control mechanisms that were once able to maintain existing proteins in their native conformation. Although the reasons for the progressive impairment of fundamental physiological processes in aging is not fully understood, it is likely that the combination of declining protein folding quality control and exposure to thermal, ionic, heavy metal or oxidative stress may be responsible for late-onset PDDs. All PDDs involve protein misfolding leading to the deposition in tissues of insoluble protein aggregates; however, the

type of aggregate formed varies between the individual diseases. In many PDDs, including Alzheimer's disease, type II diabetes, systemic amyloidosis, and transmissible spongiform encephalitis, proteins deposit as highly ordered, β-sheet-rich fibrillar aggregates known as amyloid. In other PDDs the nature of the protein deposits is fibrillar, but not amyloid – for example, Lewy bodies, which are found in Parkinson's and Alzheimer's disease. In still other PDDs, amorphous (unstructured), non-filamentous extracellular aggregates are formed. For example, such aggregates are formed by IgG light chain and/or IgG heavy chain in non-amyloidotic monoclonal IgG deposition disease (NAMIDD) [4]. In addition, drusen are amorphous extracellular deposits that accumulate in patients with age-related macular degeneration. In healthy eyes drusen are not found in the macula; however they may exist in the retinal periphery and their size and number are considered a risk factor for developing age-related macular degeneration later in life [5].

It is notable that many PDDs are associated with *extracellular* protein deposits. Thus the previous near-exclusive focus of studies on intracellular processes to control protein folding may not provide the knowledge needed to treat these diseases. Intracellular chaperones (e.g., Hsp70 and Hsp90) may be released from necrotic [6] or apoptotic [7] cells, during viral cell lysis, secreted in exosomes [8, 9], or via other specific mechanisms [10–12]; they have been discovered in human plasma and associated with cell surfaces, in particular cancer cells. Numerous extracellular roles have been postulated for these chaperones, such as cancer cell invasiveness [13] and immune presentation [14–21]. These "moonlighting" functions for normally intracellular chaperones may be very important. However, the low abundance of this class of chaperone in extracellular fluids makes it unlikely that they can play a major role in controlling the folding state of abundant extracellular proteins in body fluids.

It has only recently become apparent that abundant extracellular counterparts to the intracellular molecular chaperones exist. Clusterin was the first abundant extracellular chaperone (EC) to be identified [22, 23] but the number of known ECs continues to grow and now includes at least seven members. This chapter outlines properties of each of the proteins that may function as mammalian ECs, and proposes a model for how they act as key elements in a system to monitor and control the folding state of extracellular proteins. The model presented will also propose how the ECs may play important complementary roles in the immune system.

2 Abundant Extracellular Chaperones

There are seven currently known abundant extracellular proteins likely to function as chaperones (outlined in Table 1). The strength of the available evidence for this varies with each protein. For more detailed information see the corresponding sections below.

Table 1 Overview of the currently known extracellular chaperones

Chaperone	Abundance	Chaperone function	Disease association	References
Clusterin	35–105 μg/mL (blood plasma) 1.2–3.6 μg/mL (CSF) 2–15 mg/mL (seminal plasma)	Holdase-type chaperone activity similar to the small heat shock proteins	Associated with extracellular deposits tested including age related macular degeneration, Creutzfeldt–Jakob disease, atherosclerosis, Alzheimer's disease Upregulated in experimental models of stress Genetic association with Alzheimer's disease	[22–54]
α_2-Macroglobulin	1.5–2 mg/mL (blood plasma) 1–3.6 μg/mL (CSF)	Holdase-type chaperone activity similar to the small heat shock proteins	Promotes phagocytosis of pathogen *Trypanosoma cruzi* Associated with extracellular deposits in Alzheimer's disease, dialysis related amyloidosis and Creutzfeldt–Jakob disease Able to stimulate a cytotoxic T lymphocyte response against chaperoned peptides	[55–65]
Haptoglobin	0.3–2 mg/mL (blood plasma) 0.5–2 μg/mL (CSF)	Holdase-type chaperone activity similar to the small heat shock proteins	Upregulated during infection, neoplasia, trauma, and other inflammatory conditions Co-deposits with amyloid in senile plaques, drusen with age-related macular degeneration and in protein deposits associated with chronic glomerulonephritis	[66–74]
Apolipoprotein E	4–6.4 μg/mL (blood plasma) 1.8–5.7 μg/mL (CSF)	Stabilizes proteins in solution	Strong genetic association with Alzheimer's disease Co-localizes with Alzheimer's and Creutzfeldt-Jakob plaques	[75–81]
Serum Amyloid P Component (SAP)	40 μg/mL (blood plasma) 8.5 ng/mL (CSF)	ATP-independent refolding activity	Binds with high specificity to amyloid and is universally found in amyloid deposits Elevated SAP levels in CSF of Alzheimer's patients	[82–90]
Caseins	~80% of milk protein	α_{S1}- and β-casein have a holdase-type chaperone activity similar to the small heat shock proteins	Associated with amyloid-like deposits in mammary tissue	[26, 91–103]
α_EC-Fibrinogen	2–4.5 mg/mL (blood plasma)	Stabilizes proteins in solution	Plasma levels are elevated under periods of stress	[104–106]

2.1 Clusterin

Clusterin (also known as apolipoprotein J, sulfated glycoprotein 2, and SP-40,40) was the first normally secreted protein identified as an abundant extracellular chaperone [22]. This heat-stable glycoprotein has an extremely broad biological distribution and exhibits high sequence homology (70–80%) across a wide range of mammalian species, suggesting that it performs a fundamentally important function in vivo [107]. Clusterin has been detected in all extracellular fluids that have been tested. In humans, clusterin is present in the range of 35–105 μg/mL in blood plasma [24], 1.2–3.6 μg/mL in cerebral spinal fluid (CSF) [25], and 2–15 mg/mL in seminal plasma [25]. Determining the biological importance of clusterin has been complicated by the propensity of the protein to interact with a large number of structurally diverse molecules. It is likely that many of these interactions result from a single underlying property of clusterin, which is relevant to its primary function. Regardless, many alternative biological functions for clusterin have been proposed including roles in lipid transport [108], sperm maturation [109], complement regulation [107], membrane recycling [110], and apoptosis [111].

Clusterin is encoded by a single gene and the translated product is internally cleaved to produce two subunits, α and β, prior to secretion from the cell. Matrix-assisted laser desorption ionization mass spectrometry has identified two primary forms of human plasma clusterin at about 58 kDa and 63.5 kDa, which are likely to be different glycoforms [112]. Approximately 17–27% of the mass of clusterin is comprised of branched, sialic acid-rich, N-linked carbohydrates [112]. This high carbohydrate content, in addition to a high level of disorder and a tendency to form oligomers, has impeded structural analysis of clusterin; however, sequence analysis has allowed for the prediction of several structural elements. These include three predicted amphipathic α-helices (residues 173–184, 234–250, and 424–441) [108] and two predicted coiled-coil helices (residues 40–99 and 318–350) [113]. The five predicted α-helical regions are thought to be significant in the chaperone activity of clusterin. It has been proposed that the α-helical regions form a molten globule-like binding pocket that is the site of interaction for a variety of ligands [114].

Many reports have suggested that clusterin may have intracellular importance, for example in DNA repair [115], transcription [116], microtubule organization [117], or apoptosis [115, 118, 119]. Various mechanisms have been proposed to explain the presence of clusterin in intracellular compartments. This includes the reuptake of secreted clusterin back into the cytosol [117], retrotranslation of clusterin from the Golgi to the cytosol [120], and the generation of nuclear isoforms via alternative initiation of transcription to yield a 43-kDa isoform [121] or via alternative splicing to yield a 49-kDa isoform [122]. Given that none of these latter studies sequenced the intracellular clusterin, it is unknown whether the putative "isoforms" are indeed the result of alternative transcription initiation or splicing or whether they simply represent clusterin at different stages of maturation (e.g., cleaved or uncleaved, at different stages of glycosylation). Unambiguous structural identification of these intracellular isoforms of clusterin is required before their existence can be firmly accepted and their function(s) meaningfully assigned.

2.1.1 In Vitro Chaperone Activity

The hypothesis that clusterin may function as a molecular chaperone was first proposed over 10 years ago [22]. Since that time many studies have shown that clusterin has chaperone activity similar to that of the small heat-shock proteins (sHsps) [22, 23, 26–29, 33]. At substoichiometric concentrations, clusterin inhibits the stress-induced amorphous aggregation of a large number of unrelated client proteins by binding, in an ATP-independent manner, to areas of exposed hydrophobicity on partially unfolded intermediates [22, 26–29, 31]. While clusterin alone has no refolding activity, it can preserve heat-stressed enzymes in a state competent for subsequent ATP-dependent refolding by Hsc70 [28]. The chaperone activity of clusterin involves the sequestration of client proteins into soluble high molecular weight (HMW) complexes; when generated in vitro, these complexes have diameters of 50–100 nm and are $\geq 4 \times 10^7$ Da [31]. The maximum "loading" of clusterin appears to correspond to a mass ratio of 1:2 (clusterin:client) regardless of the client protein [31]. Immunoaffinity depletion of clusterin renders proteins in human plasma more susceptible to aggregation and precipitation [27]. Fibrinogen, ceruloplasmin, and albumin are major endogenous clients for clusterin when human plasma is subjected to physiologically relevant stress [30]. However, the method used to detect endogenous clients is biased towards those proteins that are relatively less stable and more abundant; it is likely that clusterin acts globally to stabilize a very broad range of clients in vivo.

The chaperone activity of clusterin is not limited to those proteins that form amorphous aggregates. Clusterin also inhibits the fibrillar aggregation of a large number of amyloid forming clients including amyloid β (Aβ) peptide [34, 35], PrP106–126 [36], apolipoprotein C-II [37], disease-associated variants of lysozyme [33], α-synuclein, calcitonin, κ-casein, SH3, and CCβw [32]. While clusterin appears to prevent amyloid formation in a dose dependent manner, in some cases very low levels of clusterin (relative to client protein) significantly increased amyloid formation [32]. It was proposed that when present at very low concentrations, clusterin may stabilize prefibrillar oligomers that "seed" fibril growth and are believed to be primarily responsible for amyloid-associated cytotoxicity. Thus, the clusterin:client protein ratio is an important determinant of the effects of clusterin on amyloid formation and toxicity. It is unknown exactly how clusterin is able to interfere with amyloid formation although the existing evidence suggests that it interacts predominantly with prefibrillar oligomeric species formed during the early stages of amyloid aggregation [32, 33]. These early aggregating species possess surface-exposed hydrophobicity [123]; thus the interaction of clusterin with amyloid-forming proteins may, as in the case of amorphously aggregating proteins, arise from hydrophobic interactions.

A number of investigations have focused on identifying possible interactions between members of the LDL receptor superfamily and clusterin [124–131]. Cellular internalization of clusterin via the LDL receptor megalin was the first reported clusterin-LDL receptor superfamily interaction [124]. Subsequent reports described the internalization of free clusterin and clusterin-Aβ peptide complexes by the same receptor [125, 126]. Recently, two other human members of the LDL receptor

superfamily, ApoE receptor 2 and very low density lipoprotein receptor, were reported to bind and internalize free clusterin and leptin-clusterin complexes using transfected cell models [131]. Interactions of clusterin with chicken oocyte-specific LDL receptors have also been described [128]. A recent study has suggested that megalin and LRP are capable of mediating the clusterin-dependent clearance of cellular debris into non-professional phagocytes [129]. However, the previous report of Kounnas et al. (1995) indicated that megalin, but not LRP, binds clusterin. Additional unidentified mechanisms of clusterin-dependent internalization were also suggested by Bartl et al. (2001). The affinity of clusterin binding to megalin is increased by the association of clusterin with lipids [127]. It is currently unknown how binding interactions with other molecules, such as stressed chaperone client proteins, affect the binding affinity of clusterin for megalin or other members of the LDL receptor superfamily. However, it has been shown that clusterin has independent binding sites for megalin, stressed proteins, and unstressed ligands [130].

2.1.2 Evidence for In Vivo Chaperone Action/Disease Involvement

Clusterin is found associated with extracellular protein deposits in numerous diseases including normal peripheral drusen and drusen in age-related macular degeneration patients [38], with membrane attack complex in renal immunoglobulin deposits [39], in prion deposits in Creutzfeldt-Jakob disease [40, 41], with PEX material in pseudoexfoliation (PEX) syndrome [42], in atherosclerotic plaques [43], and in amyloid plaques, or with soluble Aβ peptide in Alzheimer's disease [44, 45]. Two genome wide studies have recently implicated certain single nucleotide polymorphisms in the clusterin gene as risk factors for Alzheimer's disease [53, 54]. The overexpression of clusterin has been reported in a diverse range of renal and neurodegenerative diseases in addition to cancers, atherosclerosis, and diabetes [46]. Additionally, clusterin is upregulated in experimental models of pathological stress including oxidative stress [48], shear stress [49], proteotoxic stress (generated by inhibition of the proteasome) [50], heat stress [51], ionizing radiation [51], and exposure to heavy metals [132].

In clusterin knock-out mice, damage to testicular cells is increased after heat-shock and the removal of damaged cells is impaired [133]. After myosin-induced auto-immune myocarditis, cell damage is also more severe in clusterin-deficient mice [134], and post-ischemic brain injury is more severe [135]. Together this data suggests that stress-induced increase in clusterin expression is a cytoprotective response. In an Alzheimer's disease model, compared to control mice, mice in which the clusterin and ApoE genes were knocked out showed early disease onset and a marked increase in Aβ peptide levels and amyloid formation. The researchers concluded that apoE and clusterin work synergistically to inhibit the deposition of fibrillar Aβ [136]. A more recent study has demonstrated that clusterin knock-out mice develop progressive glomerulopathy which is characterized by the accumulation of insoluble protein deposits in the kidneys [137]. This directly implicates clusterin in the clearance of potentially pathological aggregating proteins, although the precise mechanism underlying this has yet to be described.

2.2 α_2-Macroglobulin (α_2M)

α_2M is a large secreted glycoprotein, assembled from four identical 180-kDa subunits into a 720-kDa tetramer; disulfide linked dimers of the individual 180-kDa subunits interact non-covalently to form the final tetrameric quaternary structure [138]. The secreted molecule is comprised of ~10% carbohydrate by mass. It is synthesized mainly in the liver, but is secreted from a range of different cell types (such as astrocytes) and can be found in human plasma and cerebrospinal fluid at 1,500–2,000 [56] and 1−3.6 μg/mL [57], respectively. It is best known for its ability to inhibit a broad spectrum of proteases, which it accomplishes using a unique trapping method. α_2M contains a "bait region" which undergoes limited proteolysis upon encountering a protease, resulting in a large conformational change and exposure of a thiol ester bond. The protease forms a covalent linkage with α_2M by reacting with the intramolecular thiol ester bond, which leads to further conformational changes exposing a receptor recognition site for low density lipoprotein receptor related protein (LRP). Overall, these structural changes produce a more compact molecule (known as "activated" or "fast" α_2M) and inhibits the protease by physically trapping it within a steric "cage" [56]. By directly interacting with the thiol ester bond, small nucleophiles such as methylamine can also activate α_2M [139]. Although human α_2M is best known for its protease inhibitor function, it has also been shown to bind to and promote clearance of other endogenous and exogenous molecules, consistent with a broader protective function. α_2M is known to bind to cytokines and growth factors (without converting to activated α_2M), including transforming growth factor-β (TGF-β), tumor necrosis factor-α (TNF-α), interleukin 1β (IL-1β), interleukin 8 (IL-8), platelet derived growth factor-BB (PDGF-BB), nerve growth factor-β (NGF-β), and vascular endothelial growth factor (VEGF) (reviewed in [140, 141]). The affinity of α_2M for most cytokines is higher in the activated state, and while in this state α_2M can deliver them via receptor mediated endocytosis to lysosomes for degradation [142]. In addition, α_2M has been shown to bind to the pathogen *Trypanosoma cruzi* and promote its phagocytosis [143]. α_2M has also been found to bind to endogenous proteins found in proteinaceous deposits associated with disease. α_2M is known to bind to the Aβ peptide associated with Alzheimer's disease [58, 59], β_2-microglobulin which forms insoluble deposits in dialysis related amyloidosis [60], and prion protein associated with plaques in Creutzfeldt–Jakob disease [61].

2.2.1 In Vitro Chaperone Activity

α_2M forms stable complexes with misfolded proteins to inhibit their stress-induced aggregation and precipitation but is unable to promote independently their refolding [62]. In addition, depletion of α_2M from whole human plasma renders proteins in this fluid more susceptible to aggregation and precipitation, even at 37 °C [62]. The formation of complexes between α_2M and misfolded proteins is thought to be,

at least in part, due to hydrophobic interactions [62]. The binding of a misfolded substrate protein does not activate α_2M and as a result the complex formed is not bound by LRP. However, while complexed with misfolded client proteins, α_2M remains able to interact with proteases and subsequently adopt its activated conformation and then interact with LRP [62]. Although LRP is the only known receptor for α_2M, it remains possible that non-activated α_2M/misfolded client protein complexes are taken up via other cell surface receptors. As an example, scavenger receptors have been shown to bind to methylamine activated forms of α_2M [144]. In addition to inhibiting amorphous aggregation, α_2M has been shown to inhibit amyloid fibril formation. This effect can be seen even at sub-stoichiometric levels of α_2M (as low as a 1:100 molar ratio of α_2M:substrate) [145, 146]. It is thought that α_2M interacts with lowly populated oligomeric species affecting the formation of stable nuclei from which amyloid formation proceeds [58, 146].

α_2M-client protein complexes are thought to be removed from the extracellular space by receptor mediated endocytosis. α_2M-Aβ complexes are internalized via LRP expressed on U87 cells and are subsequently degraded [58]. In addition, complexes formed from α_2M and heat-stressed citrate synthase (or glutathione-*S*-transferase, GST) that have been incubated with trypsin also bind to LRP on the surface of JEG-3 cells [62]. This uptake of complexes may protect cells from the toxicity of aggregating species. However, under certain conditions, α_2M was shown to promote the neurotoxicity of Aβ [63]. In stark contrast, using primary rat mixed neuronal cultures, others have demonstrated that α_2M can protect cells from Aβ toxicity [147]. The different effects observed may be explained by differences between systems in the extent of receptor mediated removal of complexes from the extracellular environment. This is illustrated by the demonstration that in the presence of α_2M (but not otherwise) SH-SY5Y cells that express the α_2M receptor (LRP) are more resistant to Aβ toxicity than cells that do not [63]. The protective effect of α_2M could be inhibited by RAP (a pan-specific inhibitor of LRP ligand binding). Furthermore, α_2M promoted Aβ toxicity against LRP-negative LAN5 cells but had the opposite effect with LRP-expressing LAN5 transfectants [63]. Importantly, this function has been demonstrated in vivo: the normally rapid removal of radiolabeled Aβ from mouse brain is significantly inhibited by the LDL family inhibitor RAP and antibodies against LRP-1 and α_2M.

2.2.2 Evidence for In Vivo Chaperone Action/Disease Involvement

α_2M has been found co-localized with Aβ and prion plaques in Alzheimer's disease and CJD respectively [61, 63]. In addition, levels of circulating complexes formed between α_2M and β_2m in plasma of hemodialysis patients are correlated with the severity of dialysis related amyloidosis [60]. In addition, α_2M has been found in complex with prion protein in human plasma [64]. Lastly, the ability of α_2M to promote the removal of Aβ from the extracellular space has been shown in vivo; the normally rapid removal of radiolabeled Aβ from mouse brain is significantly inhibited by the LDL family inhibitor RAP and antibodies against LRP-1 and α_2M [148].

2.2.3 Potential Application of α_2M in Anti-Cancer Treatments

α_2M shares a common receptor (α_2M receptor/ LRP1) with a variety of intracellular chaperones [149–151] which have been implicated in the re-presentation of chaperoned peptides to stimulate an immune response [8, 14, 16, 18–21, 149, 151–155]. This has led to the ability of α_2M to perform a similar immunological function being examined. It was shown that α_2M-peptide complexes are able to induce the re-presentation of the chaperoned peptides on MHC class I molecules in vitro and subsequently prime a cytotoxic T lymphocyte response in α_2M-peptide immunized mice [55]. As both intra- and extracellular chaperones have now both been shown to elicit such a response, it has been proposed that α_2M samples the extracellular space and Hsps the intracellular milieu. In this model, LRP1 facilitates the sampling of the entire antigenic milieu of an organism [55]. Unlike Hsps, which are ubiquitously expressed, many tumors do not express α_2M. Thus, in order to explore the use of α_2M-peptide complexes as an anti-cancer treatment, exogenous α_2M has been added to tumor cell lysates to generate the complexes [65]. α_2M-peptide complexes made in vitro induced anti-tumor responses and protection against tumor challenge similar to that of GP96 [156]. Thus, α_2M and perhaps the other extracellular chaperones all offer potential vehicles for peptide-specific control of the immune response and immune modulatory therapies.

2.3 Haptoglobin

Haptoglobin is a secreted glycoprotein with many known biological functions; however, it is best known as a hemoglobin binding protein. The non-covalent interaction between haptoglobin and hemoglobin is particularly strong with a reported $K_d \sim 10^{-15}$ M [66]. This interaction prevents the loss of hemoglobin and iron via glomerular filtration by redirecting the haptoglobin-hemoglobin complex to the liver [157]. The interaction of haptoglobin with hemoglobin also reduces the amount of free hemoglobin and iron available to catalyze oxidation reactions [158], and has an inhibitory effect on nitric oxide [159] and prostaglandin synthesis [160]. Haptoglobin also has a bacteriostatic effect on organisms unable to obtain heme from the hemoglobin–haptoglobin complex [161] and appears to play an important role in angiogenesis [162]. Finally, haptoglobin has been implicated in the regulation of lymphocyte transformation [163]. Haptoglobin is found in most body fluids. Its plasma concentration is between 0.3 and 2 mg/mL [67] and it is found in CSF between 0.5 and 2 μg/mL [164]. Sequence analysis has identified haptoglobin as a chymotrypsinogen-like serine protease homolog, although it has a distinct biological function [68]. Humans express one of three different haptoglobin phenotypes (Hp 1-1, Hp 1-2 or Hp 2-2) depending on the presence of two principal alleles (Hp1 and Hp2) coding for the α and β chains which associate covalently via disulfide linkage. The α^1, α^2, and β chain peptides are 9.2 kDa, 15.9 kDa, and 27.2 kDa, respectively [68]. Similar to clusterin, haptoglobin is heavily glycosylated.

2.3.1 In Vitro Chaperone Activity

Human haptoglobin specifically inhibits the precipitation of a wide variety of proteins induced by heat or oxidative stress [69]. All three human haptoglobin phenotypes exert this chaperone action, although Hp1-1 appears to be the most efficient. Like clusterin, haptoglobin forms stable, soluble, high molecular weight complexes with partially unfolded clients in an ATP-independent manner, but has no independent refolding activity. The possibility that haptoglobin holds misfolded proteins in a state competent for refolding by other chaperones is currently untested. Immunoaffinity depletion of haptoglobin from human serum significantly increases the amount of protein that is precipitated in response to stresses [165]. At substoichiometric levels, haptoglobin has been shown to inhibit amyloid formation dose-dependently by Aβ, ccβ_w, calcitonin, and the lysozyme variant I59T [165].

Haptoglobin is a known ligand of the CD11b/CD18 receptor on natural killer cells [166]. With much lower affinity, haptoglobin also binds to CD4 and CD8 receptors on T lymphocytes [167]. Neutrophils and monocytes also possess binding sites for haptoglobin and are responsible for haptoglobin uptake in peripheral blood [167]. Additionally, the acute-phase macrophage protein CD163 has been identified as a scavenger receptor for hemoglobin–haptoglobin complexes [167]. This high affinity receptor ligand interaction is Ca^{2+}-dependent and mediates endocytosis of the hemoglobin–haptoglobin complex [70]. It is possible that haptoglobin may facilitate the clearance of misfolded proteins via a similar mechanism to the clearance of hemoglobin–haptoglobin complexes, although this is yet to be investigated.

2.3.2 Evidence for In Vivo Chaperone Action/Disease Involvement

Haptoglobin is upregulated during a variety of conditions including infection, neoplasia, pregnancy, trauma, acute myocardial infarction, and other inflammatory conditions [70]. Its possible chaperone role in vivo is supported by co-deposition with amyloid in senile plaques [72], with drusen in age-related macular degeneration [73], and in protein deposits resulting from chronic glomerulonephritis [74]. Surprisingly, haptoglobin gene knockout does not impair the clearance of free plasma hemoglobin; however, haptoglobin-null mice display reduced postnatal viability and greater oxidative damage after induced hemolysis [168].

2.4 ApoE

Apolipoprotein E (ApoE) is a 35-kDa secreted glycoprotein, synthesized primarily by the liver, but can be found expressed by astrocytes, microglia, and oligodendrocytes in the brain. It exists in three isoforms – E2, E3, and E4 – which differ only by single amino acid variations. The prevalence of the alleles coding for these

isoforms, E2, E3, and E4, is approximately 7–8%, 75–80%, and 14–15%, respectively [169, 170]. ApoE is an amphipathic protein that is known for its ability to mediate transport and clearance of cholesterol, triglycerides, and other lipids [171]. It mediates lipid transport through binding to the low density lipoprotein (LDL) receptor. ApoE is best known for its association with Alzheimer's disease; APOE ε4/ε4 homozygotic individuals have a significantly greater risk of developing Alzheimer's disease [172].

2.4.1 In Vitro Chaperone Activity

ApoE has been shown to have the ability to bind to aggregation prone polypeptides, such as tau and Aβ [77, 78]. Interestingly, binding of ApoE to Aβ is isoform-dependent with the binding of ApoE4 being of lowest affinity (E2 > E3 > E4) [78, 173]. The stoichiometry of the interaction between Aβ and ApoE has been estimated at 5 Aβ peptide molecules per ApoE molecule [174]. This interaction is likely to be the driving force behind the ability of ApoE to affect the aggregation of Aβ. It has been shown both to promote and to inhibit Aβ aggregation depending on the conditions and specific variant of Aβ peptide used. The formation of complexes between ApoE and $A\beta_{1–40}$ has been shown to inhibit the formation of amyloid, at a 100:1 molar ratio of Aβ:ApoE [175]. The complexes made were added to monomeric Aβ and were unable to act as "seeds" for amyloid formation. However, the complexes formed still reacted with thioflavin T [175]. In addition, it has been shown that ApoE can prolong the lag phase of Aβ aggregation without affecting the amount of fibrillar material finally formed [176]. Similarly, ApoE lengthens the lag phase of amyloid formation from $A\beta_{29–40}$ and $A\beta_{29–42}$ by forming complexes with the respective peptides [174]. Interestingly, the E4 isotype had no effect on the lag phase. In contrast, there are many reports that suggest that ApoE can promote the formation of Aβ fibrils. ApoE was shown to enhance the formation of thioflavin T positive material from $A\beta_{1–40}$ [177], and promoted fibril formation by $A\beta_{1–42}$ (as judged by thioflavin T and transmission electron microscopy) [178].

2.4.2 Evidence for In Vivo Chaperone Action/Disease Involvement

The major focus on ApoE work has been its role in chaperoning Aβ due to its strong genetic association with Alzheimer's disease [79]. In humans ApoE has been found co-localized with Alzheimer's and CJD plaques [80]. To complicate further understanding of the role of ApoE in amyloid formation (see above), mouse studies have been similarly conflicting. In initial studies, both Aβ immunoreactivity and amyloid formation were reduced in ApoE knockout mice [179, 180]. In contrast, expression of human ApoE in transgenic mice suppressed Aβ deposition [181]. Regardless of its effect on amyloid formation, just as observed for other extracellular chaperones such as clusterin and α_2M, complexes formed between ApoE and Aβ are efficiently taken up by receptor mediated endocytosis and promote subsequent degradation

of Aβ. It has been shown that Aβ-ApoE complexes bind to the cell surface receptor megalin while free Aβ does not [182]. In addition, LRP1 binds to Aβ-ApoE complexes and internalizes them for subsequent degradation in lysosomes (or transport into plasma) [148]. Furthermore, it has been suggested that ApoE facilitates internalization and degradation of Aβ by astrocytes [81]. As Aβ is known to activate glial cells, its incorporation into complexes and its ApoE-dependent receptor mediated uptake may play a role in modulating the immune response. Consistent with this idea, it has been shown that the formation of ApoE-Aβ complexes inhibits the activation of astrocytes by Aβ [183].

2.5 Serum Amyloid P Component

Serum Amyloid P Component (SAP) is a member of the highly conserved pentraxin family and consists of five identical 25-kDa subunits arranged in a ring [184]. As for other pentraxins, SAP displays calcium-dependent ligand binding and tertiary structure similar to legume lectins [184]. It is estimated that over 8% of the mass of the molecule is N-linked oligosaccharide [184]. It has been proposed that SAP circulates as a decamer with two pentameric rings noncovalently bound [184, 185]. However, other reports claim that SAP exists as a single pentamer in the body and that the decameric form is obtained only upon purification [186, 187]. Human SAP shares approximately 51% amino acid homology with C-reactive protein, a classical human acute phase protein. In contrast, SAP does not behave as an acute phase protein in humans [82]; it is generally present in human plasma at around 40 μg/mL [83] and in CSF at around 8.5 ng/mL [84]. Although to date no clear biological function has been ascribed to SAP, it is known to interact with a diverse range of molecules in vitro. For example, SAP binds to glycosaminoglycans [188], DNA and chromatin [191–192], complement components [193, 194], fibronectin [195], C-reactive protein [196], aggregated IgG [197], phosphatidylethanolamine [197], and endotoxin [192, 198]. Of particular interest in the current context, SAP binds highly specifically to amyloid and is universally found in amyloid deposits [85–88, 199].

2.5.1 In Vitro Chaperone Activity

There is currently little evidence for the existence of efficient refolding chaperones in the extracellular milieu; however, it has been reported that SAP has ATP-independent refolding activity [89]. When present at a tenfold molar excess, SAP was able to recover 25% of the initial enzyme activity of denatured lactate dehydrogenase. Whether this activity would be enhanced by the presence of ATP or "helper" chaperones is currently unknown. Further studies are needed before the potential physiological significance of this refolding activity becomes clear. SAP binds to synthetic Aβ at physiological concentrations of Ca^{2+} [200] and binds to all types of amyloid fibrils tested in vitro [201]. SAP has a protease-resistant β-pleated

sheet structure that in the presence of Ca^{2+} is resistant to proteolysis [90]. Consequently, SAP binding to amyloid fibrils is thought to inhibit their proteolytic digestion.

2.5.2 Evidence for In Vivo Chaperone Action/Disease Involvement

SAP constitutes up to 15% of the mass of amyloid deposits in vivo, which is remarkable considering it is only present in plasma at trace concentrations. Also, strongly supporting a role for SAP in amyloid pathogenesis is the frequency with which it is found localized in amyloid deposits in vivo [85–88, 90]. SAP knockout mice are viable and fertile with no obvious abnormalities; however, they display delayed amyloid deposition in models of systemic amyloidosis [89]. These results support that SAP plays a role in amyloid pathogenesis and that inhibition of SAP binding to amyloid is a potential therapeutic target. Given that SAP does not appear to be expressed in the brain, localization of SAP with cerebral amyloid deposits suggest that either specific active transport mechanisms exist to transport it from one side of the blood–brain barrier to the other or that damage to the blood–brain barrier is sufficient to allow the protein to leak into the brain during disease. Regardless of the mechanism by which it gets there, the CSF concentration of SAP is higher in patients with Alzheimer's disease [85].

2.6 Caseins

Casein is the main constituent of milk (~80% of protein in bovine milk) and is made up of a heterogeneous mixture of phosphoproteins that includes four unrelated gene products: α_{S1}-, α_{S2}-, β-, and κ-casein. In their monomeric forms, the caseins themselves are small, ranging in molecular mass between 19 and 25 kDa. However, the casein proteins exhibit a strong tendency to associate with each other, through hydrophobic and ionic interactions, which, in the presence of calcium and other ions, leads to the formation of casein micelles [91]. The micelles range in mass between 10^3 and 3×10^6 kDa and represent the primary nutritional source of calcium (in the form of calcium phosphate) to the neonate [91]. The caseins have been classified as intrinsically disordered proteins, as they are extremely flexible, essentially unfolded, and have relatively little secondary or tertiary structure under physiological conditions [202]. Their open, dynamic and malleable conformations suggest that they exist in a molten globule-like state, with extensive regions of solvent-exposed and clustered hydrophobicity [203]. As a result, it is unlikely that detailed X-ray crystal structures of full-length casein protein will be achieved; however, three-dimensional energy-minimized molecular models are available [204, 205]. Two of the casein proteins, α_{S1}- and β-casein, have been found to have molecular chaperone-like activity, similar to the small heat shock proteins (sHsps) [26, 92]. The open, flexible nature of α_{S1}-casein and β-casein results from

the high percentage of proline residues in their amino acid sequence (9% of the amino acid sequence of α_{S1}-casein and 18% of β-casein) and lack of disulfide bonds. Both α_{S1}-casein and β-casein also possess a high degree of overall hydrophobicity, with well separated hydrophilic and hydrophobic domains. Such properties, which they share with other molecular chaperones such as the sHsps and clusterin [26], likely account for their ability to bind to a wide-range of destabilized, partially unfolded target proteins to prevent their aggregation [92].

2.6.1 In Vitro Chaperone Activity

To date, studies on the chaperone-like activity of casein proteins have been performed with bovine whole casein (comprising all four casein proteins) or with α_S-casein (comprising both α_{S1}- and α_{S2}-casein) or β-casein. Thus, α_S-casein and β-casein have been shown to inhibit the amorphous aggregation of a range of unrelated target proteins induced by heating [93–97], reduction [93, 95, 96], and UV-light [93]. They do so by forming high molecular weight complexes with the target protein, and stabilizing them in order to prevent their aggregation and potential precipitation. They have no intrinsic re-folding ability [95, 96] and thus their mechanism of action is akin to the sHsps and clusterin [26]. The chaperone-like activity of α_S-casein and β-casein against amorphously aggregating target proteins is phosphorylation-dependent, dephosphorylation decreasing their chaperone efficacy [94, 206]. The caseins are heavily phosphorylated (typically eight phosphate residues per mole for α_{S1}-casein and five for β-casein) which, apart from its role in calcium-binding and stabilization of the casein micelle, appears to play a significant role (via their negative charge) in maintaining the solubility of the complexes formed between the caseins and target proteins [207]. It has recently been suggested that the chaperone-like activity of these caseins may be exploited in order to control protein aggregation during food production [92]. α_S-Casein and β-casein also appear to possess a generic ability to prevent protein aggregation associated with fibril formation. For example, whole and β-casein inhibit heat-induced fibril formation by ovalbumin [207], α_S-casein and β-casein inhibit κ-casein fibril formation [206, 208], and α_{S1}-casein inhibits α_{S2}-fibril formation [209].

2.6.2 Evidence for In Vivo Chaperone Action/Disease Involvement

Caseins are uniquely synthesized in the mammary gland and immediately associate to form casein micelles, which are secreted into the alveolar lumen [210]. There is no direct evidence that a failure in the chaperone action of α_S-casein and β-casein is involved in disease; however, amyloid-like deposits (known as *corpora amylacea*) have been identified in mammary tissue from a variety of species [98–100], and bundles of fibrils have been reported in the cytoplasm of cells that surround these calcified deposits [101]. The proteins present in these deposits and fibrils include the caseins [102, 103]. When isolated from the other caseins, α_{S2}- and κ-casein

readily form fibrils when incubated under conditions of physiological pH and temperature (i.e., pH 7.0–7.4, 37 °C) [208, 209, 211, 212] which suggests that these proteins may form fibrils in vivo. However, fibril formation by α_{S2}- and κ-casein is inhibited by physiological concentrations of α_{S1}- and β-casein in vitro [208, 209] and thus, the tendency of caseins to associate together acts as a protective mechanism to prevent this form of aggregation. Indeed, the fact that amyloid deposits in mammary tissue are not more prevalent is most likely attributable to the chaperone-like ability of α_{S1}- and β-casein, which act to prevent the release of the amyloidogenic α_{S2}- and κ-casein precursors by binding them into casein micelles.

2.7 Fibrinogen

Fibrinogen is synthesized by the liver and circulates in human plasma at a concentration of 2–4.5 mg/mL [104]. It is the 340-kDa glycoprotein precursor to fibrin, which forms clots in the wound response. Fibrinogen is an "acute phase protein" and its levels in plasma are elevated in response to a variety of stresses including stroke, atherosclerotic diseases, age, and acute myocardial infarction [104]. Fibrinogen molecules are comprised of two sets of disulfide-linked Aα-, Bβ-, and γ-chains. Fibrin is formed after cleavage of fibrinopeptide A (FPA) from fibrinogen Aα-chains, which initiates fibrin polymerization. In addition to its well known role in providing a scaffold for clots, fibrinogen also has other biological functions involving a range of binding sites, some of which are only exposed as a consequence of fibrin formation. These other functions include recruiting platelets into clots, down-regulation of circulating levels of thrombin, and plasminogen activation [104].

2.7.1 In Vitro Chaperone Activity

Only two publications have appeared so far describing the chaperone activity of fibrinogen. The first of these presented results suggesting that human plasma fibrinogen (1) specifically, and independently of ATP, inhibited the thermally induced aggregation of citrate synthase and firefly luciferase, (2) held the heat-stressed forms of these proteins in a state competent for refolding by a rabbit reticulocyte lysate, (3) inhibited amyloid formation by yeast prion protein Sup35, and (4) inhibited heat-induced aggregation of proteins in undiluted mouse plasma [105]. These studies were described as having been done using fibrinogen sourced from a commercial supplier (which would be expected to be overwhelmingly comprised of the usual 340-kDa form). However, in a subsequent study by the same group, similar chaperone properties were attributed specifically to the α_EC C-terminal extension of fibrinogen, present only in a much less abundant 420-kDa isoform of the protein (fibrinogen-420) [106]. Fibrinogen-420 is normally present in human plasma at 20–150 mg/mL (i.e., making up about 0.4–7.5% of the

circulating fibrinogen pool). Our own experiments failed to show any chaperone activity for the 340-kDa form of fibrinogen (A. Wyatt, unpublished). The reason(s) for the apparent discrepancy between these two publications is unclear. However, the balance of evidence suggests that the abundant 340-kDa form of fibrinogen is not a chaperone, but that the α_EC moiety in fibrinogen-420 is a chaperone-active species.

2.7.2 Evidence for In Vivo Chaperone Action/Disease Involvement

The level of α_EC can be regulated by proteases (such as matrix metalloproteases and plasmin) which can rapidly release it from fibrinogen-420. It has been suggested that fibrinogen-420 acts as a delivery vehicle for α_EC [106]. Evidence for an in vivo chaperone role for fibrinogen-420/α_EC is currently limited to the demonstration that (1) proteins in plasma of fibrinogen knock-out mice aggregate to a greater extent when incubated for 48 h at 43 °C than those in the plasma of wild-type mice [106] and (2) exogenously added α_EC formed complexes with a variety of proteins in human plasma heated for 30 min at 50 °C [106]. Future work will hopefully further define the in vivo role(s) of the fibrinogen-420/α_EC chaperone activity and its potential involvement in diseases.

2.8 In Vivo Functions of Extracellular Chaperones

It is clear from the growing number of abundant ECs identified that they are likely to play very important roles in the maintenance of normal physiological functions. The precise details of these roles are currently under investigation but are likely to include (1) selective binding to exposed regions of hydrophobicity on extracellular proteins induced to misfold by (for example) various physical or chemical stresses, leading to (2) inhibition of their toxicity towards cells and (3) stabilization of their structure so that they are prevented from aggregating to form insoluble deposits. Soluble complexes formed between ECs and misfolded proteins are probably internalized via receptor-mediated endocytosis and subsequently degraded by (for example) lysosomal proteolysis. However, it is also feasible that within antigen-presenting cells ECs can direct bound protein antigens to other intracellular proteolytic systems such as the proteasome, and that peptide fragments of the degraded chaperone client proteins are later presented at the cell surface in association with class I and/or II major histocompatibility antigens. In this way, ECs may play multiple critical roles in vivo, protecting the body from the dangers of inappropriate aggregation of extracellular proteins but also playing a pivotal role in the processing of extracellular protein antigens necessary for eliciting protective immune responses (Fig. 1).

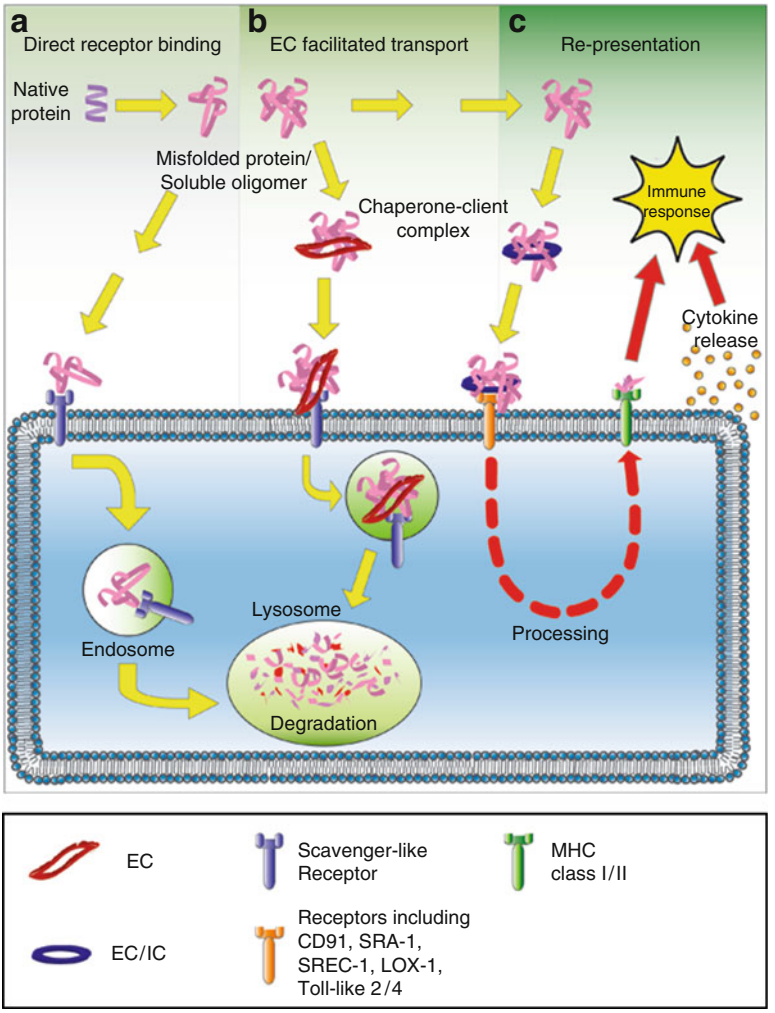

Fig. 1 Theoretical model for the involvement of ECs in extracellular proteostasis and the immune response. Under normal physiological conditions misfolded extracellular proteins are bound by (**a**) scavenger-like receptors directly, or (**b**) circulating ECs, keeping them soluble and facilitating their subsequent transport to cell surface scavenger-like receptors. EC-client protein complexes may be internalized and subsequently degraded by lysosomal proteolysis. Alternatively, on antigen presenting cells (**c**), EC (or IC)-client protein complexes may be (1) bound and internalized by a variety of receptors, (2) subsequently processed intracellularly by yet to be established mechanisms, and then (3) re-presented as peptides on the cell surface associated with major histocompatibility (MHC) antigen class I or II molecules to trigger the release of cytokines and an immune response

3 Conclusions

It is barely over a decade since the first abundant mammalian extracellular chaperone (clusterin) was identified. Since that time there have been a series of discoveries of other extracellular chaperones such that we now know there are at least 7% at (in some cases) substantial concentrations in human blood. Collectively, by mass, these chaperones account for possibly in excess of 7% of all blood proteins. The caseins are also abundant in another important extracellular fluid, milk. It will be unsurprising if further extracellular chaperones are identified in coming years. The shear abundance of these chaperones in body fluids strongly suggests that they perform vital biological functions. These functions may include roles in stabilizing misfolded proteins aggregating via either the amorphous or amyloid-forming pathways, mediating the clearance of these aggregation-prone (and often toxic) proteins from the body, and modulating the response of the immune system to extracellular antigens. The processes governing the development of the many serious human diseases linked to inappropriate aggregation of extracellular proteins are poorly understood. Clearly, advances in knowledge of extracellular chaperones will impact upon our ability to prevent and treat these diseases, and may allow us to harness better the power of the immune system to fight conditions such as cancers. Furthermore, extracellular chaperones may exert powerful but currently poorly characterized effects on the delivery and efficacy of systemically administered hydrophobic drugs. All of these considerations point to the importance of future work to identify the in vivo roles of the growing family of extracellular chaperones.

References

1. Sitia R, Braakman I (2003) Quality control in the endoplasmic reticulum protein factory. Nature 426:891–894
2. Ker YC, Chen RH (1998) Stress-induced conformational changes and gelation of soy protein isolate suspensions. Lebenson Wiss Technol 31:107–113
3. Bucciantini M et al (2002) Inherent toxicity of aggregates implies a common mechanism for protein misfolding diseases. Nature 416:507–510
4. Buxbaum J, Gallo G (1999) Nonamyloidotic monoclonal immunoglobulin deposition disease. Light-chain, heavy-chain, and light- and heavy-chain deposition diseases. Hematol Oncol Clin North Am 13:1235–1248
5. Mullins RF et al (2000) Drusen associated with aging and age-related macular degeneration contain proteins common to extracellular deposits associated with atherosclerosis, elastosis, amyloidosis, and dense deposit disease. FASEB J 14:835–846
6. Saito K, Dai Y, Ohtsuka K (2005) Enhanced expression of heat shock proteins in gradually dying cells and their release from necrotically dead cells. Exp Cell Res 310:229–236
7. Feng H et al (2001) Stressed apoptotic tumor cells express heat shock proteins and elicit tumor-specific immunity. Blood 97:3503–3512
8. Gastpar R et al (2005) Heat shock protein 70 surface-positive tumor exosomes stimulate migratory and cytolytic activity of natural killer cells. Cancer Res 65:5238–5247

9. Lancaster GI, Febbraio MA (2005) Exosome-dependent trafficking of HSP70: a novel secretory pathway for cellular stress proteins. J Biol Chem 280:23349–23355
10. Mambula SS, Calderwood SK (2006) Heat shock protein 70 is secreted from tumor cells by a nonclassical pathway involving lysosomal endosomes. J Immunol 177:7849–7857
11. Mambula SS et al (2007) Mechanisms for Hsp70 secretion: crossing membrane without a leader. Methods 43:168–175
12. Merendino AM et al (2010) Hsp60 is actively secreted by human tumor cells. PLoS One 5:e9247
13. Eustace BK et al (2004) Functional proteomic screens reveal an essential extracellular role for hsp90 alpha in cancer cell invasiveness. Nat Cell Biol 6:507–514
14. Srivastava PK et al (1998) Heat shock proteins come of age: primitive functions acquire new roles in an adaptive world. Immunity 8:657–665
15. Srivastava P (2002) Roles of heat-shock proteins in innate and adaptive immunity. Nat Rev Immunol 2:185–194
16. Basu S, Srivastava PK (1999) Calreticulin, a peptide-binding chaperone of the endoplasmic reticulum, elicits tumor- and peptide-specific immunity. J Exp Med 189:797–802
17. Maki RG et al (2007) A phase I pilot study of autologous heat shock protein vaccine HSPPC-96 in patients with resected pancreatic adenocarcinoma. Dig Dis Sci 52:1964–1972
18. Rivoltini L et al (2003) Human tumor-derived heat shock protein 96 mediates in vitro activation and in vivo expansion of melanoma- and colon carcinoma-specific T cells. J Immunol 171:3467–3474
19. Srivastava PK, DeLeo AB, Old LJ (1986) Tumour rejection antigens of chemically induced sarcomas of inbred mice. Proc Natl Acad Sci USA 83:3407–3411
20. Suto R, Srivastava PK (1995) A mechanism for the specific immunogenicity of heat shock protein-chaperoned peptides. Science 269:1585–1588
21. Udono H, Srivastava PK (1993) Heat shock protein 70-associated peptides elicit specific cancer immunity. J Exp Med 178:1391–1396
22. Humphreys DT et al (1999) Clusterin has chaperone-like activity similar to that of small heat shock proteins. J Biol Chem 274:6875–6881
23. Wilson MR, Easterbrook-Smith SB (2000) Clusterin is a secreted mammalian chaperone. Trends Biochem Sci 25:95–98
24. Murphy BF et al (1988) SP-40,40, a newly identified normal human serum protein found in the SC5b-9 complex of complement and in the immune deposits in glomerulonephritis. J Clin Invest 81:1858–1864
25. Choi NH et al (1990) Sandwich ELISA for quantitative measurement of SP-40,40 in seminal plasma and serum. J Immunol Methods 131:159–163
26. Carver JA et al (2003) Small heat-shock proteins and clusterin: intra- and extracellular molecular chaperones with a common mechanism of action and function. IUBMB Life 55:661–668
27. Poon S et al (2002) Mildly acidic pH activates the extracellular molecular chaperone clusterin. J Biol Chem 277:39532–39540
28. Poon S et al (2000) Clusterin is an ATP-independent chaperone with a very broad substrate specificity that stabilizes stressed proteins in a folding-competent state. Biochemistry 39:15953–15960
29. Poon S et al (2002) Clusterin is an extracellular chaperone that specifically interacts with slowly aggregating proteins on their off-folding pathway. FEBS Lett 513:259–266
30. Wyatt AR, Wilson MR (2010) Identification of human plasma proteins as major clients for the extracellular chaperone clusterin. J Biol Chem 285:3532–3539
31. Wyatt AR, Yerbury JJ, Wilson MR (2009) Structural characterization of clusterin-client protein complexes. J Biol Chem 284:21920–21927
32. Yerbury JJ et al (2007) The extracellular chaperone clusterin influences amyloid formation and toxicity by interacting with pre-fibrillar structures. FASEB J 21:2312–2322
33. Kumita JR et al (2007) The extracellular chaperone clusterin potentially inhibits amyloid formation by interacting with prefibrillar species. J Mol Biol 369:157–167

34. Matsubara E, Frangione B, Ghiso J (1995) Characterization of apolipoprotein J-Alzheimer's a-beta interaction. J Biol Chem 270:7563–7567
35. Oda T et al (1995) Clusterin (apoJ) alters the aggregation of amyloid beta peptide 1–42 and forms slowly sedimenting A-beta complexes that cause oxidative stress. Exp Neurol 136:22–31
36. McHattie S, Edington N (1999) Clusterin prevents aggregation of neuropeptide 106–126 in vitro. Biochem Biophys Res Commun 259:336–340
37. Hatters DM et al (2002) Suppression of apolipoprotein C-II amyloid formation by the extracellular chaperone, clusterin. Eur J Biochem 269:2789–2794
38. Crabb JW et al (2002) Drusen proteome analysis: an approach to the etiology of age-related macular degeneration. Proc Natl Acad Sci USA 99:14682–14687
39. French LE, Tschopp J, Schifferli JA (1992) Clusterin in renal tissue: preferential localization with the terminal complement complex and immunoglobulin deposits in glomeruli. Clin Exp Immunol 88:389–393
40. Sasaki K et al (2002) Clusterin/apolipoprotein J is associated with cortical Lewy bodies: immunohistochemical study in cases with alpha-synucleinopathies. Acta Neuropathol 104:225–230
41. Freixes M et al (2004) Clusterin solubility and aggregation in Creutzfeldt-Jakob disease. Acta Neuropathol 108:295–301
42. Zenkel M et al (2006) Clusterin deficiency in eyes with pseudoexfoliation syndrome may be implicated in the aggregation and deposition of pseudoexfoliative material. Invest Opthalmol Vis Sci 47:1982–1990
43. Mackness B et al (1997) Increased immunolocalization of paraoxonase, clusterin and apolipoprotein A-I in the human artery wall with the progression of atherosclerosis. Arterioscler Thromb Vasc Biol 17:1233–1238
44. Witte DP et al (1993) Platelet activation releases megakaryocyte-synthesized apolipoprotein J, a highly abundant protein in a atheromatous lesions. Am J Pathol 143:763–773
45. Ghiso J et al (1993) The cerebrospinal-fluid soluble form of Alzheimer's amyloid beta is complexed to SP-40,40 (apolipoprotein J), an inhibitor of the complement membrane-attack complex. Biochem J 293:27–30
46. Calero M et al (2000) Apolipoprotein J (clusterin) and Alzheimer's disease. Microsc Res Tech 50:305–315
47. Rosenberg ME, Silkensen J (1995) Clusterin: physiologic and pathophysiologic considerations. Int J Biochem Cell Biol 27:633–645
48. Strocchi P et al (2006) Clusterin up-regulation following sub-lethal oxidative stress and lipid peroxidation in human neuroblastoma cells. Neurobiol Aging 27:1588–1594
49. Ubrich C et al (2000) Laminar shear stress upregulates the complement-inhibitory protein clusterin. Circulation 101:352–355
50. Loison F et al (2006) Up-regulation of the clusterin gene after proteotoxic stress: implications of HSF1-HSF2 heterocomplexes. Biochem J 395:223–231
51. Michel D et al (1997) Stress-induced transcription of the clusterin/apoJ gene. Biochem J 328:45–50
52. Criswell T et al (2005) Delayed activation of insulin-like growth factor-1 receptor/Src/MAPK/Egr-1 signaling regulates clusterin expression, a pro-survival factor. J Biol Chem 280:14212–14221
53. Harold D et al (2009) Genome-wide association study identifies variants at CLU and PICALM associated with Alzheimer's disease. Nat Genet 41:1088–1093
54. Lambert JC et al (2009) Genome-wide association study identifies variants at CLU and CR1 associated with Alzheimer's disease. Nat Genet 41:1094–1099
55. Binder RJ, Karimeddini D, Srivastava PK (2001) Adjuvanticity of alpha2-macroglobulin, an independent ligand for the heat shock protein receptor CD91. J Immunol 166:4968–4972
56. Sottrup-Jensen L (1989) Alpha-macroglobulins: structure shape and mechanism of proteinase complex formation. J Biol Chem 264:11539–11542

57. Biringer RG et al (2006) Enhanced sequence coverage of proteins in human cerebrospinal fluid using multiple enzymatic digestion and linear ion trap LC-MS/MS. Brief Funct Genomic Proteomic 5:144–153
58. Narita M et al (1997) Alpha2-macroglobulin complexes with and mediates the endocytosis of beta-amyloid peptide via cell surface low-density lipoprotein receptor-related protein. J Neurochem 69:1904–1911
59. Mettenburg JM, Webb DJ, Gonias SL (2002) Distinct binding sites in the structure of alpha 2-macroglobulin mediate the interaction with beta-amyloid peptide and growth factors. J Biol Chem 277:13338–13345
60. Motomiya Y et al (2003) Circulating levels of alpha2-macroglobulin-beta2-microglobulin complex in hemodialysis patients. Kidney Int 64:2244–2252
61. Adler V, Kryukov V (2007) Serum macroglobulin induces prion protein transition. Neurochem J 1:43–52
62. French K, Yerbury JJ, Wilson MR (2008) Protease activation of alpha2-macroglobulin modulates a chaperone-like action with broad specificity. Biochemistry 47:1176–1185
63. Fabrizi C et al (2001) Role of alpha2-macroglobulin in regulating amyloid -protein neurotoxicity: protective or detrimental factor? J Neurochem 78:406–412
64. Adler V et al (2007) Alpha2-macroglobulin is a potential facilitator of prion protein transformation. Amyloid 14:1–10
65. Binder RJ (2004) Purification of alpha2-macroglobulin and the construction of immunogenic alpha2-macroglobulin-peptide complexes for use as cancer vaccines. Methods 32:29–31
66. Bowman BH, Kurosky A (1982) Haptoglobin: the evolutionary product of duplication, unequal crossing over, and point mutation. Adv Hum Genet 12:189–261
67. Baskies AM et al (1980) Serum glycoproteins in cancer patients: first reports of correlations with in vitro and in vivo parameters of cellular immunity. Cancer 45:3050–3060
68. Kurosky A et al (1980) Covalent structure of human haptoglobin: a serine protease homolog. Proc Natl Acad Sci USA 77:3388–3392
69. Pavlicek Z, Ettrich R (1999) Chaperone-like activity of human haptoglobin: similarity with a-crystallin. Collect Czech Chem Comm 64:717–725
70. Kristiansen M et al (2001) Identification of the haemoglobin scavenger receptor. Nature 409:198–201
71. Langlois MR, Delanghe JR (1996) Biological and clinical significance of haptoglobin polymorphisms in humans. Clin Chem 42:1589–1600
72. Powers JM et al (1981) An immunoperoxidase study of senile cerebral amyloidosis with pathogenetic considerations. J Neuropathol Exp Neurol 40:592–612
73. Kliffen M, de Jong PT, Luider TM (1995) Protein analysis of human maculae in relation to age-related maculopathy. Lab Invest 72:267–272
74. Tomino Y et al (1981) Immunofluorescent studies on acute phase reactants in patients with various types of chronic glomerulonephritis. Tokai J Exp Clin Med 6:435–441
75. Phillips NR, Havel RJ, Kane JP (1983) Sex-related differences in the concentrations of apolipoprotein E in human blood plasma and plasma lipoproteins. J Lipid Res 24: 1525–1531
76. Landén M et al (1996) Apolipoprotein E in cerebrospinal fluid from patients with Alzheimer's disease and other forms of dementia is reduced but without any correlation to the apoE4 isoform. Dementia 7:273–278
77. Strittmatter WJ et al (1994) Isoform-specific interactions of apolipoprotein E with microtubule-associated tau: implications for Alzheimer disease. Proc Natl Acad Sci USA 91:11183–11186
78. Strittmatter WJ et al (1993) Binding of human apolipoprotein E to synthetic amyloid b peptide: isoform specific-effects and implications for late-onset Alzheimer disease. Proc Natl Acad Sci USA 90:8098–8102
79. Corder EH et al (1993) Gene dose of apolipoprotein E type 4 allele and the risk of Alzheimer's disease in late onset families. Science 261:921–923

80. Namba Y et al (1991) Apolipoprotein E immunoreactivity in cerebral amyloid deposits and neurofibrillary tangles in Alzheimer's disease and kuru plaque amyloid in Creutzfeldt-Jakob disease. Brain Res 541:163–166
81. Koistinaho M et al (2004) Apolipoprotein E promotes astrocyte colocalization and degradation of deposited amyloid-beta peptides. Nat Med 10:719–726
82. Aquilina JA, Robinson CV (2003) Investigating interactions of the pentraxins serum amyloid P component and C-reactive protein by mass spectrometry. Biochem J 375:323–328
83. Pepys MB et al (1978) Comparative clinical study of protein SAP (amyloid P component) and C-reactive protein in serum. Clin Exp Immunol 32:119–124
84. Hutchinson WL et al (1994) The pentraxins, C-reactive protein and serum amyloid P component, are cleared and catabolized by hepatocytes in vivo. J Clin Invest 94:1390–1396
85. Botto M et al (1997) Amyloid deposition is delayed in mice with targeted deletion of the serum amyloid P component gene. Nat Med 3:885–889
86. Coria F et al (1988) Isolation and characterization of amyloid P component from Alzheimer's disease and other types of cerebral amyloidosis. Lab Invest 58:454–458
87. Breathnach SM et al (1981) Amyloid P component is located on elastic fibre microfibrils in normal human tissue. Nature 293:652–654
88. Kalaria RN et al (1991) Serum amyloid P in Alzheimer's disease. Implications for dysfunction of the blood-brain barrier. Ann NY Acad Sci 640:145–148
89. Yang GC et al (1992) Ultrastructural immunohistochemical localization of polyclonal IgG, C3, and amyloid P component on the congo red-negative amyloid-like fibrils of fibrillary glomerulopathy. Am J Pathol 141:409–410
90. Tennent GA, Lovat LB, Pepys MB (1995) Serum amyloid P component prevents proteolysis of the amyloid fibrils of Alzheimer's disease and systemic amyloidosis. Proc Natl Acad Sci USA 92:4299–4303
91. Swaisgood HE (2003) Chemistry of the caseins. In: Fox PF, McSweeney PLH (eds) Advanced dairy chemistry. Kluwer Academic/Plenum Publishers, New York
92. Thorn DC, Ecroyd H, Carver JA (2009) The two-faced nature of milk casein proteins: amyloid fibril formation and chaperone-like activity. Aust J Dairy Technol 64:36–40
93. Bhattacharyya J, Das KP (1999) Molecular chaperone-like properties of an unfolded protein, alpha(s)-casein. J Biol Chem 274:15505–15509
94. Matsudomi N et al (2004) Ability of alphas-casein to suppress the heat aggregation of ovotransferrin. J Agric Food Chem 52:4882–4886
95. Morgan PE et al (2005) Casein proteins as molecular chaperones. J Agric Food Chem 53:2670–2683
96. Zhang X et al (2005) Chaperone-like activity of beta-casein. Int J Biochem Cell Biol 37:1232–1240
97. Hassanisadi M et al (2008) Chemometric study of the aggregation of alcohol dehydrogenase and its suppression by beta-caseins: a mechanistic perspective. Anal Chim Acta 613:40–47
98. Reid IM (1972) Corpora amylacea of the bovine mammary gland. Histochemical and electron microscopic evidence for their amyloid nature. J Comp Pathol 82:409–413
99. Taniyama H et al (2000) Localized amyloidosis in canine mammary tumors. Vet Pathol 37:104–107
100. Gruys E (2004) Protein folding pathology in domestic animals. J Zhejiang Univ Sci 5:1226–1238
101. Nickerson SC (1987) Amyloid fibril formation in the bovine mammary gland: an ultrastructural study. Cytobios 51:81–92
102. Claudon C et al (1998) Proteic composition of corpora amylacea in the bovine mammary gland. Tissue Cell 30:589–595
103. Niewold TA et al (1999) Casein related amyloid, characterization of a new and unique amyloid protein isolated from bovine corpora amylacea. Amyloid 6:244–249

104. Mosesson MW (2005) Fibrinogen and fibrin structure and functions. J Thromb Haemost 3:1894–1904
105. Tang H et al (2009) Fibrinogen has chaperone-like activity. Biochem Biophys Res Commun 378:662–667
106. Tang H et al (2009) Alpha(E)C, the C-terminal extension of fibrinogen, has chaperone-like activity. Biochemistry 48:3967–3976
107. Jenne DE, Tschopp J (1992) Clusterin: the intriguing guises of a widely expressed glycoprotein. Trends Biochem Sci 17:154–159
108. de Silva HV et al (1990) Apolipoprotein J: structure and tissue distribution. Biochemistry 29:5380–5389
109. Hermo L, Barin K, Oko R (1994) Developmental expression of sulfated glycoprotein-2 in the epididymis of the rat. Anat Rec 240:327–344
110. Jordan-Starck TC et al (1992) Apolipoprotein J: a membrane policeman? Curr Opin Lipidol 3:75–85
111. Buttyan R et al (1989) Induction of the Trpm-2 gene in cells undergoing programmed death. Mol Cell Biol 9:3473–3481
112. Kapron JT et al (1997) Identification and characterization of glycosylation sites in human serum clusterin. Protein Sci 6:2120–2123
113. Lupas A (1991) Predicting coiled-coils from protein sequences. Science 252:1162–1164
114. Bailey RW et al (2001) Clusterin, a binding protein with a molten globule-like region. Biochemistry 40:11828–11840
115. Yang CR et al (2000) Nuclear clusterin/XIP8, an X-ray induced Ku70-binding protein that signals cell death. Proc Natl Acad Sci USA 97:5907–5912
116. Santilli G, Aronow BJ, Sala A (2003) Essential requirement of apolipoprotein J (clusterin) signaling for Ikappa B expression and regulation of NF-kappaB activity. J Biol Chem 278:38214–38219
117. Kang SW et al (2005) Clusterin interacts with SCLIP (SCG10-like protein) and promotes neurite outgrowth of PC12. Exp Cell Res 309:305–315
118. Debure L et al (2003) Intracellular clusterin causes juxtanuclear aggregate formation and mitochondrial alteration. J Cell Sci 116:3109–3121
119. Zhang HL et al (2005) Clusterin inhibits apoptosis by interacting with activated Bax. Nat Cell Biol 7:909–915
120. Nizard P et al (2007) Stress-induced retrotranslocation of clusterin/ApoJ into the cytosol. Traffic 8:554–565
121. Reddy KB et al (1996) Transforming growthfactor b (TGFb)-induced nuclear localization of apolipoprotein J/clusterin in epithelial cells. Biochemistry 35:6157–6163
122. Leskov KS et al (2003) Synthesis and functional analyses of nuclear clusterin, a cell death protein. J Biol Chem 278:11590–11600
123. Bucciantini M et al (2004) Pre-fibrillar amyloid protein aggregates share common features of cytotoxicity. J Biol Chem 279:31374–31382
124. Kounnas MZ et al (1995) Identification of Glycoprotein 330 as an endocytic receptor for apolipoprotein J/clusterin. Biochemistry 270:13070–13075
125. Zlokovic BV et al (1996) Glycoprotein 330 megalin: probable role in receptor-mediated transport of apolipoprotein J alone and in a complex with Alzheimer disease amyloid b at the blood–brain and blood–cerebrospinal fluid barriers. Proc Natl Acad Sci USA 93:4229–4234
126. Hammad SM et al (1997) Interaction of apolipoprotein J-amyloid B-peptide complex with low density lipoprotein receptor-related protein-2/megalin. J Biol Chem 272:18644–18649
127. Calero M et al (1999) Functional and structural properties of lipid-associated apolipoprotein J (clusterin). Biochem J 344:375–383
128. Mahon MG et al (1999) Multiple involvement of clusterin in chicken ovarian follicle development. J Biol Chem 274:4036–4044

129. Bartl MM et al (2001) Multiple receptors mediate apoJ-dependent clearance of cellular debris into nonprofessional phagocytes. Exp Cell Res 271:130–141
130. Lakins JN et al (2002) Evidence that clusterin has discrete chaperone and ligand binding sites. Biochemistry 41:282–291
131. Bajari TM et al (2003) A model for modulation of leptin activity by association with clusterin. FASEB J 17:1505–1507
132. Trougakos IP et al (2006) Clusterin/apolipoprotein J up-regulation after zinc exposure, replicative senescence or differentiation of human haematopoietic cells. Biogerontology 7:375–382
133. Bailey RW et al (2002) Heat shock-initiated apoptosis is accelerated and removal of damaged cells is delayed in the testis of clusterin/apoJ knock-out mice. Biol Reprod 66:1042
134. McLaughlin L et al (2000) Apolipoprotein J/clusterin limits the severity of murine autoimmune myocarditis. J Clin Invest 106:1105–1113
135. Wehrli P et al (2001) Inhibition of post-ischemic brain injury by clusterin overexpression. Nat Med 7:977–978
136. DeMattos RB et al (2004) ApoE and clusterin cooperatively suppress Abeta levels and deposition: evidence that ApoE regulates extracellular Abeta metabolism in vivo. Neuron 41:193–202
137. Rosenberg M et al (2002) Apolipoprotein J/clusterin prevents progressive glomerulopathy of aging. Mol Cell Biol 22:1893–1902
138. Jensen PE, Sottrup-Jensen L (1986) Primary structure of human alpha-2 macroglobulin. Complete disulfide bridge assignment and localization of two interchain bridges in the dimeric and proteinase binding unit. J Biol Chem 261:15863–15869
139. Imber MJ, Pizzo SV (1981) Clearance and binding of two electrophoretic "fast" forms of human alpha 2-macroglobulin. J Biol Chem 256:8134–8139
140. LaMarre J et al (1991) Cytokine binding and clearance properties of proteinase-activated alpha 2-macroglobulins. Lab Invest 65:3–14
141. Feige JJ et al (1996) Alpha 2-macroglobulin: a binding protein for transforming growth factor-beta and various cytokines. Horm Res 45:227–232
142. Crookston KP et al (1994) Classification of alpha 2-macroglobulin-cytokine interactions based on affinity of noncovalent association in solution under apparent equilibrium conditions. J Biol Chem 269:1533–1540
143. Araujo-Jorge TC, de Meirelles Mde N, Isaac L (1990) Trypanosoma cruzi: killing and enhanced uptake by resident peritoneal macrophages treated with alpha-2-macroglobulin. Parasitol Res 76:545–552
144. van Dijk MC et al (1992) Role of the scavenger receptor in the uptake of methylamine-activated alpha 2-macroglobulin by rat liver. Biochem J 287(Pt 2):447–455
145. Hughes SR et al (1998) Alpha2-macroglobulin associates with beta-amyloid and prevents fibril formation. Proc Natl Acad Sci USA 95:3275–3280
146. Yerbury JJ et al (2009) Alpha 2 macroglobulin and haptoglobin suppress amyloid formation by interacting with prefibrillar protein species. J Biol Chem 284:4246–4254
147. Du Y et al (1997) Alpha2-macroglobulin as a beta-amyloid peptide-binding plasma protein. J Neurochem 69:299–305
148. Shibata M et al (2000) Clearance of Alzheimer's amyloid-ss(1–40) peptide from brain by LDL receptor–related protein-1 at the blood-brain barrier. J Clin Invest 106:1489–1499
149. Basu S et al (2001) CD91, a common receptor for heat shock proteins gp96, Hsp90, hsp70 and calreticulin. Immunity 14:303–313
150. Binder RJ, Han DK, Srivastava PK (2000) CD91: a receptor for heat shock protein Gp96. Nat Immunol 1:151–155
151. Binder RJ, Srivastava PK (2004) Essential role of Cd91 in re-presentation of Gp96-chaperoned peptides. Proc Natl Acad Sci USA 101:6128–6133
152. Arnold-Schild D et al (1999) Receptor-mediated endocytosis of heat shock proteins by professional antigen-presenting cells. J Immunol 162:3757–3760

153. Henderson B et al (2010) Caught with their PAMPs down? The extracellular signaling actions of molecular chaperones are not due to microbial contaminants. Cell Stress Chaperones 15:123–141
154. Pockley AG, Muthana M, Calderwood SK (2008) The dual immunoregulatory roles of stress proteins. Trends Biochem Sci 33:71–79
155. Quintana FJ et al (2004) Inhibition of adjuvant-induced arthritis by DNA vaccination with the 70-kd or the 90-kd human heat-shock protein: immune cross-regulation with the 60-kd heat-shock protein. Arthritis Rheum 50:3712–3720
156. Binder RJ, Kumar SK, Srivastava PK (2002) Naturally formed or artificially reconstituted non-covalent alpha2-macroglobulin-peptide complexes elicit Cd91-dependent cellular immunity. Cancer Immun 2:16
157. Dobryszycka W (1997) Biological functions of haptoglobin - new pieces to an old puzzle. Eur J Clin Chem Clin Biochem 35:647–654
158. Giblett ER (1968) The haptoglobin system. Ser Haematol 1:3–20
159. Gutteridge JM (1987) The antioxidant activity of haptoglobin towards haemoglobin-stimulated lipid peroxidation. Biochimi Biophys Acta 917:219–223
160. Edwards DH et al (1986) Haptoglobin-haemoglobin complex in human plasma inhibits endothelium dependent relaxation: evidence that endothelium derived relaxing factor acts as a local autocoid. Cardiovasc Res 20:549–556
161. Lange V (1992) Haptoglobin polymorphisms - not only a genetic marker. Anthropol Anz 50:281–302
162. Barclay R (1985) The role of iron in infection. Med Lab Sci 42:166–177
163. Cid MC et al (1993) Identification of haptoglobin as an angiogenic factor in sera from patients with systemic vascularitis. J Clin Invest 91:977–985
164. Sobek O, Adam P, Seyfert OS, Kunzmann V, Schwetfeger N, Koch HC, Faulstich A (2003) Determinants of lumbar CSF protein concentration. J Neurol 250:371–372
165. Yerbury JJ et al (2005) The acute phase protein haptoglobin is a mammalian extracellular chaperone with an action similar to clusterin. Biochemistry 44:10914–10925
166. El Ghmati SM et al (1996) Identification of haptoglobin as an alternative ligand for CD11b/CD18. J Immunol 156:2542–2552
167. Wagner L et al (1996) Haptoglobin phenotyping by newly developed monoclonal antibodies: demonstration of haptoglobin uptake into peripheral blood neutrophils and monocytes. J Immunol 156:1989–1996
168. Lim SK et al (1998) Increased susceptibility in Hp knockout mice during acute hemolysis. Blood 92:1870–1877
169. Cedazo-Minguez A, Cowburn RF (2001) Apolipoprotein E: a major piece in the Alzheimer's disease puzzle. J Cell Mol Med 5:254–266
170. Zannis VI, Kardassis D, Zanni EE (1993) Genetic mutations affecting human lipoproteins, their receptors, and their enzymes. Adv Hum Genet 21:145–319
171. Li WH et al (1988) The apolipoprotein multigene family: biosynthesis, structure, structure-function relationships, and evolution. J Lipid Res 29:245–271
172. Strittmatter WJ et al (1993) Apolipoprotein E: high-avidity binding to beta-amyloid and increased frequency of type 4 allele in late-onset familial Alzheimer disease. Proc Natl Acad Sci USA 90:1977–1981
173. LaDu MJ et al (1994) Isoform-specific binding of apolipoprotein E to beta-amyloid. J Biol Chem 269:23403–23406
174. Pillot T et al (1997) Specific modulation of the fusogenic properties of the Alzheimer beta-amyloid peptide by apolipoprotein E isoforms. Eur J Biochem 243:650–659
175. Wood SJ, Chan W, Wetzel R (1996) An ApoE-Abeta inhibition complex in Abeta fibril extension. Chem Biol 3:949–956
176. Evans KC et al (1995) Apolipoprotein E is a kinetic but not a thermodynamic inhibitor of amyloid formation: implications for the pathogenesis and treatment of Alzheimer disease. Proc Natl Acad Sci USA 92:763–767

177. Castano EM et al (1995) Fibrillogenesis in Alzheimer's disease of amyloid beta peptides and apolipoprotein E. Biochem J 306(Pt 2):599–604
178. Ma J et al (1994) Amyloid-associated proteins alpha 1-antichymotrypsin and apolipoprotein E promote assembly of Alzheimer beta-protein into filaments. Nature 372:92–94
179. Bales KR et al (1997) Lack of apolipoprotein E dramatically reduces amyloid beta-peptide deposition. Nat Genet 17:263–264
180. Bales KR et al (1999) Apolipoprotein E is essential for amyloid deposition in the APP (V717F) transgenic mouse model of Alzheimer's disease. Proc Natl Acad Sci USA 96:15233–15238
181. Holtzman DM et al (1999) Expression of human apolipoprotein E reduces amyloid-beta deposition in a mouse model of Alzheimer's disease. J Clin Invest 103:R15–R21
182. Mackic JB et al (1998) Human blood–brain barrier receptors for Alzheimer's amyloid-beta 1–40. Asymmetrical binding, endocytosis, and transcytosis at the apical side of brain microvascular endothelial cell monolayer. J Clin Invest 102:734–743
183. Hu J, LaDu MJ, Van Eldik LJ (1998) Apolipoprotein E attenuates beta-amyloid-induced astrocyte activation. J Neurochem 71:1626–1634
184. Emsley J et al (1994) Structure of pentameric human serum amyloid-P component. Nature 367:338–345
185. Pepys MB et al (1994) Human serum amyloid P component is an invariant constituent of amyloid deposits and has a uniquely homogeneous structure. Proc Natl Acad Sci USA 91:5602–5606
186. Wood SP et al (1988) A pentameric form of human serum amyloid P component. Crystallization, X-ray diffraction and neutron scattering studies. J Mol Biol 202:169–173
187. Sorensen IJ et al (1995) Native human serum amyloid P component is a single pentamer. Scand J Immunol 41:263–267
188. Hawkins PN et al (1994) Concentration of serum amyloid P component in the CSF as a possible marker of cerebral amyloid deposits in Alzheimer's disease. Biochem Biophys Res Commun 201:722–726
189. Bickerstaff MCM et al (1999) Serum amyloid P component controls chromatin degradation and prevents antinuclear autoimmunity. Nat Med 5:694–697
190. Breathnach SM et al (1989) Serum amyloid P component binds to cell nuclei in vitro and to in vivo deposits of extracellular chromatin in systemic lupus erythematosus. J Exp Med 170:1433–1438
191. Sorensen IJ et al (2000) Complexes of serum amyloid P component and DNA in serum from healthy individuals and systemic lupus erythematosus patients. J Clin Immunol 20:408–415
192. de Haas CJC (1999) New insights into the role of serum amyloid P component, a novel lipopolysaccharide-binding protein. FEMS Immunol Med Microbiol 26:197–202
193. Sorensen IJ et al (1996) Binding of complement proteins C1q and C4bp to serum amyloid P component (SAP) in solid contra liquid phase. Scand J Immunol 44:401–407
194. Barbashov SF, Wang C, Nicholson-Weller A (1997) Serum amyloid P component forms a stable complex with human C5b6. J Immunol 158:3830–3858
195. de Beer FC et al (1981) Fibronectin and C4-binding protein are selectively bound by aggregated amyloid P component. J Exp Med 154:1134–1139
196. Swanson SJ, Christner RB, Mortensen RF (1992) Human serum amyloid P-component (SAP) selectively binds to immobilized or bound forms of C-reactive protein (CRP). Biochim Biophys Acta 1160:309–316
197. Brown MR, Anderson BE (1993) Receptor-ligand interactions between serum amyloid P component and model soluble immune complexes. J Immunol 151:2087–2095
198. de Haas CJC et al (1998) A synthetic lipopolysaccharide (LPS)-binding peptide based on amino acids 27–39 of serum amyloid P component inhibits LPS-induced responses in human blood. J Immunol 161:3607–3615
199. Coker AR et al (2000) Molecular chaperone properties of serum amyloid P component. FEBS Lett 473:199–202

200. Hamazaki H (1995) Ca(2+)-dependent binding of human serum amyloid P component to Alzheimer's beta-amyloid peptide. J Biol Chem 270:10392–10394
201. Pepys MB et al (1979) Binding of serum amyloid P component (SAP) by amyloid fibrils. Clin Exp Immunol 38:284–293
202. Uversky VN (2002) What does it mean to be natively unfolded? Eur J Biochem 269:2–12
203. Farrell HM Jr et al (2002) Molten globule structures in milk proteins: implications for potential new structure-function relationships. J Dairy Sci 85:459–471
204. Kumosinski TF, Brown EM, Farrell HM Jr (1993) Three-dimensional molecular modeling of bovine caseins: a refined, energy-minimized kappa-casein structure. J Dairy Sci 76:2507–2520
205. Farrell HM Jr et al (2009) Review of the chemistry of alphaS2-casein and the generation of a homologous molecular model to explain its properties. J Dairy Sci 92:1338–1353
206. Koudelka T, Hoffmann P, Carver JA (2009) Dephosphorylation of alpha(s)- and beta-caseins and its effect on chaperone activity: a structural and functional investigation. J Agric Food Chem 57:5956–5964
207. Khodarahmi R, Beyrami M, Soori H (2008) Appraisal of casein's inhibitory effects on aggregation accompanying carbonic anhydrase refolding and heat-induced ovalbumin fibrillogenesis. Arch Biochem Biophys 477:67–76
208. Thorn DC et al (2005) Amyloid fibril formation by bovine milk kappa-casein and its inhibition by the molecular chaperones alphaS- and beta-casein. Biochemistry 44:17027–17036
209. Thorn DC et al (2008) Amyloid fibril formation by bovine milk alpha s2-casein occurs under physiological conditions yet is prevented by its natural counterpart, alpha s1-casein. Biochemistry 47:3926–3936
210. Farrell HM Jr et al (2006) Casein micelle structure: what can be learned from milk synthesis and structural biology. Curr Opin Colloid In 11:135–147
211. Farrell HM Jr et al (2003) Environmental influences on bovine kappa-casein: reduction and conversion to fibrillar (amyloid) structures. J Protein Chem 22:259–273
212. Ecroyd H et al (2008) Dissociation from the oligomeric state is the rate-limiting step in fibril formation by kappa-casein. J Biol Chem 283:9012–9022

Index